EXPERIMENTAL AND ANALYTICAL STUDIES OF HYDROCARBON YIELDS UNDER DRY-, STEAM-, AND STEAM-WITH-PROPANE DISTILLATION

A Dissertation

by

NAMIT JAISWAL

Submitted to the Office of Graduate Studies of
Texas A&M University
in partial fulfillment of the requirements for the degree of

DOCTOR OF PHILOSOPHY

May 2007

Major Subject: Petroleum Engineering

EXPERIMENTAL AND ANALYTICAL STUDIES OF HYDROCARBON YIELDS UNDER DRY-, STEAM-, AND STEAM-WITH-PROPANE-DISTILLATION

A Dissertation

by

NAMIT JAISWAL

Submitted to the Office of Graduate Studies of
Texas A&M University
in partial fulfillment of the requirements for the degree of

DOCTOR OF PHILOSOPHY

Approved as to style and content by:

Chair of Committee,	Daulat D. Mamora
Committee Members,	William D. McCain
	Akhil Datta-Gupta
	Luc Ikelle
Head of Deapartment,	Steve Holditch

May 2007

Major Subject: Petroleum Engineering

ABSTRACT

Experimental and Analytical Studies of Hydrocarbon Yields Under
Dry-, Steam-, and Steam-with-Propane Distillation. (May 2007)

Namit Jaiswal, B. Eng.., University of Mumbai
M.S., University of Alaska Fairbanks;
Chair of Advisory Committee: Dr. Daulat Mamora

Simulation study has shown oil production is accelerated when propane is used as an additive during steam injection. To better understand this phenomenon, distillation experiments were performed using San Ardo crude oil (12^{o}API). For comparison purposes, three distillation processes were investigated: dry-, steam-, and steam-propane-distillation, the latter at the propane-to-steam mass ratio of 0.05 at steam injection rate 0.5 g/min.

Two sets of the distillation experiments were carried out. In the first set of experiments, the distillation temperatures ranged from 115ºC to 300ºC. Distillation pressures ranged from 0 psig to 998 psig for steam- and steam-propane distillation. The temperature-pressure combination used represented 15ºC superheated steam conditions. In the second set of experiments, the distillation temperatures ranged from 220^{o}C to 300^{o}C at 260 psig. The temperature pressure combination used represented field conditions for crude oil. For both conditions, the cell was kept at each temperature plateau (cut) until no increase occurs in distillation yields. Distillation yields were collected at each cut, and the volume and weight of water and hydrocarbon measured. Based on these experiments, a thermodynamic modeling framework was developed that describes distillation effect and oil production for steam distillation experiments. The model is based on composition of crude oil, molecular weight of heavy fraction. The analytical model results are compared against the experimental data for synthetic crude and crude oil to verify the validity of the model.

Main results of the study may be summarized as follows. The yields for steam distillation for saturated conditions of T_{sat+15^oC} and P_{sat} is 10 % and with addition of 5% of

propane to steam no significant increase occurs in distillation yields. The yields for steam distillation for field conditions of 260 psig and temperature range (220 ~300^{o}C) is 18 % and with addition of 5% of propane to steam no significant increase in distillation yields. The results indicate that propane has minimal distillation effect on the heavy oil. This occurs possibly because of lesser amount of light fractions in the heavy oil that enhance the separation of components in the oil caused by the concentration gradient.

DEDICATION

This dissertation is dedicated to my parents, my brother and my wife who have rejoiced with me in the good times and encouraged me to move forward through the bad, for their love, patience and sacrifices.

ACKNOWLEDGEMENTS

I would like to acknowledge the Halliburton Center for Unconventional Reservoirs for funding my research from 2005 to 2007 and Ramey Laboratory Research Program from 2004 to 2005. The Ramey Laboratory Program was a consortium of Chevron, ConocoPhillips and Total. Halliburton Center for Unconventional Reservoirs is funded by Anadarko, Baker Hughes, BP, Chevron, ConocoPhillips, El Paso, ExxonMobil, Halliburton, IHS, Nexen, Newfield, Saudi Aramco, Schlumberger and Total.

I would like to thank my advisor, Dr. Daulat Mamora, for believing in me and helping me out when everything was nebulous . His constant encouragement and creative ideas have always motivated me to work beyond my ability. My sincere appreciation goes to my advisory committee members, Dr. Bill McCain, Dr. Akhil Datta-Gupta and Dr. Luc Ikelle, for guidance and support throughout the course of this research.

I would like to thank Jose Rivero for his constant guidance and help in the laboratory during the course of this work. Further, I would like to thank my fellow graduate researchers, Marjorie, Ekene, Roly, Azer, Eric and Ahmed, for providing a challenging multicultural and intellectual environment. I would especially like to thank Eric Matus for his help and company whether for conducting my experiments or lunch at Northgate.

I would like to thank my friends Varun, Vaibhav, Sandeep, Brinjit, Ushank, Bharath, Ravi, Kola, Angeni, Gina and Celia. Their ongoing support during these years has been invaluable. I don’t know how I would have survived in Texas without the warmth of friends. I would like to especially thank Zuher Syihab for everything he has done for me and for making my stay at A&M a memorable one.

I remain grateful to my parents for their support throughout all my years in school and for their unwavering love and my brother, Nitesh Jaiswal, and especially my wife, Tanuja. Without their help and motivation to continue my studies, this dissertation would not have been possible.

TABLE OF CONTENTS

LIST OF FIGURES

FIGURE Page

FIGURE Page

FIGURE Page

LIST OF TABLES

CHAPTER I

INTRODUCTION

Several mechanisms have been identified which contribute to oil displacement during a heavy oil steamflood. These include viscosity reduction, thermal expansion, gas drive and steam distillation.[1]

In the past eight years, steam injection studies have been conducted at the Department of Petroleum Engineering (Texas A&M University) to evaluate the feasibility of using additives (propane, distillate) during steam injection. The studies were conducted using Duri intermediate oilfield (20^{o}API), San Ardo heavy oil (12^{o}API) and Hamaca extra heavy oilfield (8^{o}API).

1.1 Steam-Propane Injection in Heavy Oil

Several steamflood experiments have been conducted in past at Texas A&M University, in which steam is injected simultaneously with propane. The superheated steam at 230^{o}C was injected at 5.5 ml/min (San Ardo) by Simangunsong (2005)[2], 170^{o}C and 3.5 ml/min (Hamaca) by Rivero (2003)[3] and 260^{o}C and 5.5 ml/min (Duri) by Nesse (2004)[4] , with the cell outlet pressure at 270 psig (San Ardo), 50 psig (Hamaca) and 500 psig (Duri). Runs were made with propane/steam mass ratios (PSR) ranging from 0:100 to 5:100. Propane-steam ratio (PSR) 0.05 was identified as optimum concentration.

The following are the main results observed for steam-propane compared to pure steam injection -

(a) The start of oil production is accelerated by 19% (Hamaca), 30% (Duri) and 33% (San Ardo).

This dissertation follows the style and format of SPE *Journal of Petroleum Technology.*

(b) Steam injectivity is approximately three times higher

(c) The steam front velocity is higher, indicating greater partitioning of distilled fractions into the propane stream that appears to act as a very efficient carrier gas.

In addition, Plazas (2002)[5] conducted distillation experiments of two Venezuela crude oil types for up to 360°C. The following are the main results are shown in **Fig. 1.1**.

a) For 25.1°API crude oil, the yield with steam-propane distillation, 63 wt% of original oil, is significantly higher than that with pure steam distillation, 42 wt% of original oil**.**

b) For 34.2°API crude oil, yields for steam-propane and for pure steam distillations are very similar, about 54 wt% of original oil.

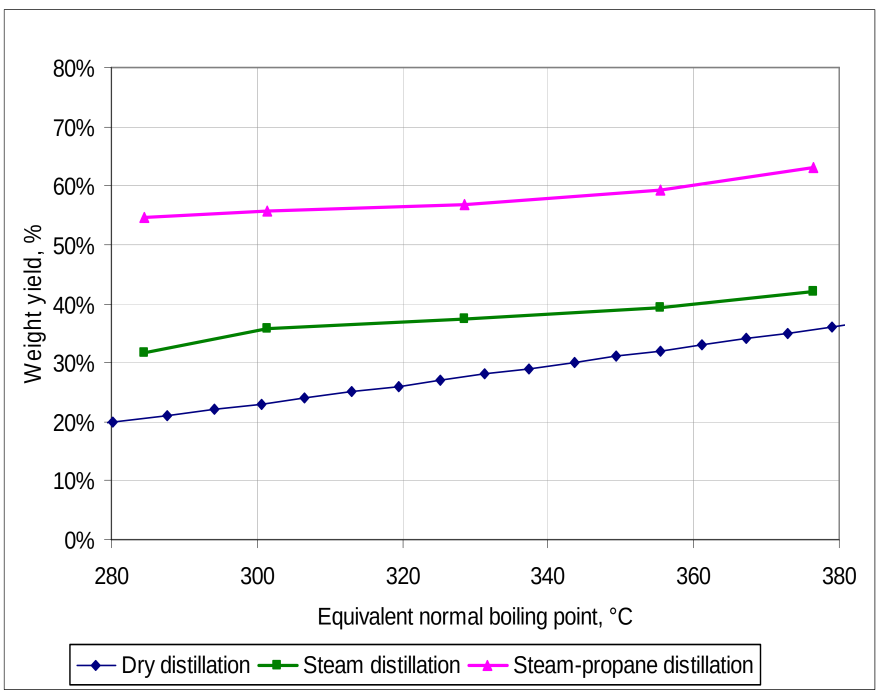

Figure 1.1: Distillation of two Venezuela crude oils (Plazas, 2002).[5]

Recently, Simangunsong et al. (2006) [6] developed an analytical model to describe the process of production acceleration with steam-propane injection[6]. The proposed research aims at obtaining a better understanding of the process involved during steam-propane distillation and associated oil recovery mechanisms during steam-propane injection. This research therefore emphasis on understanding distillation effect of propane as a steam additive during steam injection.

Steam injection is a well-known Enhanced Oil Recovery (EOR) process that has been successfully used in the field for some fifty years. A description of the oil recovery mechanisms and physics under steam injection follows.

1.1.1 Heat and Mass Transport during Steam Injection

Steam is injected into a reservoir containing particularly intermediate and heavy oil to improve the oil production rate and recovery. The injected steam is typically wet-steam with a steam quality of about 80%. The latent and sensible heat contained in the steam is imparted to both oil (and any other fluids in the reservoir) and the reservoir matrix, resulting in their temperature increase. Heating of the oil results in the following beneficial effects, [7,8]

a) Oil viscosity is significantly reduced particularly for intermediate and heavy oils–resulting in lower flow resistance, thus increasing the oil production rate.

b) Steam distillation of the lighter hydrocarbon fractions significant for lights oils–occur in the steam zone. The lighter fractions being in the gaseous phase can travel deeper into the colder regions of the reservoir, where they condense, reducing the oil viscosity, density, and interfacial tension. Oil viscosity reduction results in an increase in oil production rate. The produced oil is upgraded by reduction of the oil produced density.

c) The oil undergoes thermal expansion and viscosity reduction, which constitutes a drive mechanism.

During steam injection, the heat and mass transfer at the steam oil interface is a complex process that is not fully understood. To understand the process of steam-propane distillation, we need to understand the physics of distillation in general. The process of distillation is briefly described in the following section.

1.1.2 Steam Distillation

Steam distillation plays an important role during steamflooding. Indirect evidence of solvent bank formation in the field has been observed in light oil steamfloods and also in laboratory experiments, where a significant fraction of the oil is distillable during steam injection. The experiments have shown that the fraction of light ends (< C_{10}) in the produced oil is increased until steam breakthrough and then decreased following steam breakthrough (Sarathi et al., 1988).[9].

Figure 1.2 illustrates the steam distillation mechanism as it occurs during this thermal enhanced oil recovery process. There is condensate bank in between steam zone and original oil. As steam front moves this bank size increases. This bank is formed as light hydrocarbons are distilled from oil remaining in the steam zone.

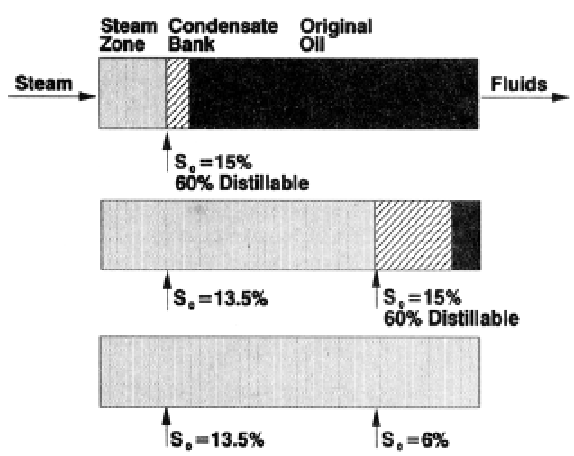

Figure 1.2: Steam distillation mechanism. [9]

To quantify the impact of steam distillation on production from a particular reservoir, one must first know the distillation characteristics of the oil. Batch distillation of a small quantity of the oil is one method of obtaining this information.

To date, there is no analytical model (we have only a tentative theory) to describe the process of production acceleration with steam-propane injection and the higher yields for steam-propane distillation. There is only one study done by Ramirez (2004) [7] for synthetic sample (mixture of normal C5, C6, C7, C8, C9, C10 & C15) to understand steam propane distillation. This study was carried out to understand the process involved during steam-propane distillation and associated oil recovery mechanisms during steam-propane injection.

One benefit resulting from the distillation of heavy oil during a steamflood is that the light distillates can act as a solvent to lower the viscosity of the original oil. As previously discussed, the vaporized distillate mixes with the original oil ahead of the steam condensation zone. Depending on the quantity of light hydrocarbon available to mix with the oil, viscosity can decrease by 1 order of magnitude (Shu et al, 1984)[10].

The boiling points of organic compounds can give important clues to other physical properties. A liquid boils when its vapor pressure is equal to the atmospheric pressure. Vapor pressure is determined by the kinetic energy of molecules. Kinetic energy is related to temperature, mass and velocity of the molecules. When the temperature reaches the boiling point, the average kinetic energy of the liquid particles is sufficient to overcome the forces of attraction that hold molecules in the liquid state. Then these molecules break away from the liquid to form a gaseous phase. Molecules with the most independence in individual motions achieve sufficient kinetic energy (velocities) to escape into the vapor phase at lower temperatures. The vapor pressure will be higher and therefore the compound will boil at a lower temperature. Molecules that strongly interact or bond with each other through a variety of intermolecular forces cannot move easily or rapidly and therefore, do not achieve the kinetic energy necessary to escape the liquid state. Therefore, molecules with strong intermolecular forces will have higher boiling points.

Number of electrons per molecule, molecular polarizability, and contact between chains increases with increasing chain length resulting in greater intermolecular London attractive forces. The data may be plotted to graphically illustrate this trend, as shown in **Fig. 1.3**. For hydrocarbons in general the higher the molecular weight the higher is the boiling point of the component.

Ramirez (2004)[7] concluded that, during steam-propane distillation of oil, the steam/propane vapor strips the more volatile components from the oil because it encourages a decrease of the boiling point of these components. The steam enriched with the propane and light components, flow through the steam zone to the condensation front where both steam and light hydrocarbons condense. The condensed hydrocarbons are miscible with the oil, reducing overall viscosity of liquids hydrocarbon. In other words, steam/propane distillation begins when the total vapor pressure (steam and propane) in the presence of two immiscible liquids (water and oil exerting its own vapor pressure at the temperature of the system) equals the total pressure on the system.

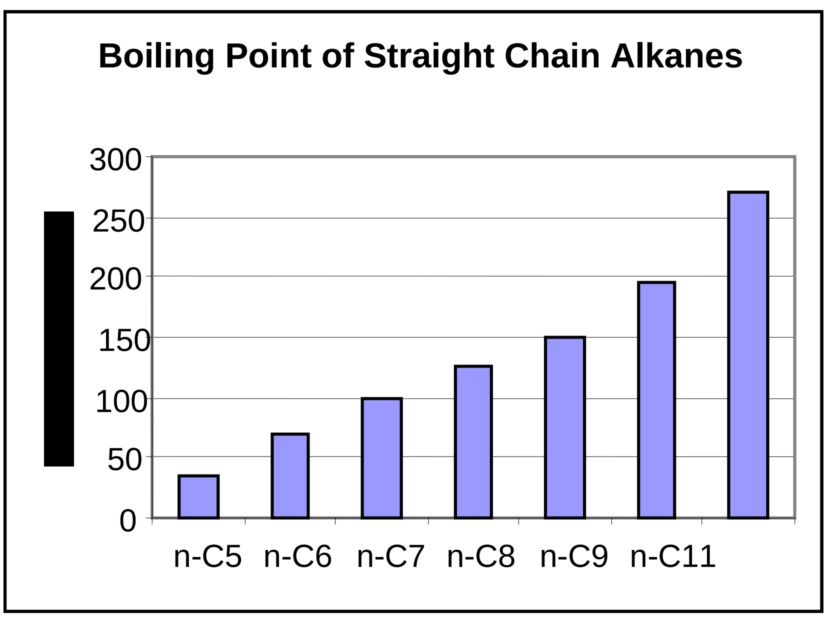

Figure 1.3: Increase in boiling point of alkanes with increasing carbon number.

Ramirez (2004)[7] in his study with synthetic hydrocarbon, identified that the role of propane is that it reduces the boiling point of some light oil components. As a result, oil will begin distilling at temperatures much lower than the normal boiling points of its constituents. As a consequence, the distillation yield increases.

The material balance on the distillation yields of synthetic hydrocarbons will help to develop a process model for the partial distillation using steam/propane. The theory and experimental method presented in this work should be particularly useful in applications to the steam-propane flood process using any additive to show the importance of vaporization in total oil recovery. The value of this study is to establish laboratory distillation measurements to quantify oil recovery efficiency during steam/propane injection and develop numerical modeling framework for this process and quantify the effect of additives.

1.2 Objectives of Study

In this research, laboratory experiments were conducted to determine the boiling points and yields during the distillation of a San Ardo crude oil from California Field. The main objectives of this research are as follows.

(a) To verify experimentally that propane reduces the boiling points of some components of San Ardo heavy oil.

(b) To investigate types of mechanisms during distillation of San Ardo oil under steam injection with propane.

(c) To investigate the effect of propane in upgrading oil.

(d) To develop a new systematic procedure to analyze the performance of steam-propane injection in oil reservoirs and match the synthetic sample and experimental study previously carried out.

(e) To correlate steam-propane distillation yields for some crude oils and synthetic hydrocarbons to generate steam-propane distillation data that could be used to develop the input data necessary for compositional steamflood simulation.

To achieve these objectives crude oil (San Ardo heavy oil) was distilled in a laboratory apparatus at various conditions of temperature and pressure. Three types of distillation will be used dry- steam- and steam-propane distillation.

1.2.1 Deliverables

The collection of experimental steam distillation data for several heavy oils under a variety of reservoir and steam process recovery conditions would be very time consuming. Therefore there is need to develop a model to predict distillate yield under any set of conditions for any heavy oil, requiring only the simulated distillation (SIMDIS) trace (i.e. percent off vs. normal boiling temperature) of the oil. The expected deliverables from this work are as follows.

(a) A systematic procedure to quantify distillation yields of crude oils under steam-propane injection.

(b) Quantification of changes in distillation yields with propane as a steam additive during steam injection and develop framework for predicting performance of other additives.

(c) Finally, this would provide better understanding of oil recovery mechanisms under steam-propane injection.

1.2.2 Model Applications

The total amount of distillate generated in the field depends on the volume of residual oil contacted by steam. The volume of reservoir swept by steam can be estimated from an analytical model like that of Marx and Langenheim (1959)[11] or from a black oil simulator. The total volume of hydrocarbon distilled can be estimated using this scheme. A result of this study would be the applicable in actual field cases estimate oil recovery under distillation effect using steam-propane injection.

CHAPTER II

LITERATURE REVIEW

An exhaustive literature review of distillation and steam injection as an enhanced oil recovery method was performed. Main results of the literature review are summarized in the following.

The principal mechanisms responsible for oil recovery during steam injection are thermal expansion of the oil, viscosity reduction, and steam distillation. Steam distillation is the main mechanism that reduces the residual oil saturation behind the hot-water front during steamflood particularly for light and medium oils.

The vaporizing effect of hydrocarbons is induced by increasing the system temperature, and it is reflected by the increase in the system pressure. Steam will evolve from the aqueous phase and strip some hydrocarbon component from the oleic phase. Sin the pressure of the system is increased; the apparent bubble point of the water is consequently increased. This will cause the higher boiling point hydrocarbons to vaporize at the elevated saturation temperatures. Volek and Pryor (1972)[12] showed that very low residual oil (<3%) can be obtained in volatile reservoir by a combination of steam displacement and steam distillation. Wu and Brown (1975)[13] reported steam distillation of crude oils ranging in gravity from 9-36^{o}API at pressures from 200 psia to500 psia and steam temperatures from 387^{o}F to 600^{o}F in porous media. Their laboratory results showed that steam distillation yields appeared to be independent of the porous media and the steam injection rate, but depended on the reservoir crude oil composition. Therefore, understanding the distillation effect of steam and more recently the effect due to little concentration of propane in the steam on oil facilitates the prediction of fluid behavior in steam injection processes.

The first mathematical description of the distillation process was developed by Rayleigh (1901). In his classical analytical work, Rayleigh described mathematically the batch distillation process but limited to binary mixtures. Later, Holland and Welch (1957)[14] developed steam batch distillation calculations for a mixture of volatile components that might be partially separated from its nonvolatile components at temperature such that volatile components do not decompose. Their calculations were based on the theoretical requirement that the partial pressure of the steam in vapor stream rising from the still is less than the saturated pressure of steam at the temperature of the still. This assumes the absence of liquid water, and the batch process is carried out at the conditions of constant still temperature and constant total pressure. The total pressure is maintained constant by increasing the rate of flow of steam to compensate for the decrease of the concentration of the lower boiling components.

Later Willman *et al.* (1961)[1] reported high oil recoveries by steam injection identifying the principal mechanisms responsible for additional oil as.(1) thermal expansion oil, (2) viscosity reduction, and (3) steam distillation. Recovery by steam injection is greater for lighter oils because they contain a greater fraction of steam-distillable components. Appreciable amounts of even low gravity crude oils are steam distillable, and that residual oil left after steam injection is essentially independent of the initial oil saturation. Finally, it was observed that residual oil was lower in gravity than the initial crude oil because it has been steam-stripped of light ends.

Sukkar (1966)[15] proposed a method of calculating oil distilled during steamflooding of light oil. This method used relative velocities of steam, condensing steam front and velocities that described the rate at which particular oil components were being distilled. The solution was influenced by reservoir properties and oil composition. Results of other investigators have indicated that steam distillation yield is independent of reservoir properties, and the author emphasized that the oil distilled is not necessarily oil recovered.

Barb (1967) [16] developed some integral-difference equations describing the batch distillation column process. Barb assumed that the mole fraction of each component in the liquid leaving a plate is equal to its mean value in the liquid holdup on the plate. This may not necessarily be true in the case of steam-propane distillation.

Johnson *et al.* (1971)[17] presented a method to calculate oil vaporization during steamflooding. Three quantities were calculated sequentially as follows.

(a) The volume of steam condensed at the steam front,
(b) The volume of immobile oil left behind the hot-water zone, and
(c) Percentage of oil vaporized as a function of volume of steam and volume of immobile oil left behind the hot-water zone.

The oil vaporization involved a series of flash calculations for which an appropriate set of equilibrium ratios (K-values) was required. Oil composition corresponding to Bureau of Mines routine method to determine distillation fractions were used in the calculations. The results were in essence dictated by the selected K-values. Comparisons with experimental data showed that the method overestimated the amount of oil vaporized.

Volek and Pryor (1972)[12] reduced oil viscosity and the residual oil saturation below that obtainable by waterflooding using steam distillation drive. They studied the mechanisms involved in the steam distillation process, finding that steam driving light oil leaves a residual oil saturation of less than 8%, and increases the average gravity of the oil by recovering a greater fraction of the light components from the reservoir crude oil. This study was done only with light oil reservoir.

Alikhan and Ali (1974)[18] found that an important effect involved in the steam displacement phase of the process is steam distillation of the light hydrocarbons. Distilled fractions are carried farther downstream where they help to lower the viscosity of the cold original oil, increasing its mobility. They observed that light hydrocarbon injection was highly effective in the case where the core initially contained residual oil saturation as compared to straight steam slug injection but they did not give more importance and neither any explanation to this fact. They concluded that from the recovery point of view, it is advantageous to use a low viscosity light hydrocarbon slug and a small slug size. Their experimental study involved oil recovery from a porous medium by the injection of light hydrocarbon slug, followed by a steam slug, which is in turn, driven by a conventional waterflood.

Alikhan and Ali [18] also found that the light hydrocarbon slug, injected prior to the steam slug in a core, initially containing residual oil saturation, improved the oil recovery as compared to a straight steam slug run. The light hydrocarbon, in view of the prevailing adverse mobility ratio, mixes with the original in-place oil, and helps to lower its viscosity. The viscosity is further reduced by the heat from the injected steam slug, leading to an improvement in the mobility ratio, and hence an improvement in the displacement efficiency. The steam distillation effects recover a large proportion of the light hydrocarbon slug. It is concluded that from the recovery ratio (volume of oil recovered divided by hydrocarbon slug volume) point of view, it is advantageous to use a low viscosity light hydrocarbon slug, and a small slug size. The optimum slug size depends on the in-place oil, as well as the steam slug size, for a given steam temperature. The temperature profiles and the heat loss rate measurement indicated that the combination, light hydrocarbon slug-steam slug process, utilizes the maximum amount of heat injected.

The injected cold water effectively recovers the heat contained in the hot porous medium, transporting it farther downstream; however, the recovery of the heat contained in the adjacent formation is low. The authors showed that the process is highly effective particularly when the porous medium initially contains residual oil saturation. The displacement of oil by the proposed process involves a number of effects. The hydrocarbon slug is dispersed rapidly into the oil phase in view of the favorable mobility ratio involved. The increase in the oleic phase volume (assuming that initially the oil saturation is residual) leads to the development of an oil bank, at the rear of which there is an extensive transition zone containing the oil and the hydrocarbon in varying proportions. Effectively, this creates a graded oil viscosity zone, which is desirable in displacement by a number of mechanisms discussed by other authors. An important effect involved in the steam displacement phase of the process is steam distillation of the light hydrocarbons. The distilled fractions are carried farther downstream, where they help lower the viscosity of the cold in-place oil, thus increasing its mobility. On the whole, oil is efficiently displaced by the steam front, and at the same time its production is facilitated at the outlet end.

Alikhan and Ali[18] mention too that in the final phase of the process, cold water is injected to displace the in-place fluids. The cold water essentially leads to the transformation of the steam slug into a hot water bank. At the same time, the heat contained in the hot porous matrix near the inlet end is transported downstream. A fraction of the heat conducted into the adjacent formations is also recovered. As a result, the overall heat utilization efficiency of the process is improved. In addition to the effects considered above, gravity segregation of the fluids, and temperature variation of the relative permeabilities would affect the overall process.

Experimental results of Wu and Brown (1975)[13] show that in saturated steam distillation, yields are mainly dependent on the oil composition and may not correlate with the crude API gravity. Six crude oils ranging from 9^{o}API to 36^{o}API were used. Cumulative yields ranged from 7 to 68 volume percent. Results indicated that yields were independent of the porous medium used, steam injection rate and initial oil volume.

Wu and Brown shows that changes in steam saturation pressure and temperature have insignificant effect on the yields; however, superheated steam increases significantly the yields for some crude oils. The authors recognized that steam distillation is one of the major mechanisms responsible for high oil recovery by steam flooding. Based on laboratory steam flood and fluid flow in porous media experiments they identified these mechanisms as: (1) steam distillation (including gas stripping), (2) steam displacement, (3) viscosity reduction, (4) thermal expansion, (5) gravity segregation, (6) relative permeability and capillary pressure variation, (7) solution gas drive, (8) oil-phase miscible drive, and (9) emulsion drive. The most important of these mechanisms, steam distillation and steam displacement, take place in the steam zone. In the steam zone, the pressure and temperature gradients are generally small indicating stable saturated steam conditions. The presence of steam vapor phase in the steam zone with two liquid phases (heated crude oil and hot water) induces vaporization of light oil fractions and water. These oil and water vapors are displaced downstream by the steam and condensed in the solvent and hot water banks. Rapid vaporization of oil and water disturbs and redistributes a portion of oil in the pores and, thus, effects a more efficient displacement of the crude oil by the injected steam.

Wu (1975)[13] concluded that steam distillation is an important part of steam drive, which is responsible for the low residual oil saturation of a steamflood.[19] Steam distillation is a process of separating the light fractions from the crude oil by the action of steam.

Rhee and Doscher (1980)[19] indicated the importance of the compositional effect on the solvent displacement mechanism in steamflooding. Steam distillation is affected strongly by the composition of the crude oil. Even crude oils having the same gravity can show significant differences in steam distillation characteristics depending on their compositions. Therefore, the effect of the composition should be considered carefully.

Wu and Elder (1983)[20] and Wu and Elder (1980) [21] established some correlations to estimate the amount of vaporized oil caused by steam distillation. These correlations were based on 16 crude oils within a minimum standard error of 4.3%. Steam distillation yields of sixteen crude oils obtained from various parts of the United States were determined at a saturated-steam pressure of 215 psia. At the steam distillation factor of 15 (V_w/V_{oi} = 15) the yield ranges from 12 to 56% of initial oil volume. V_w is volume of steam (cold water equivalent) injected, and V_{oi} is original oil volume, both volumes expressed in the same unit. Main conclusions of their studies are as follows.

1. The effect of pressure on the ultimate steam distillation yields (when $V_w/V_{oi} > 15$) appears to be small. However, its effect may be significant for $V_w/V_{oi} < 15$).

2. Simple regression analysis results indicate the following.

(a) The steam distillation yield increases linearly with respect to the API gravity. The API gravity can predict the steam distillation yields within a standard error of 5.6% (in yield).

(b) The steam distillation yield decreases logarithmically with respect to the oil viscosity (100°F). When the oil viscosity is less than 10cs (at 100°F) the relationship is uncertain. Above 10 cs at 100°F, the oil viscosity can be used to estimate the steam distillation yields within a standard error of 4.3%.

(c) The steam distillation yield increases as the characterization factor of the crude oils increases. However, this is not a good parameter for correlation.

(d) The steam distillation yield increases linearly with respect to the simulated distillation yield. This parameter can be used to predict the steam distillation within a standard error of 4.5%.

Duerksen and Hsueh (1983)[22] reported a correlation between steam distillation yield, API gravity, and wax content of crude oils. Research shows in a steam distillation of crude oils that for low-wax crude oils, steam distillation yield correlates closely with API gravity. For both high and low-wax crude oils, steam distillation yield correlates closely with API gravity and wax content. Vaporization, transport, and condensation of the hydrocarbons fractions are dynamic processes that displace the lighter hydrocarbon fractions and generate a distillate bank that miscible drives the oil to producing wells. When matching steam distillation data obtained in their laboratory, they found that distillation efficiency factor decreased as the pressure increased. The decrease in distillation efficiency was attributed to the reduction in specific volume of steam with increasing pressures.

Langhoff and Wu (1986)[23] used the Holland and Welch method and a simulated distillation data to calculate crude-oil/water/vapor separations on a hexane/decane system and for 16 crude oils. The approach satisfactorily predicted the overhead yields of 13 out of 16 crude oils with an average error of 12% (±3.6% in yield). The overhead yields obtained were expressed as a function of the steam distillation factor. This method required only simulated crude oil distillation data for the separation calculation.

A method using steam distillation tests to estimate 3-phase K-values of mixtures of pure hydrocarbons with water was developed by Billman (1989)[24] and Goite (2001)[25]. Three-phase separation data was obtained for temperature range from 150^{o}F to 500^{o}F and pressures from 0 psig to 1,000 psig in a constant volume cell. These conditions included a liquid water phase, a liquid hydrocarbon phase, and a vapor phase consisting of hydrocarbon and water vapors. The pure n-alkane components used ranged from n-hexane through n-dodecane. The author concluded that steam distillation data was useful in determining overall yields but did not provide compositional information for determining 3-phase K-values.

Later a new method to calculate 3-phase K-values of crude oil fractions was developed by Lanclos (1990)[26]. This method was based on the theoretical considerations developed by Billman[24] with some modifications to increase the accuracy of the 3-phase K-values calculation procedure and to extend the procedure for the calculation of 3-phase K-values of crude oil fractions. The method of Lanclos[26] assumed that the crude oils were composed of a mixture of pure hydrocarbon components due to lack of correlations relevant to crude oil fractions. The author concluded that the data obtained could be used to estimate 3-phase K-values of pure hydrocarbons ranging from n-C_5 to n-C_{12}. Lanclos observed that the liquid hydrocarbon density-temperature correlations had very little effect on the 3-phase K-value calculations for all ranges of hydrocarbon components and crude oil fractions.

Lim (1991)[27] developed a general method to calculate steam distillation yield and to quantify oil quality changes during steam injection. Steam distillation data from the literature could be correlated with the steam distillation yield obtained from the Department of Energy (DOE) crude oil assays. Lim found that the steam distillation yield could be significant, even for heavy crude oils. Data from 454 California crude oil samples from the DOE were analyzed that gave the following relationship.

$$\text{Volume \% Yield} = 1.75 \times {}^{o}\text{API} \qquad (2.1)$$

Forero (1992)[28] developed a new semiempirical computer model to calculate 3-phase K-values of n-alkanes in the presence of an aqueous phase using 3-phase isochoric experimental data generated by Billman.[24] This method uses the vapor phase composition from the lab data and the Peng-Robinson equation of state. The 3-phase K-values for n-C_6, n-C_7, n-C_8, n-C_9, n-$C_{10,}$ and n-C_{12} were calculated for temperatures raging from 200^{o}F to 500^{o}F. Results of this study indicated that the mutual solubility between the two liquids phases significantly affect the lighter hydrocarbon K-values at temperatures above 350^{o}F. For the heavier components the effect of mutual solubility is insignificant. The calculated 3-phase K-values were compared to the published 2-phase K-values obtained from Gas Processor's Association charts. The 3-phase K-values were considerably larger than published 2-phase K-values indicating the need for 3-phase K-values for reservoir process simulations.

Mokrys and Butler (1993)[29] studied steam-propane as part of the "Vapex" process. This process was designed to recover heavy oils effectively, and also obtain a partial upgrading of heavy crude in-situ. Simultaneous steam-propane injection into the scaled model is a variation on the Steam Assisted Gravity Drainage (SAGD) with propane forming a low temperature oil production zone that spreads laterally away from the steam zone at the injector/producer. In this process the steam creates a limited hot region in which propane is stripped from the draining oil and recycled internally. The cooler propane spreads laterally into the reservoir where it dilutes, upgrades and recovers oil. The steam is used to create a limited hot region in the vicinity of the injector/producer in which the propane is stripped from the draining oil and recycled into the laterally spreading, cooler propane chamber. As a result of this internal recycling mechanism the gas-oil ratios are low and the latent heat of propane vapor is transported to the oil/propane interface that is receding deeper into the cold reservoir. This was the first work where the propane-recovered oil could be upgraded in situ and thus is higher quality than the original oil.

The physical mechanism of lean gas injection into volatile oil reservoirs to recover oil by vaporization was studied by Espie *et al.* (1994)[30]. In this research the composition of the gas used included C_3 at 1.26 mole%. The experiments were conducted at reservoir conditions using core from the Prudhoe Bay reservoir. They pointed out that reservoir oil recovery efficiency by vaporization depends upon thermodynamics partitioning of oil components into the gas. Finally, the principal findings of this study showed: (1) The C_{6+} recovery by vaporization after 9.47 PV of lean gas injected was 28.4% of the target oil remaining after the equilibrium gas-flood, (2) Compositional analysis of the effluent stream and the core residual oil showed high recovery of components up to C_{12} with steadily declining recoveries up to C_{20}, (3) Mass balances over the total fluid, total hydrocarbons, C_{6+}, water and on a hydrocarbon component basis confirmed the accuracy of the experimental results.

Beladi (1995)[31] reported results of research on determination of *K*-values.[30] The approach consisted of four parts.

(a) 3-phase isochoric distillation (SWID) tests were developed to obtain the vapor phase compositions of binary, ternary, quaternary, and crude oil systems in presence of water for the temperature range, 250°F to 500°F.

(b) Compositional empirical balance model (EMBM) was developed to calculate pure component mixtures, pseudo components and water three-phase K-values using lab vapor phase conditions.

(c) Corrections were devised for three-phase K-values of binary systems (C_8/H_2O through C_{20}/H_2O) for the temperature range 250°F to 500°F.

(d) Ternary, quaternary and crude oil systems multi-component three-phase K-values were calculated using EMBM. These 3-phase K-values were used to examine the binary 3-phase K-value and their applicability to multi-component and pseudo component systems.

A consistent pseudoization technique was used to calculate pseudo-component's K-values of crude oil. Also, empirical mutual solubility correlations are proposed for both the hydrocarbon solubility in aqueous phase and the water solubility in the oleic phase. EMBM incorporated the new correlations for mutual solubilities, critical properties, and fluid densities to calculate the 3-phase compositions. EMBM compositions were used to calculate the 3-phase K-values. A comparison between EMBM compositions and existing equation of state compositions (EOS) was provided. Commercial thermal compositional reservoir simulators use 2-phase K-values compensated by water vapor pressures instead of 3-phase K-values gas-oil-water equilibrium K-values. When reservoir simulation is performed on 3-phase processes the distillation mechanism and effects of water on the oleic phase are neglected. This is due to scarceness of the three-phase experimental data for the reservoir conditions of high temperatures at their saturation pressures. This research emphasizes the properties and phase behavior of n-decane and n-eicosane and crude oil pseudocomponents. This experimental set-up was used to perform:

(a) Static system pressure test (SPT): These tests are performed on every sample to obtain the saturation system pressures of hydrocarbon/water mixtures. It is important to have the static pressure data to insure that three-phase near equilibrium conditions are reached for SWID tests.

(b) Stage-wise isochoric distillation test (SWID): At each stage of the distillation the system is brought to equilibrium before the distillate samples are removed from the vapor phase. This test is conducted under a stepwise increase of temperature for each stage. For each stage the vapor phase is partially and slowly removed as distillate for compositional analysis. Knowing the composition of every component removed, the overall composition is calculated by material balance. The remaining components in the cell are used for the next stage of test at higher temperature.

A comprehensive semi-empirical (CSA) approach to calculate 3-phase water/hydrocarbons equilibrium was developed by Tandia (1995)[32.] Lab data (stagewise isochoric distillation data) and Peng-Robinson EOS were used. The author considered mutual solubility between water and hydrocarbons. The CSA calculates phase equilibria by applying the thermodynamic equalities between phases and material balance of the systems. The approach also includes a self-tuning algorithm that allows the user to tune the input parameters, for instance vapor phase composition (y_i).

Goite (1999)[33] reported experimental results of steam-propane injection for Morichal heavy oil. Results appear to indicate optimal concentration of propane lies somewhere in the region of 5%. Significant acceleration in oil production was observed.

Mamora and Sutadiwiria (1999)[34] developed an analytical model for light oil recovery by steam distillation for a vertical sand pack containing a 3-component liquid mixture, cyclohexane, n-octane, and water. Study shows that steam distillation of oil does not occur at equilibrium conditions because it is a dynamic process. Moreover, oil recovery by steam distillation is largely dependent on the steam saturation point and injection rate. Their model describes the advance of steam-oil interface, temperature profile in the sand mix, and cyclohexane production, and it is in satisfactory agreement with the experimental data.

Following Goite (1999) [33]'s study of propane as an additive in steam injection, Ferguson *et al.* (2001)[35] continued the research using a constant steam mass rate. Several tests were performed to determine the optimum propane-steam mass ratio. Acceleration of production was found in the steam-propane runs when compared to steam alone. The optimum propane/steam mass ratio was found to be around 5:100. The acceleration in oil production was thought to be due to the dry distillation process in which the lighter oil fractions are vaporized and carried by propane. On contact with the colder part of the reservoir, the light fractions condense and are miscible with the oil, thus lowering the interfacial tension and decreasing the viscosity of the oil.

Later, Tinss (2001)[36] carried out steam-propane experiments using the "optimum" found in Ferguson's study, 5:100 propane-steam mass ratio, on a 21ºAPI Kulin oil. The same effect of production acceleration was observed in these experiments. Viscosity and density measurements indicated an increment in API gravity and a reduction of viscosity in the produced oil. Furthermore, injectivity was improved with the addition of propane to the steam. A slight reduction in the maximum injection pressure from 85 psig to 78 psig was observed in the experiments.

Distillation study considering the injection of steam using propane as an additive was conducted by Plazas (2002)[5]. The experimental study measured the yields for a light crude oil (34.2°API) and an intermediate crude oil (25.1°API). Propane to steam ratio of 5:100 was used in the distillation runs. Steam and steam-propane distillations were performed at five temperature cuts for each run, 110°C, 150°C, 200°C, 250°C and 300°C at slightly superheated conditions getting volumetric yields. A comparison with dry distillation was included. The steam distillation showed higher yield (43.1 wt%) and the steam-propane distillation gave an even higher yield (63.1 wt%), almost twice the yield obtained during dry distillation (36.0 wt%). These results indicated a remarkable improvement obtained using propane as an additive to steam distillation at the experimental conditions and for the intermediate oil only. For both crude oils, in general, viscosities of the distilled fractions were similar for both steam and steam-propane distillation.

Ramirez (2004)[7], conducted a series of experiments using steam-propane injection to evaluate the role of propane on Hamaca extra-heavy oil.[5] Four propane-steam mass ratios were used: 0:100, 2.5:100, 5:100, and 10:100. The same effect of production acceleration was observed in these experiments. The use of propane as an additive to steam resulted in injection pressures lower than those of pure steam injection, and that improvement of injectivity was observed even with propane-steam ratio as low as 2.5:100.

Ramirez (2004)[7], conducted a series of distillation experiments using steam-propane injection on synthetic crude. Results of this study can be summarized as follows. First, the hydrocarbon yield for equi-weight mixture of normal Alkanes (C_5, C_6, C_7, C_8, C_9, C_{10} & C_{15}) at 125ºC is highest with steam-propane distillation (74 wt%) compared to steam distillation (58 wt%), and lowest with dry distillation (36 wt%). This explains in part the oil production acceleration observed in steam-propane displacement experiments. Second, the final hydrocarbon yield at 300ºC however is the same for the three distillation processes. This observation is in line with the fact that oil recoveries were very similar in steam- and steam-propane displacement experiments. Third, based on the yields of individual hydrocarbon components, steam-propane distillation lowers the apparent boiling points of the hydrocarbons significantly. This phenomenon may be the most fundamental effect of propane on hydrocarbon distillation, which results in a higher yield during steam-propane distillation and oil production acceleration during steam propane displacement. Fourth, experimental K-values are higher in distillations with steam-propane for the components n-hexane, n-heptane, n-octane, and n- nonane. Fifth, vapor fugacity coefficients for each component are higher in distillations with steam propane than with steam. Finally, Gibbs excess energy is overall lower in distillations with steam-propane than with steam.

CHAPTER III

STEAM DISTILLATION

The phase behavior of reservoir fluids is an important phenomenon in petroleum production, particularly in enhanced oil recovery processes. The practical limit of how much of a reservoir fluid can be distilled, is obtained in steam distillation experiments originally developed by Wu and Elder, 1980.[21] Laboratory steam distillation experiments have generally been conducted as dynamic tests, which may or may not be near equilibrium. Experiments near equilibrium with extensive analysis of the phases yields values for the vapor-liquid equilibrium ratios, another way of assessing the importance of compositional changes in steamflood.

3.1 Experimental Analysis

To quantify the impact of steam distillation on oil production from a particular reservoir, one must first know the distillation characteristics of the oil. Batch distillation of a small quantity of the oil is one method of obtaining this information. Steam distillation can be performed in several ways depending on results required (Beladi, 1995).[31]

3.1.1 Static System Pressure Test (SPT):

Static system pressure is run for hydrocarbons (HC) in the presence of a water phase [three-phase, vapor-liquid-liquid (VLL) equilbria] and in the absence of a water [two-phase, vapor-liquid (VL) equilbria]. These tests are used as indication of equilibrium conditions in distillation tests. It is important to have the static pressure data to insure that equilibrium or near equilibrium condition is reached for stage wise isochoric distillation (SWID). The results of these tests can also be used to tune EOS approaches.

3.1.2 Dynamic Distillation Tests:

Dynamic distillation tests are performed to investigate the effect of steam injection rate on the steam distillation yields. This testing procedure is primarily used to obtain the maximum steam distillation yield.

3.1.3 Stagewise Isochoric Distillation (SWID) tests:

The SWID test is a stagewise distillation test. At each stage, the system is brought to equilibrium before the distillate sample is removed from the vapor phase. Ramirez (2004) [7] conducted modified SWID test for synthetic hydrocarbon by injecting steam and steam-propane to quantify effect of propane. There are two ways to perform SWID tests –

SWID-1: This test is conducted under stepwise increase of temperature for each stage. The equilibrium is reached between the stages. After the equilibrium is reached, the distillate sample removed for compositional analysis of the vapor phase. From the volumes of the distillate and the composition of the hydrocarbon phase, the new overall composition in the cell is calculated by the mole balance. The remaining components with the calculated overall compositions are used for the next stage of the test (at a higher temperature). This method was originally reported as semistatic test.

SWID-2: This test was originally developed by Beladi (1995)[31] to estimate K-values for steam-hydrocarbon mixture. This test is conducted at constant temperature for all stages. The equilibrium is reached between the stages. After the equilibrium is reached, the distillate sample is removed for compositional analysis of the vapor phase. From the volumes of the distillate and the composition in the cell is calculated by the mole balance. The remaining components with the calculated overall compositions are used for the next stage of test (at the same temperature). This is test procedure can examine the compositional effects on the K-values.

In SWID test (SWID-1 or SWID-2), after each stage of equilibrium, the overhead samples including hydrocarbon and water vapors are withdrawn from the vapor phase and are condensed. The hydrocarbons are separated from the water and their volumes are measured. The HC sample is collected for chromatography analysis.

3.2 Thermodynamic Analysis

To describe analytically dry-, steam-, and steam-propane distillation processes, thermodynamic description of the hydrocarbon synthetic mixture can be made assuming thermodynamic liquid-vapor equilibrium exists during the distillation process. [37,38,39,40].

Figure 3.1 shows a sketch for the distillation process. Hydrocarbon sample is placed in a cell and the system, cell with hydrocarbon, is kept at constant pressure and temperature for a period of time at each temperature cut.[41,42,] The system is considered during each temperature cut to approximate thermodynamic equilibrium for each type of distillation: dry-, steam-, and steam-propane distillation. Two-phase flash calculation can be stated as follows. Given a number of initial moles *F*, with a mole fraction of components z_i, $i = 1, 2, 3, \ldots, n$ find the number of moles in the gas and liquid phases, *V* and *L*, keeping pressure and temperature constants during the distillation process.

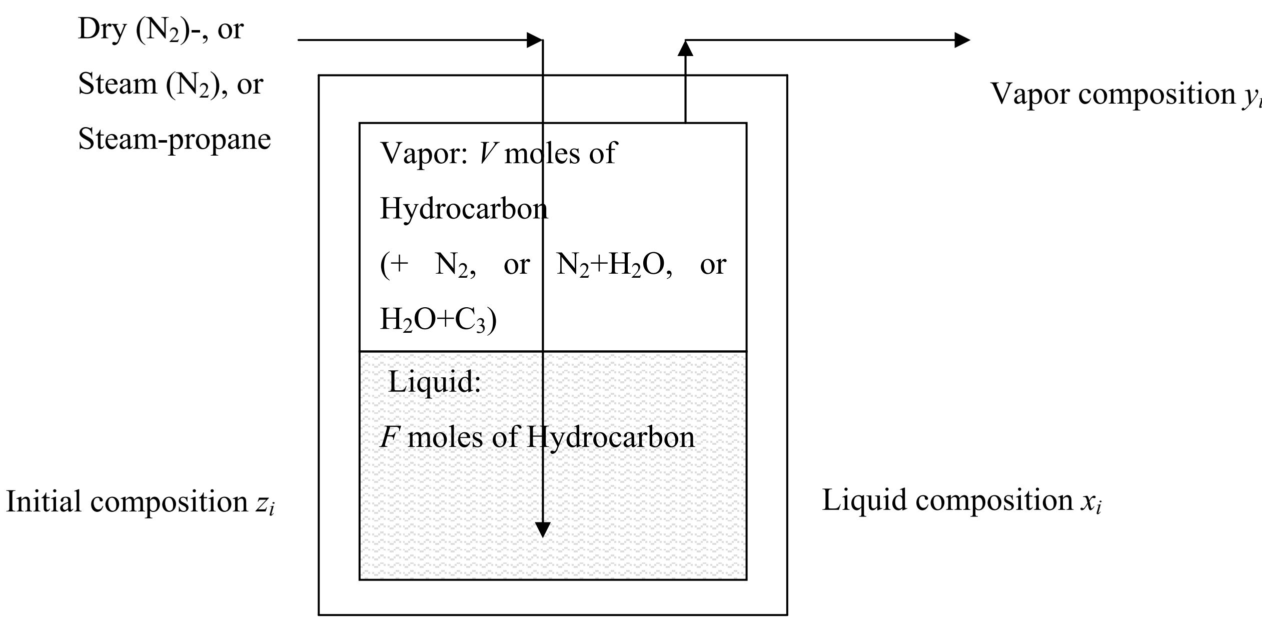

Figure 3.1: Schematic diagram of distillation at constant *T* and *P*.

Assuming equilibrium [43,44,45] we can describe distillation at each temperature cut as a two-phase flash separation process.

$$Fz_i = x_i L + y_i V \quad i = 1, 2, \ldots, n \tag{3.1}$$

The mole fraction constraints assure that the total sum of mole fractions in a given phase is equal to unity

$$\sum_i^n x_i = 1 \tag{3.2}$$

$$\sum_i^n y_i = 1 \tag{3.3}$$

In the **Eq. 3.1** there are 2 unknowns in x_i and y_i and two unknowns in V and L. A successive substitution technique permit searches only an unknown variable, the fraction of vapor V/F. The equilibrium ratio K_i is defined as

$$K_i = \frac{y_i}{x_i}, \quad i = 1,2,\ldots, n \tag{3.4}$$

Combining the **Eq. (3.4)** and **(3.1)** we have,

$$Lx_i + VK_i x_i = Fz_i, \quad i = 1,2,\ldots, n \tag{3.5}$$

Now,

$$L = F - V \tag{3.6}$$

Combining the **Eq. (3.5)** and **(3.6)** and solving for x_i we have,

$$x_i = \frac{z_i}{1 + (K_i - 1)(V/F)} \quad i = 1,2,\ldots, n \tag{3.7}$$

Similarly, for y_i we have,

$$y_i = \frac{K_i z_i}{1 + (K_i - 1)(V/F)} \quad i = 1,2,\ldots, n \tag{3.8}$$

Let define $\beta = V/f$, the mole fraction vaporized. Combining **Eq. (3.7)** and (**3.8**), the flash condition is as follows.

$$f(\beta) = -1 + \sum_i^n x_i = -1 + \sum_i^n \frac{z_i}{1 + \beta(K_i - 1)} = 0 \tag{3.9}$$

and the corresponding Newton-Raphson algorithm is

$$\beta^{k+1} = \beta^k + \frac{-1 + \sum_{1}^{n} \frac{z_i}{1+\beta(K_i - 1)}}{\sum_{i}^{n} \frac{(K_i - 1)z_i}{[1+\beta(K_i - 1]^2}} \tag{3.10}$$

where k is the index of iteration.

An objective function that can often lead to more rapid convergence is that of Rachford—Rice that uses the following expression [46,47, 48].

$$f(\beta) = \sum_{1}^{n} y_i - \sum_{1}^{n} x_i = 0 \tag{3.11}$$

Then the flash calculation using Rachford-Rice is given by

$$f(\beta) = \sum_{i}^{n} \frac{(K_i - 1)z_i}{1+\beta(K_i - 1)} = 0 \tag{3.12}$$

and the Newton-Raphson algorithm is given by

$$\beta^{k+1} = \beta^k + \frac{\sum_{1}^{n} \frac{(K_i - 1)z_i}{1+\beta(K_i - 1)}}{\sum_{1}^{n} \left[\frac{K_i - 1}{1+\beta(K_i - 1)}\right]^2 z_i} \tag{3.13}$$

On the other hand, as we know the equations that define the two-phase flash are the equality of chemical potentials. The chemical potential, G, of a component of a mixture is defined as

$$dG_i = RTd \ln f_i \tag{3.14}$$

with a property called fugacity f_i. The reference value of fugacity in this equation is considered as

$$\lim_{P \to 0} f_i = y_i P = P_i \tag{3.15}$$

The meaning is that as pressure approaches to zero the fluid approaches ideal behavior and the fugacity of a component approaches the partial pressure of that component. A useful term is fugacity coefficient for each component in a mixture which is defined as the ratio of fugacity to partial pressure. That is,

$$\phi_i = \frac{f_i}{y_i P} \tag{3.16}$$

Fugacity coefficient for each component in a mixture can be defined as

$$\ln\phi_i = \frac{1}{RT}\int_{\infty}^{V}\left(\frac{RT}{V} - (\frac{\delta P}{\delta n_i})_{T,V,n_i}\right)dV - \ln z \tag{3.17}$$

where z is *z*-factor. This fugacity coefficient can be evaluated using an Equation of State (EOS). One the most used widely EOS equations in petroleum engineering is the Peng-Robinson EOS.

Peng-Robinson[44] EOS is as follows.

$$\left[P + \frac{RT}{V_M - b} - \frac{a_T}{V_M(V_M + b)(b(V_M - b)}\right](V_M - b) = RT \tag{3.18}$$

This EOS arranged into cubic form is expressed as

$$V_M{}^3 - (\frac{RT}{P} - b)V_M{}^2 + (\frac{a_T}{P} - \frac{2bRT}{P} - 3b^2)V_M - b(\frac{a_T}{P} - \frac{bRT}{P} - b^2) = 0 \tag{3.19}$$

with

$$b = 0.07780\frac{RT_c}{P_c} \tag{3.20}$$

$$a_c = 0.45724\frac{R^2T_c{}^2}{P_c} \tag{3.21}$$

The term b is a constant, and the term a_T varies with temperature; a_c is its values at the critical temperature. The term a_T resides in α, that is determined as

$$a_T = a_c\alpha \tag{3.22}$$

where α is defined as

$$\alpha = \left[1 + m(1 - T_r{}^{0.5})\right]^2 \tag{3.23}$$

with m given by

$$m = 0.3796 + 1.485\omega - 0.1644\omega^2 + 0.01667\omega^3 \tag{3.24}$$

where acentric factor ω is a constant. The last correlation was expanded for ω in the range of $0.1 < \omega < 2.0$. Substitution of

$$V_M = zRT / P \tag{3.25}$$

into the Peng-Robinson EOS gives

$$z^3 - (1-B)z^2 + (A - 2B - 3B^2)z - (AB - B^2 - B^3) = 0 \tag{3.26}$$

where

$$A = \frac{a_T P}{R^2 T^2} \tag{3.27}$$

and

$$B = \frac{bP}{RT} \tag{3.28}$$

which is a cubic equation with real coefficients. Thus, three values of z-factor are the roots of this cubic equation. These three roots are all real when pressure and temperature are on the vapor pressure line, which is when liquid and gas are present. One real root and two complex roots exist when temperature is above the critical temperature. If there is only one root, temperature is above the critical temperature, If there are three real roots, the largest is the z-factor of the equilibrium gas and the smallest is the z-factor of the equilibrium liquid. The cubic equation can be used to complete the integration of the EOS to evaluate the fugacity coefficient, resulting in the following.

$$\ln(\frac{f_g}{P}) = z_g - 1 - \ln(z_g - B) - \frac{A}{2^{1.5} B} \ln\left[\frac{z_g + (2^{0.5} + 1)B}{z_g - (2^{0.5} - 1)B}\right] \tag{3.29}$$

and

$$\ln(\frac{f_L}{P}) = z_L - 1 - \ln(z_L - B) - \frac{A}{2^{1.5} B} \ln\left[\frac{z_L + (2^{0.5} + 1)B}{z_L - (2^{0.5} - 1)B}\right] \tag{3.30}$$

Equations **(3.29)** and **(3.30)** are applied twice: once with the liquid z-factor and the other with the gas z-factor to calculate the fugacity of the liquid and the fugacity of the gas respectively.

When working with mixtures the same expressions apply except that $a\alpha$ and b are evaluated for a mixture using a set of mixing rules. In our case, we used the most common mixing rule, the linear mixing rule for b. That is,

$$b = \sum_i y_i b_i \tag{3.31}$$

and

$$a_T = \sum_i \sum_j y_i y_j (a_{T_i} a_{T_j})^{0.5} (1 - \delta_{ij}), \tag{3.32}$$

where subscripts *i,j* refer to components, and also

$$\delta_{ii} = \delta_{jj} = 0 \tag{3.33}$$

and

$$\delta_{ij} = \delta_{ji} \tag{3.34}$$

Some values of δ_{ij} are reported in literature[40,] and values of the coefficients for the individual components are calculated as

$$b_j = 0.07780 \frac{RT_{cj}}{P_{cj}} \tag{3.35}$$

and

$$a_{Tj} = a_c a_j \tag{3.36}$$

where

$$a_{c_j} = 0.45724 \frac{R^2 T_{cj}^{\ 2}}{P_{cj}} \tag{3.37}$$

and

$$\alpha_j = \left[1 + (0.3796 + 1.485\omega_j - 0.1644\omega_j^2 + 0.01667\omega^3)(1 - T_{rj}^{\ 0.5})\right]^2 \tag{3.38}$$

As before, Peng-Robinson EOS can be written as

$$z^3 - (1-B)z^2 + (A - 2B - 3B^2)z - (AB - B^2 - B^3) = 0 \tag{3.39}$$

where

$$A = \frac{a_T P}{R^2 T^2} \tag{3.40}$$

and

$$B = \frac{bP}{RT} \tag{3.41}$$

The three roots are all real when pressure and temperature are such that the mixture is two phase. There will be only one root and two complex roots when the mixture is single phase. When the roots are obtained, the lowest root is the *z*-factor of the liquid, and the highest root is the *z*-factor of the gas, and the middle root is discarded[49].

3.3 Analytical Models

Northrop and Venkatesan (1993)[50] Model: They considered the batch steam distillation at total pressure P_t of volatile component a, having vapor pressure P_a, in solution with nonvolatile component b. Assuming that Raoult's law is applicable, it can be shown that (Winkle, 1967) [51]

$$dN_a = -Ex_a P_a dN_s / \left(P_t - Ex_a P_a\right) \tag{3.42}$$

dN_a is the incremental moles of component a distilled, dN_s is the incremental moles of steam added, X_a is the mole fraction of a in the liquid phase, and E is the vaporization efficiency, which accounts for mass-transfer resistance in the process. Crude oils typically contain thousands of compounds, so that individually accounting for each one is not practical. Thus, n pseudocomponents are defined to represent different boiling fractions of the crude oil. Assuming each psuedocomponent j is independent of the others, **Eq. 3.42** becomes

$$dN_j = -Ex_j P_j (T) dN_s / (P_t - \sum_{k=1}^{n} Ex_k P_k) \text{ ---} \tag{3.43}$$

where N_j is the moles of component J distilled. The dependence of P_j on temperature T has been made explicit. In a heavy oil system, the sum of partial pressures $\sum_{k=1}^{n} Ex_k P_k (T)$ of the pseudocomponents will generally be much smaller than that of the total system pressure P_t. Also, $x_j \approx N_J / N_{oi}$, where N_{oi} is the initial number of moles of oil. These assumptions greatly simplify the analysis

$$dN_j = -\left(EN_j \frac{P_j(T)}{P_t N_{oi}} \right) dN_s \tag{3.44}$$

Integrating **Eq. 3.43** using boundary conditions of $N_j = N_{jo}$ at $N_s = 0$, and $N_s = N_{sf}$, we obtain

$$N_{jf} \big/ N_{jo} = \exp\left(-EP_j(T) \frac{N_{sf}}{P_t N_{oi}} \right) \tag{3.45}$$

The total yield of component j as distillate is

$$N_{jo} - N_{jf} = N_{jo}\left(1 - \exp(-EP_j(T) \frac{N_{sf}}{P_t N_{oi}} \right) \tag{3.46}$$

Distillate yields are usually expressed as function of the total volume of steam (cold water equivalent), V_w and the initial volume of steam (cold water equivalent), V_w and the initial volume of oil, V_{oi}. Thus, N_{sf} can be replaced by $(V_{oi}\rho_o/M_o)$, where ρ denotes the density of the appropriate phase and M_o is the average molecular weight of the oil.

Eq. 3.46 applies to a single pseudocomponent. To account for all distillable components, a summation must be performed.

$$Y = \sum_{j=1}^{n} N_{jo}\left(1 - \exp\left[-EP_j(T) \frac{N_{sf}}{P_t N_{oi}} \right] \right) \text{-------} \tag{3.47}$$

In the limit of small $N_{jo,}$ the summation can be converted to an integral, if $P_j(T)$ is defined as continuous function of N_{jo}.

Van Winkle Model (1967)[51] : This model is an analytical expression for estimating the quantity of steam required to distill a given quantity of steam required to distill a desired quantity of volatile material using Raoult's and Daltons Laws. For a volatile-nonvolatile to pseudocomponent system, the final expression relating the amount of volatile component A distilled (a) to the amount of steam injected (s) is

$$\frac{s}{a_o} = \frac{P_t}{EP_a\left(Y_a - (b_o / a_o)\ln(1 - Y_a\right)} - Y_a \tag{3.48}$$

where $Y_a = (a_o - a)/a_o$. In **Eq. 3.48**, *E* is the distillation efficiency factor (which reflects deviation from equilibrium conditions), is the only adjustable parameter. A value of unity for *E* indicates complete equilibrium between the steam and volatile component. Note that this expression gives steam volume explicitly for a given yield, rather than yield for a given steam volume.

Chevron STMD5 Model : Hsueh et al. (1982)[39] developed a number simulator called STMD5 to calculate the steam distillation yield of crude oils. The six step algorithm is based on the Peng-Robinson equation of state uses a flash calculation to compute yield at each time step. This method solution is reasonable, although rather complicated. In my research, I have used the ASPEN Plus ® process simulator which uses this method.

Additional to the above work, Wu and Elder (1983)[20] developed correlation of crude oil steam distillation yields with basic crude oil properties for experiments reported by Wu (1980).[21]

CHAPTER IV

EXPERIMENTAL APPARATUS AND PROCEDURE

4.1 Experimental Apparatus

The original distillation apparatus was set up by Ramirez (2004) [7]. In this study, some modifications were made to improve the existing apparatus. A schematic diagram of the experimental apparatus used in the study is shown in **Fig. 4.1**. The measurement points for temperature and pressure are also indicated in **Fig. 4.1. Figures 4.2 – 4.3** show main components of the apparatus. The experimental set-up is comprised of five main components fluid injection system, distillation cell, fluid production system, gas composition measurement system, and data recording system

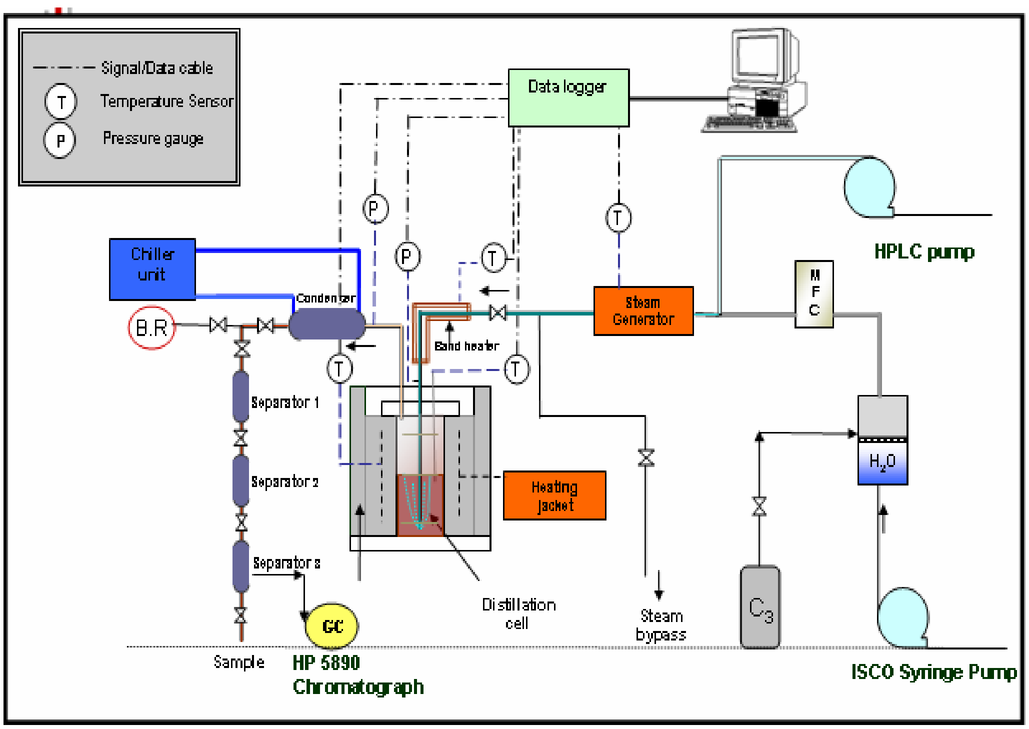

Figure 4.1: Schematic diagram of experimental apparatus.

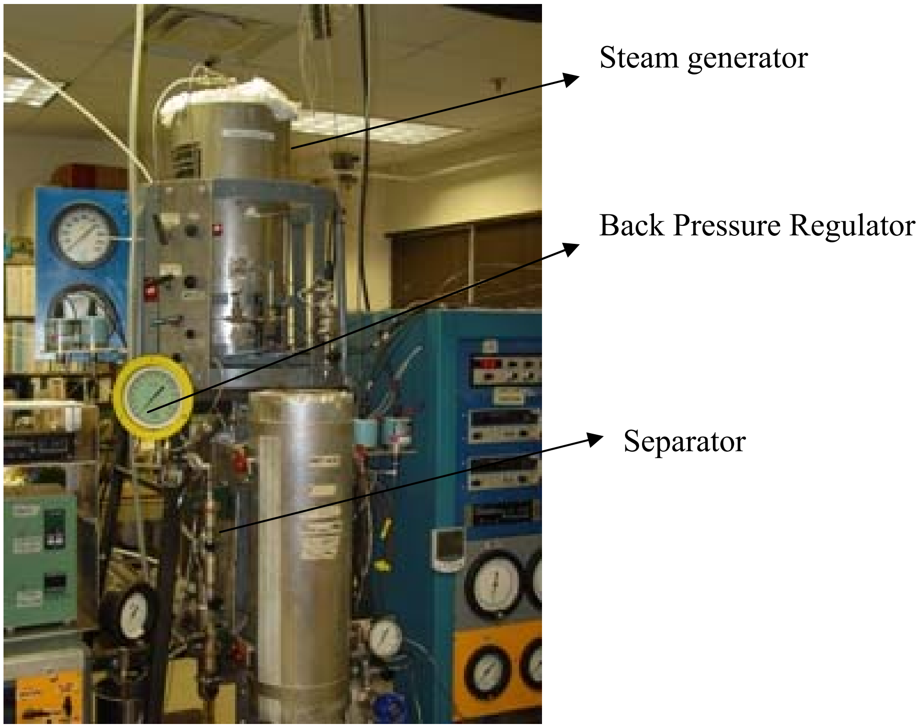

Figure 4.2: Front view of experimental setup.

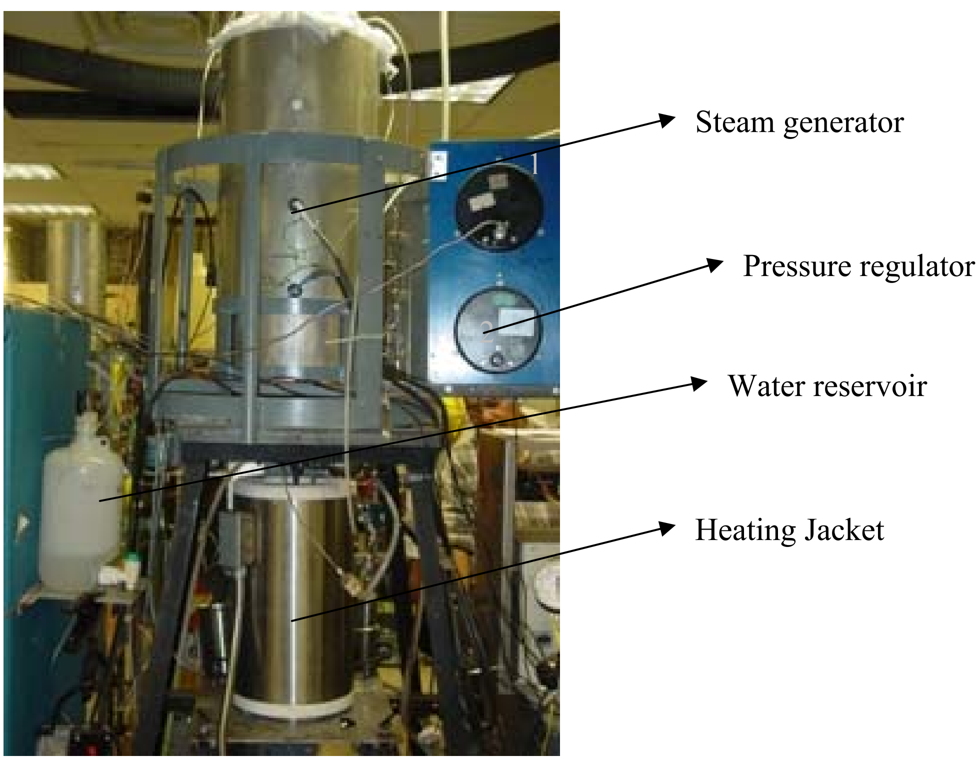

Figure 4.3: Rear view of experimental setup.

4.1.1 Fluid Injection System

Fluid injection system consists of three parts: nitrogen injection, steam injection, and propane injection.

(i) Nitrogen injection

Nitrogen is kept under pressure in a gas tank. A backpressure valve controls the gas injection pressure and a gas mass flow controller regulates the nitrogen gas injection rate in the case of dry- and steam-distillation at 0.025 g/min. The nitrogen is mixed with steam in the case of steam distillation at the steam generator inlet.

(ii) Steam injection

A High Performance Liquid Chromatography (HPLC) pump feeds water to the steam generator at a constant rate of 0.5 g/min. The pump is maintained at back pressure of 900 psig to avoid pulse flow effect. The water is mixed with nitrogen in the case of steam distillation, and with propane in the case of steam-propane distillation before the steam generator in both cases. Mixing takes place after the back pressure regulator.

(iii) Propane injection

Propane injection was specially designed for this experimental setup as shown in **Fig. 4.4**. This design allowed the flow of liquid propane at any desired pressure 0-1000 psig. It consists of water/gas collector, piston tube cylinder and syringe pump. Constant N_2 gas pressure is applied over water level on collector unit to pump propane. Flow of propane is regulated using mass flow controller. Mass flow controller is calibrated using water with ISCO 500D syringe pump.

4.1.2 Distillation Cell

The distillation cell (**Fig. 4.5**) is a stainless steel cylinder with an internal diameter of 5.4 cm, wall thickness of 1 cm and a height of 17.5 cm. The ends of the cell are sealed off by end caps that provide metal-to-metal seal. The top end cap is connected to a 1/8 in. line through which the distilled.

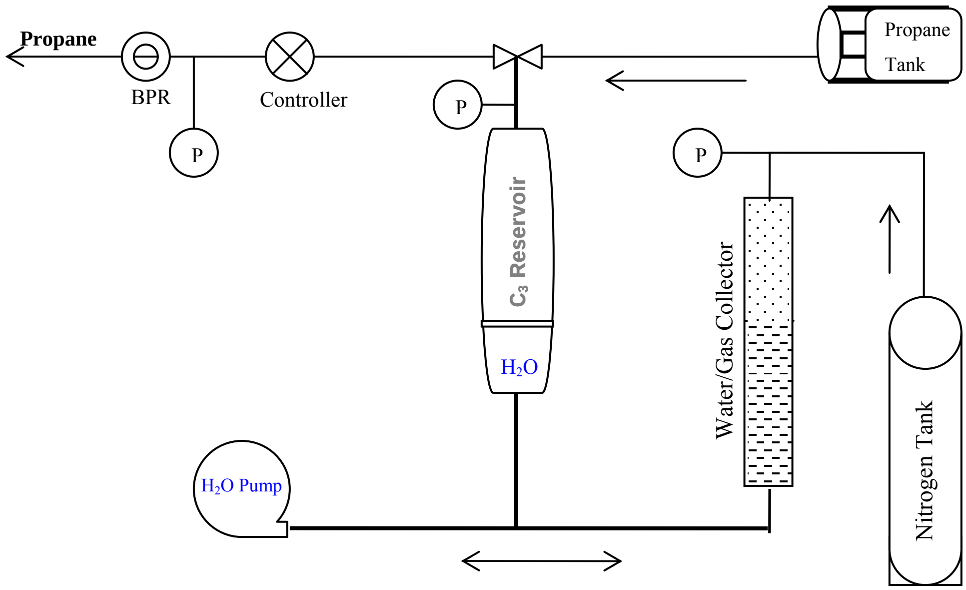

Figure 4.4: Propane injection system.

A 1/8 inch injection line (connected at the top end cap) goes to the bottom of the cell, through which nitrogen, steam, or steam-propane is injected. A thermocouple (Type K) is inserted through the top end cap into the cell (the tip at the cell mid-height) to measure the temperature e inside the cell. Three perforated plates are attached to the injection line and help diffusion of the injected gas **(Fig. 4.6).** The distillation cell is placed in a heating jacket (**Fig. 4.7).** The temperature of the heating jacket is controlled by a temperature controller. A band heater is placed around the injection line and is connected to a temperature controller. This band heater is used to heat the injection tube to keep the steam injected at the required superheated conditions. Glass wool is used to cover the top of the cell to minimize heat losses.

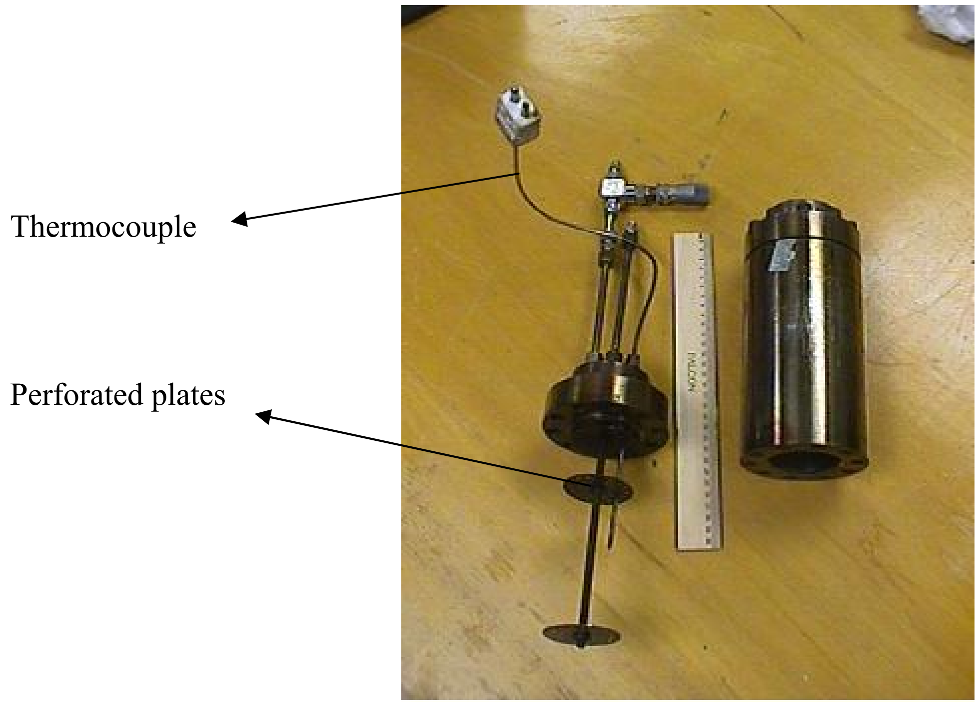

Figure 4.5: Distillation cell with plates.

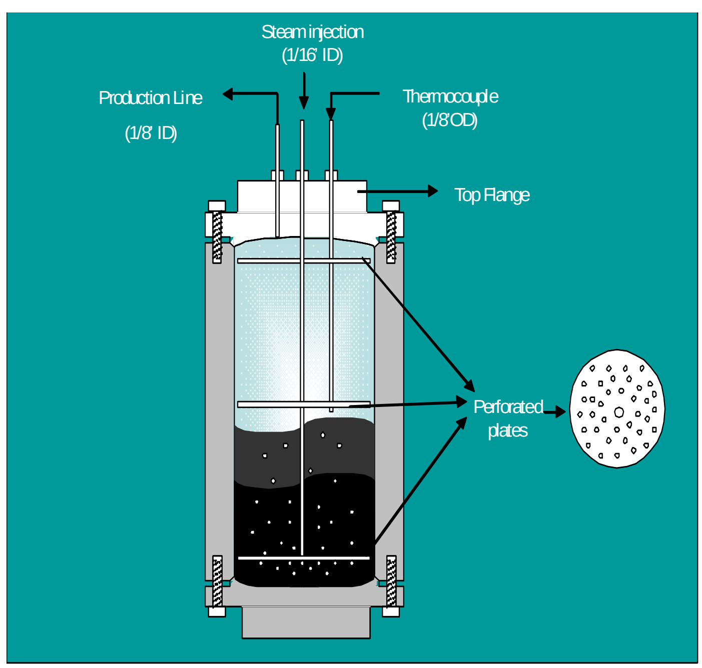

Figure4.6: Cross-section of distillation cell.

Figure 4.7: Heating jacket.

Figure 4.8: Three stage separator.

4.1.3 Fluid Production System

The fluids leaving the cell are produced through a line which is connected to a set of separators (**Fig. 4.8**) and a condenser. A backpressure regulator maintains the cell outlet pressure at a constant predetermined level during the experiment. A chiller unit provides cold water for the condenser kept at 10^{o}C during the distillation process. There are three separators in the system which permits collection of the distillate samples at low pressure. The distillate samples are collected in polypropylene centrifuge tube after the third separator.

4.1.4 Gas Chromatograph System

The distillate collected in the polypropylene tubes are kept at low temperature. Using a 1 µl syringe a distillate sample is injected into a gas chromatograph **(Fig. 4.9)** to determine the compound and composition of the distillate.

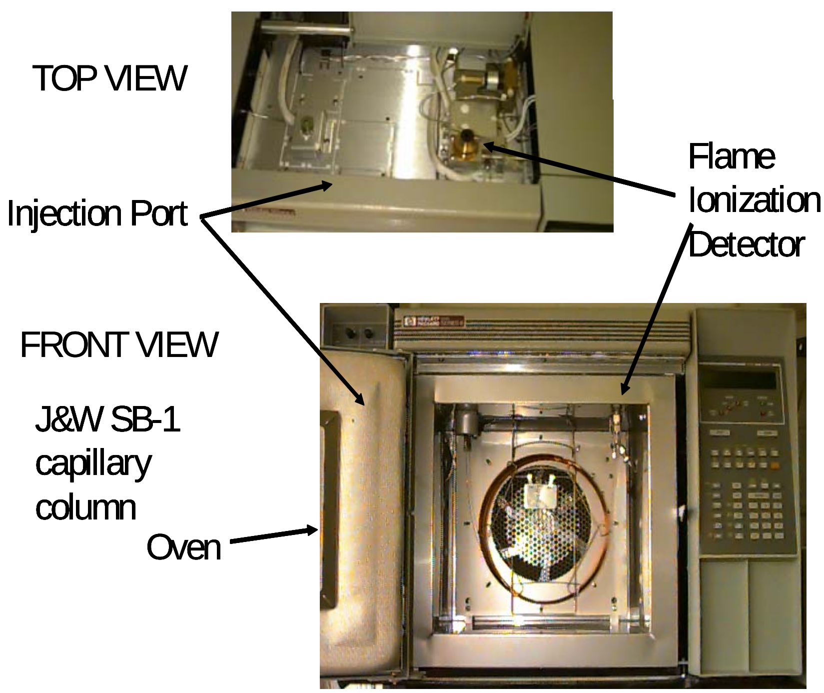

Figure 4.9: Key components of gas chromatograph – HP 5890 Series II.

4.1.5 Data Measurement and Recording System

A data logger and a personal computer are used to record the following parameters: time, cell temperature, jacket temperature, steam temperature, band heater temperature, injection pressure, outlet pressure, and propane or nitrogen injection rate. The parameters are recorded at 30-second intervals. **Table 4.1** shows list of components used in this experiments.

Summary of the main components of the apparatus follows.

1. HPLC pump: A High Performance Liquid Chromatograph pump supplies water to the steam generator at a very accurate rate.
2. Steam generator: An electric powered steam generator of 1000 watts maximum power and rated at a maximum pressure of 2000 psi and a maximum temperature of 1200^{o}F provides the steam necessary for the experiments.
3. Distillation cell: The stainless steel cell with internal diameter 5.4 cm and a long of 17.5 cm (volume approximated of 400.79 cm^3)
4. Heating jacket: The heating jacket consists of a 43.18 cm long and 27.94 cm OD of stainless steel cylinder.
5. Temperature controller: A dual-circuit temperature controller is used to maintain constant temperature of the steam generator and the other controls the heating jacket temperature.
6. Three-stage separation and collection system: It is used to reduce the pressure to enable sampling. The distilled is collected at a polypropylene tube fixed at the end of the third separator.
7. Mass flow controller: Regulates the mass rate of nitrogen and propane injected into the line of the steam generator. This mass flow controller regulates in the case of propane liquid and vapor propane.
8. Gas chromatographs: The gas chromatographs analyze the composition of the vapor samples collected at the end of the third separator.
9. Data logger/recording system: Measures and records pressure, temperature, and injection gas rates data for every 30 seconds.

Table 4.1: List of components, materials and equipments used for the experiments.

Water reservoir	4-liter plastic container
HPLC pump	Beckman. Model 100A
Steam generator	Custom-made by Texaco. Max. pressure: 2000 psig. Max. temperature: 1200 ºF
Distillation cell	Stainless steel tube. Long: 17.5 cm. I.D.: 5.4 cm.
Temperature controller	Digi-Sense. Model 2186-10A, 20 Amp peak
Temperature Controller	Omega EN9000A
Temperature Controller	Eurotherm 808
Mass Flow Controller	Brooks. Model 5850E series. Max. flow 1000 cm^3/min
GC-FID assembly	(1) Hewlett Packard 5890 Series II (2) J & W Scientific -DB-1, 0.53µm, 15 m. (3) HP 3396A Integrator
Data logger	Hewlett Packard data acquisition unit. Model 3497A with 44422A T-couple acquisition assembly.
Back-pressure regulator	Tescom Corporation. Max. pressure 500 psig
Chiller unit	Hasskriss Co. Model R100
Pressure transducer	Validyne. model DP15-TL. Max. pressure: 320 psig.
Tubing	¼-in., 1/8-in. and 1/16-in. stainless steel tubing with Swagelock and Autoclave connections.
Control valves	Autoclave Engineers ¼-in. Withey ¼-in., 1/8-in.
Thermocouples	Omega JMQSS-020. Type J. Sheath diameter .020-in.
Gauges	HEISE, CM-105620 and CM-105618, Bourdon tube 403 ST-ST. Max. pressure 500 psig.
Electronic balance	METTLER PM 4600 Delta Range. Capacity 10.45 kg.
Balance	OHAUS Heavy duty. Capacity 20 kg.
Thermometer	Kessler. ASTM 40C

Table 4.1 Continued

Hydrocarbon/ Crude Oil	Dewatered San Ardo Field Crude Oil
Synthetic hydrocarbon	n-Pentane, n-Hexane, n-Heptane, n-Octane, n-Nonane, n-Decane, and n-Pentadecane at 99.99% pure.
Paint thinner	Commercial paint thinner
Nitrogen tank	Botco, Nitrogen compressed, 1500 psig.
Conical sample bottles	Nalgene. Polipropylene Centrifuge tube. Size 50 ml.
Temperature bath	GCA/Precision Scientific

4.2 Experimental Procedure

This section describes the experimental method used for carrying out distillation experiments on San Ardo crude oil. Basically, three different types of distillation were carried out, (1) at atm conditions, (2) at field conditions (3) 15^{o}C above steam saturation conditions. A step wise but generic experimental procedure is described in the following sub-section.

4.2.1 Cell Preparation

First, San Ardo oil is dewatered and stored in air tight container. All the glass material used is cleaned with iso-propanol and dried with nitrogen. The apparatus including the lines are thoroughly cleaned to prevent any contamination in the distillation process.

Pressure transducers and mass flow controller are calibrated. This will be done every time before the experiment for each type of distillation. Pressure transducer is calibrated using a dead weight tester. Mass flow controller is calibrated for nitrogen and propane. The HPLC pump for water is calibrated using a measuring cylinder and stop watch for 0.5 ml/min rate.

The weighed San Ardo crude oil is poured into the cell filling up approximately half cell volume (201.0 ml). Once the cell is properly closed, it is pressure tested to 1000 psig with nitrogen for leaks. After the pressure test a thermocouple is attached externally to the body of the cell with aluminum tape at approximately third of depth of the cell.

The set up of the whole assembly consists of placing the cell inside the heating jacket and connecting all the lines. The valve connecting the steam generator to the distillation cell is closed. At this point the apparatus is pressure tested again with nitrogen until 1000 psig. After this pressure test the apparatus is ready for the experiment.

4.2.2 Distillation Procedure

The following steps were followed for collecting each distillation yields

1. The steam generator is conditioned to the starting temperature. The pressure in the steam generator is increased by increasing pressure at back pressure regulator. Water is injected using HPLC pump at 0.5 ml/min rate. If propane is used , the intial pressure of propane cylinder must be kept at a higher pressure than the steam generator (approximately 100 psig).
2. In the case of dry distillation nitrogen is injected to the cell through the steam generator line at a 5:100 mass ratio of nitrogen to water. The rate of water injected in steam distillation is 0.5 g/min. In the case of steam-propane distillation, once the pressure and temperature conditions are stabilized (observing the values graphically recorded in the monitor of the recording system), the propane is injected into the steam generator (if the case includes propane injection). Subsequently the valve connecting the steam generator to the distillation cell is open. The time at which injection starts is recorded.
3. The distillate is collected for the 45-60 min of production in interval of 2 min. Distillate is collected in centrifuge bottles until the there is no production of hydrocarbon. Cell inlet and outlet pressures are recorded. Distillation yield consist of water and hydrocarbon are measured and material balance calculations are performed at the end of experiment. The liquid samples are kept in a freezer after the readings of volume and weight to avoid evaporating some fractions.
4. When the limiting temperature of 300ºC is reached the valve connecting the steam generator and the cell is closed, and all the equipment are turned off.

Three types of distillation were carried out during this research

1. Stagewise Continuous Isochronic Isobaric Distillation -

In this case, 115ºC of superheated steam is injected in cell with same temperature. Temperature of system (steam + cell) was gradually increased to 300^{o}C with 10^{o}C increment. The distillation yields at each increment are collected. The temperatures and pressures of system are presented in **Table 4.2**.

Table 4.2: Temperature cuts for each distillation.

Cut No.	Temperature ºC	Pressure psia	Pressure Psig
1	115	14.7	0.0
2	130	24.84	10.14
3	140	34.41	19.71
4	150	46.62	31.92
5	160	61.96	47.26
6	170	80.96	66.26
7	180	104.21	89.51
8	190	132.34	117.64
9	200	166.04	151.34
10	210	206.07	191.37
11	220	253.22	238.52
12	230	308.35	293.65
13	240	372.39	357.69
14	250	446.32	431.62
15	260	531.18	516.48
16	270	628.07	613.37
17	280	738.17	723.47
18	290	862.72	848.02
19	300	1003.01	988.31

These conditions were selected according to the boiling points of the component of the synthetic hydrocarbon. The conditions of distillation were selected according to the steam tables at a saturation temperature 15ºC below the temperatures mentioned in the table to assure superheated steam.

2. Ambient Condition Distillation

Hydrocarbon distillation was performed at constant pressure of 1 atm. The temperature was increased from 110^{o}C to 280^{o}C in steps of 10^{o}C. Production lines are closed after each to cut until system attains new temperature conditions.

3. Field Condition Distillation

These test were similar to ambient condition distillation except the system is at 265 psig (reservoir pressure) and first temperature cut is at 210^{o}C, which is 10^{o}C above the saturation temperature of steam.

4.2.3 Gas Chromatograph Analysis (GC-FID)

GC-FIDs are best for detecting hydrocarbons, and other easily flammable components. They are very sensitive to these components, and response tends to be linear across a wide range of concentrations. The GC-FID (Flame Ionization detector) was used to determine the composition of distillation yields. GC-FID for distillation yields are carried out at split mode but for analyzing crude oil it was carried in splitless mode.

Following were the steps followed to get best results in analyzing composition of distillation yields

1. Turn on GC and integrator.
2. Make sure that all the internal regulators are closed (carrier, hydrogen, air). This is optional, once adjusted should not be changed.
3. Make sure that all the detector valves are closed (air, hydrogen, aux gas).
4. Make sure that all the injection regulators are off (column head pressure, total flow, septum purge).
5. Set oven initial temperature (value) at 30ºC.
6. Set oven final temperature (value) at 325ºC.
7. Set initial oven time to 0 min.

8. Set final oven time to 10 min.
9. Set oven temperature ramping rate to 5ºC/min.
10. Set injection port B temperature to 340ºC.
11. Set detector B temperature to 350ºC.
12. Allow the unit, at least 30 mins to thermally stabilize. (*MUST*)
13. Open the hydrogen cylinder and set the regulator to 60/70 psi. Set the internal carrier gas regulator to 40 psi.
14. Connect the flowmeter to the inlet vent hose. Open the total flow regulator to 100 ml/min. This is the split vent flow rate.
15. Connect the flowmeter to the detector outlet. Open the column head pressure regulator to 1 ml/min. This is the carrier gas (hydrogen) rate through the column.
16. Connect the flowmeter to the septum purge hose. Open the septum purge regulator to 3 ml/min. This is the septum purge flow rate.
17. The flow rates described in steps 14, 15 and 16 are all related to each other. This means that a change in one of them will change the other two. Therefore, in order to correctly set the flows, steps 14, 15 and 16 should be repeated until all the rates are steady.
18. Connect the flowmeter in the detector outlet. You should only be measuring the carrier gas rate through the column (1 ml/min).
19. Open the hydrogen valve in the detector manifold (the rate should go down and then stabilize).
20. Set the hydrogen internal regulator so the flowrate at the detector outlet is 31 ml/min. This procedure sets the hydrogen fuel rate to 30 ml/min. The total flow rate is: carrier hydrogen (1 ml/min) + fuel hydrogen (30 ml/min) = 31 ml/min.
21. Open the air cylinder regulator to 60 psi.
22. Open the air valve in the detector manifold (the rate should go down and then stabilize).

23. Set the air internal regulator so the flowrate at the detector outlet is 461 ml/min. This procedure sets the air rate to 430 ml/min. The total flow rate is: carrier hydrogen (1 ml/min) + fuel hydrogen (30 ml/min) + air (430 ml/min) = 460 ml/min.
24. Remove the flowmeter connection from the detector outlet. Press the FID ignitor. You should hear a "pop" sound.
25. Turn on the detector by pressing: DET + B + ON. Display the detector signal by pressing SIG 1. Wait as long as necessary until the signal stabilizes.

4.2.4 Quantitative Evaluation of the Chromatogram

A chromatogram can be evaluated for quantitative analysis in one of two ways, by the measurement of either peak area or peak heights.

Peak Area Measurements

The total area count of the peak is proportional to the total mass of solute contained in the peak. The area of a peak is the integration of the mass per unit volume (concentration) of solute eluted from the column with respect to time.

Peak Height Measurement

Peak height is inversely related to the peak width. If peak height are to be used for analytical purposes, all parameters that can affect the peak width must be held constant. This means capacity factor of peak must be held constant and consequently composition of solvent must be held constant

CHAPTER V

SIMULATION OF DISTILLATION YIELDS

In this study, a numerical simulation model was developed using a commercial phase equilibrium software tool called *ASPEN Plus* ®. Equations described in previous chapters are used in this model to calculate steam distillation yield of crude oils. This model is based on the Peng-Robinson equation of state (EOS) and uses a flash calculation to compute yield at each step of distillation. This approach is based on algorithm of Hsueh et al (1982)[39] called STMD5 and originally developed to calculate steam volume for obtaining desired distillation yield. This unique modeling frame work can eventually be used for different crude oils, to study quantification of steam-additive effects on distillation yields

The calculation procedure and assumptions used are as follows:

1. The volumetric rate element of steam is pumped into the distillation cell containing a known volume of sample crude. The process is assumed continuous so as to attain equilibrium. In experimental condition, there may be less than 100% contact of vapor and liquid phase due to, for example, channeling in the equipment. So a fraction (5~10%) of steam would be considered ineffective. The remaining part of the steam is assumed to mix completely with the crude sample.
2. This mixture is flashed into vapor and liquid phases using K-values equation described in Chapter III. The densities and concentrations of each hypothetical component in liquid and vapor phases are calculated using the Peng-Robinson EOS. Since the system temperature is above the saturated steam temperature, no separate liquid water can be included in equilibrium calculations. The solubility of liquid water in oil at a given temperature and pressure is assumed to be higher than the amount of water dissolved in oil which is in equilibrium with steam in the vapor phase.
3. The volume and composition of the vapor phase is recalculated after combining the vapor from the current time-step with the bypassed steam and reflux from the previous time step.

4. Total vapor formed is assumed to be distilled yield. This is in line with experiments in which we wait till there is no incremental production of hydrocarbon yields.
5. The liquid remaining in the cell is moved to another flash unit to allow to mix with new volume else of steam. The calculation steps are repeated for the next cut (T,P).

5.1 Model Validation

The validity of the simulator and the assumption used in *ASPEN Plus* modeling framework was tested with a steam distillation of synthetic hydrocarbon. This framework is based on Raoult's and Dalton's laws (equations (1) and (2)), Van Winkle (1967) [51] who showed that for a simple mixture consisting of a_o moles of volatile component b_o moles of nonvolatile component, the moles of steam consumed, s during steam distillation can be calculated as follows.

$$\frac{s}{a_o} = \frac{P_T}{EP_a}\left[Y_a - \left(\frac{b_o}{a_o}\right)\ln(1 - Y_a)\right] - Y_a$$

where,

$$Y_a = \left(\frac{a_o - a}{a_a}\right)$$

Where P_a is the vapor pressure of volatile component A and E is the efficiency factor.

The validity of the model was tested with a multi-component crude oil undergoing a gas chromatographic analysis. These experiments were performed by Ramirez, (2004) [7]. **Figures 5.1-5.2** and **Fig. 5.3** are yield curves for dry distillation experiment carried out at 1 Atm condition. **Figures 5.4**, **5.5** and **5.6** are yield curves for steam distillation at various temperature pressure conditions for synthetic hydrocarbon. Finally, **Fig. 5.7** and **Fig. 5.8** are yield curve for steam–propane distillation of synthetic hydrocarbon. Details of these experiments are presented by Ramirez's (2004).[7]

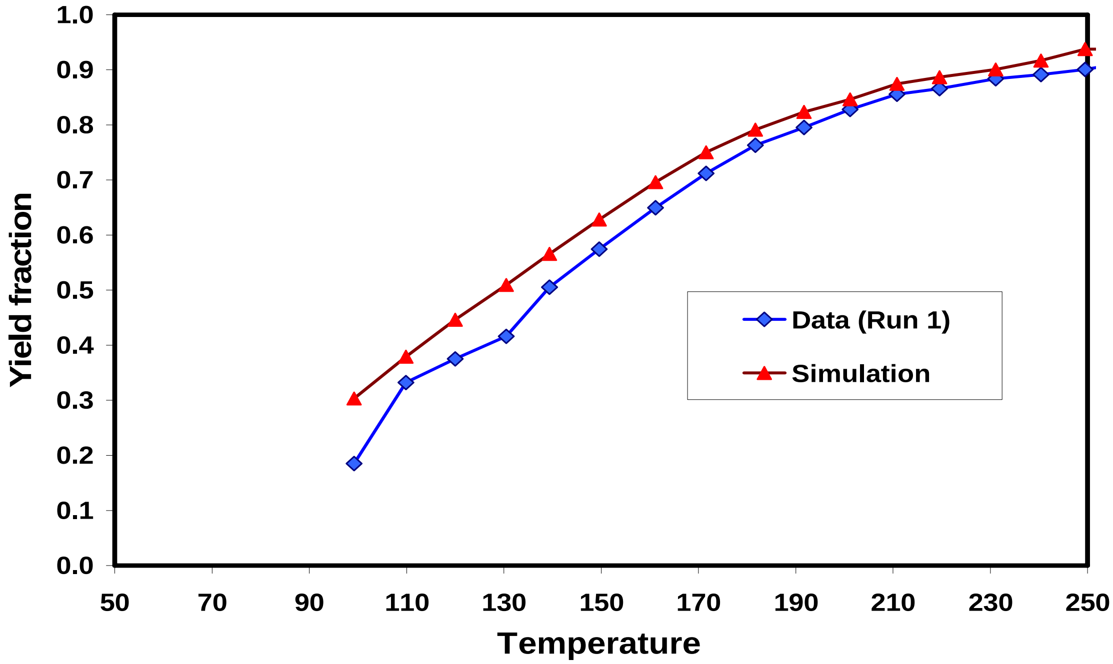

Figure 5.1: Comparison of experimental and simulation result for dry distillation of synthetic hydrocarbon (Run 1).

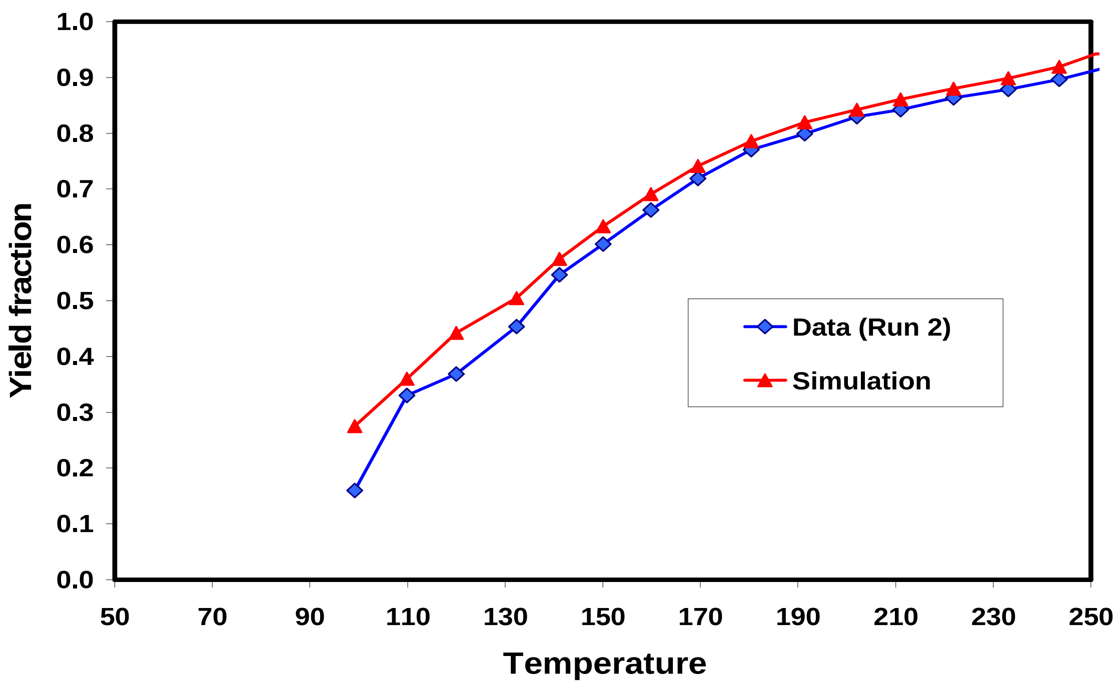

Figure 5.2: Comparison of experimental and simulation result for dry distillation of synthetic hydrocarbon (Run 2).

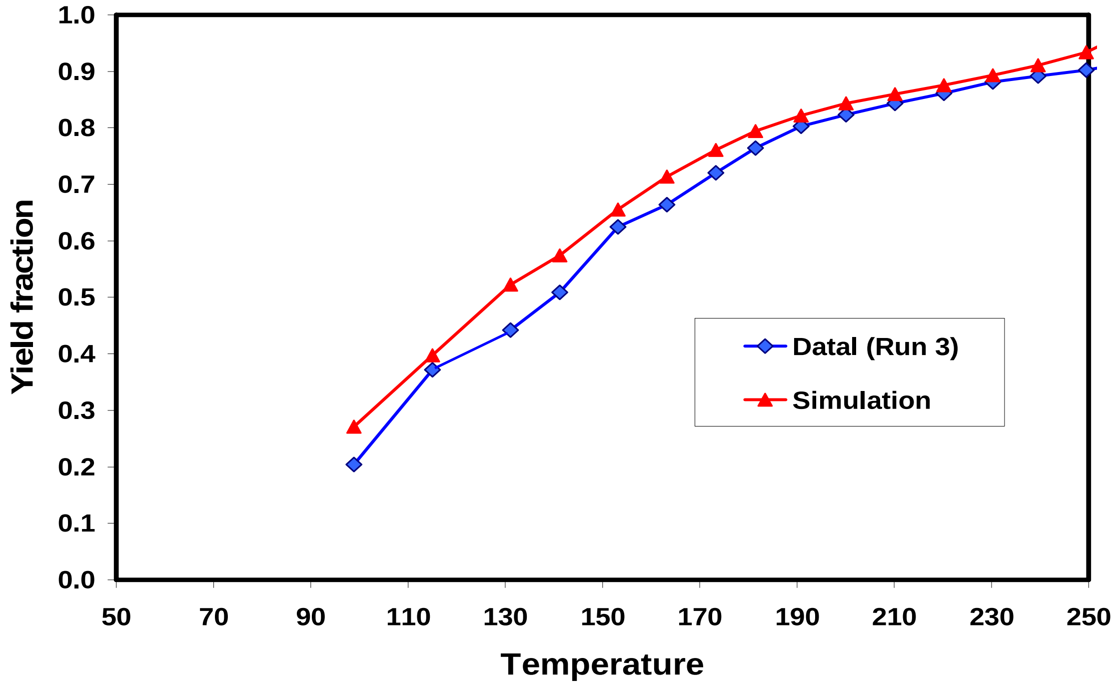

Figure 5.3: Comparison of experimental and simulation result for dry distillation of synthetic hydrocarbon (Run 3).

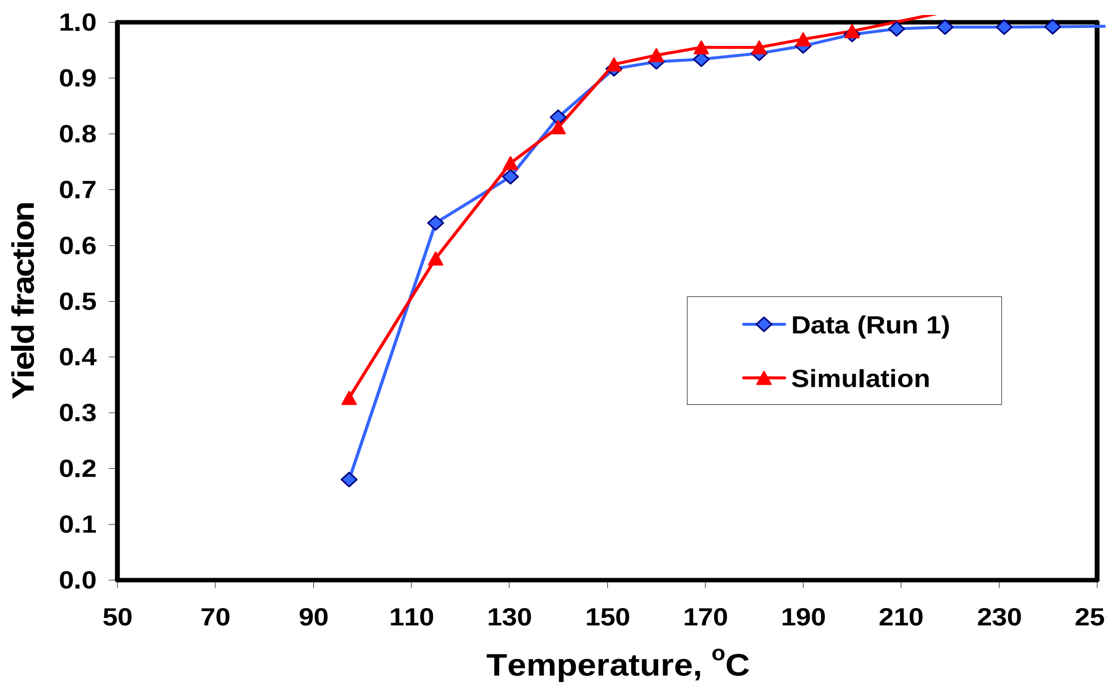

Figure 5.4: Comparison of experimental and simulation result for steam distillation of synthetic hydrocarbon (Run 1).

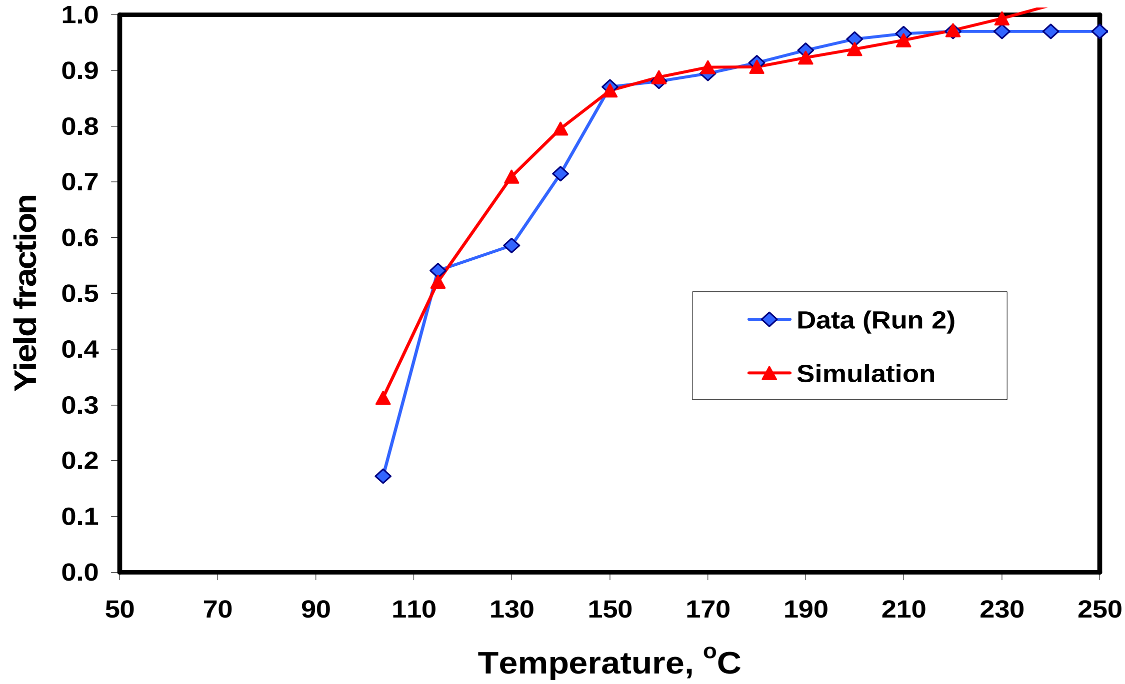

Figure 5.5: Comparison of experimental and simulation result for steam distillation of synthetic hydrocarbon (Run 2).

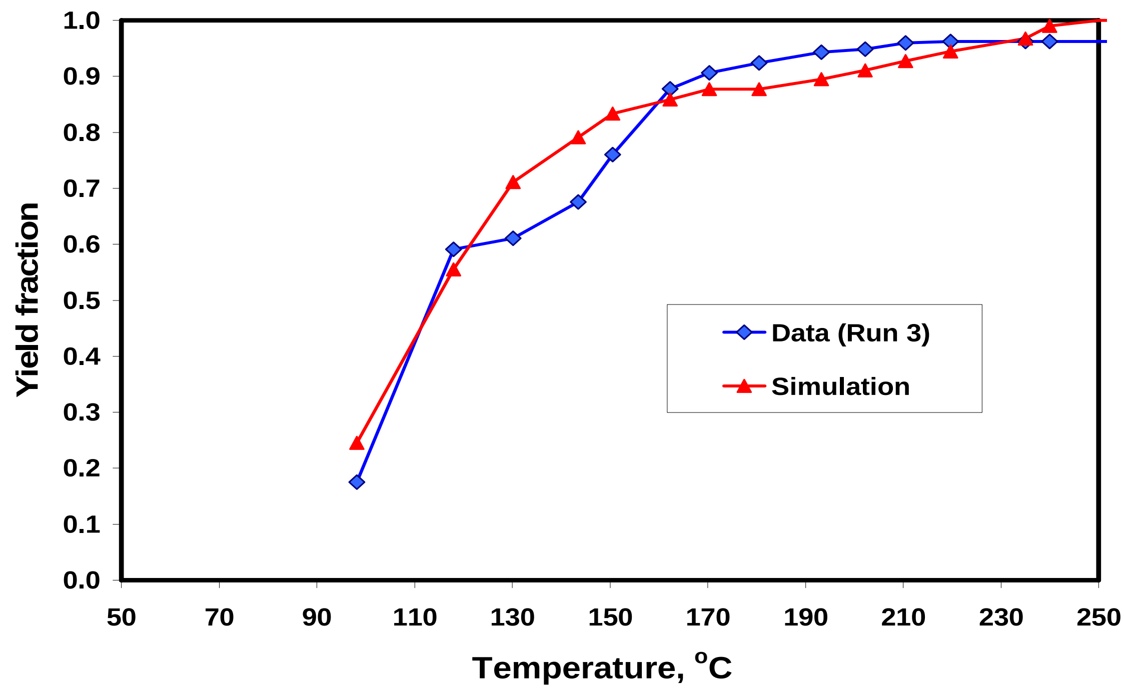

Figure 5.6: Comparison of experimental and simulation result for steam distillation of synthetic hydrocarbon (Run 3).

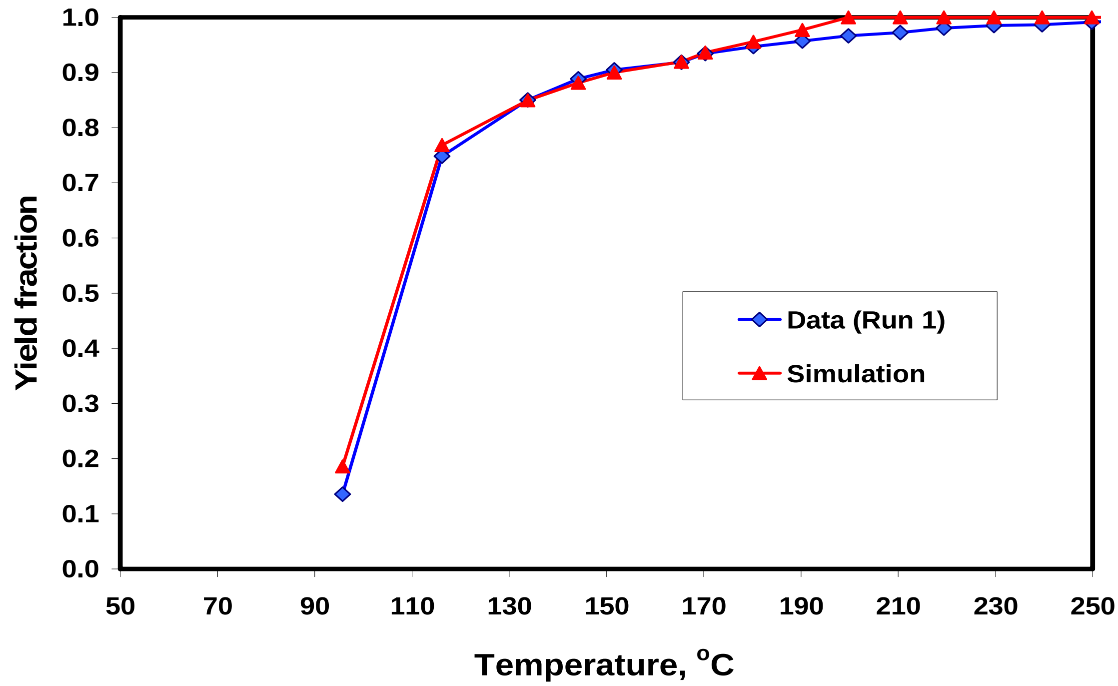

Figure 5.7: Comparison of experimental and simulation result for steam-propane distillation of synthetic hydrocarbon (Run 1).

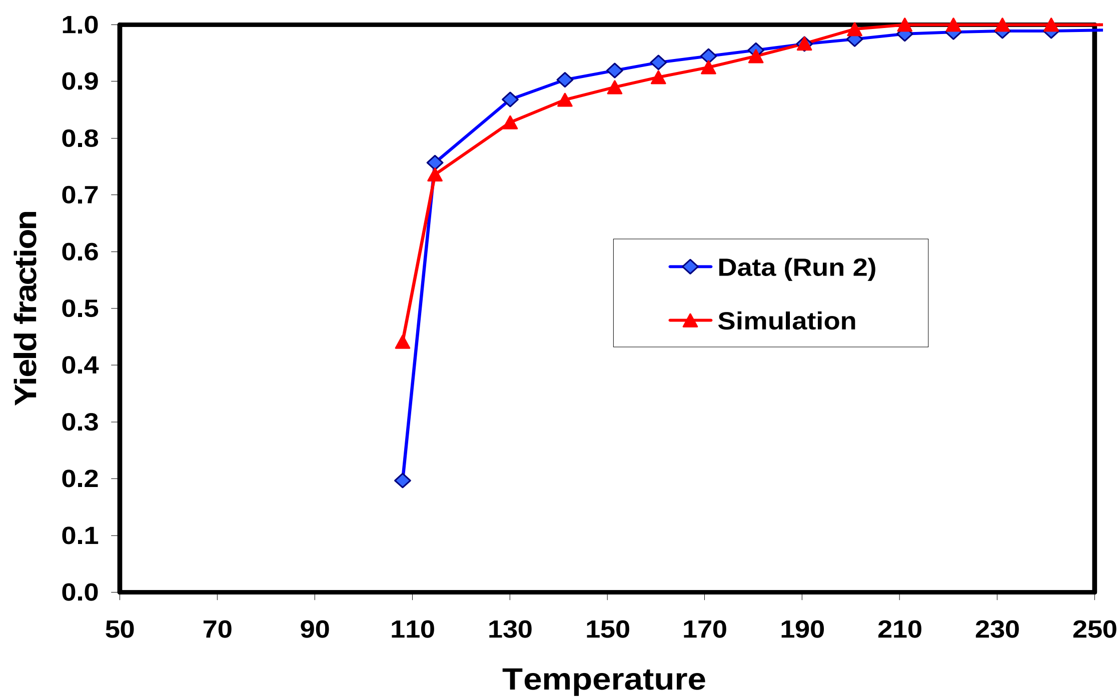

Figure 5.8: Comparison of experimental and simulation result for steam-propane distillation of synthetic hydrocarbon (Run 2).

Thus, the plots show good agreement in simulation and experimental results. Distillation efficiency of ~29% was used all the simulation runs to match experimental data. There is offset between simulation and experimental results at low temperature data. This usually occurs as experiments were not exactly carried out at constant pressure but performed at fluctuating pressures and cut simulations are carried out at constant pressures and constant temperature. Hence, where are pressures are steady the results are in good agreement.

CHAPTER VI

EXPERIMENTAL RESULTS

The phase equilibrium behavior of reservoir fluids is an important phenomenon in petroleum production, particularly in enhanced oil recovery processes. However, phase behavior for heavy oils (< 15^{o} API) under steamflood has generally been felt to be unimportant thus neglected. The practical limit of how much of a reservoir fluid can be distilled, is obtained in dynamic steam distillation experiments and with this research this can be predicted by using fluid composition. Thermodynamic properties of components of San Ardu fluid were derived using Katz and Firoozabadi data and are shown in **Appendix A**. The fluid composition of San Ardo crude oil and its chromatogram is presented in **Appendix A.** The crude shows bimodal distribution and significant biodegradation.

This chapter contains the experimental data, calculated results and simulation results modeled for each distillation type: dry, steam-, and steam-propane distillation. Each sub-section is followed by discussion about the results and there implication. Finally at the end, distillation results for steam + other additives are predicted using the calibrated simulation model.

6.1 Overview of Results

These experimental results include:

a. Temperature profiles: inside steam-generator, the cell, heating jacket, band heater around the injection line before the cell
b. Pressure profiles: cell inlet pressure, cell outlet pressure, and cell differential pressure
c. Compositional analyses of distillate by gas chromatography are shown in **Appendix C.**
d. Material balance for each distillation cut.
e. Experimental and simulated oil cumulative in weight and volume.

f. Experimental and simulated oil fraction produced at each cut.

The following parameters were kept constant for all the runs:

a. Temperature and pressure of system during each cut
b. Nitrogen rate mass injection in dry distillations of 0.025 g/min
c. Steam injection rate of 0.5 g/min
d. Propane to steam mass ratio injection of 5:100

A comparison of the two distillation process (varying T_{sat}, P_{sat} and field conditions) is shown at the end of this chapter. The data analyses and interpretations are presented individually for each run. In addition, a global comparison between the various cases is also made.

6.2 Atmospheric Condition Distillation

Distillation experiments were performed at constant 1 atmospheric condition using dry nitrogen.

6.2.1 Dry Distillation

The yields measured for the two dry distillation runs are summarized in **Table 6.1** and **Table 6.2**. Actual results for simulation and GC analysis are presented in **Appendix B** and **Appendix C** respectively. The temperature profiles of the dry distillations runs are shown in **Fig 6.1** and **Fig. 6.4**. These plots indicate the good control of temperature during the whole process. Dry distillation run no.1 showed an oil recovery of 15% until 1200 min of distillation with an experimental error of 10.25% and dry distillation run no. 2 showed an oil recovery of 14.6% with an experimental error of 8.5%. The experimental error was calculated based on a material balance of oil. The fraction oil rates plots as function of temperature for the dry distillation runs are shown in **Fig. 6.2** and **Fig. 6.4**. The oil yield plots as function of temperature for the dry distillation runs are shown in **Fig 6.3**, **Fig.6.5** .and **Fig. 6.7.** show comparison between average distillation yields for this study and the one in literature (Lolley, 1997).[52]

Table 6.1: Oil Yields at Distillation Temperatures (Dry distillation -run 1).

Cut. NO.	Temp ^{o}C	Volume of liquid , ml				Weight of liquid, gm				Fractional Recovery %
		V_{water}	V_{oil}	V_{total}	Cum_{oil}	W_{water}	V_{oil}	W_{oil}	Cum_{oil}	
1	105	0	2.00	2.00	1.50	0	0.85	1.70	1.70	0.72
2	115	0	2.00	2.00	3.50	0	0.77	1.53	3.23	1.37
3	125	0	1.50	1.50	5.00	0	0.56	0.84	4.07	1.73
4	135	0	0.50	0.50	5.50	0	1.78	0.89	4.96	2.11
5	145	0	1.00	1.00	6.50	0	0.59	0.59	5.55	2.36
6	155	0	0.00	0.00	6.50	0	0.00	0.00	5.55	2.36
7	165	0	0.75	0.75	7.25	0	0.63	0.47	6.02	2.56
8	175	0	0.75	0.75	8.00	0	0.72	0.54	6.56	2.79
9	185	0	0.75	0.75	8.75	0	0.49	0.37	6.93	2.95
10	195	0	3.50	3.50	12.25	0	0.44	1.54	8.47	3.60
11	205	0	1.00	1.00	13.25	0	0.66	0.66	9.13	3.89
12	215	0	3.00	3.00	16.25	0	0.98	2.94	12.07	5.14
13	225	0	2.00	2.00	18.25	0	0.81	1.61	13.68	5.82
14	235	0	2.00	2.00	20.25	0	1.05	2.09	15.77	6.71
15	245	0	2.00	2.00	22.25	0	0.98	1.96	17.73	7.54
16	255	0	3.50	3.50	25.75	0	1.15	4.04	21.77	9.26
17	265	0	3.95	3.95	29.70	0	0.76	3.01	24.78	10.54
18	275	0	4.25	4.25	33.95	0	0.85	3.62	28.40	12.09
19	285	0	4.00	4.00	37.95	0	0.87	3.49	31.89	13.57
20	295	0	4.04	4.04	41.99	0	0.99	4.01	35.90	15.28

*Initial weight of hydrocarbon = 235 g.

Table 6.2: Oil Yields at Distillation Temperatures (Dry distillation-run 2).

Cut. NO.	Temp ^oC	Volume of liquid , ml				Weight of liquid, gm				Fractional Recovery %
		V_{water}	V_{oil}	V_{total}	Cum_{oil}	W_{water}	V_{oil}	W_{oil}	Cum_{oil}	
1	98	0	2.00	2.00	1.50	0	1.03	2.05	2.05	0.91
2	115	0	2.00	2.00	3.50	0	1.05	2.10	4.15	1.84
3	130	0	1.50	1.50	5.00	0	0.93	1.40	5.55	2.47
4	140	0	0.50	0.50	5.50	0	1.28	0.64	6.19	2.75
5	150	0	0.50	1.00	6.00	0	0.77	0.39	6.58	2.92
6	160	0	0.00	0.00	6.00	0	0.00	0.50	7.08	3.14
7	170	0	0.75	0.75	6.75	0	0.36	0.27	7.35	3.26
8	180	0	0.75	0.75	7.50	0	0.89	0.67	8.02	3.56
9	190	0	0.75	0.75	8.25	0	0.75	0.56	8.58	3.81
10	200	0	3.50	3.50	11.75	0	0.27	0.94	9.52	4.23
11	210	0	1.00	1.00	12.75	0	0.84	0.84	10.36	4.60
12	220	0	3.00	3.00	15.75	0	0.70	2.09	12.45	5.53
13	230	0	2.00	2.00	17.75	0	0.98	1.97	14.42	6.41
14	240	0	2.00	2.00	19.75	0	0.87	1.73	16.15	7.18
15	250	0	2.00	2.00	21.75	0	1.15	2.29	18.44	8.19
16	260	0	3.50	3.50	25.25	0	0.84	2.94	21.38	9.50
17	270	0	3.50	3.50	28.75	0	1.07	3.74	25.12	11.16
18	280	0	4.25	4.25	33.00	0	0.91	3.87	28.99	12.88
19	290	0	4.00	4.00	37.00	0	0.96	3.84	32.83	14.59
20	300	0	4.04	4.04	41.04	0	1.03	4.16	36.99	16.44

*Initial weight of hydrocarbon = 225 g

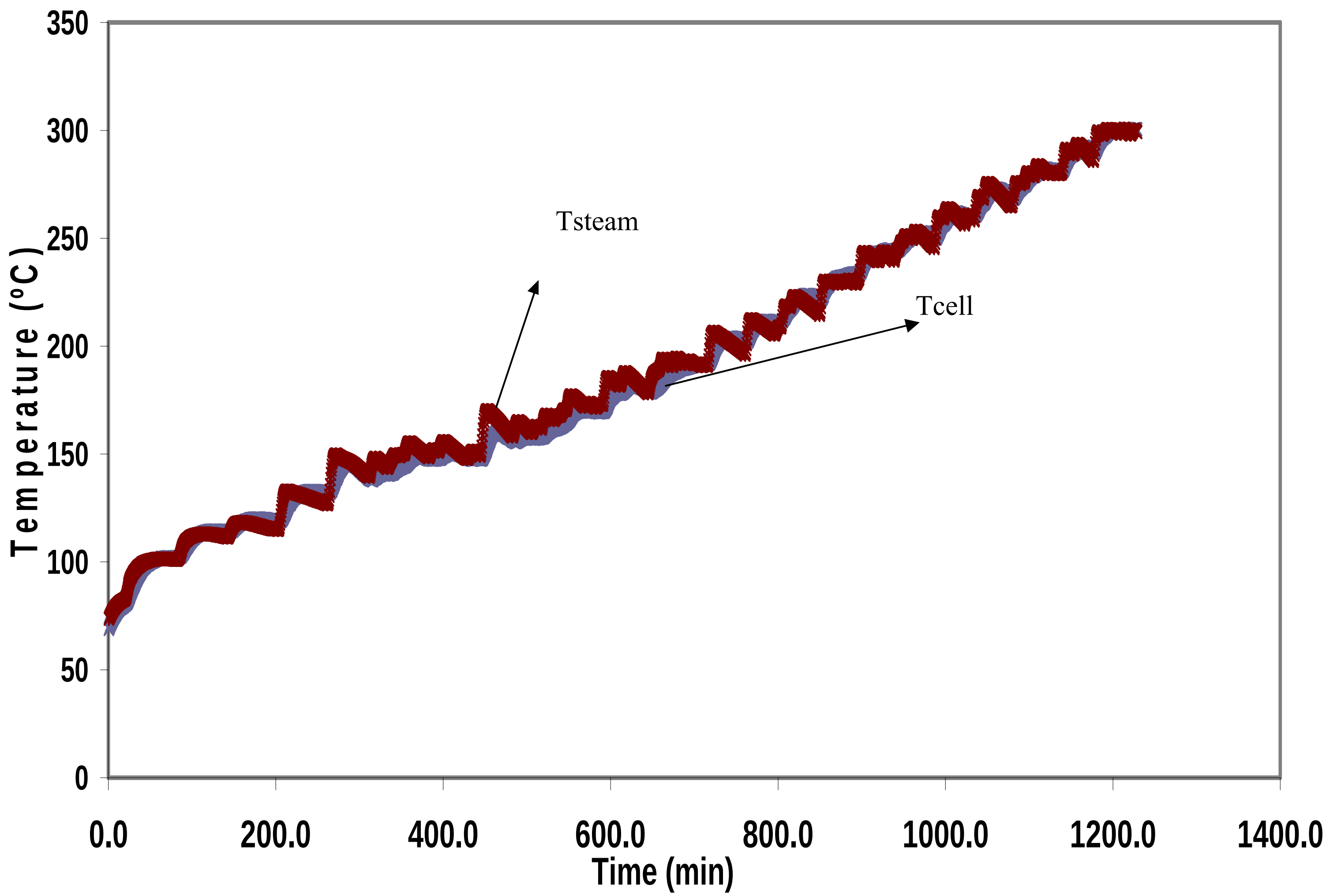

Figure 6.1: Temperature vs time for dry distillation of San Ardo crude (Run - 1).

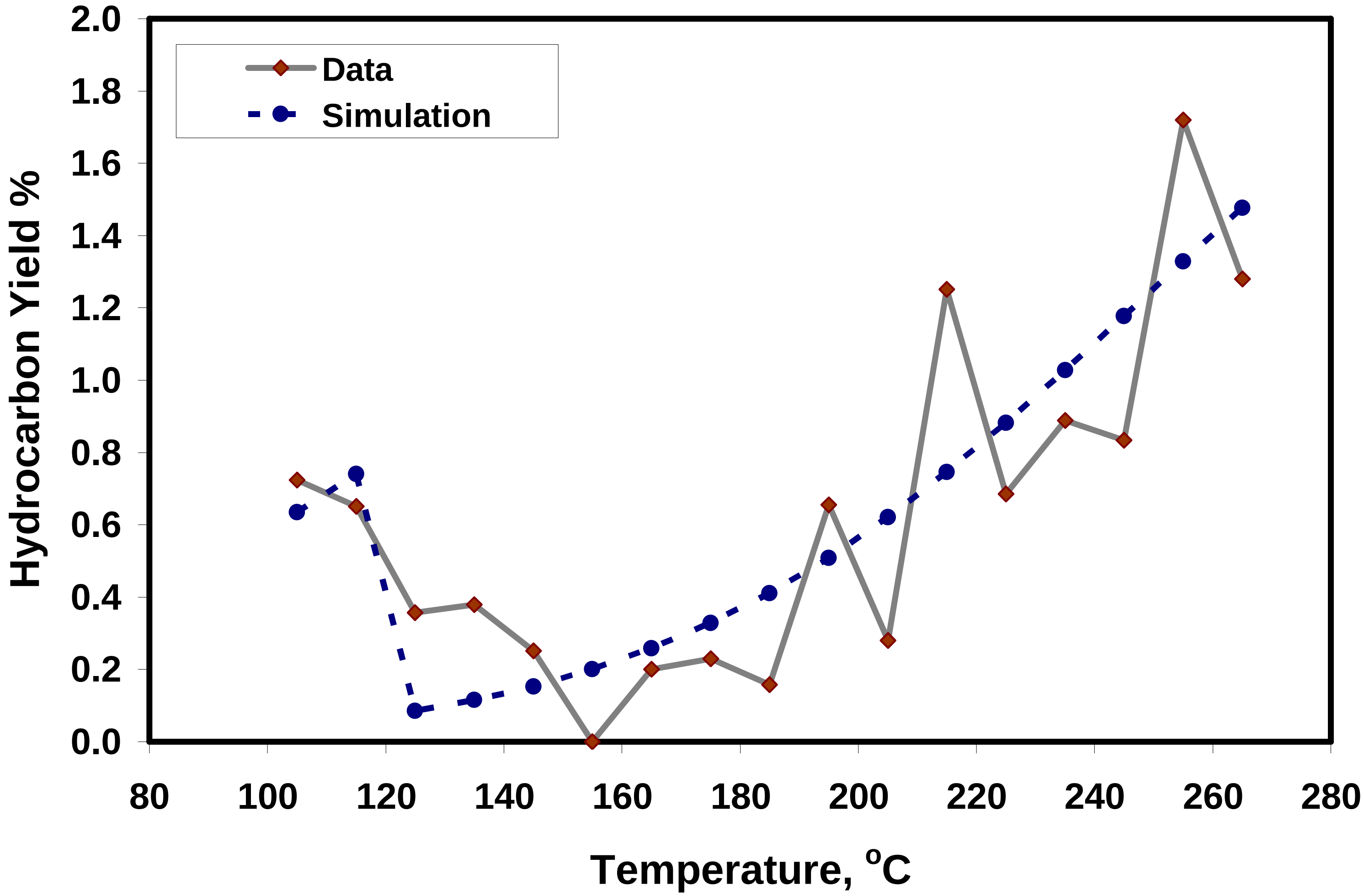

Figure 6.2: Fractional oil rates for dry distillation of San Ardo crude (Run 1).

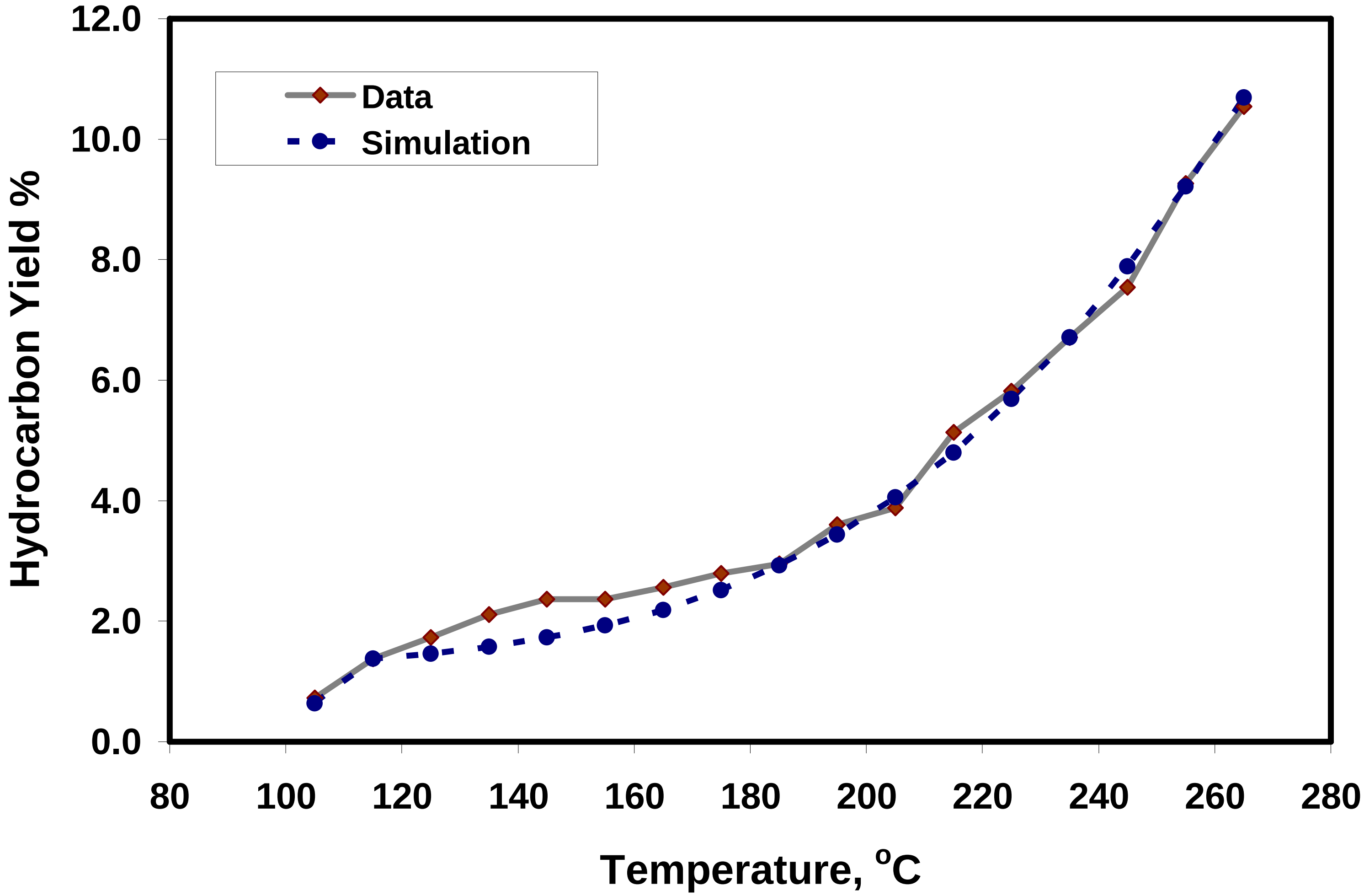

Figure 6.3: Cumulative oil yields for dry distillation of San Ardo crude (Run 1).

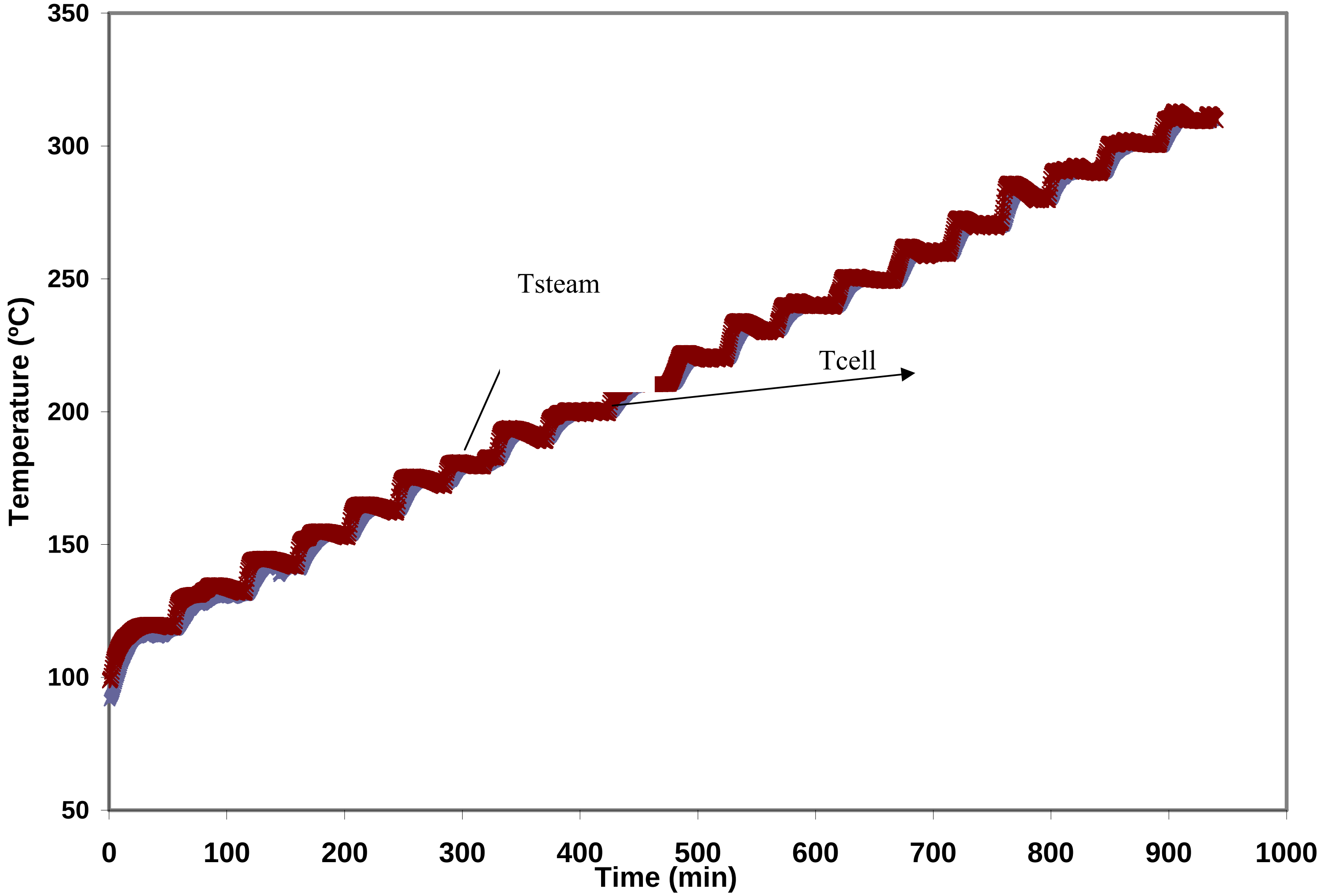

Figure 6.4: Temperature vs time for dry distillation of San Ardo crude (Run 2).

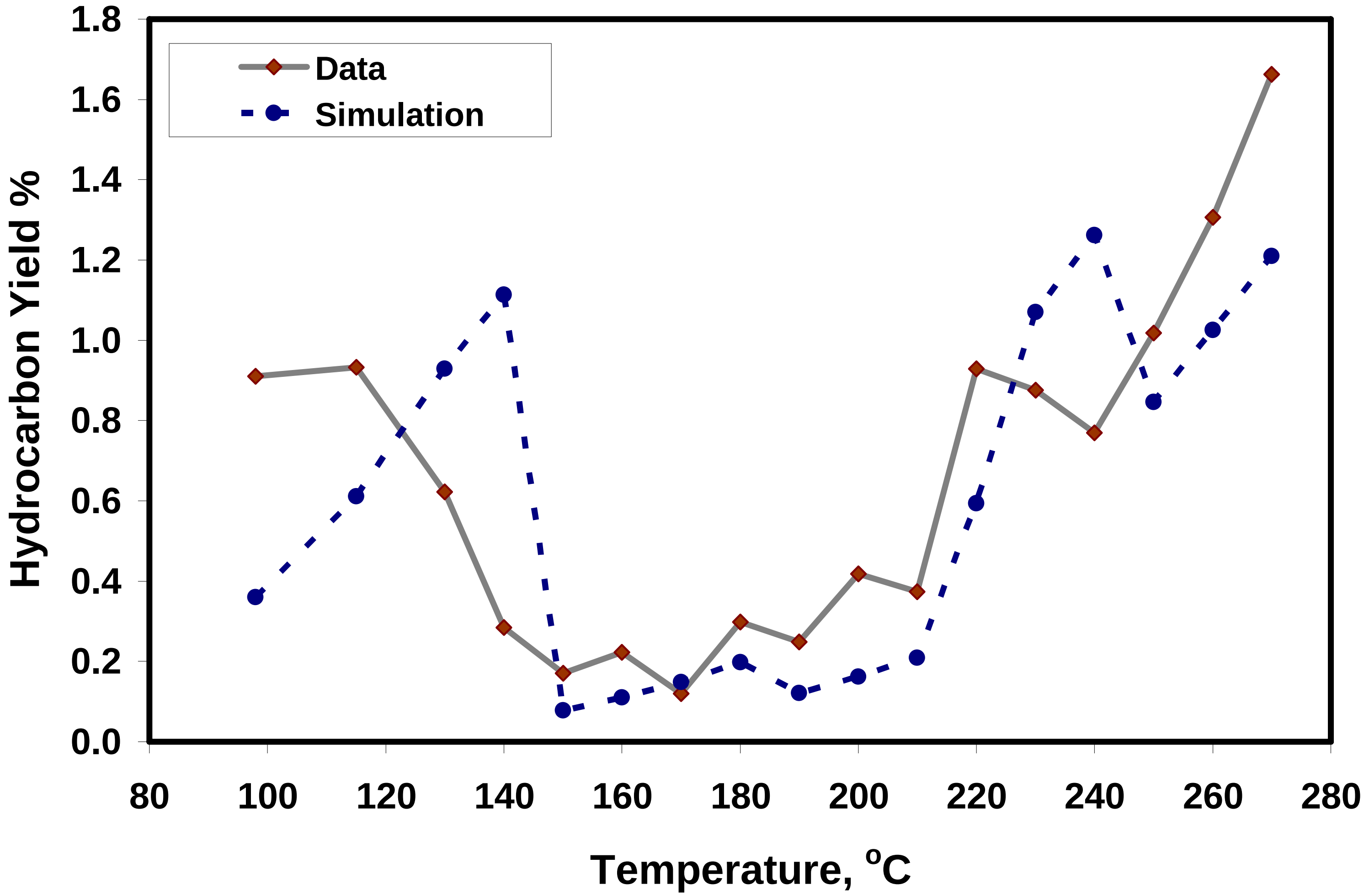

Figure 6.5 : Fractional oil rates for dry distillation of San Ardo crude (Run 2).

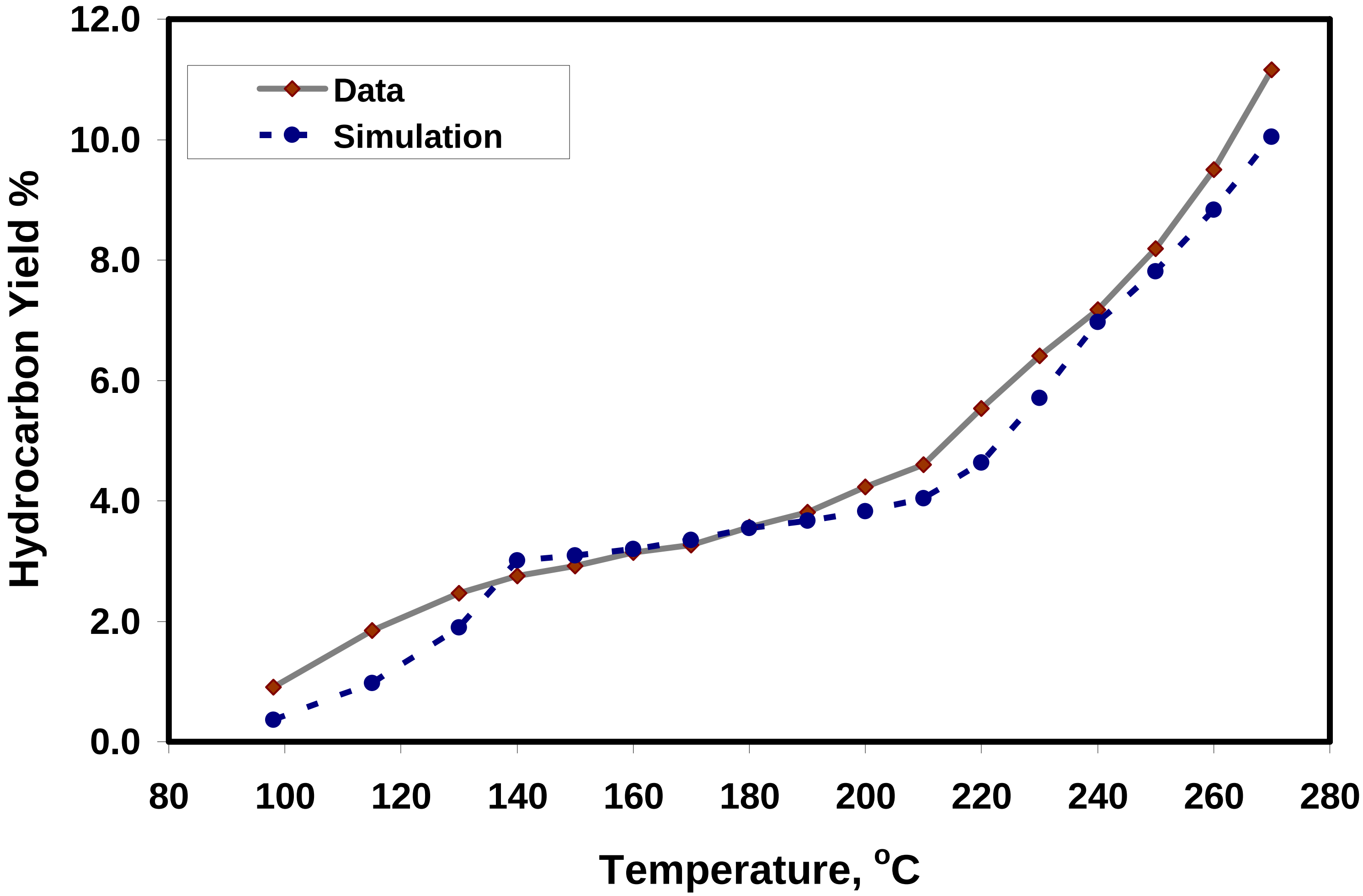

Figure 6.6: Cumulative oil yields for dry distillation of San Ardo crude (Run 2).

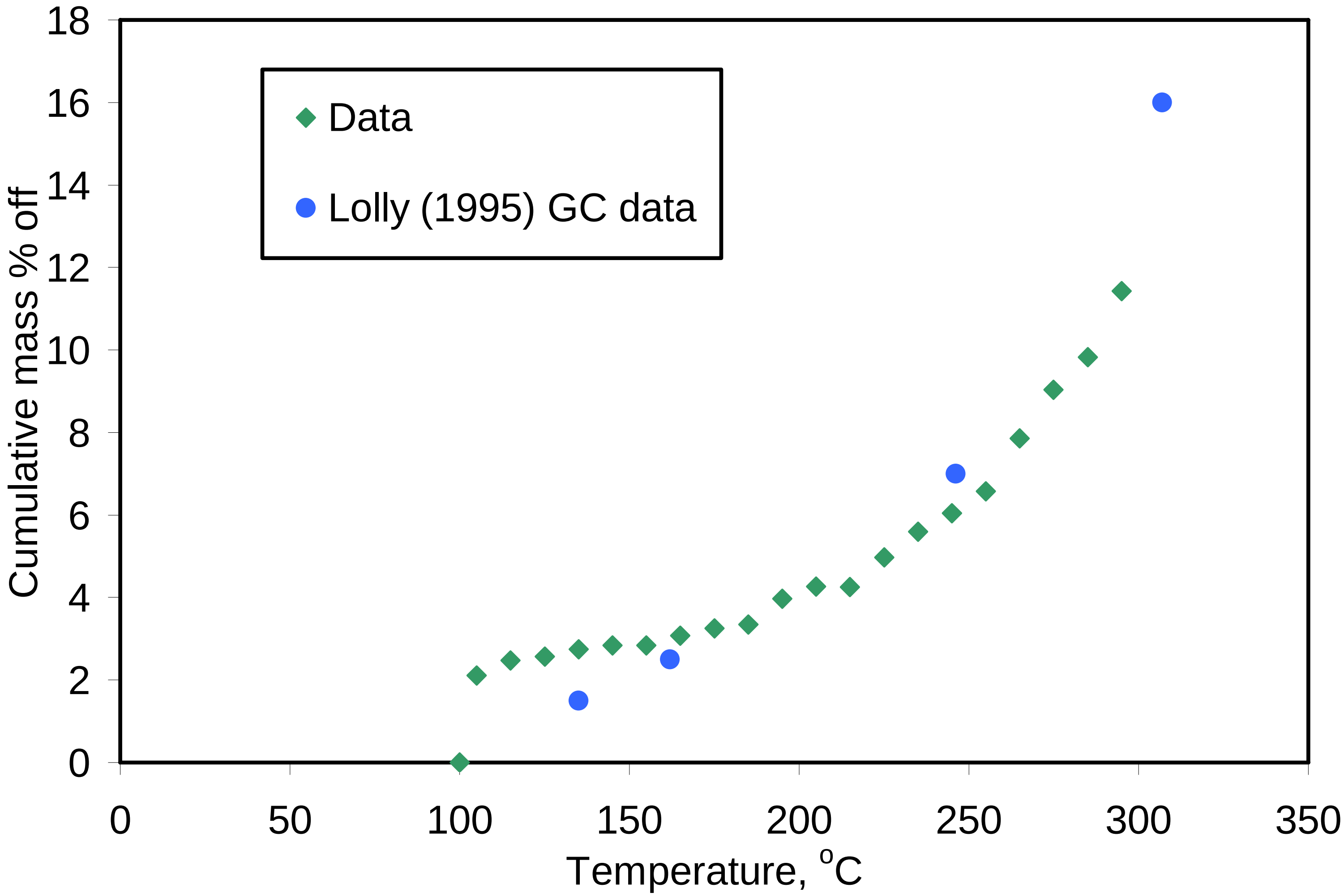

Figure 6.7: Comparison between experimental and Lolly (1997)[52] data.

6.3 Isochoric Isobaric Distillation – (P_{sat} and $T_{sat+15C}$)

In this section results from two sets of experiments using steam and steam propane for temperature and pressure shown in **Table 4.2** are presented.

6.3.1 Steam Distillation

The yields measured for the two steam distillation runs are shown in **Table 6.3**and **6.4**. The temperature profiles of the two steam distillation runs are shown in **Figs. 6.8 – 6.12**. These plots show good control of temperature during the runs. The profiles of pressures during the runs are shown in **Figs. 6.9 – 6.13** indicating very stable pressures at each cut. The fractional oil production at each temperature cut is show in **Figs 6.10** and **6.14** .The oil yield plots as a function of temperature for every steam distillation are shown in **Figs. 6.11-6.15.** Steam distillation run no.1 showed an oil recovery of 9.1% at 300ºC with an experimental error of 9.9%. Steam distillation run no. 2 showed a recovery of 10.0% with an experimental error of 5.8% at 300ºC. The experimental error was calculated based on a material balance of oil. From these plots it is evident that the amount of oil purely distilled off for these conditions is merely 10 wt. Thus, there is not a significant amount of oil being distilled at such high temperature and pressure conditions.

Table 6.3: Oil Yields at Distillation Temperatures (Steam distillation-run 1).

Cut. NO.	Temp ^{o}C	pressure psi	Volume of Liquid , ml				Weight of liquid, gms				Fractional Recovery %
			V_{oil}	V_{water}	V_{total}	Cum_{oil}	W_{oil}	W_{water}	W_{total}	Cum_{oil}	
1	115	0	6.50	23.50	30.00	6.50	4.05	22.61	26.66	4.05	1.833
2	130	10.1	2.50	18.00	20.50	9.00	0.88	17.32	18.20	4.93	2.231
3	140	19.7	2.25	27.75	30.00	11.25	1.86	26.70	28.56	6.79	3.072
4	150	31.9	2.00	11.00	13.00	13.25	0.65	10.58	11.23	7.44	3.367
5	160	47.2	2.50	27.50	30.00	15.75	0.40	26.46	26.86	7.84	3.548
6	170	66.2	1.50	22.50	24.00	17.25	0.24	21.65	21.89	8.08	3.656
7	180	89.5	3.00	33.00	36.00	20.25	0.75	31.75	32.50	8.83	3.995
8	190	117.6	1.50	25.50	27.00	21.75	0.13	24.53	24.66	8.96	4.054
9	200	151.3	4.00	35.00	39.00	25.75	1.37	33.67	35.04	10.33	4.674
10	210	191.3	1.50	28.50	30.00	27.25	0.50	27.42	27.92	10.83	4.900
11	220	238.5	2.50	30.50	33.00	29.75	1.52	29.34	30.86	12.35	5.588
12	230	293.6	3.00	28.00	31.00	32.75	0.15	26.94	27.09	12.50	5.656
13	240	357.6	4.00	42.00	46.00	36.75	2.11	40.40	42.51	14.61	6.611
14	250	431.6	2.50	30.50	33.00	39.25	0.74	29.34	30.08	15.35	6.946
15	260	516.4	2.50	38.50	41.00	41.75	1.27	37.04	38.31	16.62	7.520
16	270	613.3	2.00	45.00	47.00	43.75	0.23	43.29	43.52	16.85	7.624

*Initial oil = 221 g

Table 6.4: Oil yields at distillation temperatures (Steam distillation-run 2).

Cut. NO.	Temp ^oC	Pressure psi	Volume of Liquid , ml				Weight of liquid, gms				Fractional Recovery %
			V_{oil}	V_{water}	V_{total}	Cum_{oil}	W_{oil}	W_{water}	W_{total}	Cum_{oil}	
1	115	0	7.50	42.50	50.00	7.50	5.80	40.89	46.69	5.80	2.50
2	130	10.1	3.50	32.00	35.50	11.00	1.47	30.78	32.25	7.27	3.13
3	140	19.7	3.00	30.00	33.00	14.00	0.99	28.86	29.85	8.26	3.56
4	150	31.9	3.00	32.00	35.00	17.00	1.39	30.78	32.17	9.65	4.16
5	160	47.2	3.50	30.00	33.50	20.50	2.01	28.86	30.87	11.66	5.03
6	170	66.2	2.50	32.50	35.00	23.00	0.93	31.27	32.20	12.59	5.43
7	180	89.5	2.00	31.00	33.00	25.00	0.10	29.82	29.92	12.69	5.47
8	190	117.6	3.00	34.00	37.00	28.00	0.75	32.71	33.46	13.44	5.79
9	200	151.3	3.00	36.00	39.00	31.00	1.13	34.63	35.76	14.57	6.28
10	210	191.3	2.00	28.00	30.00	33.00	0.61	26.94	27.55	15.18	6.54
11	220	238.5	3.00	27.50	30.50	36.00	1.78	26.46	28.24	16.96	7.31
12	230	293.6	2.00	29.00	31.00	38.00	0.32	27.90	28.22	17.28	7.45
13	240	357.6	4.00	63.00	67.00	42.00	0.91	60.61	61.52	18.19	7.84
14	250	431.6	2.50	36.50	39.00	44.50	0.62	35.11	35.73	18.81	8.11
15	260	516.4	4.50	36.50	41.00	49.00	1.67	35.11	36.78	20.48	8.83
16	270	613.3	2.00	31.00	33.00	51.00	0.44	29.82	30.26	20.92	9.02

*Initial Oil = 235 gms

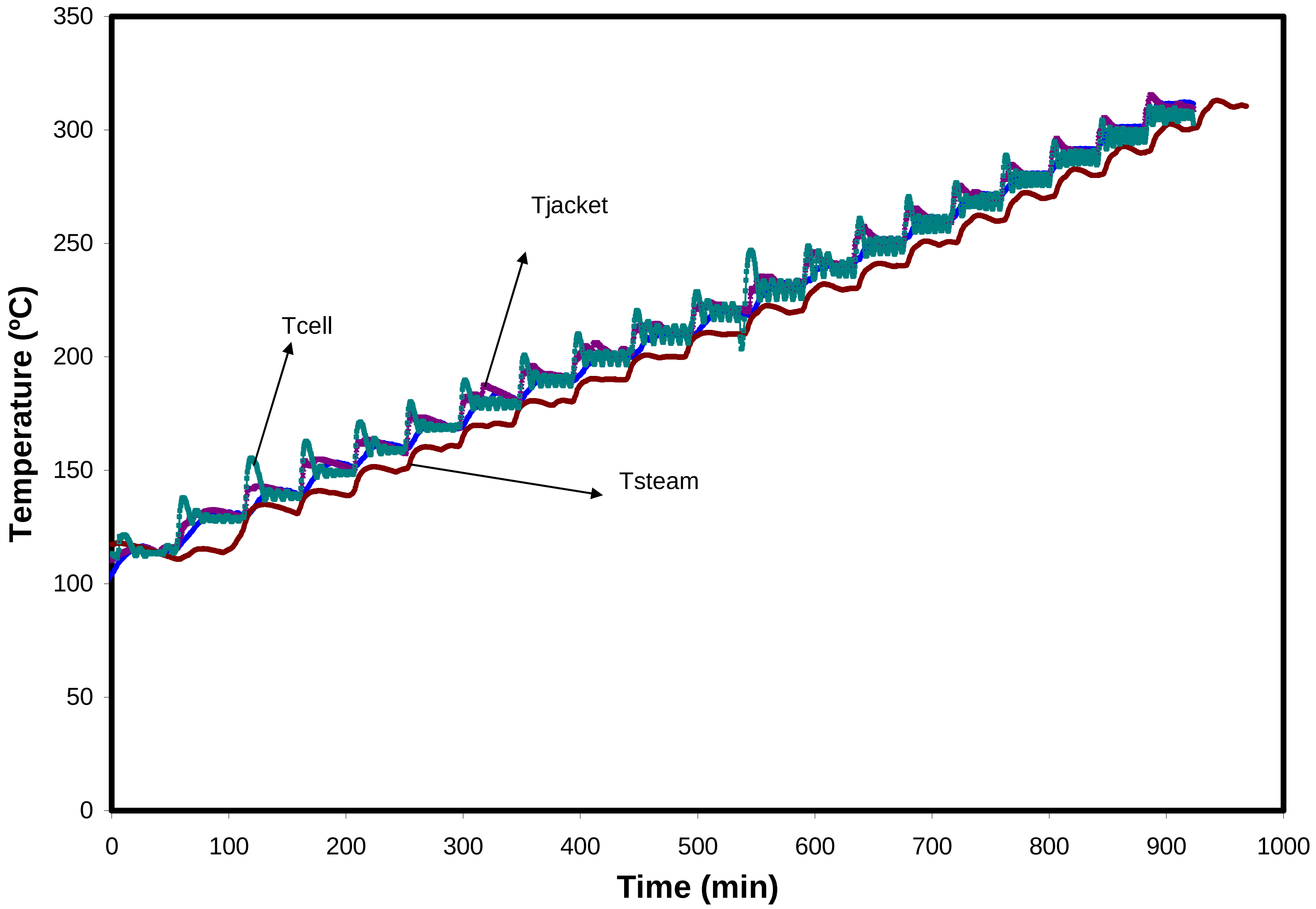

Figure 6.8: Temperature vs time for steam distillation of San Ardo crude (T_{sat+15}, P_{sat}) (Run –1).

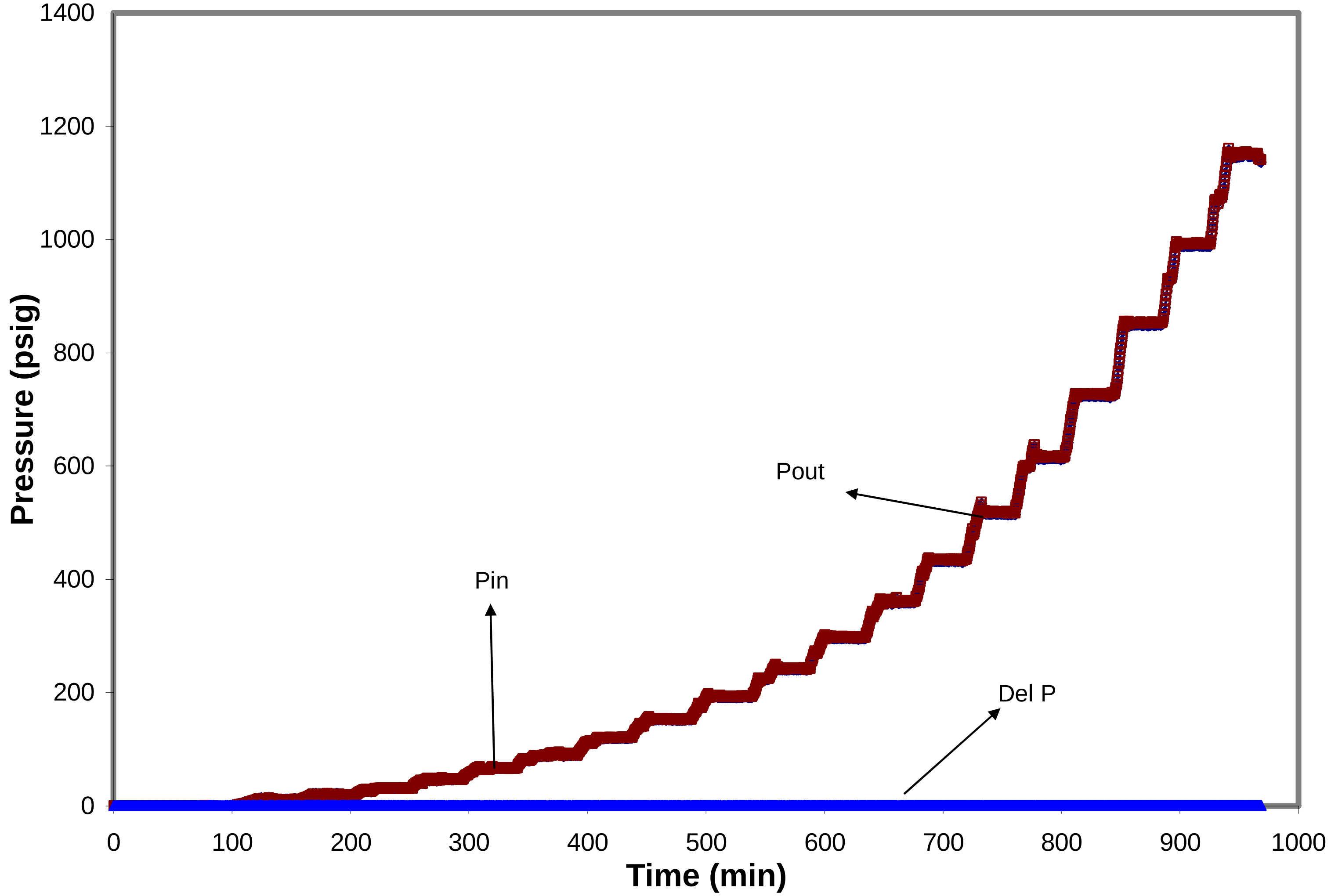

Figure 6.9: Pressure vs time for steam distillation of San Ardo crude (T_{sat+15}, P_{sat}) (Run –1).

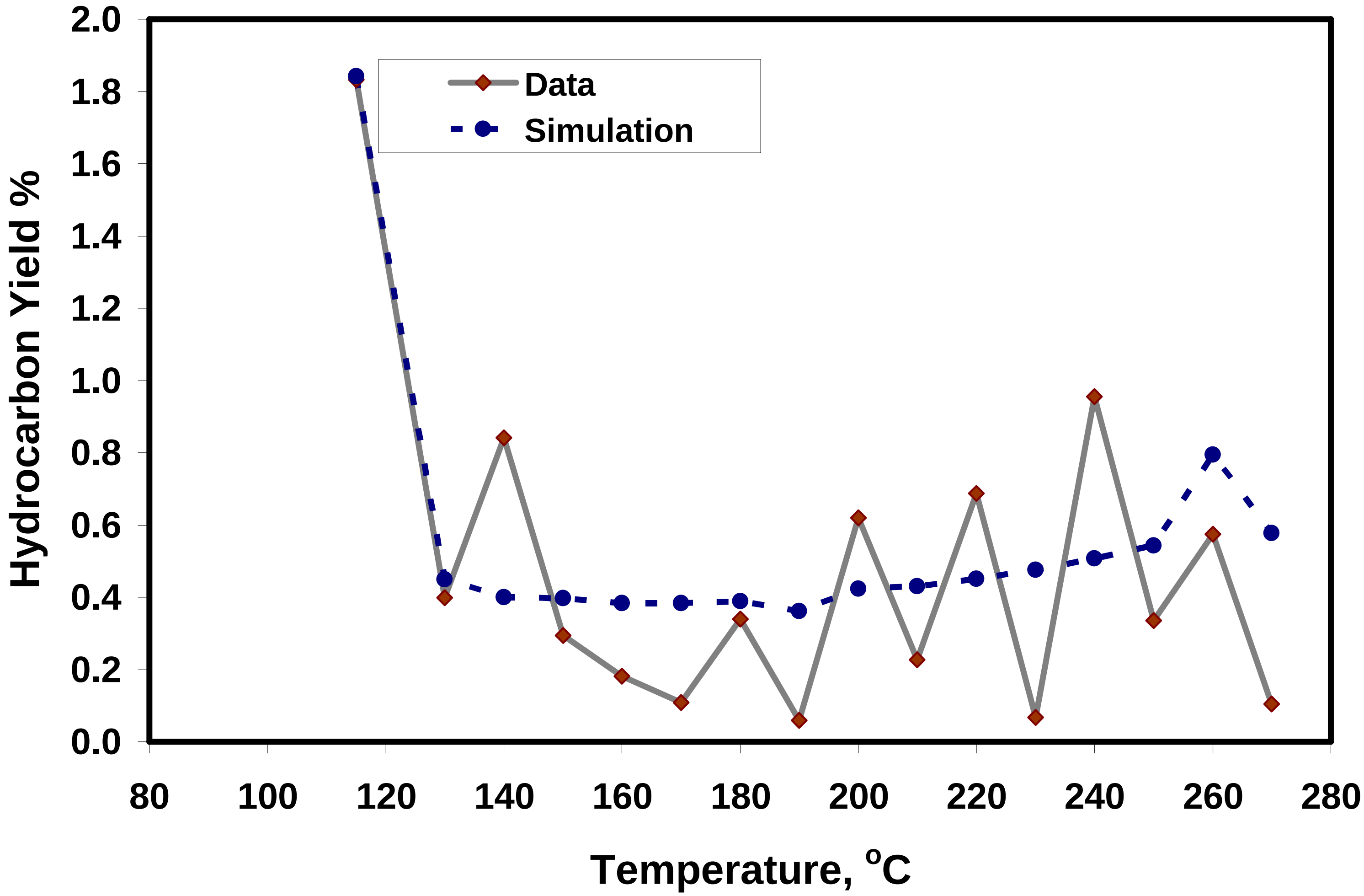

Figure 6.10: Fractional oil rates for steam distillation of San Ardo crude (Run-1).

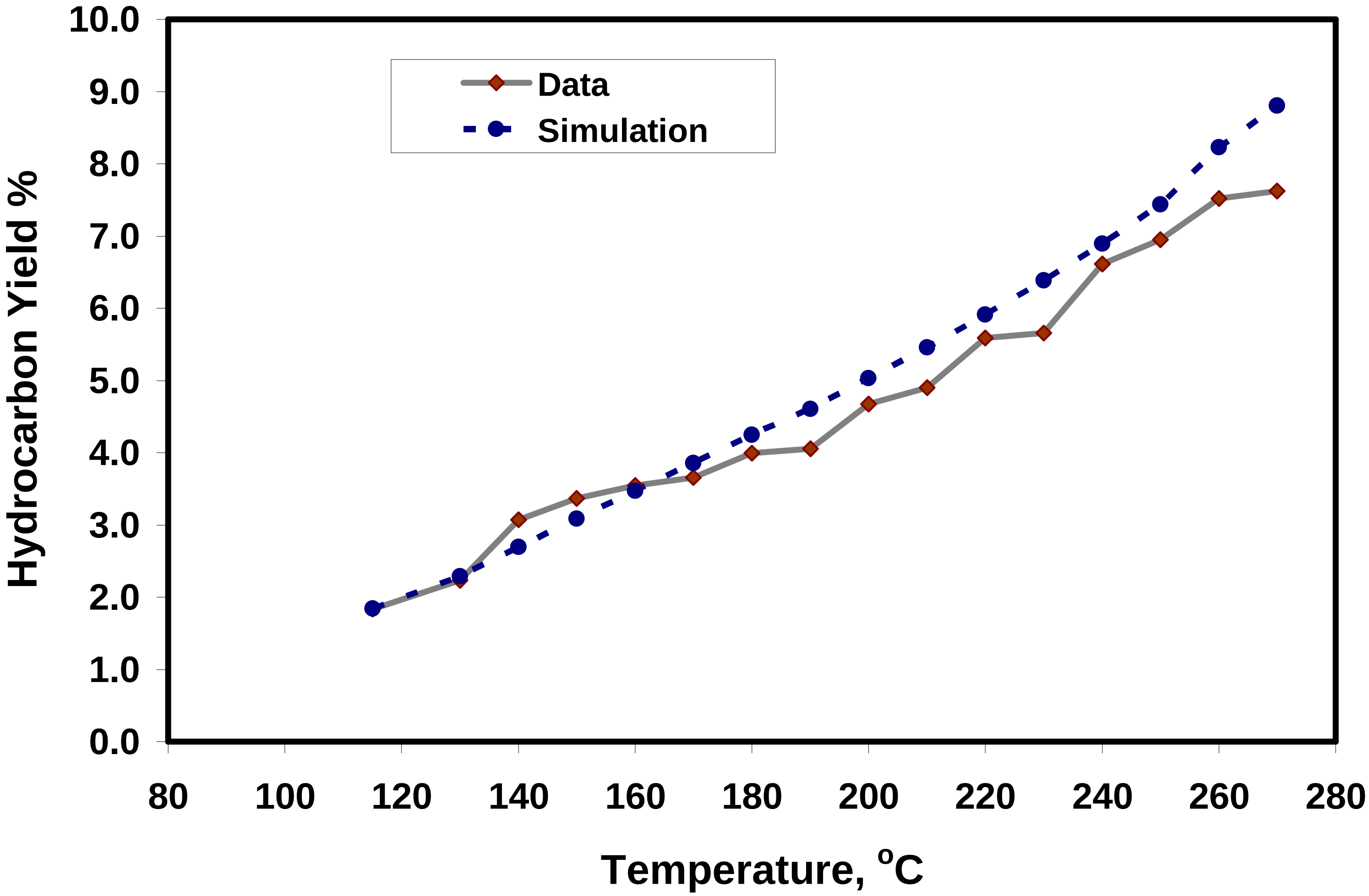

Figure 6.11: Cumulative oil yields for steam distillation of San Ardo crude (Run – 1).

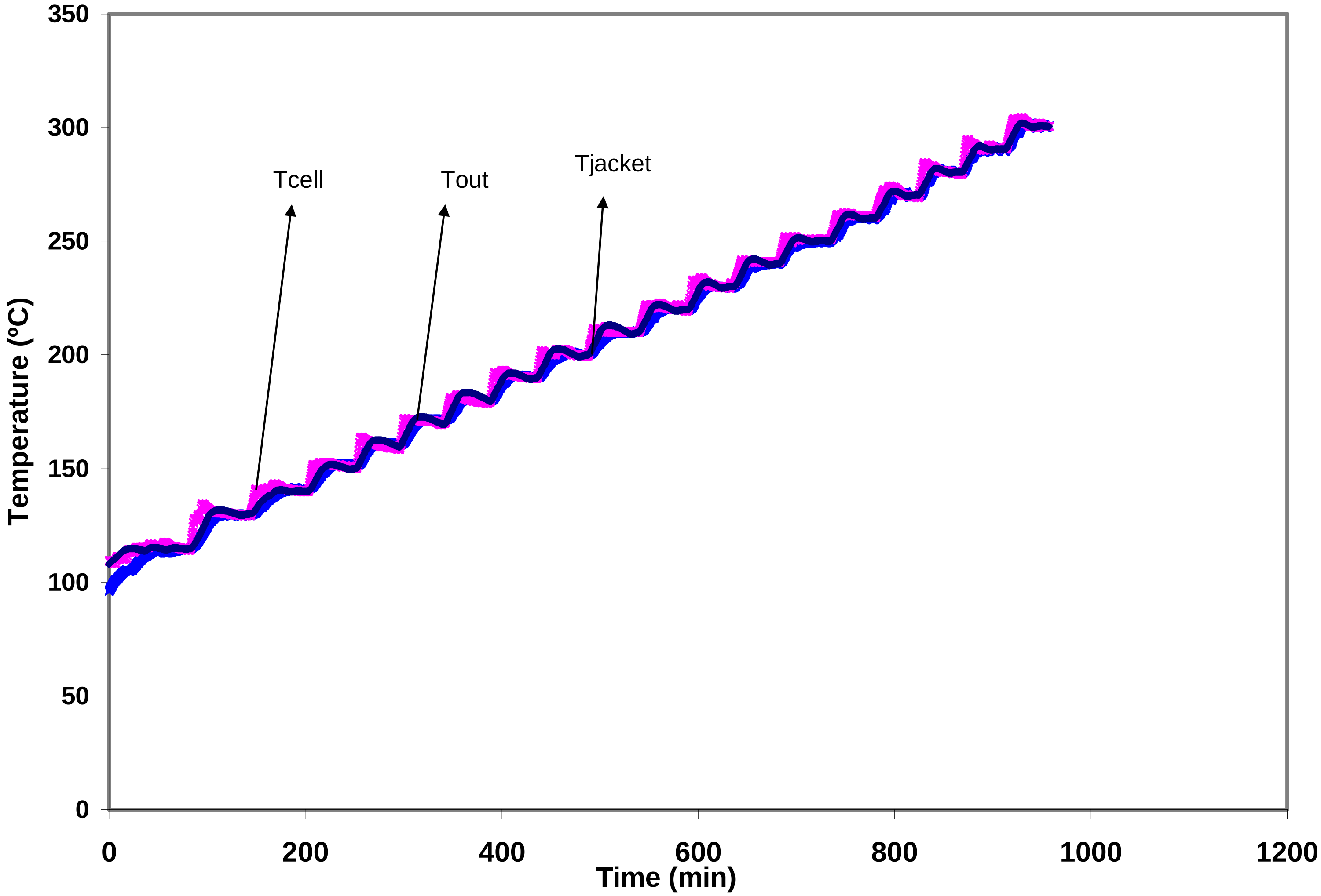

Figure 6.12: Temperature vs time for steam distillation of San Ardo crude (T_{sat+15}, P_{sat}) (Run –2).

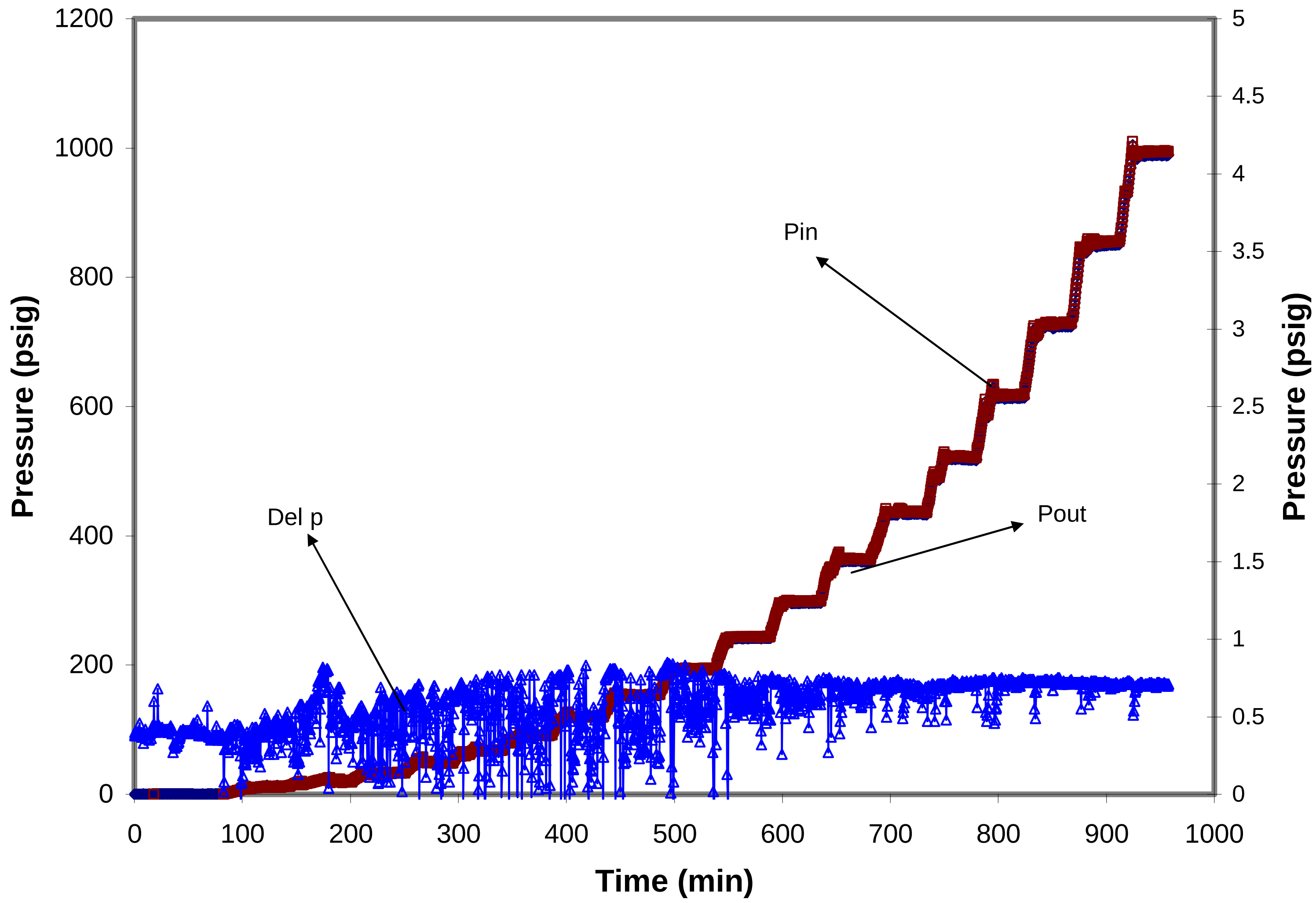

Figure 6.13: Pressure vs time for steam distillation of San Ardo crude (T_{sat+15}, P_{sat}) (Run –2).

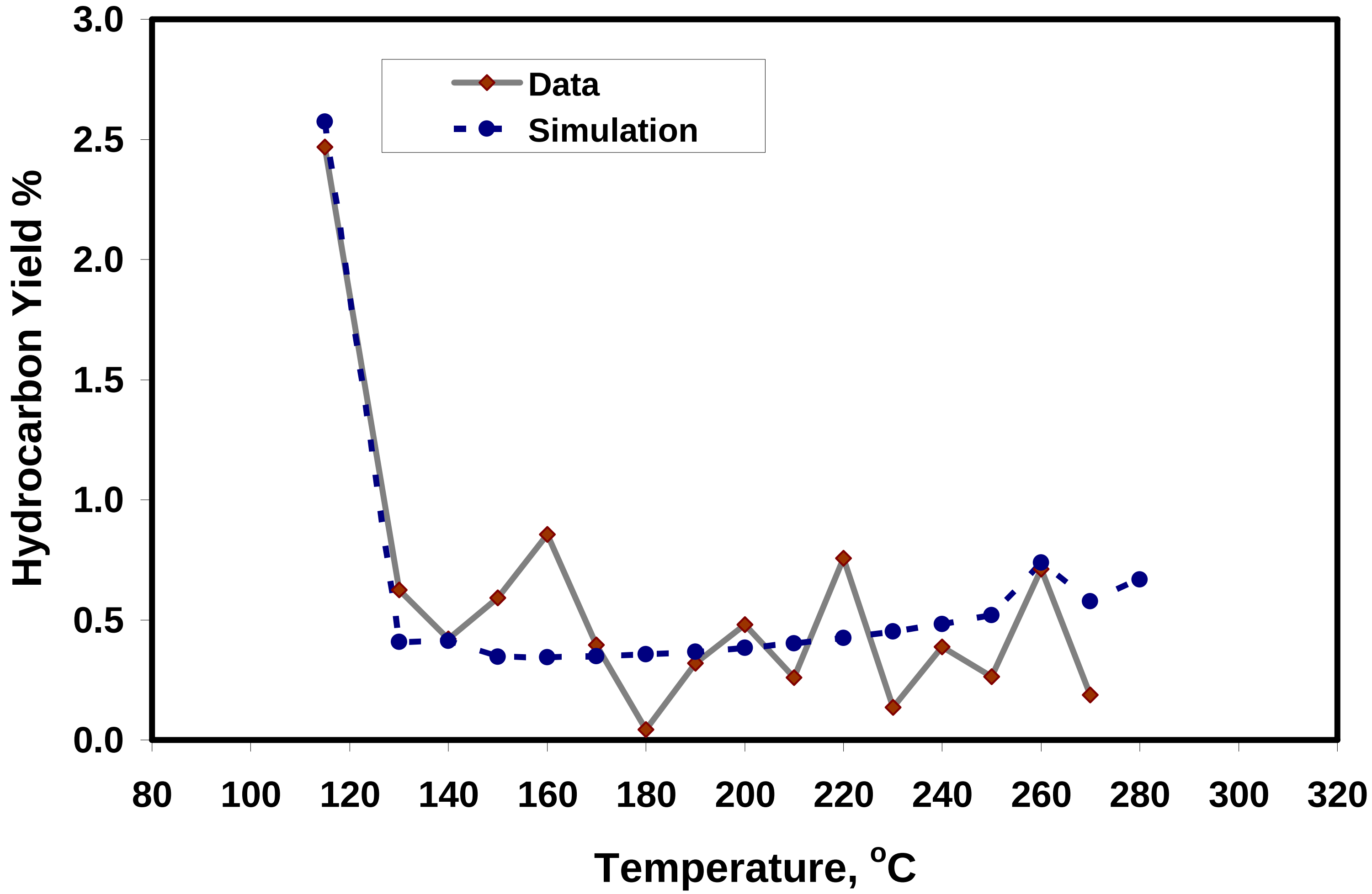

Figure 6.14: Fractional oil rates for steam distillation of San Ardo crude (Run-2).

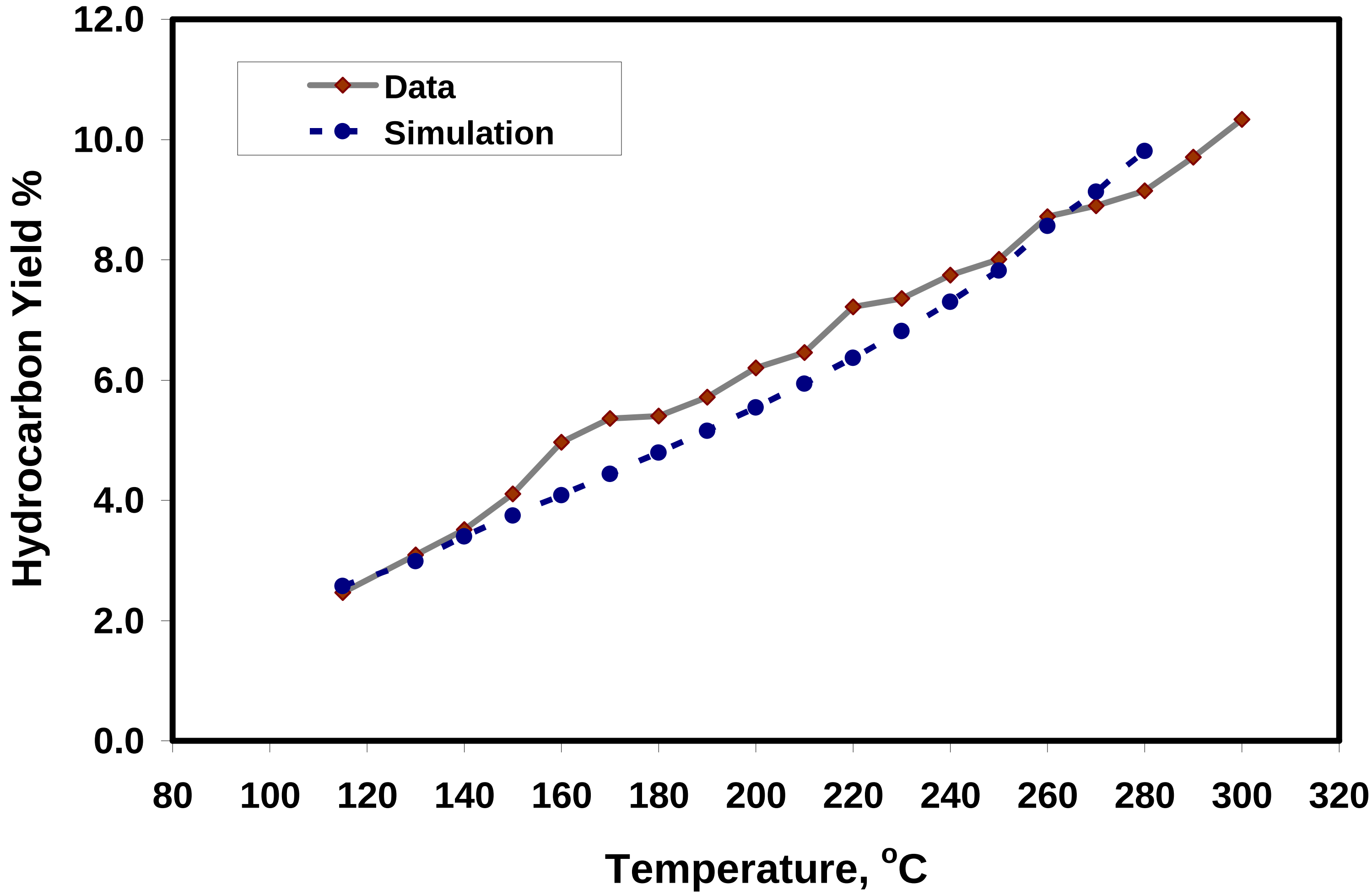

Figure 6.15: Cumulative oil yields for steam distillation of San Ardo crude (Run-2)..

6.3.2 Steam-Propane Distillation

Measured distillate yields are summarized in **Table 6.5 - 6.6** for the steam-propane runs. The temperature profiles for this run are shown in **Fig 6.16** and **Fig 6.20**. These plots indicate stable of temperatures at each cut are stable during the runs. The profiles of pressures during runs are shown **Fig 6.17 and Fig 6.21**. The fraction of oil produced at each temperature cut is shown for run 1 and run 2 is shown in **Fig 6.18** and **Fig 6.22**

The oil yield plots as a function of temperature for each steam-propane distillation run are shown in **Fig 6.19** and **Fig 6.23** Steam-propane distillation run no. 1 showed an oil recovery of 8.7 % at 300ºC with an experimental error of 9.4 %. Steam–propane distillation run no. 2 showed an oil recovery of 9.7 % with an experimental error of 8.9 % at 270ºC. The experimental error was calculated considering the material balance of oil. From the oil yield plots one can observe that about almost similar amount (4 wt % and 10 wt%) of the hydrocarbons is distilled off at around 150 ^{o}C and 270ºC, for steam-propane than in the steam- or dry distillations processes. The absolute amount of hydrocarbon distilled off in the process is very low (~ 10%) So, achieving acceleration in production using additives would be a difficult process to quantify. In core flooding experiments propane was found to be accelerating production only and there was no increase in cumulative production for San Ardo crude oil (Simangunsong, 2005) [6]. So the similar experiments were performed for field conditions and results are presented in the next subsection.

Table 6.5 : Oil yields at distillation temperatures (Steam Propane distillation-run 1).

Cut. NO.	Temp °C	Pressure psi	Volume of Liquid , ml				Weight of liquid, g				Fractional Recovery %
			V_{oil}	V_{water}	V_{total}	Cum_{oil}	W_{oil}	W_{water}	W_{total}	Cum_{oil}	
1	118	0	3.5	25	30	3.5	3.62	24.05	29.50	3.62	1.63800905
2	132	10.1	2.6	26	20.5	6.1	1.65	25.012	18.88	5.27	2.38461538
3	139	19.7	0.5	27.5	30	6.6	0.42	26.455	29.61	5.69	2.57466063
4	149	31.9	2.5	29	13	9.1	0.46	27.898	11.65	6.15	2.78280543
5	161	47.2	2.5	31	30	11.6	0.5	29.822	27.90	6.65	3.00904977
6	170	66.2	1.5	32.5	24	13.1	1	31.265	22.74	7.65	3.46153846
7	180	89.5	1	36	36	14.1	0.56	34.632	33.75	8.21	3.71493213
8	191	117.6	0.5	29.5	27	14.6	0.38	28.379	25.63	8.59	3.88687783
9	202	151.3	1.5	31	39	16.1	1.45	29.822	36.37	10.04	4.54298643
10	210	191.3	1	30	30	17.1	0.68	28.86	29.00	10.72	4.85067873
11	219	238.5	2.5	32	33	19.6	0.75	30.784	32.02	11.47	5.19004525
12	230	293.6	3	27.5	31	22.6	2.15	26.455	28.15	13.62	6.16289593
13	241	357.6	4	31	46	26.6	1.75	29.822	44.11	15.37	6.95475113
14	250	431.6	1	27.5	33	27.6	0.68	26.455	31.24	16.05	7.26244344
15	260	516.4	0.5	33.5	41	28.1	0.48	32.227	39.77	16.53	7.47963801
16	271	613.3	2	41	47	30.1	0.75	39.442	45.23	17.28	7.81900452
17	279	723.4	1	31	30	31.1	0.65	29.822	28.32	17.93	8.11312217
18	290	848	1	34	37.5	32.1	0.86	32.708	36.34	18.786	8.50045249
19	300	988	3	32	32	35.1	0.5	30.784	29.40	19.286	8.72669683

*Initial Oil = 210 gms

Table 6.6: Oil yields at distillation temperatures (Steam Propane distillation-run 2).

Cut. NO.	Temp ^oC	Bottle, wt gms	Volume of Liquid , ml				Weight of liquid, gms				Fractional Recovery %
			V_{water}	V_{oil}	V_{total}	Cum_{oil}	W_{water}	W_{oil}	W_{total}	Cum_{oil}	
1	115	10.76	22.5	6	28.5	6	21.71	4.11	36.58	4.11	2.12
2	115	10.8	24.5	1.5	26	7.5	23.64	0.71	35.15	4.82	2.49
3	130	10.79	32.5	2.5	35	10	31.36	1.12	43.27	5.93	3.06
4	140	10.7	25	2	27	12	24.13	1.02	35.84	6.95	3.59
5	150	10.7	21	1.5	22.5	13.5	20.27	0.55	31.51	7.49	3.87
6	160	10.7	29.5	2	31.5	15.5	28.47	0.85	40.02	8.35	4.31
7	170	10.71	24	0	24	15.5	23.16	0.13	34.00	8.48	4.38
8	180	10.7	29.5	2.5	32	18	28.47	0.80	39.97	9.28	4.79
9	190	10.72	33.5	3	36.5	21	32.33	2.07	45.12	11.35	5.86
10	200	10.71	21.5	-0.3	21.2	20.7	20.75	0.08	31.54	11.43	5.90
11	210	10.8	24	0	24	20.7	23.16	0.00	33.96	11.43	5.90
12	220	10.81	31	0.5	31.5	21.2	29.92	0.59	41.31	12.02	6.20
13	230	10.71	39.5	4.5	44	25.7	38.12	2.04	50.87	14.06	7.26
14	240	10.73	36	2	38	27.7	34.74	0.99	46.46	15.05	7.77
15	250	10.74	25.5	2.5	28	30.2	24.61	0.80	36.15	15.85	8.18
16	260	10.81	24.5	4.5	29	34.7	23.64	2.20	36.65	18.05	9.32
17	270	10.69	25	5	30	39.7	24.13	1.08	35.89	19.13	9.87

*Initial Oil = 193.7 gms

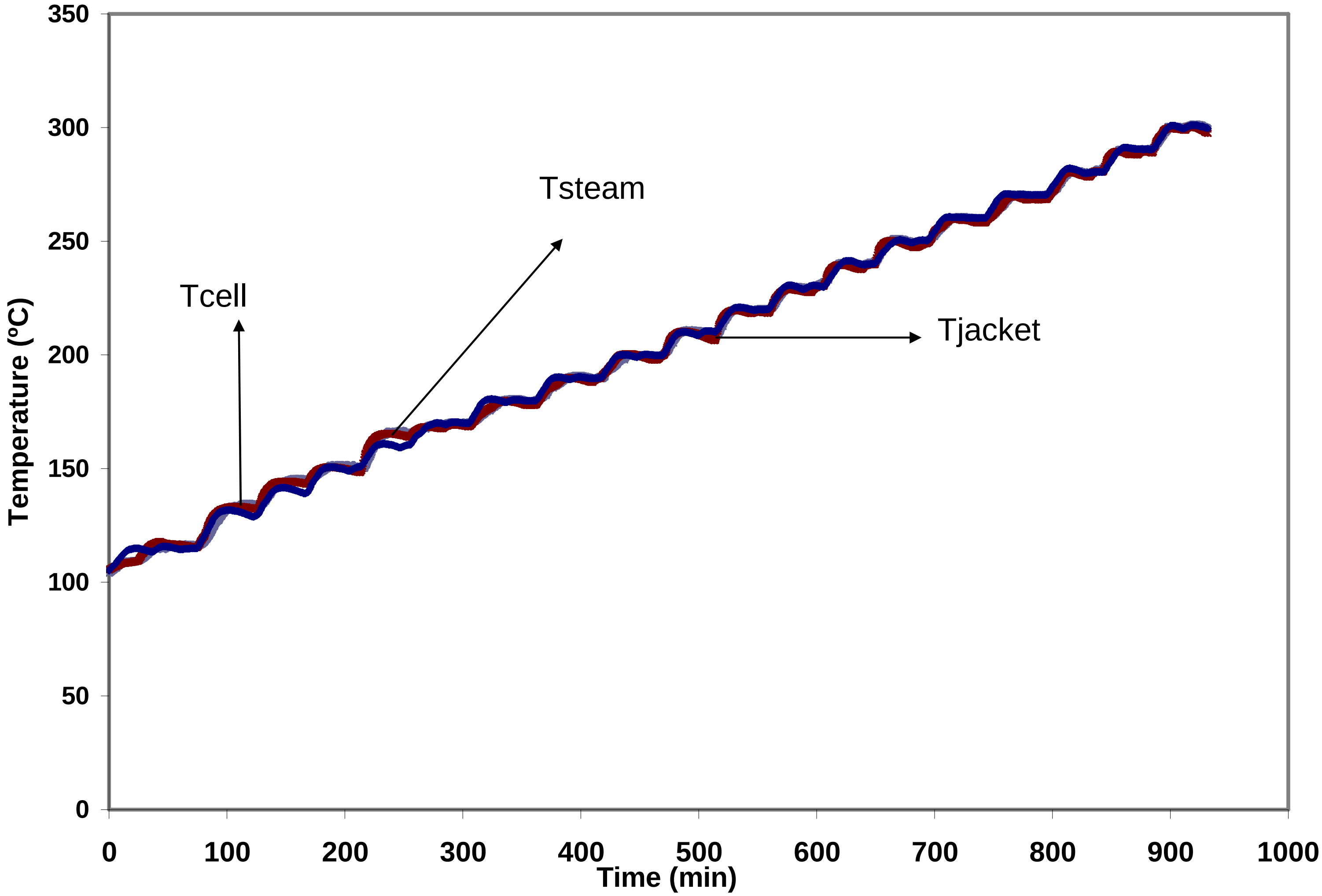

Figure 6.16: Temperature vs time for steam propane distillation of San Ardo crude (T_{sat+15}, P_{sat}) (Run–1).

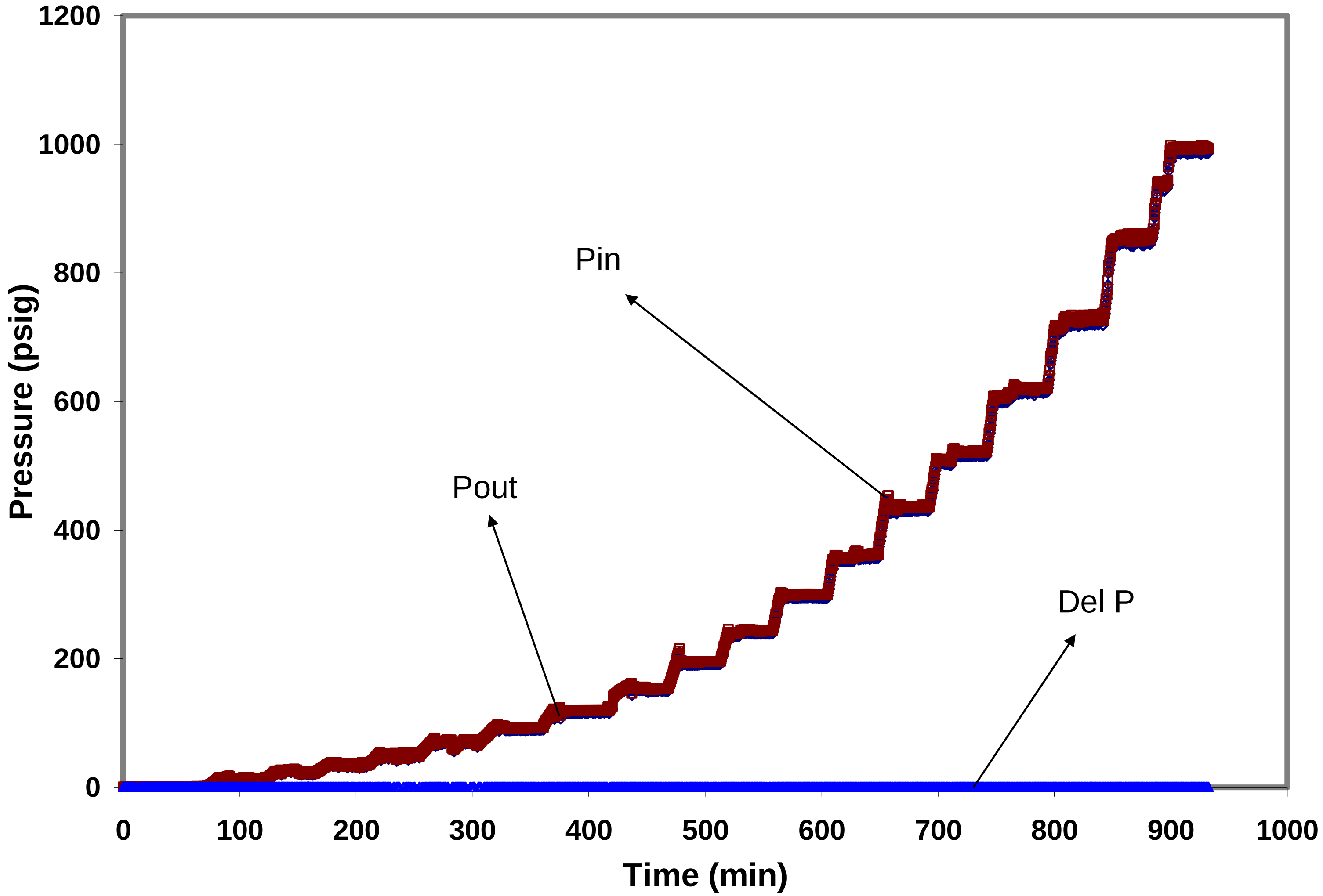

Figure 6.17 : Pressure vs time for steam propane distillation of San Ardo crude (T_{sat+15}, P_{sat}) (Run–1).

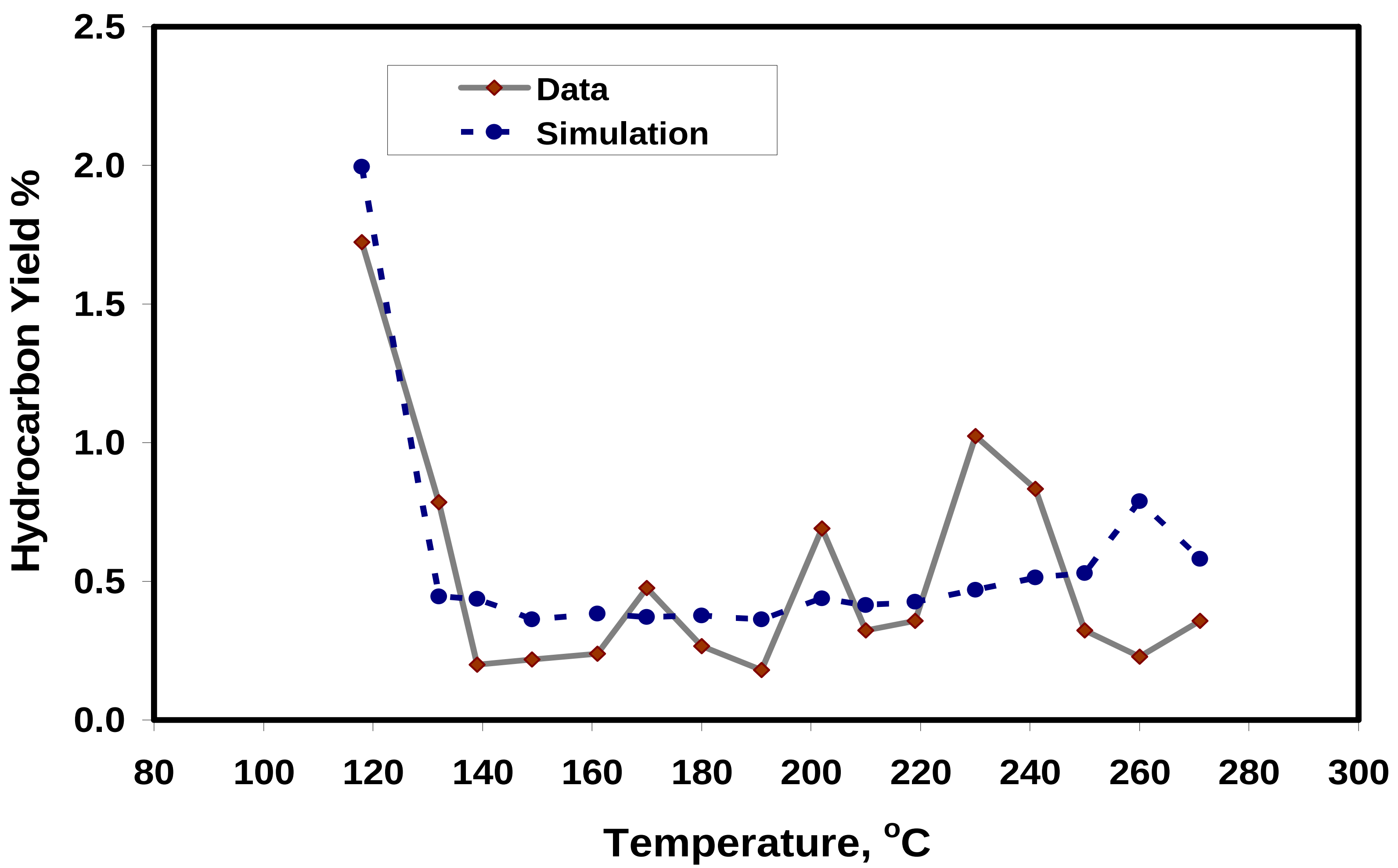

Figure 6.18: Fractional oil rates for steam propane distillation of San Ardo crude (Run-1).

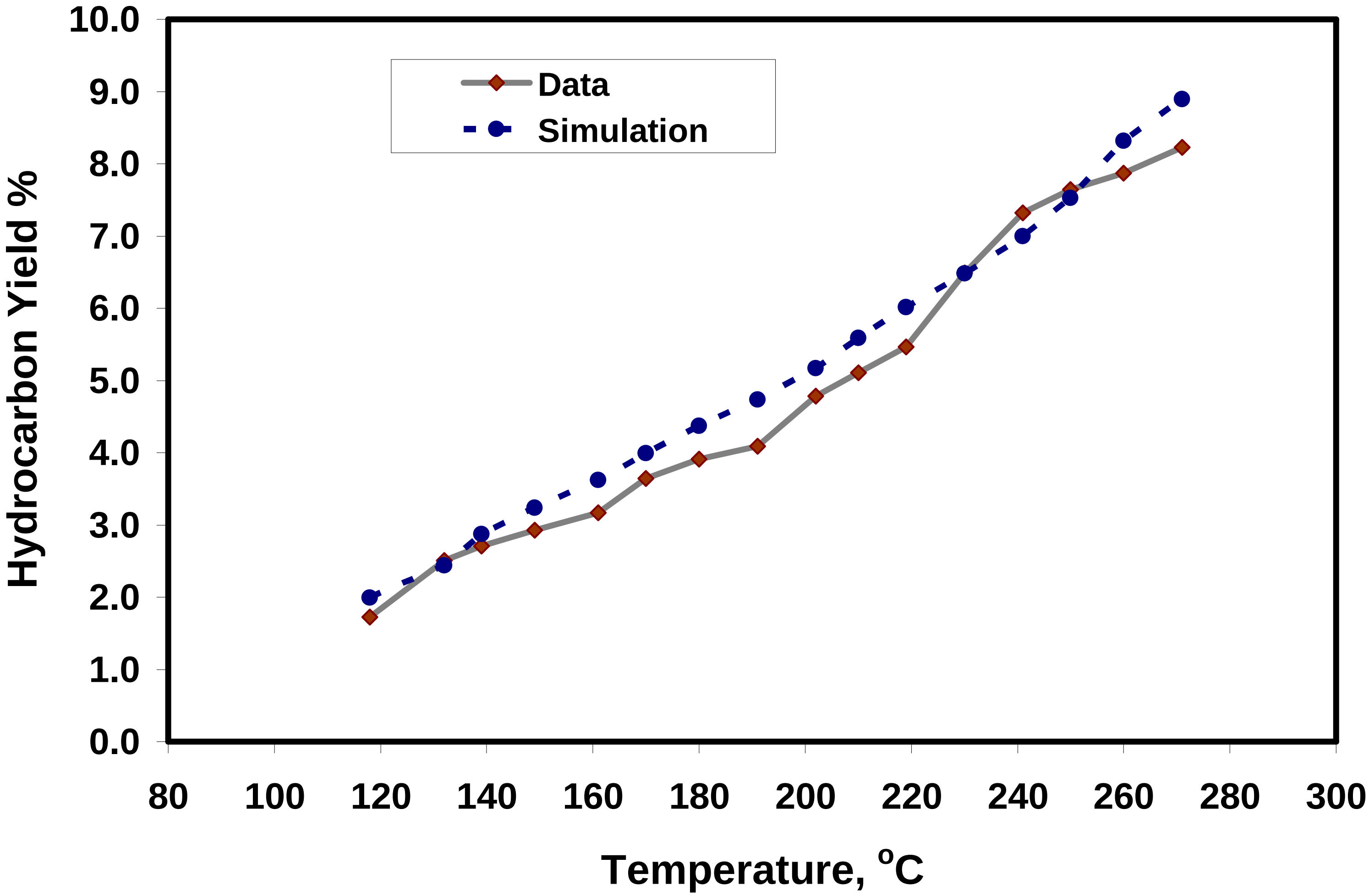

Figure 6.19: Cumulative oil yields for steam propane distillation of crude (Run–1).

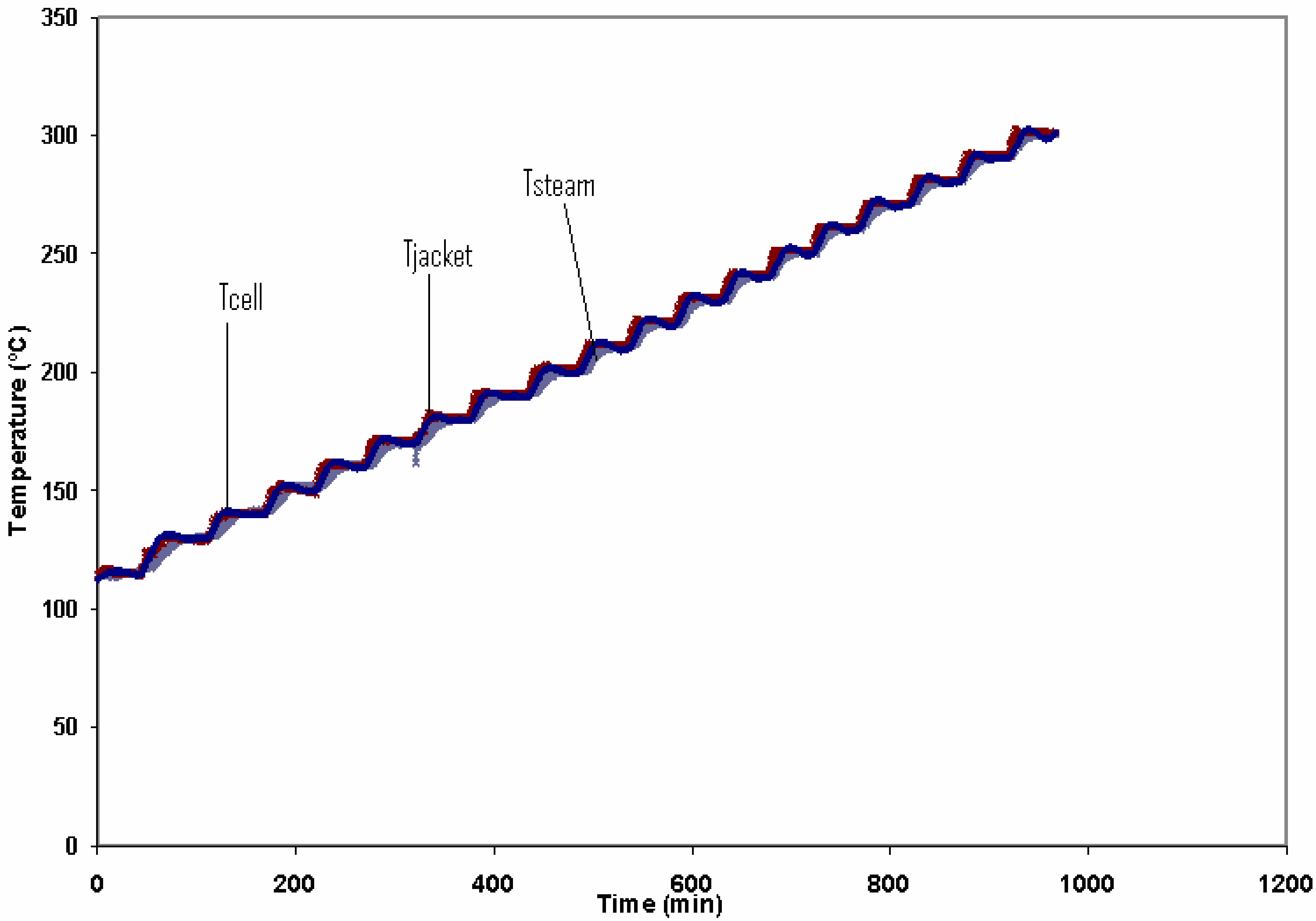

Figure 6.20: Temperature vs time for steam propane distillation of San Ardo crude (T_{sat+15}, P_{sat}) (Run –2).

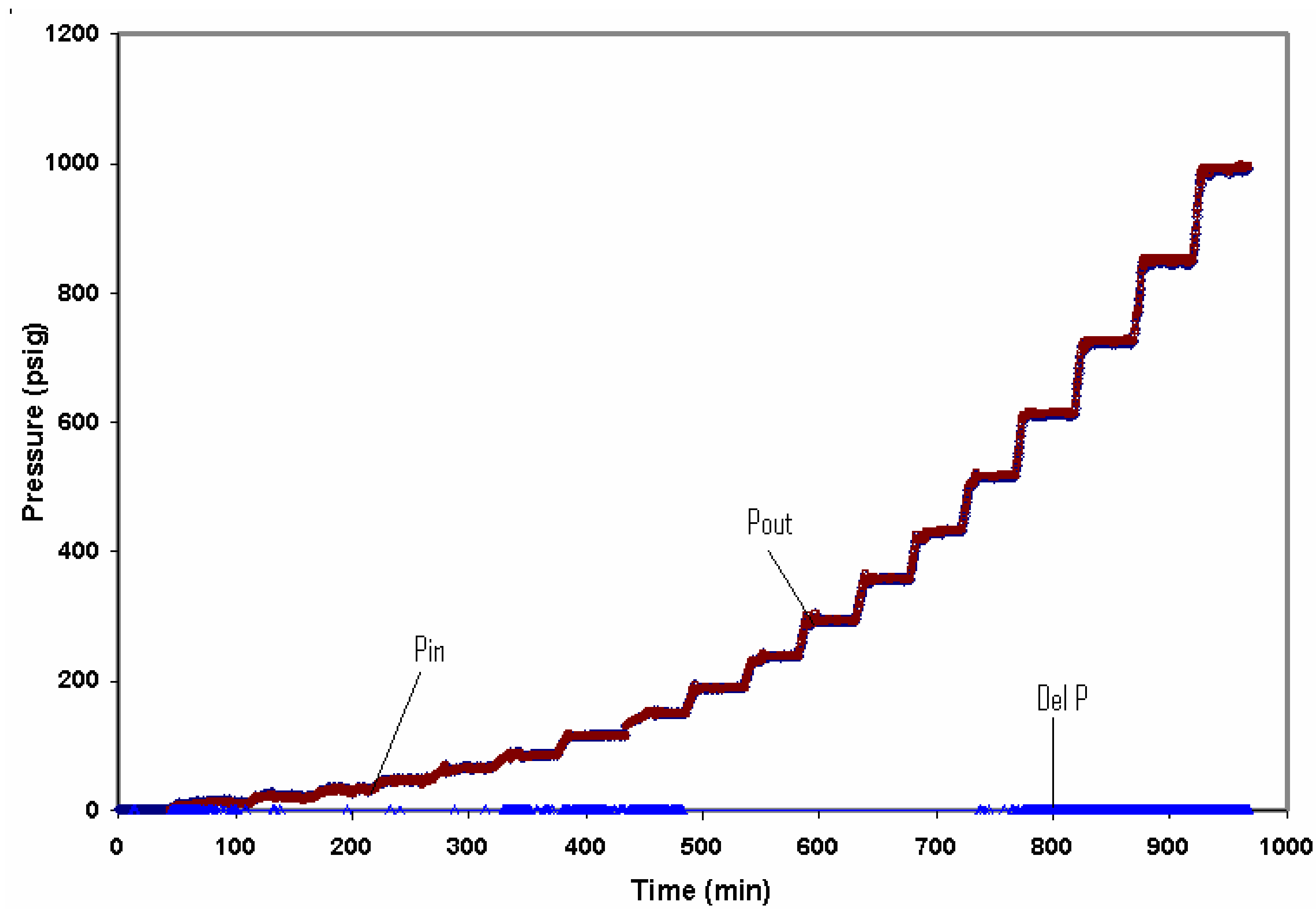

Figure 6.21: Pressure vs time for steam propane distillation of San Ardo crude (T_{sat+15}, P_{sat}) (Run –2).

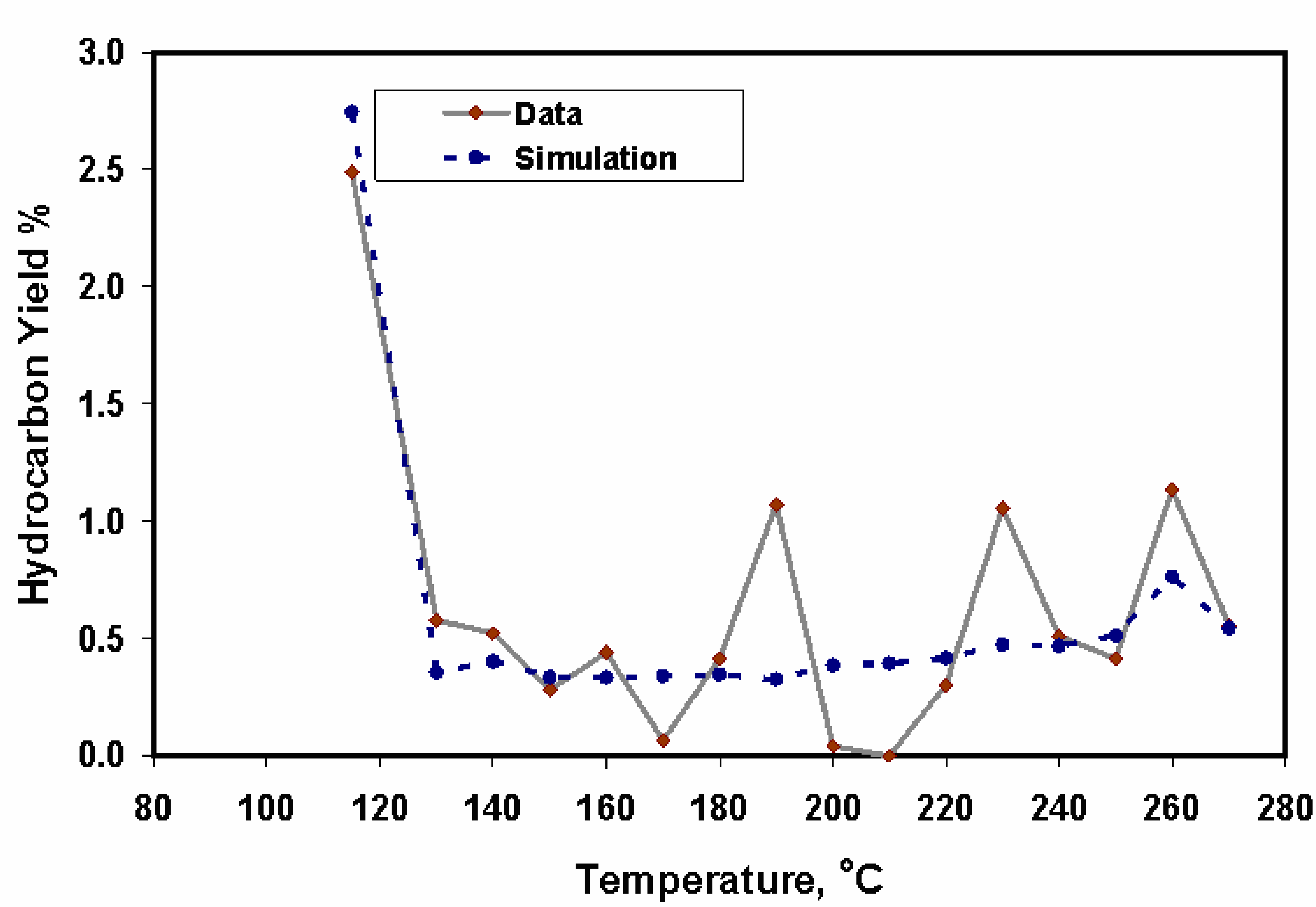

Figure 6.22: Fractional oil rates for steam propane distill ation of San Ardo crude (Run - 2).

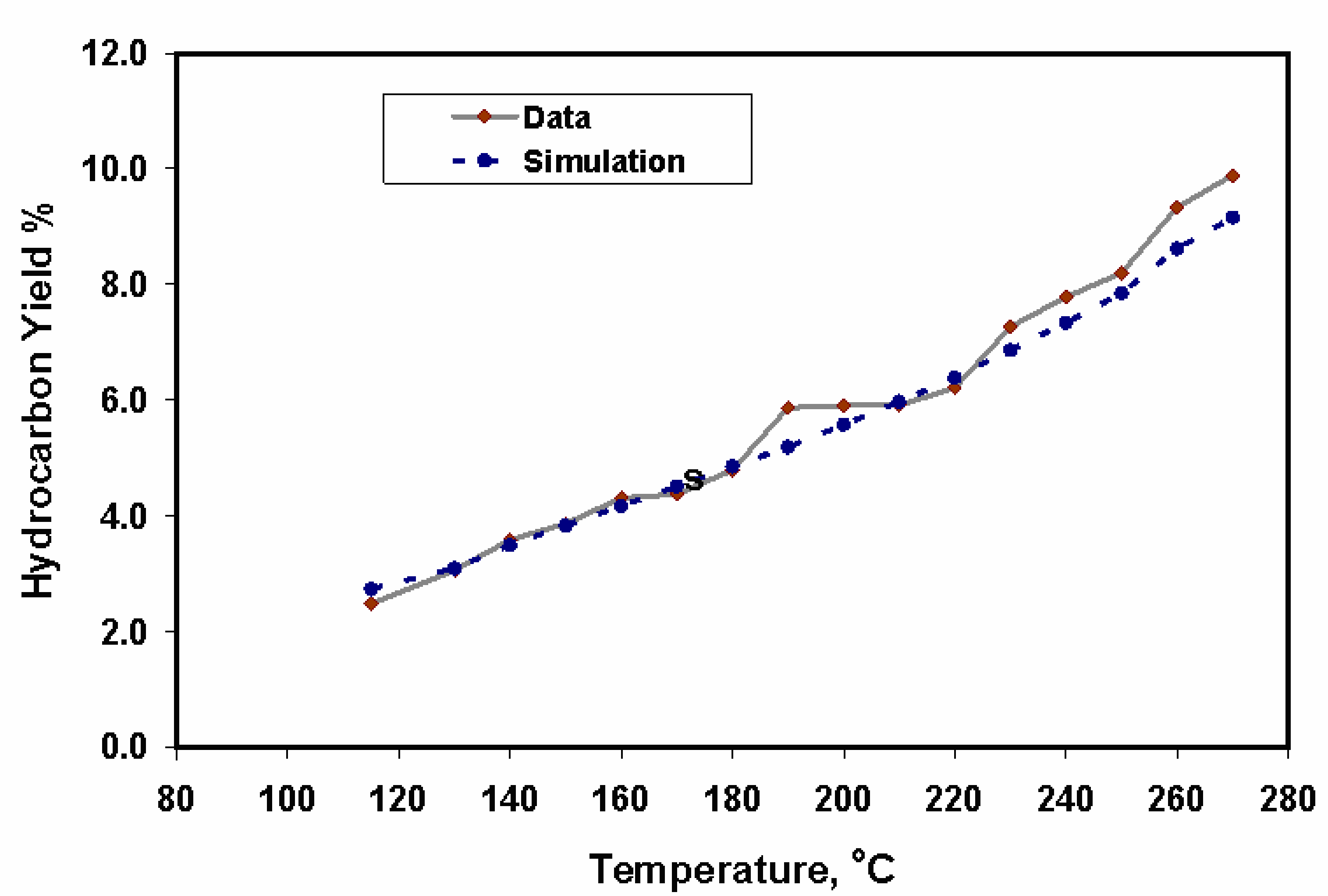

Figure 6.23: Cumulative oil yields for steam propane distillation of crude (Run–2).

6.4 Field Condition (Isobaric) Distillation – (P_{field} and $T_{sat+10C}$)

In this distillation cuts were obtained for temperature from 210°C to 300°C and at constant pressure of 260psig. These pressure conditions are similar to one in field and temperature variation corresponds to incremental increase in crude temperature after steam injection. Two sets of experiments were performed for steam and steam-propane injection at 0.5 ml/min with (5% additive).

6.4.1 Steam Distillation

The yields measured for the two steam distillation runs are shown in the **Table 6.7 – 6.8.** A typical chromatogram for one analysis is shown in the **Appendix B**. The temperature profiles of the two steam distillation runs are shown in **Fig 6.24** and **Fig 6.28**. . The pressure profiles of the two steam distillation runs are shown in **Fig 6.25** and **Fig 6.29**. These plots show good control of temperature during the runs. The fractional oil production at each temperature cut is show in **Fig. 6.26** and **Fig 6.30**.The oil yield plots as a function of temperature for every steam distillation are shown in **Fig 6.27** and **Fig 6.31.** Steam distillation run no. 1 showed an oil recovery of 18.75% at 300ºC with an experimental error of 11.48%. Steam distillation run no. 2 showed a recovery of 18.2% with an experimental error of 8.32% at 300ºC. The experimental error was calculated based on a material balance of oil. From these plots its evident that amount of oil purely distilled off for these conditions is 18 %. Thus, there is not significant amount of oil being distilled for such high temperature and field pressure conditions.

Table 6.7: Oil yields at distillation temperatures and field pressure (Steam distillation-run 1).

Cut. NO.	Temp ^{O}C	Volume of Liquid , ml				Weight of liquid, gms				Fractional Recovery %
		V_{oil}	V_{water}	V_{total}	Cum_{oil}	W_{oil}	W_{water}	W_{total}	Cum_{oil}	
1	230	23.00	7.00	30.00	7.00	23.00	4.07	37.87	4.07	2.375
2	240	10.75	7.25	18.00	14.25	10.75	7.24	28.29	11.31	6.599
3	240	34.00	5.00	39.00	19.25	34.00	2.05	46.90	13.36	7.795
4	250	30.00	7.00	37.00	26.25	30.00	4.79	45.92	18.15	10.589
5	260	37.00	5.00	42.00	31.25	37.00	2.80	51.12	20.95	12.223
6	270	31.50	4.50	36.00	35.75	31.50	2.06	44.32	23.01	13.425
7	280	36.00	4.50	40.50	40.25	36.00	3.65	49.94	26.66	15.554
8	290	36.50	5.50	42.00	45.75	36.50	3.28	51.08	29.94	17.468
9	300	40.50	4.50	45.00	50.25	40.50	2.24	53.77	32.18	18.775

*Initial Oil = 171.4 g

Table 6.8: Oil yields at distillation temperatures and field pressure (Steam distillation-run 2).

Cut. NO.	Temp ^{o}C	Volume of Liquid , ml				Weight of liquid, gms				Fractional Recovery %
		V_{oil}	V_{water}	V_{total}	Cum_{oil}	W_{oil}	W_{water}	W_{total}	Cum_{oil}	
1	228	27.50	4.50	32.00	4.50	26.68	3.62	41.05	3.62	1.776
2	240	23.00	5.00	28.00	11.50	22.31	7.75	40.85	11.37	5.583
3	249	32.00	6.00	38.00	17.50	31.04	2.40	44.25	13.77	6.762
4	260.5	30.50	6.00	36.50	23.50	29.59	5.88	46.25	19.64	9.649
5	270	38.00	4.00	42.00	27.50	36.86	2.22	49.84	21.86	10.739
6	276	31.00	6.00	37.00	33.50	30.07	7.87	48.75	29.73	14.606
7	280	39.00	1.50	40.50	35.00	37.83	1.40	50.05	31.13	15.294
8	290	30.00	12.00	42.00	47.00	29.10	2.26	42.15	33.39	16.404
9	300	43.00	3.50	46.50	50.50	41.71	3.65	56.15	37.04	18.197

*Initial Oil = 203.5 g

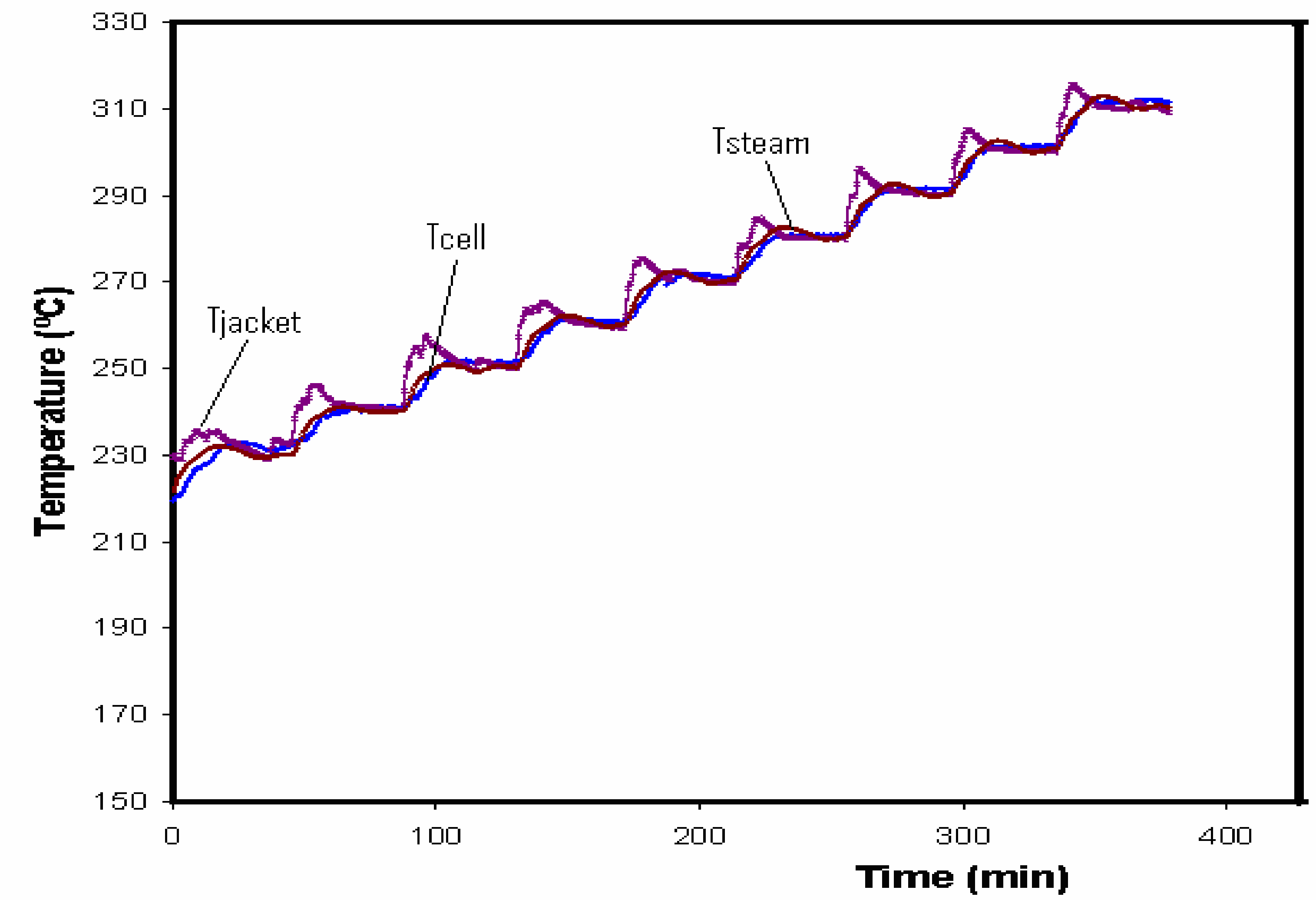

Figure 6.24: Temperature vs time for steam distillation of San Ardo crude (Field) (Run –1).

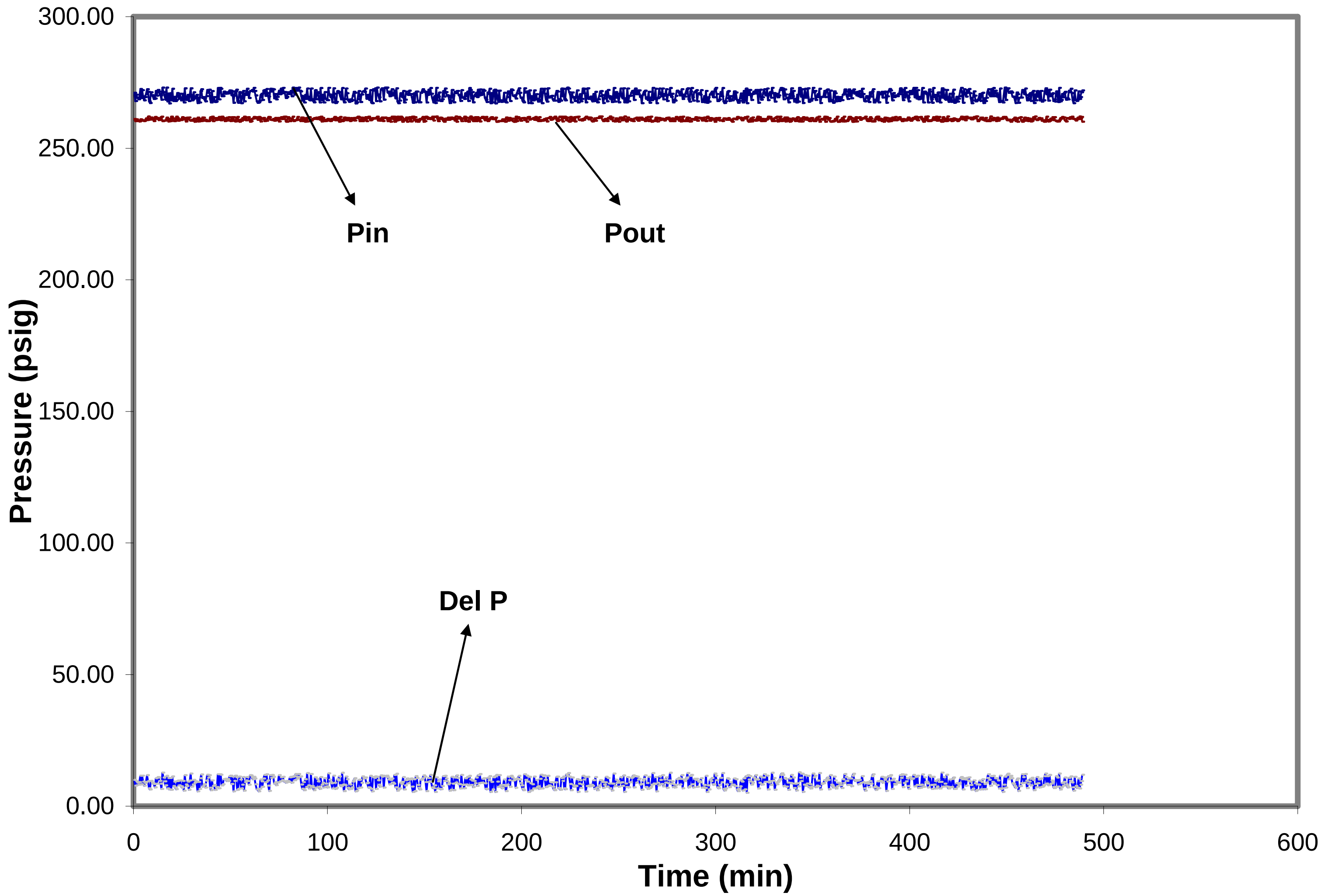

Figure 6.25: Pressure vs time for steam distillation of San Ardo crude (Field) (Run –1).

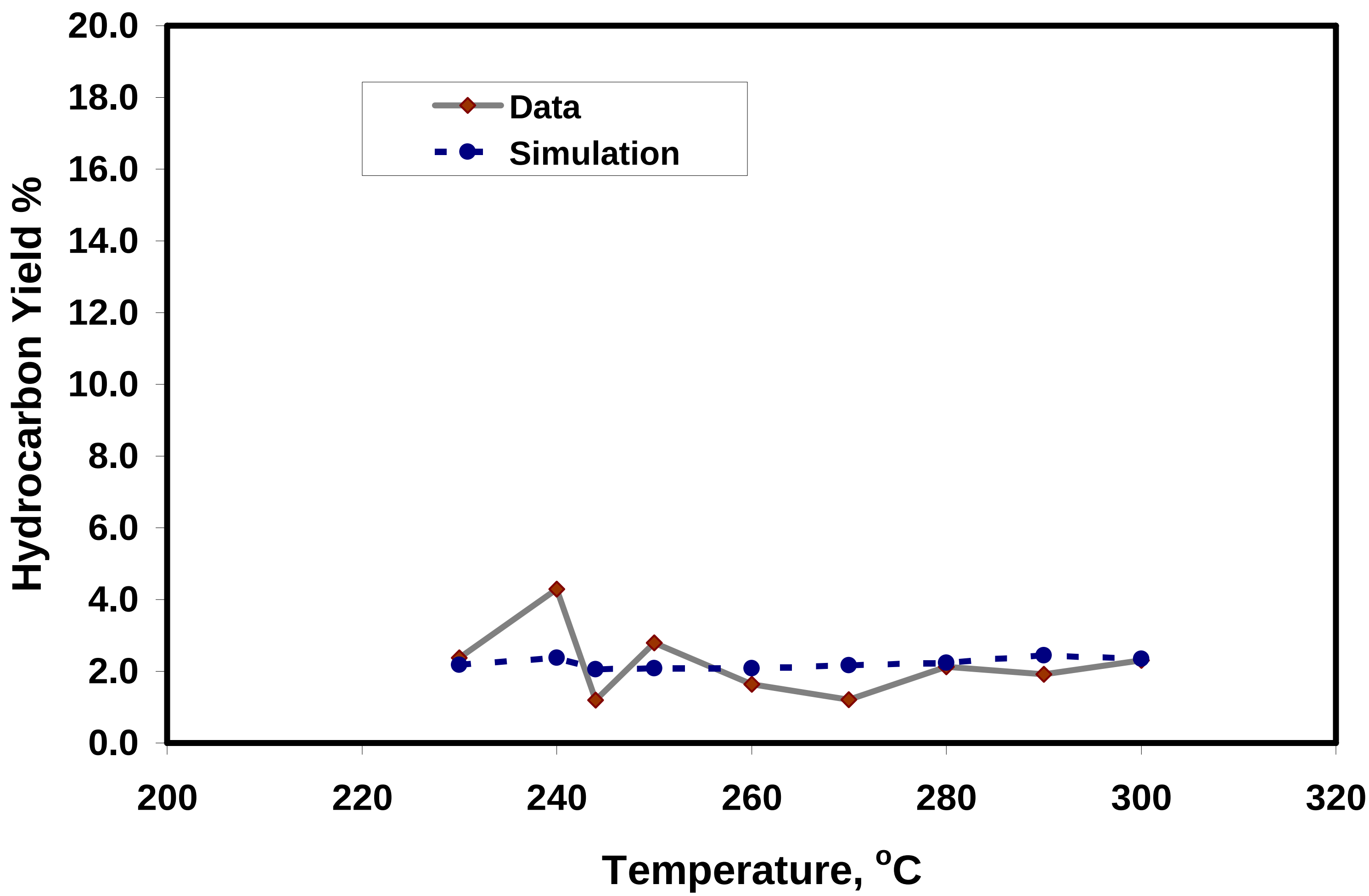

Figure 6.26: Fractional oil rates for steam distillation of San Ardo crude (Run-1).

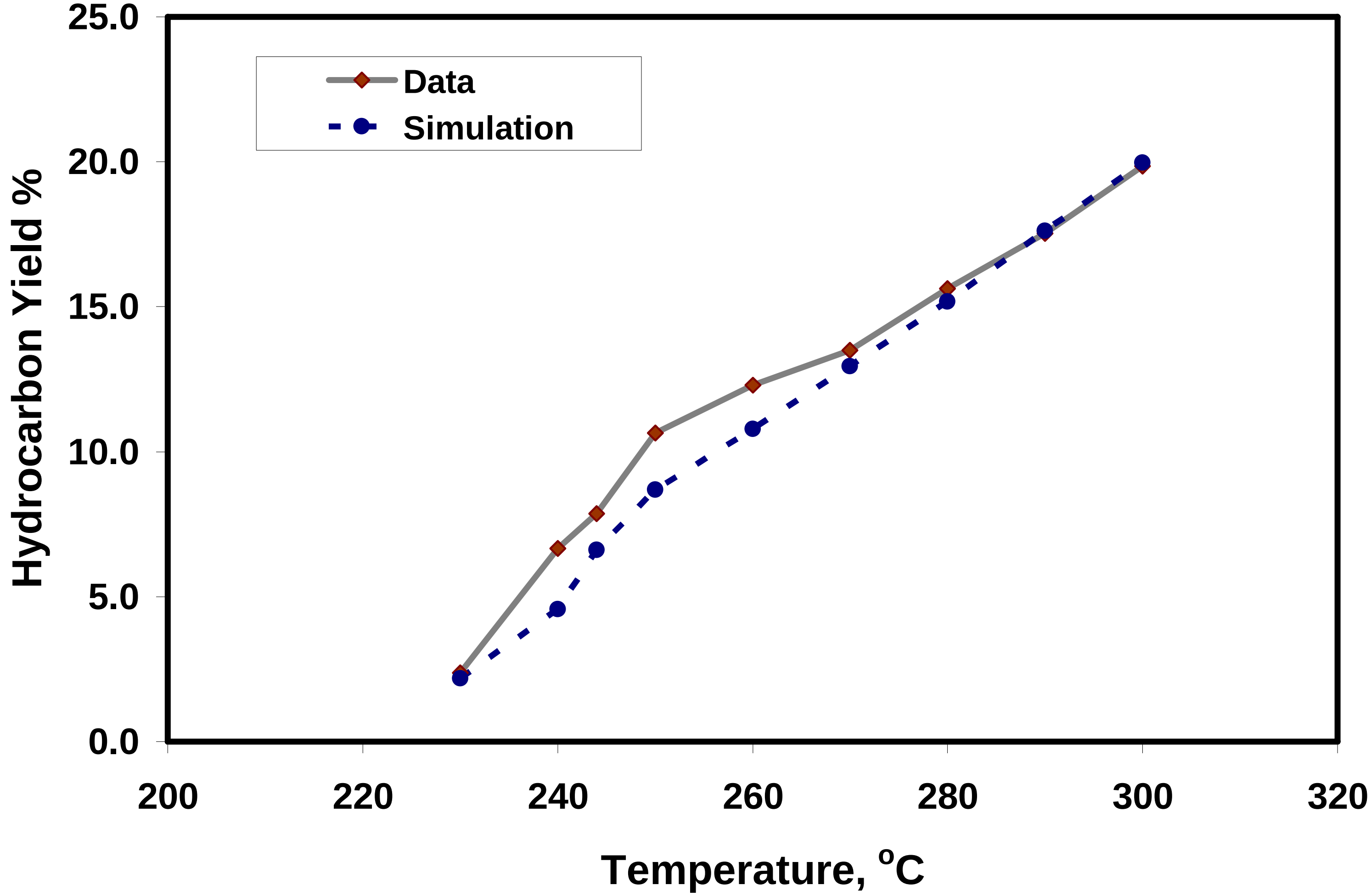

Figure 6.27: Cumulative oil yields for steam distillation of San Ardo crude (Run-1).

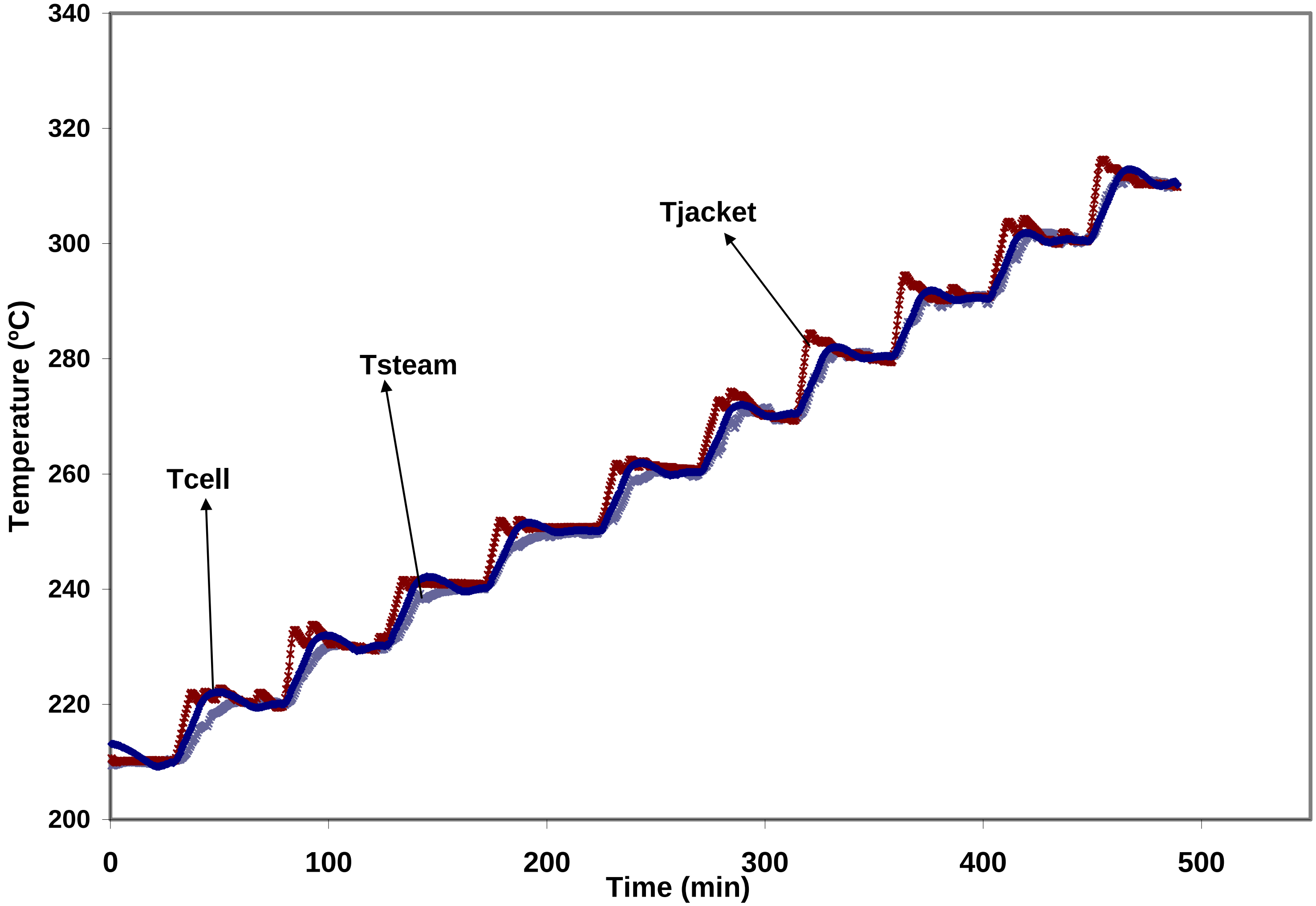

Figure 6.28: Temperature vs time for steam distillation of San Ardo crude (Field) (Run–2).

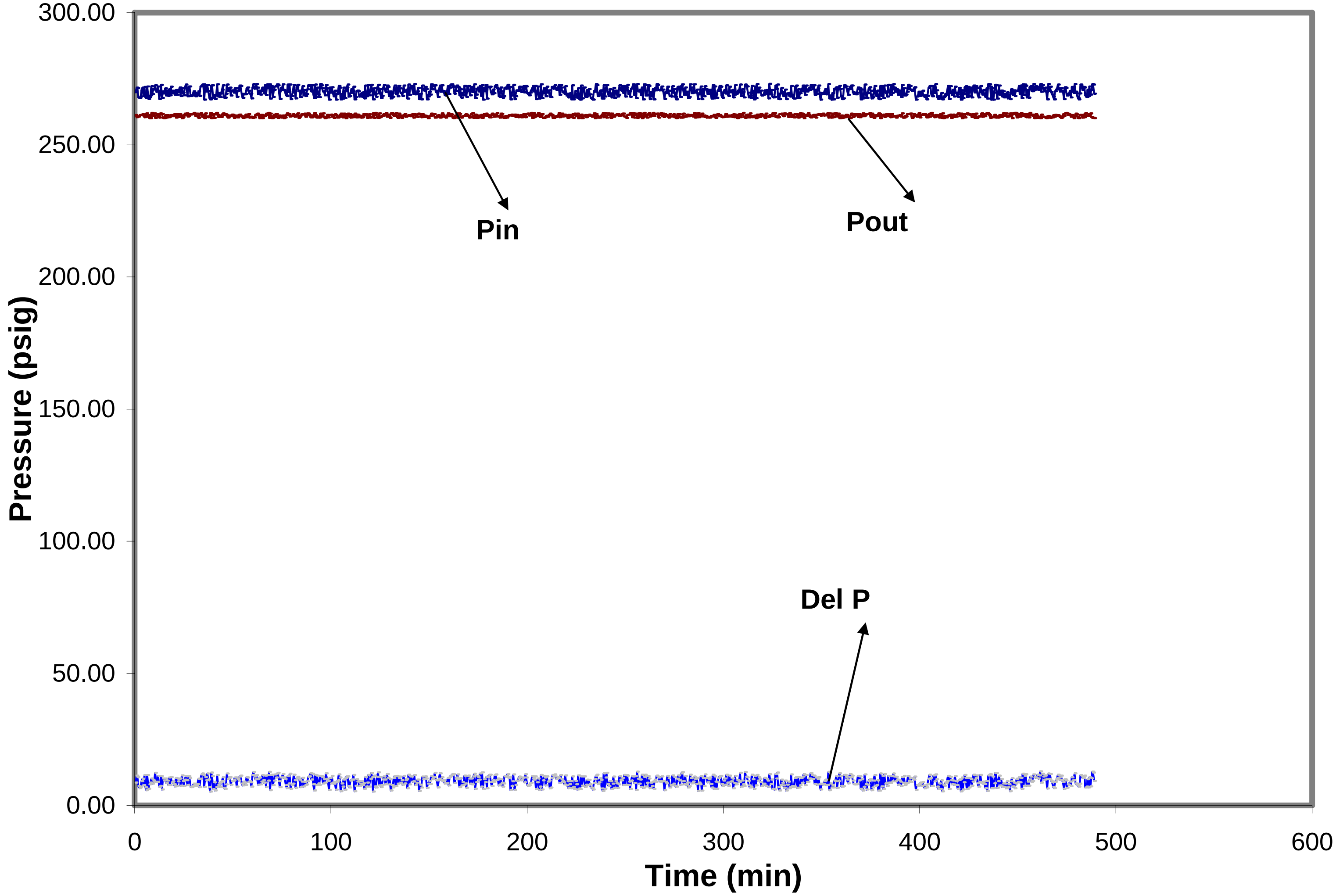

Figure 6.29: Pressure vs time for steam distillation of San Ardo crude (Field) (Run–2).

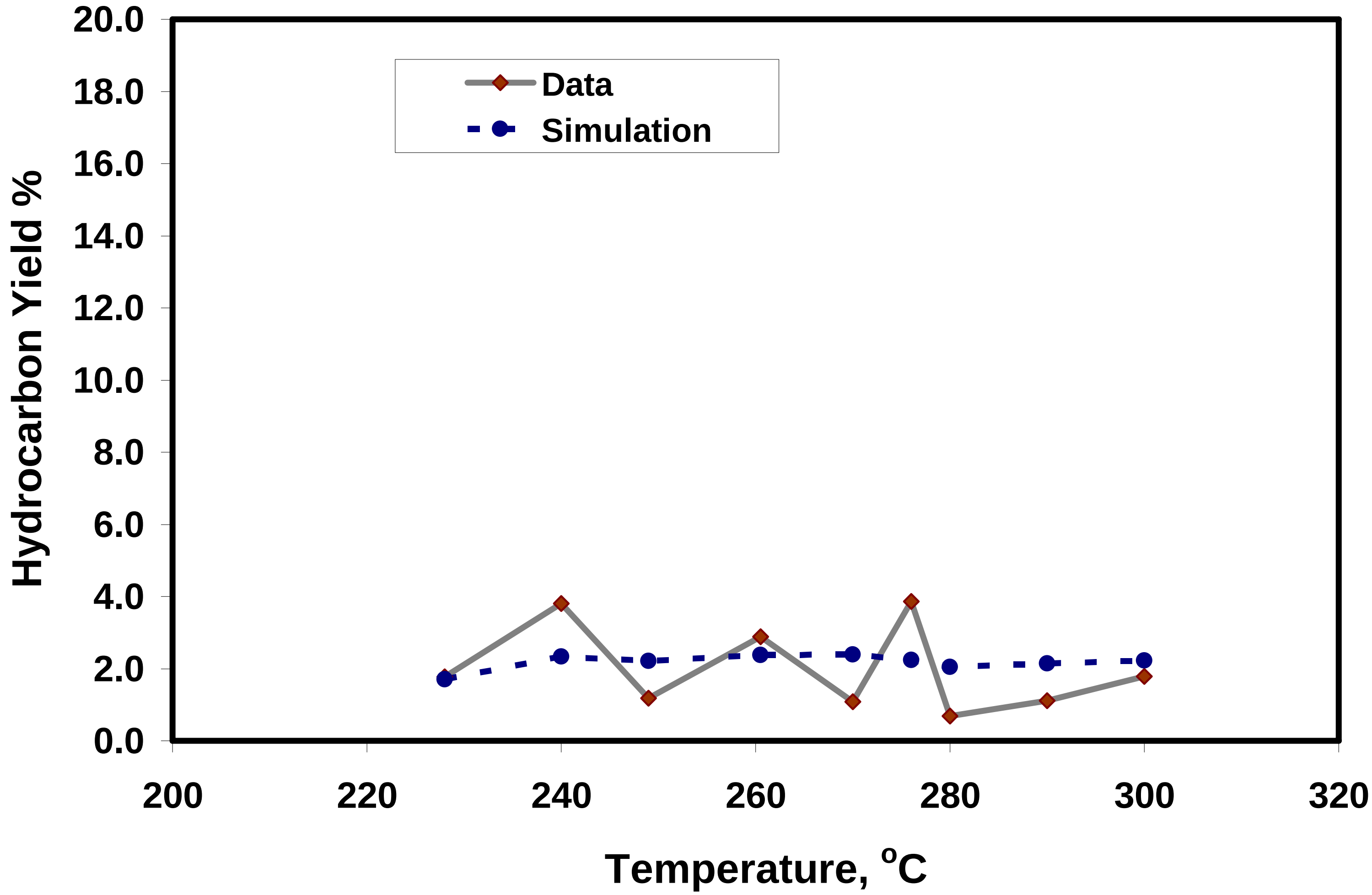

Figure 6.30: Fractional oil rates for steam distillation of San Ardo crude (Run-2).

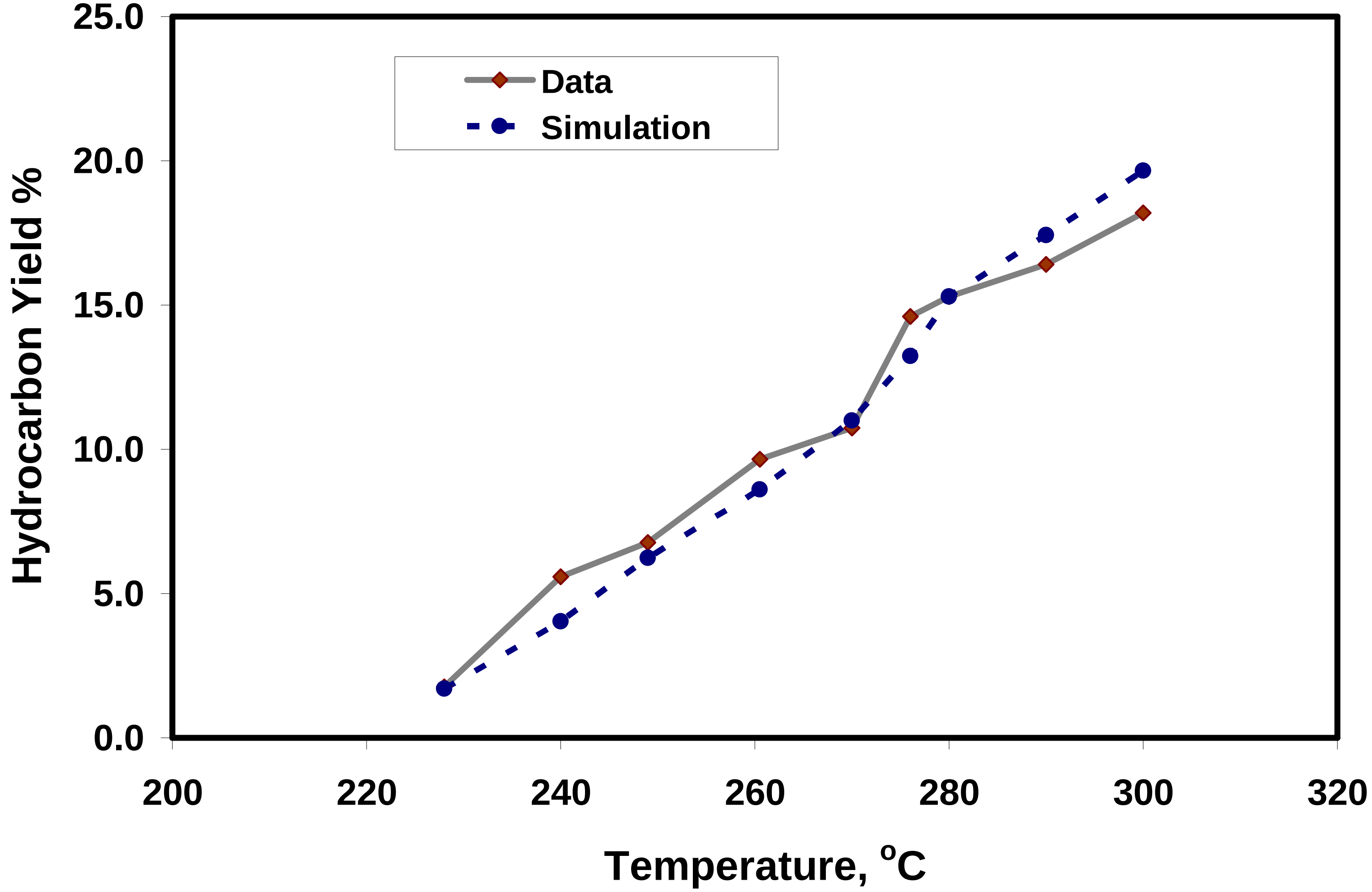

Figure 6.31: Cumulative oil yields for steam distillation of San Ardo crude (Run-2).

6.4.2 Steam-Propane Distillation

Measured distillate yields are summarized in **Table 6.9** and **Table 6.10** for the steam-propane runs. The gas chromatograph analyses (GC) for the hydrocarbon distillate are presented in **Appendix B**. The temperature profiles for this run are shown in **Fig. 6.32** and **Fig. 6.36**. These plots indicate stable of temperatures at each cut during the runs. The pressure profiles for this run are shown in **Fig. 6.33**. The fraction of oil produced at each temperature cut is shown for run 1 and run 2 is shown in **Fig. 6.34** and **Fig. 6.37.** The oil yield plots as a function of temperature for each steam-propane distillation run are shown in **Fig. 6.35** and **Fig. 6.38.** Steam-propane distillation run no. 1 showed an oil recovery of 18.83 % at 300ºC with an experimental error of 11.38%. Steam–propane distillation run no.2 showed an oil recovery of 17.74 % with an experimental error of 10.65% at 300ºC. The experimental error was calculated considering the material balance of oil. From the oil yield plots one can observe that about almost similar amount 18 % of the hydrocarbons is distilled off at around 300ºC, for steam propane than in the steam- or dry distillations processes. The absolute amount of hydrocarbon distilled off in the process is less (~ 18%) Although its more than the Isochronic Isobaric method but, achieving acceleration in production using additives would be difficult process to quantify. Ramirez, (2004)[7] had observed acceleration in production for intermediate hydrocarbons (C6-C10) when synthetic crude was used. However, in San Ardo crude only 4 % of total crude is intermediate hydrocarbons, which can be another possible reason for not observing significant acceleration in production. So the similar experiments should be performed using different additives. The thermodynamic model developed during this study can actually be used predict the effect of other additives on distillation process of steamflood.

Table 6.9: Oil yields at distillation temperatures and field pressure (Steam propane distillation-run 1).

Cut. NO.	Temp ^{O}C	Volume of Liquid , ml				Weight of liquid, g				Fractional Recovery %
		V_{oil}	V_{water}	V_{total}	Cum_{oil}	W_{oil}	W_{water}	W_{total}	Cum_{oil}	
1	230	24.00	6.00	30.00	6.00	24.00	4.06	38.84	4.06	2.256
2	235	11.50	6.00	17.50	12.00	11.50	4.02	26.45	8.08	4.489
3	245	33.00	6.00	39.00	18.00	33.00	4.37	48.12	12.45	6.917
4	250	31.00	6.00	37.00	24.00	31.00	2.66	44.76	15.11	8.393
5	260	38.00	4.00	42.00	28.00	38.00	1.12	49.84	16.23	9.015
6	270	30.00	6.00	36.00	34.00	30.00	7.91	48.77	24.14	13.409
7	280	39.00	1.50	40.50	35.50	39.00	0.26	50.05	24.40	13.554
8	290	30.00	12.00	42.00	47.50	30.00	7.81	49.11	32.21	17.893
9	300	42.00	4.00	46.00	51.50	42.00	1.42	54.55	33.63	18.682

*Initial Oil = 180 g

Table 6.10: Oil yields at distillation temperatures and field pressure (Steam propane distillation-run 2).

Cut. NO.	Temp ^{O}C	Volume of Liquid , ml				Weight of liquid, gms				Fractional Recovery %
		V_{oil}	V_{water}	V_{total}	Cum_{oil}	W_{oil}	W_{water}	W_{total}	Cum_{oil}	
1	229	1.00	28.50	29.50	28.50	2.29	27.65	29.93	2.29	1.10
2	240	5.00	23.00	28.00	11.50	6.79	22.31	29.10	9.08	4.36
3	249	6.50	31.50	38.00	43.00	3.42	30.56	33.97	12.49	6.00
4	257	6.00	30.50	36.50	73.50	4.45	29.59	34.03	16.94	8.14
5	265	4.00	38.00	42.00	111.50	3.21	36.86	40.07	20.15	9.69
6	270	5.50	30.50	36.00	142.00	7.21	29.59	36.79	27.35	13.15
7	279	3.00	32.00	35.00	174.00	5.71	31.04	36.75	33.06	15.89
8	290	12.00	30.00	42.00	204.00	2.24	29.10	31.34	35.30	16.97
9	299	0.50	42.00	42.50	246.00	1.60	40.74	42.34	36.90	17.74

*Initial Oil = 208 gms

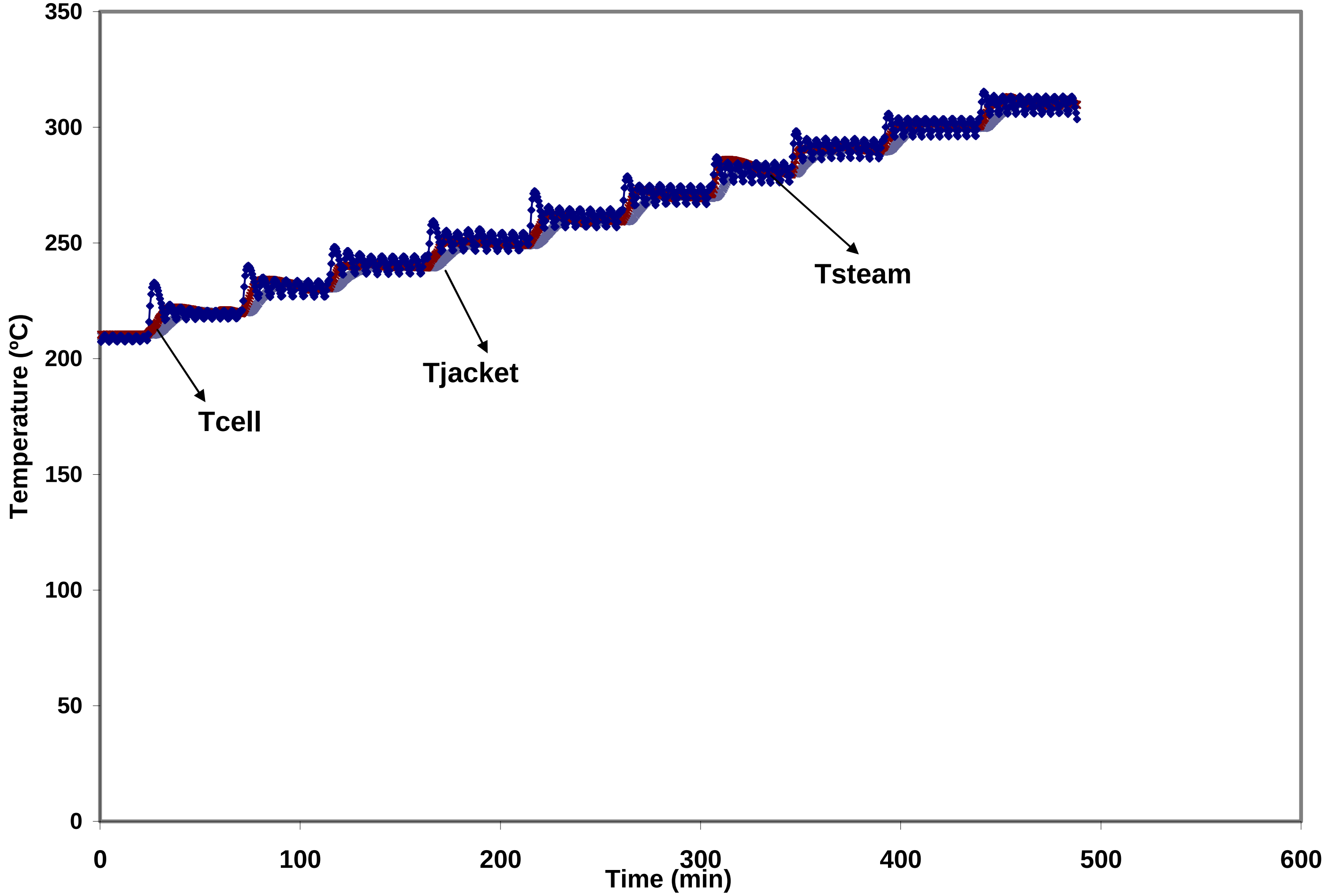

Figure 6.32: Temperature vs time for steam propane distillation (Field) (Run–1).

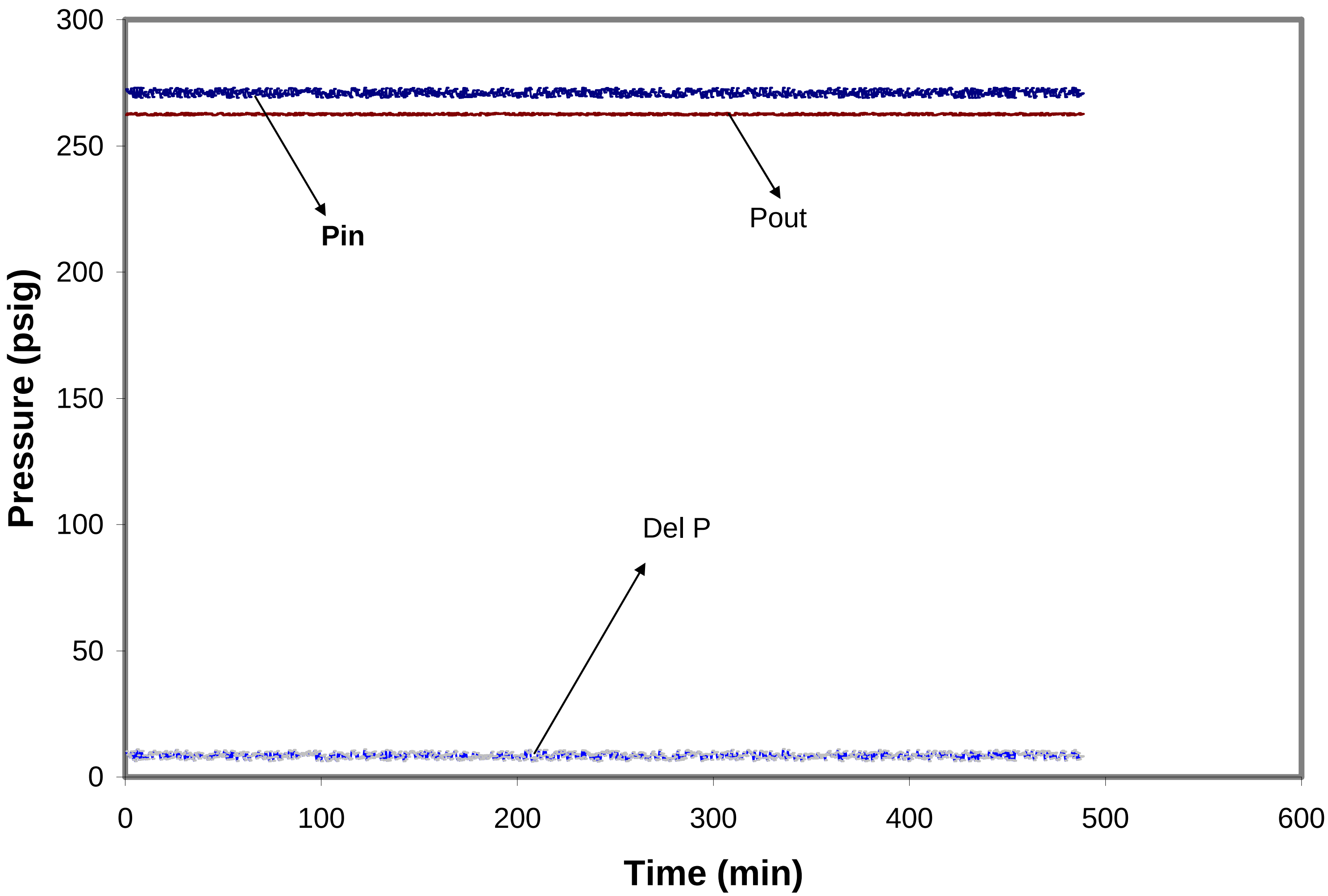

Figure 6.33: Pressure vs time for steam propane distillation (Field) (Run–1).

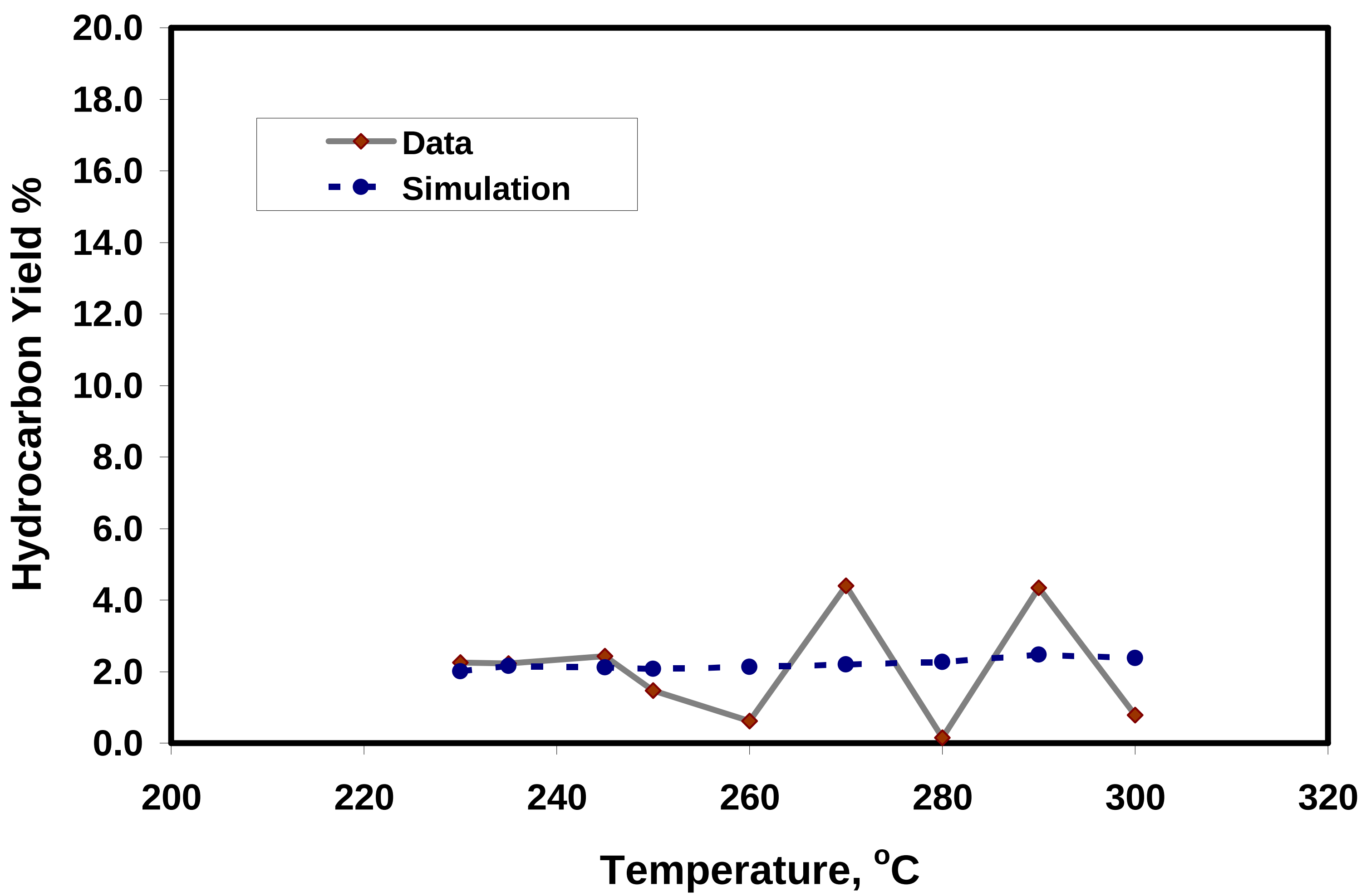

Figure 6.34: Fractional oil rates for steam propane distillation of San Ardo crude (Run-1).

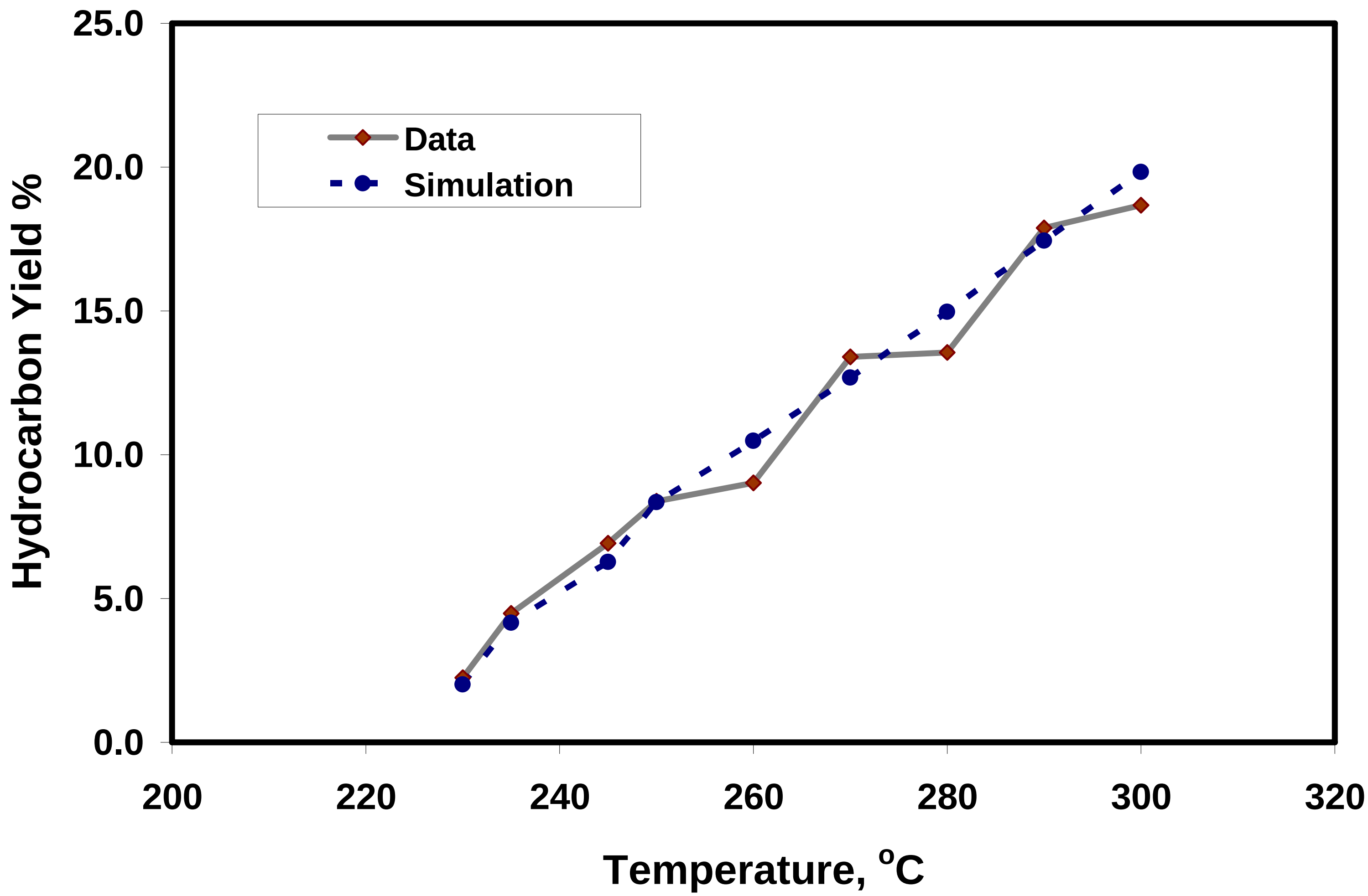

Figure 6.35: Cumulative oil yields for steam propane distillation of San Ardo crude (Run-1).

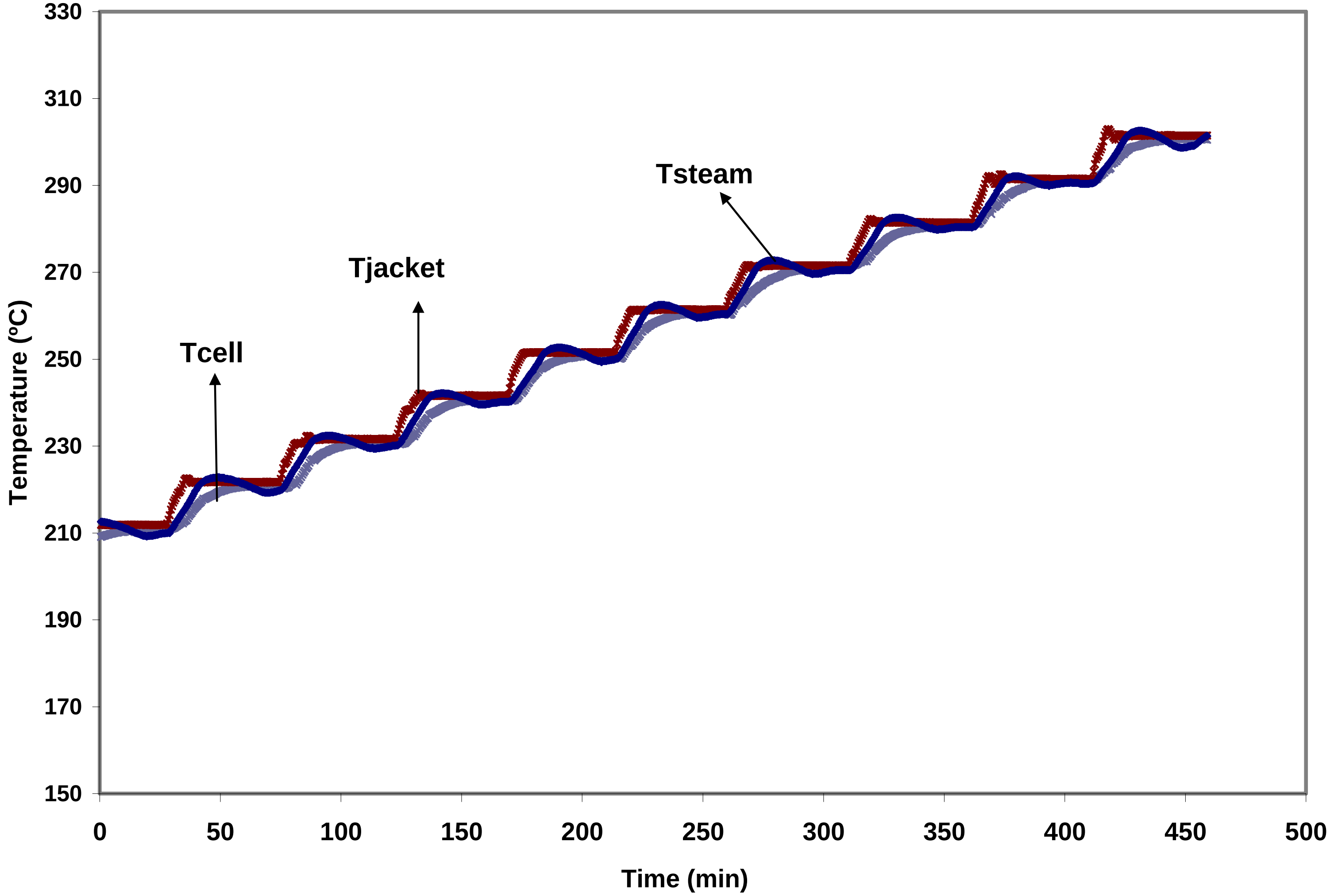

Figure 6.36 : Temperature vs time for steam propane distillation (Field) (Run–2).

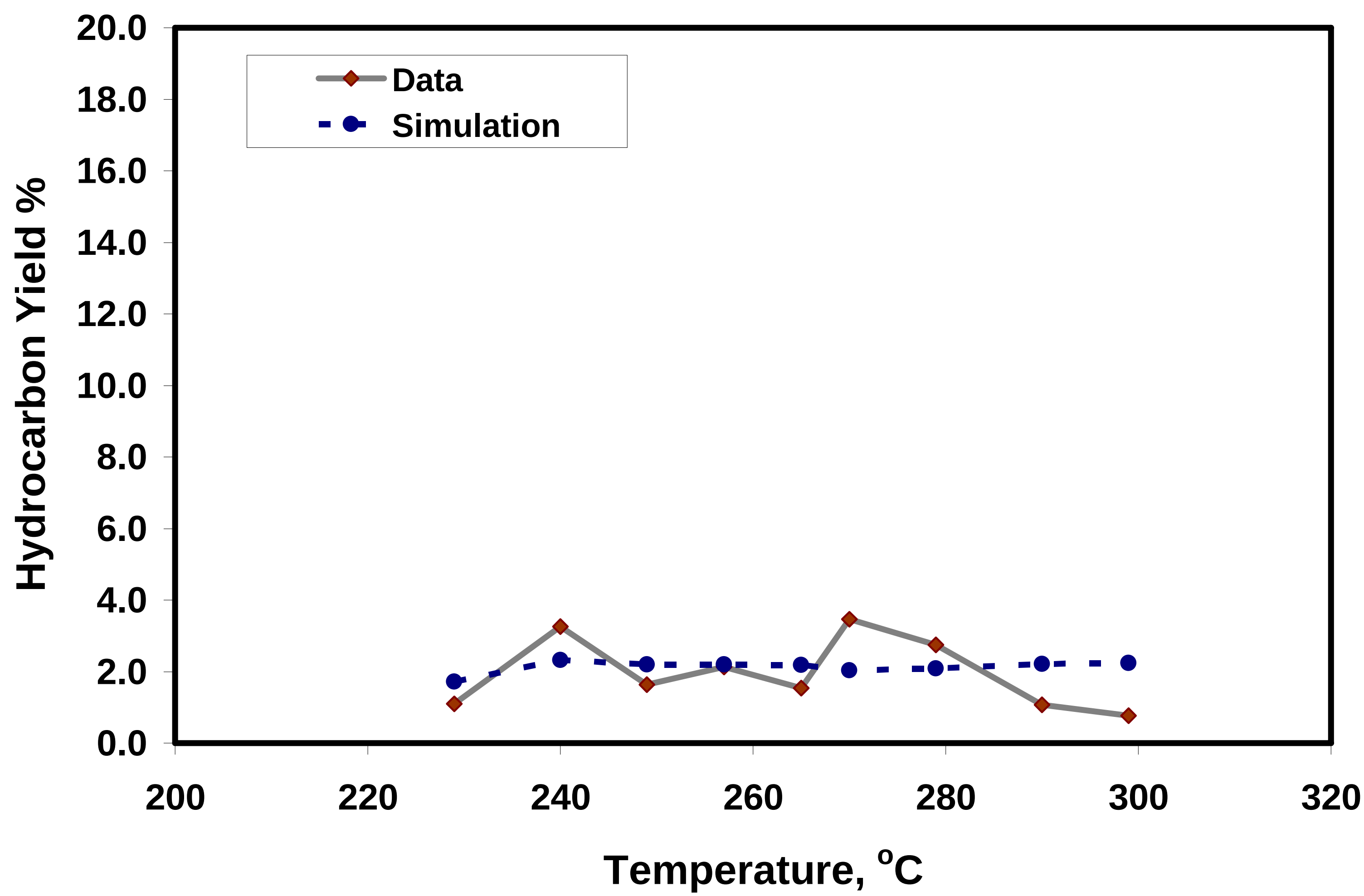

Figure 6.37: Fractional oil rates for steam propane distillation of San Ardo crude (Run-2).

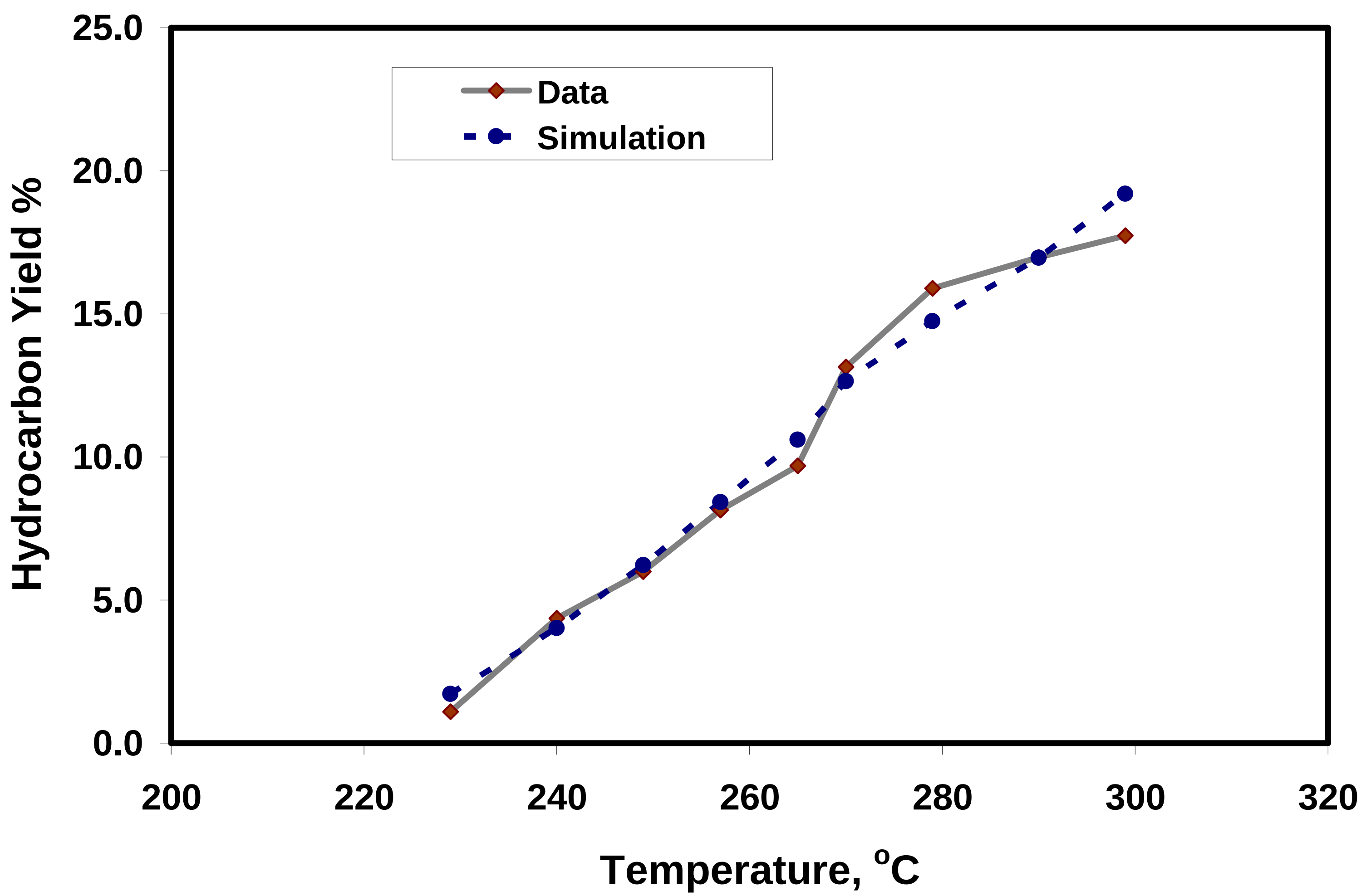

Figure 6.38: Cumulative oil yields for steam propane distillation of San Ardo crude (Run– 2).

6.5 Comparison and Discussion of Experimental Results

The individual run oil yields for each distillation run and type are shown in **Fig. 6.39** and **Fig. 6.40**. As can be seen from these plots, the oil yield with steam-propane distillation is similar to that with steam distillation. From these plots one can see that the steam-propane distillation gives same yields as steam. The yields for steam distillation for saturated condition and field condition is merely 10% and 18% respectively. Ramirez, (2004)[7] had observed acceleration in production for intermediate hydrocarbons (C_6-C_{10}) when synthetic crude was used[7]. However, in San Ardo crude only ~ 4 % of total crude is intermediate hydrocarbons and 0.5% of component which showed acceleration for Ramirez, (2004)[7]. There is no significant interaction of propane and higher hydrocarbons. Although, literature suggest propane interacts very well with normal hydrocarbons (Alkanes), heavy oils are usually biodegraded and devoid of significant normal hydrocarbons. Moreover, with so low yield, achieving significant acceleration in production using additives would be a difficult process to quantify, where transport mechanism is vaporization only. Thus, these two important reasons can be attributed for not observing significant acceleration in production/distillation effects.

It is proposed that similar experiments should be performed using different steam additives such as petroleum distillate, hexane. The thermodynamic model developed during this study can actually be used predict the effect of other additives on distillation process of steamflood in several minutes

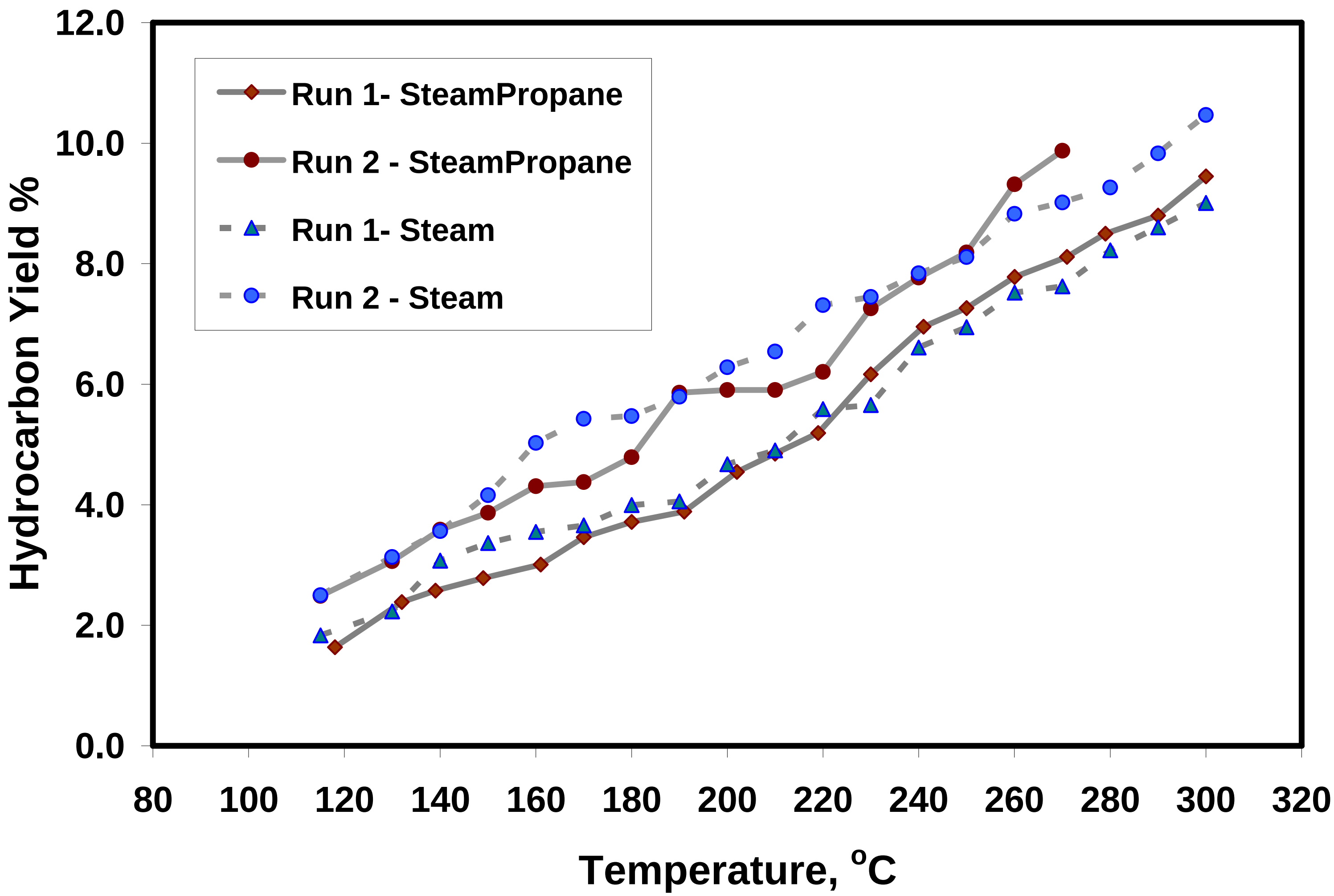

Figure 6.39: **Comparative study for steam and steam propane distillation data at Tsat + 15°C, Psat conditions.**

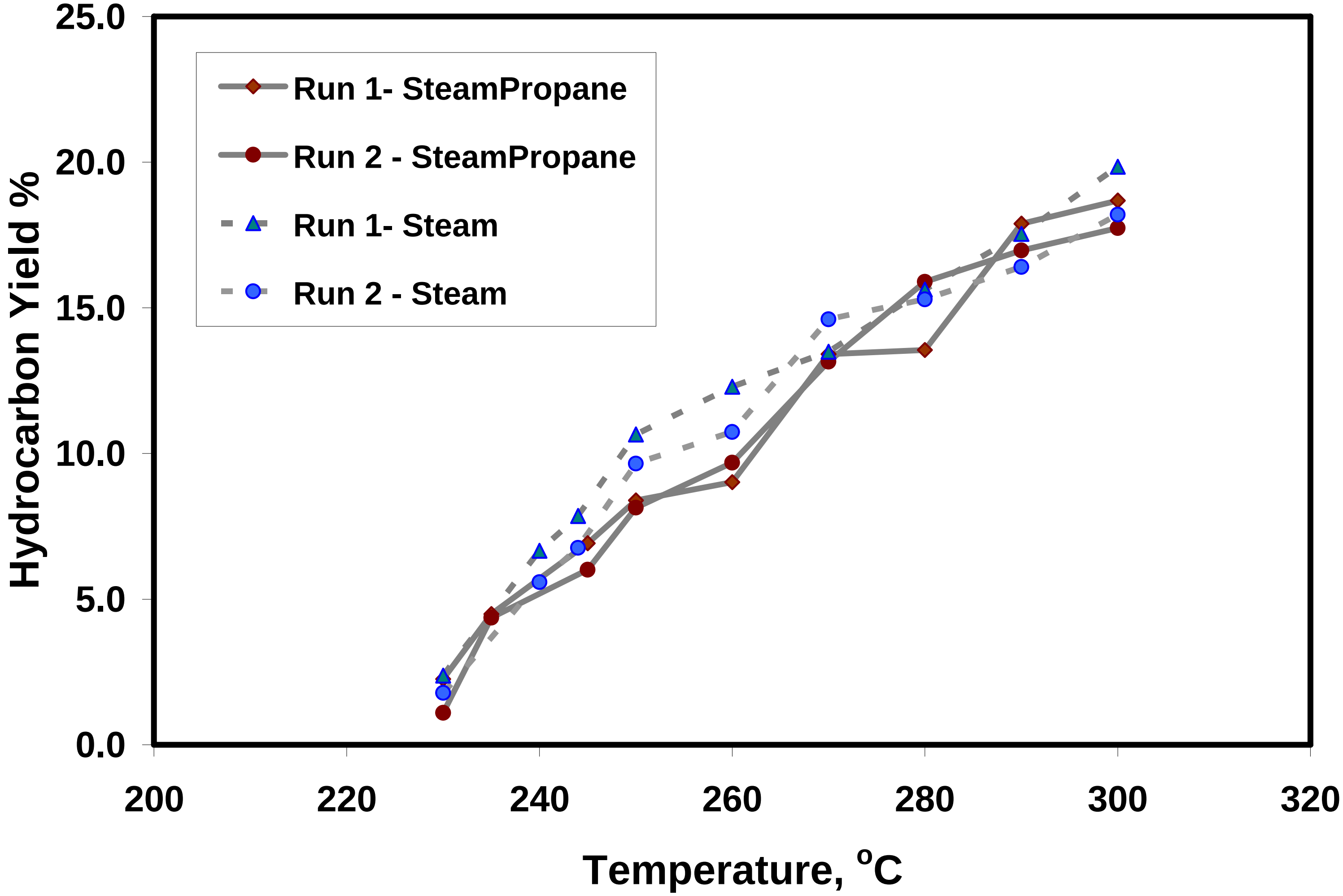

Figure 6.40: Comparison of steam and steam propane distillation data at Field conditions (260 psig).

CHAPTER VII

SUMMARY, CONCLUSIONS AND RECOMMENDATIONS

The overall objective of this research was to investigate the effect of propane as a steam additive on the distillation yield of crude oils in general and San Ardo oil in particular

7.1 Summary

Distillation experiments were performed using a San Ardo crude oil. Three distillation processes were used: dry-, steam-, and steam-propane (PSR 0.05). Dry distillation experiments were carried out at one atmosphere, temperature range of 115°-300°C. Steam- and steam-propane distillation experiments were conducted at the following conditions,

a. Superheated steam conditions (15°C above T_{sat}), temperature/pressure range of 115°C/0 psig - 300°C/998 psig.
b. Field conditions (260psig), temperature range of 220°C – 300°C

Produced hydrocarbon distillate weight and composition were determined. New thermodynamic model was developed to quantify the effect of propane on distillation of the crude. The model was validated for synthetic crude oil and for San Ardo crude oil.

7.2 Conclusions

Based on the experimental results and analysis of the data, the following conclusions may be drawn.

a. Steam distillation yields for saturated conditions of T_{sat+15}°C and P_{sat} is 10 % and with addition of 5 wt% of propane to steam there is no significant increase in distillation yields.
b. Steam distillation yields for field conditions of 260 psig and temperature of range (220 ~300°C) is 18 % and with addition of 5% of propane to steam there is no significant increase in distillation yields.

c. A thermodynamic model was developed, which requires only composition of crude oil to carry out distillation effect study. The model was validated using literature data and compared with experimental results in this study.

d. Based on distillation yields, fraction of crude oil in intermediate range will determine lowering of hydrocarbon boiling points or increase distillation yield by steam-propane injection.

7.3 Recommendations

a. Propane may not be the only or ideal steam additive. It is therefore recommended to investigate the effect of other alkanes on distillation yield (C_2, n-C_4, n-C_5, etc.) or a "cocktail" of the light n-alkanes.

b. Perform distillation experiments using more hydrocarbon components– including varying the proportion of the components, before proceeding to using crude oils to fully understand the process.

c. Understanding the effect of oil typing and this can help in determine the need for modification in thermodynamic model..

NOMENCLATURE

ACRONYMS

EOS Equation of State

PF Poynting Factor

LETTERS

A	$=a_T P/R^2T^2$, derived parameter of Peng-Robinson EOS
A'_j	derived parameter of Peng-Robinson EOS for mixtures
a_c	attraction parameter of Peng-Robinson EOS at critical conditions, (atm liters^2 ^{o}K/gmol), (psia ft^3 ^{o}R/lbmol)
a_T	attraction parameter of Peng-Robinson EOS, (liters/gmol)^2, (ft^3/lbmol)^2
B	$= bP/RT$, derived parameter of the Peng-Robinson EOS
B'_j	derived parameter of Peng-Robinson EOS for mixtures
b	residual volume parameter of the Peng-Robinson EOS, liters/gmol, ft^3/lbmol
b_i	residual volume parameter of the Peng-Robinson EOS of species i in a mixture, liters/gmol, ft^3/lbmol
F	total mass or mol number of a system
f	fugacity, bar, Torr, psia, atm
f_g	gas fugacity, bar, Torr, psia, atm
f_L	liquid fugacity, bar, Torr, psia, atm
G	specific Gibbs energy, Kjoules/gmol
K_i	$= y_i/x_i$, vaporization equilibrium ratio
K_i^C	$= y_i/x_i$, vaporization equilibrium ratio calculated
K_i^T	$= y_i/x_i$, trial vaporization equilibrium ratio
L	amount of a liquid phase, mass, or mol number, gmols or grams
m	parameter of Peng-Robinson EOS as acentric factor function and reduced temperature
n	number of the species in the system
P	pressure of a system, bar, Torr, psia, atm
P_c	critical pressure, bar, Torr, psia, atm

P_i	partial pressure of a species *i*, bar, Torr, psia, atm
R	gas constant
T	temperature, °K, °R, °C, °F
T_c	critical temperature
V	amount of vapor phase, gmols or grams
V_M	specific volume in Peng-Robinson equation, liters/gmol, liters/kg, ft^3/lbmol, ft^3/lb
x_i	mol fraction of a species in a liquid-phase mixture
y_i	mol fraction of a species in a vapor-phase mixture
z_g	gas compressibility factor
z_i	mol fraction of a species in all phases of a system
z_L	liquid compressibility factor
z	$= PV/RT$, compressibility factor

GREEK LETTERS

α	parameter of Peng-Robinson EOS
β	mol fraction vaporized
γ_i	activity coefficient of species *i*
δ_{ij}	binary interaction parameters for Peng-Robinson EOS
ε	objective function
ϕ_i	$= f_i/P$, fugacity coefficient of a specie *i* in a mixture
ϕ_i^V	$= f_i/P$, fugacity coefficient of a specie *i* in a vapor phase mixture
ϕ_i^L	$= f_i/P$, fugacity coefficient of a specie *i* in a liquid phase mixture
ω	acentric factor

SUBSCRIPTS

i	identifying a species in a mixture, as in x_i

SUPERSCRIPTS

k	iteration index
sat	property at saturation conditions, as in P^{sat} = vapor pressure

V	vapor phase
L	liquid phase

REFERENCES

1. Willman, B.T. et al.: "Laboratory Studies of Oil Recovery by Steam Injection," JPT (June 1961) 731.
2. Simangunsong, R.: "Experimental and Analytical Modeling Studies of Steam Injection with Hydrocarbon Additives to Enhance Recovery of San Ardo Heavy Oil" M.S. Thesis, Texas A&M University, College Station, TX (2005).
3. Rivero, J.A.: "Experimental Studies of Enhancement of Injectivity and in-situ Oil Upgrading by Steam Propane Injection for the Hamaca Oil Field," M.S. Thesis, Texas A&M University, College Station, TX (2003).
4. Nesse, T.: "Experimental Comparison of Hot Water/Propane Injection to Steam/Propane Injection for Recovery of Heavy Oil," M.S. Thesis, Texas A&M University, College Station, TX (2004).
5. Plazas, P.G.: "Experimental Study of Oil Fields and Properties of Light and Medium Venezuelan Crude Oils under Steam and Steam Propane Distillation," M.S. Thesis, Texas A&M University., College Station, TX (2002).
6. Simangunsong, R., Jaiswal, N.J., and Mamora, D. D.: "Improved Analytical Model and Experimentally Calibrated Studies of Steam Injection with Hydrocarbon Additives to Enhance Heavy Oil Recover," paper 100703 presented at the 2006 SPE Annual Technical Conference and Exhibition held in San Antonio, TX, 24–27 September 2006.
7. Ramirez, M. A., "Experimental and Analytical Studies of Hydrocarbon Yields under Dry-, Steam-, and Steam with Propane-Distillation," Ph.D. Dissertation, Texas A&M University, College Station, TX (2004).
8. Green, D and Willhite, G.P.: *Enhanced Oil Recovery*, Textbook Series, SPE, Richardson, TX (1998) 6, 1.
9. Sarathi, P. S.; Roark, D.; Strycker, A. R. "Light Oil Steamflooding A Laboratory Study," SPE 17447 presented at th 58th Annual California Regional Meeting of the SPE., Bakersfield, CA, March 23-25, 1988, 431-442.
10. Shu, W. R. "A Viscosity Correlation for Mixtures of Heavy Oil, Bitumen, and Petroleum Fractions," *Soc. Pet. Eng. J.* 1984, Jun, 277-292.

11. Marx, J. W., and Langenheim R. H.: "Reservoir Heating by Hot Fluid Injection," *Trans. AIME*, **216**:312-315, 1959.

12. Volek, C.W. and Pryor, J.A.: "Steam Distillation Drive – Brea Field, California," *JPT* (August 1972) 899.

13. Wu, C.H. and Brown, A.: "A Laboratory Study on Steam Distillation in Porous Media," paper 5569 presented at the 1975 SPE Annual Meeting, Dallas, TX, 28 September-1 October.

14. Holland, C.D. and Welch, N.E.: "Steam Batch Distillation Calculations", *Petroleum Refiner* (May 1957) 251.

15. Sukkar, J.K.: "Calculation of Oil Distilled during Steam Flooding of Light Crude," paper 1609 presented at the 1966 SPE of AIME Annual Meeting, Dallas, TX, 2-5 October.

16. Barb, D.K.: Solution of Problems Involving the Separation of Multi-Component Mixtures by Batch Distillation, Ph.D. Dissertation, Texas A&M University, College Station, TX (1967).

17. Johnson, F.S., Walker, C.J. and Bayazeed, A.F.: "Oil Vaporization during Steamflooding" *JPT* (July 1971) 731.

18. Alikhan, A.A. and Ali, S.M.F.: "Heavy Oil Recovery by Steam-Driven Hydrocarbon Slugs from Linear Porous Media," paper 5019 presented at the 1974 SPE of AIME, Houston, TX, 6-9 October.

19. Rhee, S.W. and Doscher, T.M.: "A Method for Predicting Oil Recovery by Steamflooding including the effects of Distillation and Gravity Override," *Soc. Pet. Eng. J.* (Aug. 1980) 249-266.

20. Wu, C.H. and Elder, R.B.: "Correlation of Crude Oil Steam Distillation Yields with Basic Crude Oil Properties," *SPEJ* (December 1983) 937.

21. Wu, C. H. and Elder, R.B.: U.S.DOE Final Report 1980, DOE/ET-12357-3, pp 7-16.

22. Duerksen, J.H. and Hsueh, L.: "Steam Distillation of Crude Oils," *Soc.Pet. Eng. J.* (April 1983) 265-269.

23. Langhoff, J.A. and Wu, C.H.: "Calculation of High Temperature Crude Oil/Water/Vapor Using Simulated Distillation Data," *SPERE* (Sept. 1986) 483-489.

24. Billman, A.L.: "Estimation of 3-Phase Separation K-Values using Laboratory 3-Phase Separation Tests," M.S. Thesis, Texas A&M University, College Station, TX (Dec. 1989).

25. Goite, J.G., Mamora, D.D. and Fergurson, M.A.: "Experimental Study of Morichal Heavy Oil Recovery Using Combined Steam and Propane Injection," paper 69566 presented at the

2001 SPE Latin American and Caribbean Petroleum Engineering Conference, Buenos Aires, 25–28 March.

26. Lanclos, R.P.: A Three-Phase K-Value Study for Pure Hydrocarbon/Water and Crude Oil/Water Systems, M.S. Thesis, Texas A&M University, College Station, TX (Dec. 1990).
27. Lim, K.T.: "Steam Distillation Effect and Oil Quality Change during Steam Injection," M.S. Thesis, Standford University, Palo Alto, CA (1991).
28. Forero, R.: "Three-Phase K-Values for n-Alkanes Co-Existing with Water at High Temperatures," M.S. Thesis, Texas A&M University, College Station, TX (May 1992).
29. Mokrys, I.J. and Butler, R.M.: "In-situ Upgrading of Heavy Oils and Bitumen by Propane Deasphalting: the Vapex Process," paper 25452 presented at the 1993 SPE Production and Operations Symposium, Oklahoma City, OK, 21-23 March.
30. Espie, A.A. et al.: "An Evaluation of Oil Recovery by Vaporization," paper 27812 presented at the SPE/DOE Ninth Symposium on Improved Oil Recovery, Tulsa, OK, 17-20 April, 1994.
31. Beladi, M.K.: "Three-Phase Hydrocarbon/Water Separation and K-Values," Ph.D. Dissertation, Texas A&M University, College Station, TX (Dec. 1995).
32. Tandia, B.K.: "A New Comprehensive Semiempirical Approach to Calculate Three-Phase Water/Hydrocarbons Equilibria," M.S. Thesis, Texas A&M University, College Station, Texas (Dec. 1995).
33. Goite, J.G.: "Experimental Study of Morichal Heavy Oil Recovery Using Combined Steam and Propane Injection," M.S. Thesis, Texas A&M University., College Station, TX (1999).
34. Mamora, D.D. and Sutadiwiria, G.: "An Analytical Model for Light Oil Recovery by Steam Distillation," paper 54094 presented at the 1999 SPE International Thermal Operations and Heavy Oil Symposium, Bakersfield, CA, 17-19 March.
35. Ferguson, M.A., Mamora, D.D., and Goite, J.G.: "Steam-Propane Injection for Production Enhancement of Heavy Morichal Oil," paper 69689 presented at the 2001 International Thermal Operations and Heavy Oil Symposium, Porlamar, Venezuela, 12-14 March.
36. Tinss, J.C.: "Experimental Studies of Steam-Propane Injection to Enhance Recovery of an Intermediate Crude Oil," M.S. Thesis, Texas A&M University, College Station, TX (2001).
37. Walas, S.M.: *Phase Equilibria in Chemical Engineering*, McGraw-Hill Book Co., New York (1985).

38. Maitland, G.C., Rigby, M., Smith,E.B., Wakeham, W.A., I*ntermolecular Forces: Their Origin and Determination*, Clarendon Press, Oxford, 1981.
39. Hsueh, L; Hong, K. C.; Duerksen, J.H.: "Simulation of High Pressure and High Temperature Steam Distillation of Crude Oils," 2^{nd} UNITAR Int. Conference on Heavy Crude and Tar Sands, Caracus, Venezuela, 1982, 924-935.
40. Rachford, H.H. and Rice, J.D.: "Procedure for Use of Electronic Digital Computers in Calculating Flash Vaporization Hydrocarbon Equilibrium," *Trans. Soc. Pet. Eng*., **195** 327-337, 1952.
41. Smith, J.M. and Van Ness, H.C.: *Introduction to Chemical Engineering Thermodynamics*, fourth edition, McGraw-Hill Book Co., New York (1987).
42. McCain, W.D.: *The Properties of Petroleum Fluids*, second edition, PennWell Publishing Co., Tulsa, OK (1990).
43. Sandler, S.I.: *Chemical and Engineering Thermodynamics*, second edition, John Wiley & Sons, Inc., New York, (1989).
44. Peng D.Y. and Robinson, D.B., *I.E.C. Fund*., **15**, 59(1976).
45. Robinson, D.B., Kalara, H., and Rempis, H.: "The Equilibrium Phase Properties of a Synthetic Sour Gas Mixture and a Simulated Natural Gas Mixture," GPA Research Report No. RR-31, Tulsa, OK, May 1978.
46. Knapp. H. et al.: *Vapor-Liquid Equilibria for Mixtures of Low Boiling Substances*, DECHEMA Chemistry Data Series, Vol. VI, Scholium Intl Frankfurt/Main, (1982).
47. Orbey, H. and Sandler, S.I.: *Cubic Equations of State and Their Mixing Rules*, Cambridge University Press, Cambridge, (1998).
48. Firoozabadi, A.: *Thermodynamics of Hydrocarbon Reservoirs*, first edition, McGraw-Hill Book Co., New York (1999).
49. Prausnitz, J.M. et al.: *Computer Calculations for Multicomponent Vapor-Liquid and Liquid-Liquid Equilibria*, first edition, Prentice-Hall, Inc., Lebanon, Indiana (1980).
50. Northrop, P. S. and Venkatesan, V. N.: "Analytical Steam Distillation Model for Thermal Enhanced Oil Revocery Processes," *Ind. Eng. Chem, Res*., 1993, **32**, 2039-2046.
51. Winkle, V. M.: "*Vapor-Liquid Equilibria in Distillation,"* McGraw-Hill; New York, 1967; pp 178-185.

52. Lolley, C.S., and Richardson, W.C.: "Compositional Input for Reservoir Simulation of Heavy Oils with Application to the San Ardo Field," paper SPE 37538 presented at the 1997 SPE International Thermal Operations and Heavy Oil Symposium, Bakersfield, CA, 10-12 February.
53. Aguilar, R. A. and McCain, W. D.: "An Efficient Tuning Strategy to Calibrate EOS for Compositional Simulation," paper 77382 presented at the 2002 SPE Annual Technical Conference and Exhibition, San Antonio, TX, 29 Sept – 2 Oct.

APPENDIX A

San Ardo Crude Analysis

This section shows elemental analysis of San Ardo crude, there thermodynamic properties and chromatograph on GC-FID system.

For are the correlation used for estimating thermodynamic properties [53] ,

Whitson characterization factor, K_w

$$K_w = \left[\frac{\xi \cdot \gamma_{plus}}{z_{plus} \cdot M_{plus}} \right]^{-0.84573}$$

Where, ξ

$$\xi = \sum_{i=n}^{45} \left[4.5579 \cdot M_i^{0.15178} \right]^{-\frac{1}{0.84573}} z_i . M_i$$

Specific gravity, γ

$$\gamma_i = \left[\frac{K_w}{4.5579 \cdot M_i^{0.15178}} \right]^{-\frac{1}{0.84573}}$$

Critical pressure (P_c) calculation,

$$\begin{aligned} \log p_{ci} = {} & 2.8290406 + (0.94120109 \cdot 10^{-3}) \cdot T_{bi} \\ & - (0.30474749 \cdot 10^{-5}) \cdot T_{bi}^{2} \\ & - (0.20887611 \cdot 10^{-4}) \cdot API_i \cdot T_{bi} \\ & + (0.15184103 \cdot 10^{-8}) \cdot T_{bi}^{3} \\ & + (0.11047899 \cdot 10^{-7}) \cdot API_i \cdot T_{bi}^{2} \\ & - (0.48271599 \cdot 10^{-7}) \cdot API_i^{2} \cdot T_{bi} \\ & + (0.13949619 \cdot 10^{-9}) \cdot API_i^{2} \cdot T_{bi}^{2} \end{aligned}$$

Critical temperature (T_c) calculation,

$$
\begin{aligned}
T_{ci} = 768.07121 + 1.7133693 \cdot T_{bi} \\
- (0.10834003 \cdot 10^{-2}) \cdot T_{bi}^{\ 2} \\
- (0.89212579 \cdot 10^{-2}) \cdot API_i \cdot T_{bi} \\
+ (0.38890584 \cdot 10^{-6}) \cdot T_{bi}^{\ 3} \\
+ (0.5309492 \cdot 10^{-5}) \cdot API_i \cdot T_{bi}^{\ 2} \\
+ (0.327116 \cdot 10^{-7}) \cdot API_i^{\ 2} T_{bi}^{\ 2}
\end{aligned}
$$

Where,

$$API_i = \frac{141.5}{\gamma_i} - 131.5$$

Table A.1: Composition of San Ardo crude oil using GC-FID capillary column.

Component	Mol%	Weight%
Methane	0.00	0.00
Ethane	0.00	0.00
Propane	0.00	0.00
i-Butane	0.00	0.00
n-Butane	0.00	0.00
neo-Pentane	0.00	0.00
i-Pentane	0.00	0.00
n-Pentane	0.00	0.00
Hexanes	0.04	0.01
M-C-Pentane	0.01	0.00
Benzene	0.00	0.00
Cyclohexane	0.01	0.00
Heptanes	0.05	0.01
M-C-Hexane	0.05	0.01
Toluene	0.01	0.00
Octanes	0.29	0.08
E-Benzene	0.10	0.03
M/P-Xylene	0.03	0.01
O-Xylene	0.04	0.01
Nonanes	0.58	0.18
T-M-Benzene	0.14	0.04
Decanes	1.46	0.50
Undecanes	2.71	0.95
Dodecanes	4.00	1.54
Tridecanes	4.87	2.05
Tetradecanes	4.33	1.97
Pentadecanes	5.08	2.51
Hexadecanes	4.75	2.53
Heptadecanes	4.03	2.29
Octadecanes	4.02	2.42
Nonadecanes	3.75	2.37
Eicosanes	3.20	2.11
Heneicosanes	3.07	2.14
Docosanes	2.55	1.87
Tricosanes	2.38	1.82
Tetracosanes	2.19	1.74
Pentacosanes	2.07	1.71
Hexacosanes	1.87	1.61
Heptacosanes	1.80	1.61
Octacosanes	1.75	1.63
Nonacosanes	1.84	1.77
Triacontanes	1.78	1.78
Hentriacontanes	1.53	1.58
Dotriacontanes	1.44	1.53
Tritriacontanes	1.26	1.39
Tetratriacontanes	1.21	1.37
Pentatriacontanes	1.11	1.30
Hexatriacontanes plus	28.60	53.53
Totals	100.00	100.00

Measured Properties		
Whole Sample Density	0.9745	$g.cc^{-1}$ @ 60°F
Whole Sample Mol.Wt.	417.0	$g.mol^{-1}$

Plus Fraction Calculated Properties	Density $g.cc^{-1}$ @ 60°F	Mole Weight $g.mole^{-1}$
Heptanes Plus	0.9745	417.1
Undecanes Plus	0.9772	425.3
Eicosanes Plus	1.0184	562.6
Triacontanes Plus	1.0664	705.4
Hexatriacontanes Plus	1.0981	780.7

Subtotals	Mole %	Weight %
Heptanes	0.07	0.01
Octanes	0.35	0.09
Nonanes	0.75	0.23
Decanes	1.60	0.54

Notes
Calculated properties derived from Katz & Firoozabadi data.

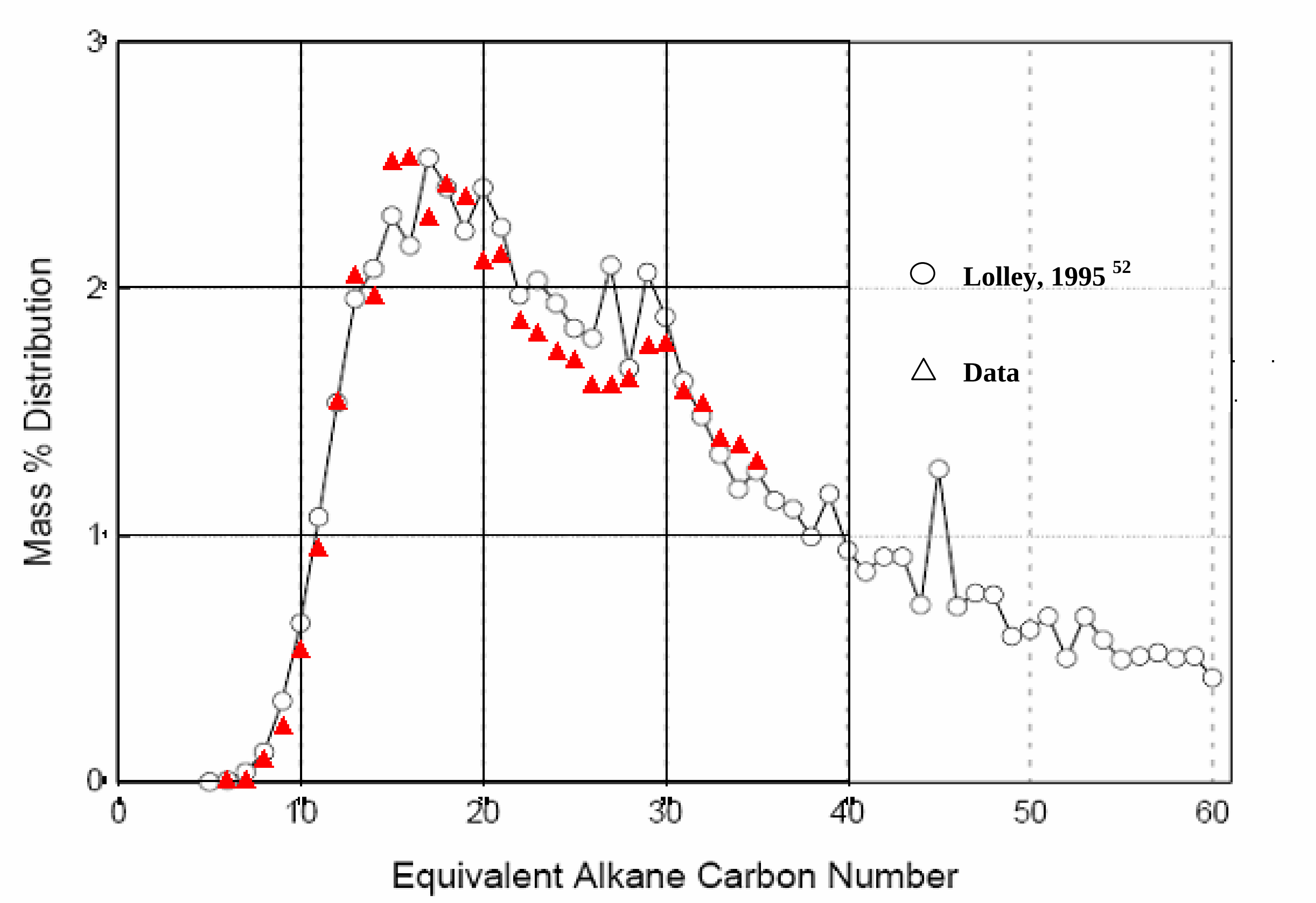

Figure A.1: Comparison of laboratory composition analysis with literature data.

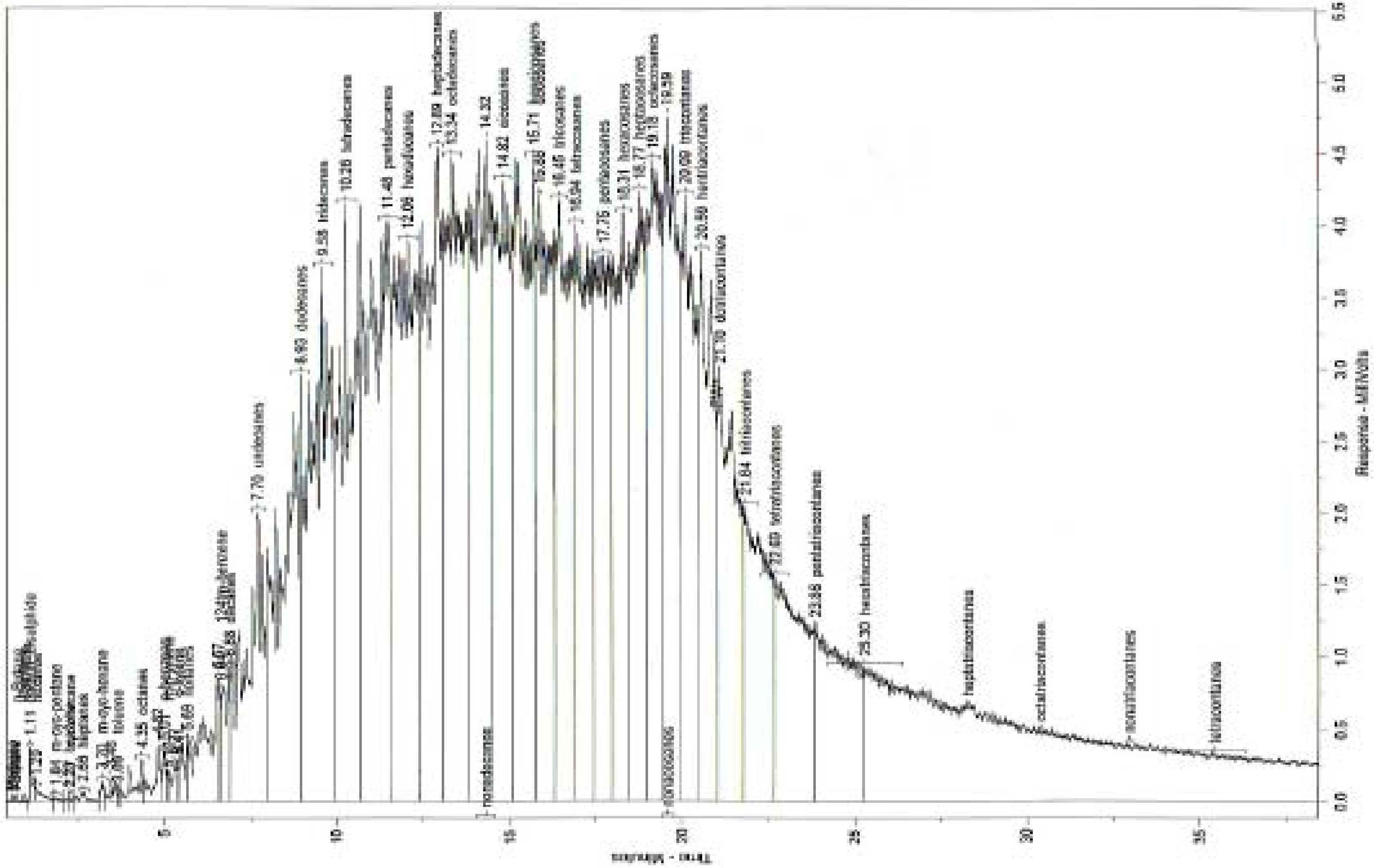

Figure A.2 : Chromatogram of San Ardo crude.

Table A.2 : Estimated property used for simulating experiments.

Hydrocarbon Group	Mol. Wt, Mi	ξ	k	γ	T_B ^oF	P_c psia	T_c ^oR
C_6	86.17	0.1746	11.7374	0.7390	147.00	455.000	913.000
C_7	96	0.1746	11.7374	0.7413	197.50	472.040	974.957
C_8	107	0.1695	11.7374	0.7559	242.00	440.025	1021.955
C_9	121	0.1669	11.7374	0.7728	288.00	411.371	1071.220
C_{10}	134	0.1614	11.7374	0.7871	331.00	384.371	1116.280
C_{11}	147	0.1548	11.7374	0.8002	369.00	362.217	1156.096
C_{12}	161	0.1484	11.7374	0.8134	407.00	340.923	1195.575
C_{13}	175	0.1413	11.7374	0.8257	441.00	323.087	1230.870
C_{14}	190	0.1345	11.7374	0.8380	476.00	305.078	1266.664
C_{15}	206	0.1277	11.7374	0.8502	511.00	287.816	1302.080
C_{16}	222	0.1209	11.7374	0.8617	542.00	273.764	1333.537
C_{17}	237	0.1133	11.7374	0.8719	572.00	259.993	1363.105
C_{18}	251	0.1058	11.7374	0.8809	595.00	250.858	1386.350
C_{19}	263	0.0977	11.7374	0.8883	617.00	241.542	1407.668
C_{20}	275	0.0902	11.7374	0.8954	641.00	231.180	1430.167
C_{21}	291	0.0840	11.7374	0.9046	664.00	223.304	1452.987
C_{22}	305	0.0772	11.7374	0.9122	686.00	215.435	1474.000
C_{23}	318	0.0719	11.7374	0.9191	707.00	208.032	1493.651
C_{24}	331	0.0657	11.7374	0.9257	727.00	201.418	1512.317
C_{25}	345	0.0604	11.7374	0.9326	747.00	195.326	1531.044
C_{26}	359	0.0555	11.7374	0.9393	766.00	189.932	1548.810
C_{27}	374	0.0511	11.7374	0.9462	784.00	185.430	1565.909
C_{28}	388	0.0468	11.7374	0.9525	802.00	180.855	1582.537
C_{29}	402	0.04	11.74	0.96	817.00	177.695	1596.833
C_{30}	416	0.04	11.74	0.96	834.00	173.855	1612.409
C_{31}	430	0.04	11.74	0.97	850.00	170.569	1627.120
C_{32}	444	0.03	11.74	0.98	866.00	167.443	1641.697
C_{33}	458	0.03	11.74	0.98	881.00	164.817	1655.436
C_{34}	472	0.03	11.74	0.99	895.00	162.653	1668.346
C_{35}	486	0.02	11.74	0.99	908.00	160.910	1680.436
C_{36+}	781	0.29	11.74	1.08	1177.83	156.778	1920.047

APPENDIX B

Simulation Results

In this section data from Aspen simulation of all experiments are presented. Simulation was performed on elemental basis. Equilibrium time of 1 hour was used for all the simulation. For each experimental condition the composition of distillates are presented. Feed used for this are presented in Appendix A and distillation efficiency of 29 % was used for all simulation.

Table B.1 Results from simulated dry distillation of crude at 1 atm condition for 105 °C to 185 °C(Run-1).

	Distillation Cuts @ Temp °C								
Mass Flow gm/hr	**105**	**115**	**125**	**135**	**145**	**155**	**165**	**175**	**185**
WATER	0.00E+00	0.00E+00	0.00E+00	0.00E+00	0.00E+00	0.00E+00	0.00E+00	0.00E+00	0.00E+00
PROPA-01	0.00E+00	0.00E+00	0.00E+00	0.00E+00	0.00E+00	0.00E+00	0.00E+00	0.00E+00	0.00E+00
N-PEN-01	0.00E+00	0.00E+00	0.00E+00	0.00E+00	0.00E+00	0.00E+00	0.00E+00	0.00E+00	0.00E+00
NITROGEN	1.50E+00	1.50E+00	1.50E+00	1.50E+00	1.50E+00	1.50E+00	1.50E+00	1.50E+00	1.50E+00
METHY-02	0.00E+00	0.00E+00	0.00E+00	0.00E+00	0.00E+00	0.00E+00	0.00E+00	0.00E+00	0.00E+00
CYCLOHEX	0.00E+00	0.00E+00	0.00E+00	0.00E+00	0.00E+00	0.00E+00	0.00E+00	0.00E+00	0.00E+00
HEXANES	1.94E-02	3.71E-03	4.05E-03	3.41E-03	2.66E-03	1.90E-03	1.25E-03	7.45E-04	4.03E-04
METHY-01	1.50E-02	6.06E-03	2.62E-03	2.77E-03	2.79E-03	2.65E-03	2.36E-03	1.97E-03	1.53E-03
TOLUE-01	0.00E+00	0.00E+00	0.00E+00	0.00E+00	0.00E+00	0.00E+00	0.00E+00	0.00E+00	0.00E+00
HEPTANES	1.66E-02	5.36E-03	3.11E-03	3.11E-03	2.92E-03	2.58E-03	2.12E-03	1.61E-03	1.13E-03
OCATANES	1.03E-01	5.36E-02	1.65E-02	1.87E-02	2.01E-02	2.06E-02	2.00E-02	1.82E-02	1.55E-02
ETHYL-02	2.98E-02	2.07E-02	4.27E-03	5.14E-03	5.95E-03	6.62E-03	7.04E-03	7.12E-03	6.81E-03
M-XYL-01	9.39E-03	6.87E-03	1.32E-03	1.61E-03	1.90E-03	2.14E-03	2.31E-03	2.37E-03	2.31E-03
O-XYL-01	8.78E-03	6.76E-03	1.21E-03	1.49E-03	1.77E-03	2.02E-03	2.22E-03	2.32E-03	2.31E-03
NONANES	1.55E-01	1.21E-01	2.14E-02	2.65E-02	3.16E-02	3.63E-02	3.99E-02	4.19E-02	4.18E-02
1,2,4-C9	1.92E-02	2.05E-02	2.43E-03	3.21E-03	4.13E-03	5.16E-03	6.25E-03	7.31E-03	8.22E-03
C10	2.57E-01	2.67E-01	3.27E-02	4.29E-02	5.48E-02	6.79E-02	8.15E-02	9.44E-02	1.05E-01
C11	2.79E-01	3.46E-01	3.46E-02	4.74E-02	6.35E-02	8.28E-02	1.05E-01	1.30E-01	1.56E-01
C12	2.38E-01	3.33E-01	2.99E-02	4.26E-02	5.92E-02	8.06E-02	1.07E-01	1.39E-01	1.76E-01

C13	1.69E-01	2.55E-01	2.19E-02	3.22E-02	4.62E-02	6.50E-02	8.95E-02	1.21E-01	1.59E-01
C14	8.14E-02	1.30E-01	1.11E-02	1.68E-02	2.48E-02	3.59E-02	5.10E-02	7.11E-02	9.70E-02
C15	4.99E-02	8.35E-02	7.18E-03	1.12E-02	1.71E-02	2.55E-02	3.72E-02	5.34E-02	7.52E-02
C16	2.55E-02	4.42E-02	3.88E-03	6.22E-03	9.72E-03	1.49E-02	2.23E-02	3.28E-02	4.73E-02
C17	1.16E-02	2.09E-02	1.87E-03	3.08E-03	4.95E-03	7.76E-03	1.19E-02	1.79E-02	2.65E-02
C18	7.13E-03	1.31E-02	1.20E-03	2.02E-03	3.31E-03	5.29E-03	8.28E-03	1.27E-02	1.91E-02
C19	4.09E-03	7.72E-03	7.23E-04	1.24E-03	2.07E-03	3.37E-03	5.37E-03	8.36E-03	1.28E-02
C20	1.99E-03	3.86E-03	3.71E-04	6.52E-04	1.11E-03	1.85E-03	3.00E-03	4.77E-03	7.43E-03
C21	1.12E-03	2.23E-03	2.19E-04	3.94E-04	6.87E-04	1.17E-03	1.93E-03	3.12E-03	4.95E-03
C22	5.46E-04	1.11E-03	1.12E-04	2.06E-04	3.68E-04	6.36E-04	1.07E-03	1.77E-03	2.85E-03
C23	3.00E-04	6.27E-04	6.48E-05	1.22E-04	2.21E-04	3.91E-04	6.72E-04	1.13E-03	1.85E-03
C24	1.64E-04	3.51E-04	3.71E-05	7.13E-05	1.32E-04	2.38E-04	4.17E-04	7.12E-04	1.19E-03
C25	9.10E-05	2.00E-04	2.17E-05	4.25E-05	8.05E-05	1.48E-04	2.64E-04	4.58E-04	7.77E-04
C26	4.93E-05	1.11E-04	1.23E-05	2.47E-05	4.76E-05	8.91E-05	1.62E-04	2.86E-04	4.93E-04
C27	2.90E-05	6.66E-05	7.56E-06	1.54E-05	3.04E-05	5.79E-05	1.07E-04	1.92E-04	3.36E-04
C28	1.69E-05	3.99E-05	4.63E-06	9.67E-06	1.94E-05	3.77E-05	7.09E-05	1.29E-04	2.30E-04
C29	1.16E-05	2.79E-05	3.30E-06	7.01E-06	1.43E-05	2.82E-05	5.38E-05	9.97E-05	1.80E-04
C30	4.30E-06	1.09E-05	0.00E+00	3.00E-06	6.39E-06	1.31E-05	2.60E-05	4.98E-05	9.29E-05
C31	2.44E-06	6.28E-06	0.00E+00	1.79E-06	3.88E-06	8.07E-06	1.62E-05	3.15E-05	5.94E-05
C32	0.00E+00	3.64E-06	0.00E+00	0.00E+00	2.39E-06	5.07E-06	1.04E-05	2.05E-05	3.92E-05
C33	0.00E+00	2.04E-06	0.00E+00	0.00E+00	0.00E+00	3.07E-06	6.37E-06	1.28E-05	2.49E-05
C34	0.00E+00	0.00E+00	0.00E+00	0.00E+00	0.00E+00	2.08E-06	4.37E-06	8.90E-06	1.75E-05
C35	0.00E+00	0.00E+00	0.00E+00	0.00E+00	0.00E+00	0.00E+00	2.93E-06	6.04E-06	1.21E-05
C36+	0.00E+00	7.43E-06	0.00E+00	0.00E+00	6.54E-06	1.51E-05	3.35E-05	7.15E-05	1.48E-04

Table B 2: Results from simulated dry distillation of crude at 1 atm conditions (195^{o}C to 265^{o}C) (Run-1).

	Distillation Cuts @ Temp ^{o}C							
Mass Flow gm/hr	**195**	**205**	**215**	**225**	**235**	**245**	**255**	**265**
WATER	0.00E+00	0.00E+00	0.00E+00	0.00E+00	0.00E+00	0.00E+00	0.00E+00	0.00E+00
PROPA-01	0.00E+00	0.00E+00	0.00E+00	0.00E+00	0.00E+00	0.00E+00	0.00E+00	0.00E+00
N-PEN-01	0.00E+00	0.00E+00	0.00E+00	0.00E+00	0.00E+00	0.00E+00	0.00E+00	0.00E+00
NITROGEN	1.50E+00	1.50E+00	1.50E+00	1.50E+00	1.50E+00	1.50E+00	1.50E+00	1.50E+00
METHY-02	0.00E+00	0.00E+00	0.00E+00	0.00E+00	0.00E+00	0.00E+00	0.00E+00	0.00E+00
CYCLOHEX	0.00E+00	0.00E+00	0.00E+00	0.00E+00	0.00E+00	0.00E+00	0.00E+00	0.00E+00
HEXANES	1.97E-04	8.64E-05	3.40E-05	1.19E-05	3.72E-06	1.03E-06	0.00E+00	0.00E+00
METHY-01	1.09E-03	7.17E-04	4.29E-04	2.33E-04	1.14E-04	4.99E-05	1.96E-05	6.84E-06
TOLUE-01	0.00E+00	0.00E+00	0.00E+00	0.00E+00	0.00E+00	0.00E+00	0.00E+00	0.00E+00
HEPTANES	7.27E-04	4.26E-04	2.26E-04	1.08E-04	4.64E-05	1.78E-05	6.07E-06	1.84E-06
OCATANES	1.23E-02	8.98E-03	6.01E-03	3.66E-03	2.02E-03	9.97E-04	4.41E-04	1.74E-04
ETHYL-02	6.12E-03	5.13E-03	3.99E-03	2.85E-03	1.86E-03	1.10E-03	5.86E-04	2.80E-04
M-XYL-01	2.11E-03	1.80E-03	1.43E-03	1.04E-03	6.90E-04	4.16E-04	2.26E-04	1.10E-04
O-XYL-01	2.17E-03	1.91E-03	1.56E-03	1.18E-03	8.16E-04	5.14E-04	2.93E-04	1.50E-04
NONANES	3.93E-02	3.46E-02	2.84E-02	2.14E-02	1.48E-02	9.32E-03	5.29E-03	2.69E-03
1,2,4-C9	8.84E-03	9.04E-03	8.73E-03	7.91E-03	6.66E-03	5.16E-03	3.67E-03	2.37E-03
C10	1.12E-01	1.13E-01	1.07E-01	9.57E-02	7.92E-02	6.04E-02	4.20E-02	2.66E-02
C11	1.80E-01	1.99E-01	2.11E-01	2.12E-01	2.00E-01	1.76E-01	1.43E-01	1.07E-01
C12	2.17E-01	2.59E-01	2.98E-01	3.28E-01	3.44E-01	3.41E-01	3.16E-01	2.73E-01

C13	2.05E-01	2.57E-01	3.13E-01	3.69E-01	4.17E-01	4.50E-01	4.60E-01	4.42E-01
C14	1.30E-01	1.70E-01	2.17E-01	2.70E-01	3.25E-01	3.76E-01	4.17E-01	4.40E-01
C15	1.04E-01	1.41E-01	1.87E-01	2.43E-01	3.07E-01	3.77E-01	4.46E-01	5.07E-01
C16	6.71E-02	9.35E-02	1.28E-01	1.72E-01	2.25E-01	2.87E-01	3.56E-01	4.27E-01
C17	3.85E-02	5.49E-02	7.71E-02	1.06E-01	1.43E-01	1.89E-01	2.43E-01	3.04E-01
C18	2.82E-02	4.09E-02	5.85E-02	8.20E-02	1.13E-01	1.52E-01	2.01E-01	2.58E-01
C19	1.92E-02	2.84E-02	4.12E-02	5.88E-02	8.24E-02	1.13E-01	1.53E-01	2.01E-01
C20	1.14E-02	1.71E-02	2.52E-02	3.67E-02	5.24E-02	7.34E-02	1.01E-01	1.36E-01
C21	7.70E-03	1.18E-02	1.77E-02	2.61E-02	3.79E-02	5.40E-02	7.56E-02	1.04E-01
C22	4.52E-03	7.01E-03	1.07E-02	1.60E-02	2.37E-02	3.43E-02	4.88E-02	6.80E-02
C23	2.97E-03	4.69E-03	7.26E-03	1.11E-02	1.65E-02	2.43E-02	3.51E-02	4.97E-02
C24	1.94E-03	3.11E-03	4.88E-03	7.54E-03	1.14E-02	1.70E-02	2.49E-02	3.58E-02
C25	1.29E-03	2.10E-03	3.34E-03	5.23E-03	8.05E-03	1.22E-02	1.80E-02	2.63E-02
C26	8.30E-04	1.37E-03	2.22E-03	3.52E-03	5.48E-03	8.38E-03	1.26E-02	1.86E-02
C27	5.75E-04	9.62E-04	1.58E-03	2.54E-03	4.00E-03	6.19E-03	9.41E-03	1.40E-02
C28	4.00E-04	6.79E-04	1.13E-03	1.84E-03	2.94E-03	4.60E-03	7.08E-03	1.07E-02
C29	3.16E-04	5.43E-04	9.13E-04	1.50E-03	2.43E-03	3.84E-03	5.97E-03	9.09E-03
C30	1.69E-04	2.98E-04	5.16E-04	8.73E-04	1.45E-03	2.35E-03	3.73E-03	5.81E-03
C31	1.09E-04	1.95E-04	3.41E-04	5.83E-04	9.76E-04	1.60E-03	2.56E-03	4.03E-03
C32	7.31E-05	1.33E-04	2.35E-04	4.07E-04	6.89E-04	1.14E-03	1.85E-03	2.94E-03
C33	4.70E-05	8.64E-05	1.55E-04	2.72E-04	4.65E-04	7.79E-04	1.28E-03	2.05E-03
C34	3.36E-05	6.25E-05	1.13E-04	2.01E-04	3.47E-04	5.88E-04	9.72E-04	1.57E-03
C35	2.34E-05	4.40E-05	8.08E-05	1.45E-04	2.53E-04	4.31E-04	7.20E-04	1.18E-03
C36+	2.95E-04	5.74E-04	1.08E-03	2.00E-03	3.58E-03	6.27E-03	1.07E-02	1.79E-02

Table B 3:Results from simulated dry distillation of crude at 1 atm condition (98 ^oC to 190 ^oC) (Run-2).

	Distillation Cuts @ Temp ^oC								
Mass Flow gm/hr	**98**	**115**	**130**	**140**	**150**	**160**	**170**	**180**	**190**
WATER	0.00E+00	0.00E+00	0.00E+00	0.00E+00	0.00E+00	0.00E+00	0.00E+00	0.00E+00	0.00E+00
PROPA-01	0.00E+00	0.00E+00	0.00E+00	0.00E+00	0.00E+00	0.00E+00	0.00E+00	0.00E+00	0.00E+00
N-PEN-01	0.00E+00	0.00E+00	0.00E+00	0.00E+00	0.00E+00	0.00E+00	0.00E+00	0.00E+00	0.00E+00
NITROGEN	1.50E+00	1.50E+00	1.50E+00	1.50E+00	1.47E+00	1.50E+00	1.50E+00	1.50E+00	1.46E+00
METHY-02	0.00E+00	0.00E+00	0.00E+00	0.00E+00	0.00E+00	0.00E+00	0.00E+00	0.00E+00	0.00E+00
CYCLOHEX	0.00E+00	0.00E+00	0.00E+00	0.00E+00	0.00E+00	0.00E+00	0.00E+00	0.00E+00	0.00E+00
HEXANES	2.73E-02	9.90E-03	2.35E-03	3.78E-04	1.60E-05	1.29E-05	9.49E-06	6.45E-06	2.47E-06
METHY-01	1.81E-02	1.29E-02	6.28E-03	2.07E-03	1.08E-04	1.11E-04	1.05E-04	9.42E-05	4.34E-05
TOLUE-01	0.00E+00	0.00E+00	0.00E+00	0.00E+00	0.00E+00	0.00E+00	0.00E+00	0.00E+00	0.00E+00
HEPTANES	2.11E-02	1.24E-02	4.87E-03	1.29E-03	6.39E-05	6.13E-05	5.42E-05	4.52E-05	1.98E-05
OCATANES	1.15E-01	1.03E-01	6.38E-02	2.68E-02	1.48E-03	1.61E-03	1.63E-03	1.58E-03	7.62E-04
ETHYL-02	3.00E-02	3.43E-02	2.84E-02	1.61E-02	9.43E-04	1.10E-03	1.20E-03	1.26E-03	6.44E-04
M-XYL-01	9.24E-03	1.11E-02	9.63E-03	5.73E-03	3.40E-04	4.00E-04	4.43E-04	4.72E-04	2.43E-04
O-XYL-01	8.48E-03	1.06E-02	9.69E-03	6.12E-03	3.66E-04	4.36E-04	4.89E-04	5.29E-04	2.75E-04
NONANES	1.49E-01	1.89E-01	1.75E-01	1.12E-01	6.73E-03	8.02E-03	9.03E-03	9.79E-03	5.11E-03
1,2,4-C9	1.63E-02	2.67E-02	3.41E-02	3.07E-02	1.97E-03	2.53E-03	3.08E-03	3.65E-03	2.02E-03
C10	2.20E-01	3.53E-01	4.38E-01	3.83E-01	2.45E-02	3.11E-02	3.76E-02	4.42E-02	2.44E-02
C11	2.21E-01	4.11E-01	6.18E-01	6.68E-01	4.45E-02	5.91E-02	7.51E-02	9.32E-02	5.34E-02
C12	1.78E-01	3.71E-01	6.40E-01	8.06E-01	5.57E-02	7.69E-02	1.02E-01	1.32E-01	7.81E-02

C13	1.22E-01	2.74E-01	5.19E-01	7.21E-01	5.13E-02	7.29E-02	9.94E-02	1.33E-01	8.11E-02
C14	5.67E-02	1.37E-01	2.79E-01	4.17E-01	3.06E-02	4.47E-02	6.28E-02	8.66E-02	5.41E-02
C15	3.37E-02	8.70E-02	1.89E-01	2.98E-01	2.25E-02	3.38E-02	4.87E-02	6.91E-02	4.43E-02
C16	1.68E-02	4.58E-02	1.05E-01	1.72E-01	1.33E-02	2.05E-02	3.02E-02	4.39E-02	2.88E-02
C17	7.49E-03	2.16E-02	5.15E-02	8.74E-02	6.94E-03	1.10E-02	1.66E-02	2.46E-02	1.65E-02
C18	4.52E-03	1.36E-02	3.35E-02	5.83E-02	4.72E-03	7.59E-03	1.17E-02	1.76E-02	1.20E-02
C19	2.55E-03	7.96E-03	2.04E-02	3.62E-02	2.99E-03	4.89E-03	7.66E-03	1.18E-02	8.14E-03
C20	1.22E-03	3.98E-03	1.06E-02	1.93E-02	1.63E-03	2.72E-03	4.34E-03	6.78E-03	4.78E-03
C21	6.72E-04	2.30E-03	6.32E-03	1.18E-02	1.02E-03	1.73E-03	2.81E-03	4.48E-03	3.22E-03
C22	3.21E-04	1.15E-03	3.27E-03	6.23E-03	5.50E-04	9.55E-04	1.58E-03	2.56E-03	1.87E-03
C23	1.73E-04	6.47E-04	1.91E-03	3.72E-03	3.35E-04	5.93E-04	1.00E-03	1.65E-03	1.22E-03
C24	9.29E-05	3.62E-04	1.11E-03	2.20E-03	2.02E-04	3.64E-04	6.26E-04	1.05E-03	7.92E-04
C25	5.07E-05	2.06E-04	6.51E-04	1.32E-03	1.24E-04	2.28E-04	3.99E-04	6.81E-04	5.23E-04
C26	2.70E-05	1.14E-04	3.73E-04	7.74E-04	7.41E-05	1.39E-04	2.47E-04	4.28E-04	3.34E-04
C27	1.56E-05	6.86E-05	2.32E-04	4.89E-04	4.78E-05	9.10E-05	1.65E-04	2.90E-04	2.30E-04
C28	8.96E-06	4.11E-05	1.43E-04	3.09E-04	3.08E-05	5.97E-05	1.10E-04	1.97E-04	1.59E-04
C29	6.05E-06	2.87E-05	1.03E-04	2.26E-04	2.29E-05	4.50E-05	8.41E-05	1.53E-04	1.25E-04
C30	2.16E-06	1.12E-05	4.30E-05	9.85E-05	1.04E-05	2.13E-05	4.13E-05	7.75E-05	6.55E-05
C31	0.00E+00	6.47E-06	2.55E-05	5.93E-05	6.36E-06	1.32E-05	2.59E-05	4.93E-05	4.21E-05
C32	0.00E+00	3.75E-06	1.53E-05	3.62E-05	3.96E-06	8.36E-06	1.67E-05	3.23E-05	2.80E-05
C33	0.00E+00	2.11E-06	8.83E-06	2.13E-05	2.38E-06	5.11E-06	1.04E-05	2.03E-05	1.79E-05
C34	0.00E+00	0.00E+00	5.73E-06	1.41E-05	0.00E+00	3.48E-06	7.15E-06	1.42E-05	1.27E-05
C35	0.00E+00	0.00E+00	3.63E-06	9.07E-06	0.00E+00	2.31E-06	4.82E-06	9.72E-06	8.79E-06
C36+	0.00E+00	7.68E-06	3.61E-05	9.38E-05	1.12E-05	2.58E-05	5.58E-05	1.16E-04	1.09E-04

Table B 4:Results from simulated dry distillation of crude at 1 atm condition (200 ^{o}C to 270 ^{o}C) (Run-2).

	Distillation Cuts @ Temp ^{o}C							
Mass Flow gm/hr	**200**	**210**	**220**	**230**	**240**	**250**	**260**	**270**
WATER	0.00E+00	0.00E+00	0.00E+00	0.00E+00	0.00E+00	0.00E+00	0.00E+00	0.00E+00
PROPA-01	0.00E+00	0.00E+00	0.00E+00	0.00E+00	0.00E+00	0.00E+00	0.00E+00	0.00E+00
N-PEN-01	0.00E+00	0.00E+00	0.00E+00	0.00E+00	0.00E+00	0.00E+00	0.00E+00	0.00E+00
NITROGEN	1.50E+00	1.50E+00	1.54E+00	1.51E+00	1.50E+00	1.49E+00	1.50E+00	1.50E+00
METHY-02	0.00E+00	0.00E+00	0.00E+00	0.00E+00	0.00E+00	0.00E+00	0.00E+00	0.00E+00
CYCLOHEX	0.00E+00	0.00E+00	0.00E+00	0.00E+00	0.00E+00	0.00E+00	0.00E+00	0.00E+00
HEXANES	1.99E-06	1.48E-06	1.59E-06	7.76E-07	0.00E+00	0.00E+00	0.00E+00	0.00E+00
METHY-01	4.28E-05	3.95E-05	6.12E-05	4.67E-05	2.12E-05	6.64E-06	3.47E-06	1.63E-06
TOLUE-01	0.00E+00	0.00E+00	0.00E+00	0.00E+00	0.00E+00	0.00E+00	0.00E+00	0.00E+00
HEPTANES	1.85E-05	1.62E-05	2.26E-05	1.51E-05	5.99E-06	1.68E-06	7.82E-07	0.00E+00
OCATANES	7.90E-04	7.71E-04	1.31E-03	1.13E-03	5.78E-04	2.00E-04	1.16E-04	6.00E-05
ETHYL-02	7.10E-04	7.40E-04	1.43E-03	1.46E-03	8.90E-04	3.55E-04	2.39E-04	1.45E-04
M-XYL-01	2.71E-04	2.85E-04	5.59E-04	5.80E-04	3.62E-04	1.46E-04	9.99E-05	6.17E-05
O-XYL-01	3.10E-04	3.31E-04	6.67E-04	7.21E-04	4.70E-04	1.97E-04	1.40E-04	8.99E-05
NONANES	5.76E-03	6.15E-03	1.24E-02	1.34E-02	8.71E-03	3.64E-03	2.57E-03	1.65E-03
1,2,4-C9	2.44E-03	2.80E-03	6.47E-03	8.47E-03	6.80E-03	3.34E-03	2.81E-03	2.18E-03
C10	2.92E-02	3.33E-02	7.59E-02	9.78E-02	7.70E-02	3.73E-02	3.10E-02	2.36E-02
C11	6.67E-02	7.97E-02	1.98E-01	2.90E-01	2.63E-01	1.42E-01	1.33E-01	1.15E-01
C12	1.01E-01	1.25E-01	3.34E-01	5.41E-01	5.52E-01	3.25E-01	3.35E-01	3.25E-01

C13	1.08E-01	1.38E-01	3.85E-01	6.71E-01	7.44E-01	4.67E-01	5.18E-01	5.44E-01
C14	7.39E-02	9.69E-02	2.82E-01	5.22E-01	6.20E-01	4.11E-01	4.84E-01	5.45E-01
C15	6.20E-02	8.33E-02	2.51E-01	4.87E-01	6.11E-01	4.22E-01	5.23E-01	6.22E-01
C16	4.11E-02	5.64E-02	1.74E-01	3.50E-01	4.57E-01	3.26E-01	4.19E-01	5.19E-01
C17	2.40E-02	3.36E-02	1.06E-01	2.19E-01	2.96E-01	2.17E-01	2.87E-01	3.68E-01
C18	1.78E-02	2.53E-02	8.11E-02	1.71E-01	2.35E-01	1.76E-01	2.37E-01	3.11E-01
C19	1.22E-02	1.76E-02	5.75E-02	1.23E-01	1.73E-01	1.31E-01	1.80E-01	2.41E-01
C20	7.31E-03	1.07E-02	3.55E-02	7.75E-02	1.11E-01	8.57E-02	1.20E-01	1.63E-01
C21	5.00E-03	7.43E-03	2.50E-02	5.55E-02	8.07E-02	6.34E-02	9.00E-02	1.25E-01
C22	2.96E-03	4.47E-03	1.52E-02	3.44E-02	5.07E-02	4.05E-02	5.83E-02	8.20E-02
C23	1.96E-03	3.01E-03	1.04E-02	2.38E-02	3.57E-02	2.89E-02	4.22E-02	6.02E-02
C24	1.29E-03	2.01E-03	7.05E-03	1.63E-02	2.48E-02	2.03E-02	3.01E-02	4.35E-02
C25	8.64E-04	1.37E-03	4.86E-03	1.14E-02	1.76E-02	1.46E-02	2.19E-02	3.20E-02
C26	5.61E-04	8.99E-04	3.24E-03	7.72E-03	1.20E-02	1.01E-02	1.54E-02	2.27E-02
C27	3.91E-04	6.36E-04	2.32E-03	5.60E-03	8.84E-03	7.52E-03	1.15E-02	1.73E-02
C28	2.74E-04	4.51E-04	1.67E-03	4.08E-03	6.53E-03	5.62E-03	8.72E-03	1.32E-02
C29	2.18E-04	3.63E-04	1.36E-03	3.35E-03	5.42E-03	4.71E-03	7.39E-03	1.13E-02
C30	1.18E-04	2.03E-04	7.79E-04	1.97E-03	3.27E-03	2.91E-03	4.67E-03	7.29E-03
C31	7.69E-05	1.33E-04	5.18E-04	1.32E-03	2.22E-03	1.99E-03	3.22E-03	5.07E-03
C32	5.19E-05	9.12E-05	3.59E-04	9.29E-04	1.57E-03	1.43E-03	2.34E-03	3.72E-03
C33	3.36E-05	5.98E-05	2.38E-04	6.24E-04	1.07E-03	9.81E-04	1.62E-03	2.61E-03
C34	2.41E-05	4.35E-05	1.75E-04	4.63E-04	8.02E-04	7.44E-04	1.24E-03	2.01E-03
C35	1.69E-05	3.08E-05	1.25E-04	3.35E-04	5.86E-04	5.49E-04	9.24E-04	1.51E-03
C36+	2.17E-04	4.07E-04	1.71E-03	4.69E-03	8.40E-03	8.08E-03	1.39E-02	2.34E-02

Table B.5: Results from simulated steam distillation of crude at different T_{sat+15} & P_{sat} conditions (115 ^oC to 200 ^oC) (Run-1).

	Distillation Cuts @ Temp ^oC								
Mass Flow gm/hr	**115**	**130**	**140**	**150**	**160**	**170**	**180**	**190**	**200**
WATER	2.95E+01	2.79E+01	2.91E+01	2.94E+01	2.92E+01	2.92E+01	2.90E+01	2.81E+01	2.96E+01
PROPA-01	0.00E+00	0.00E+00	0.00E+00	0.00E+00	0.00E+00	0.00E+00	0.00E+00	0.00E+00	0.00E+00
N-PEN-01	0.00E+00	0.00E+00	0.00E+00	0.00E+00	0.00E+00	0.00E+00	0.00E+00	0.00E+00	0.00E+00
NITROGEN	1.50E+00	1.50E+00	1.50E+00	1.50E+00	1.50E+00	1.50E+00	1.50E+00	1.49E+00	1.50E+00
METHY-02	0.00E+00	0.00E+00	0.00E+00	0.00E+00	0.00E+00	0.00E+00	0.00E+00	0.00E+00	0.00E+00
CYCLOHEX	0.00E+00	0.00E+00	0.00E+00	0.00E+00	0.00E+00	0.00E+00	0.00E+00	0.00E+00	0.00E+00
HEXANES	5.64E-02	2.79E-03	6.15E-04	1.59E-04	4.34E-05	1.31E-05	4.26E-06	1.41E-06	5.95E-07
METHY-01	5.17E-02	4.83E-03	1.88E-03	8.37E-04	3.76E-04	1.81E-04	9.10E-05	4.44E-05	2.74E-05
TOLUE-01	0.00E+00	0.00E+00	0.00E+00	0.00E+00	0.00E+00	0.00E+00	0.00E+00	0.00E+00	0.00E+00
HEPTANES	5.36E-02	4.16E-03	1.38E-03	5.23E-04	2.03E-04	8.59E-05	3.81E-05	1.66E-05	9.21E-06
OCATANES	3.91E-01	4.49E-02	2.07E-02	1.08E-02	5.55E-03	3.04E-03	1.71E-03	9.20E-04	6.22E-04
ETHYL-02	1.31E-01	1.89E-02	1.07E-02	6.72E-03	4.13E-03	2.66E-03	1.74E-03	1.07E-03	8.32E-04
M-XYL-01	4.26E-02	6.41E-03	3.74E-03	2.42E-03	1.52E-03	1.01E-03	6.73E-04	4.21E-04	3.32E-04
O-XYL-01	4.13E-02	6.46E-03	3.90E-03	2.61E-03	1.70E-03	1.16E-03	7.99E-04	5.13E-04	4.17E-04
NONANES	7.39E-01	1.18E-01	7.15E-02	4.80E-02	3.13E-02	2.12E-02	1.46E-02	9.37E-03	7.54E-03
1,2,4-C9	1.20E-01	2.42E-02	1.81E-02	1.48E-02	1.16E-02	9.33E-03	7.54E-03	5.57E-03	5.19E-03
C10	1.56E+00	3.12E-01	2.29E-01	1.84E-01	1.41E-01	1.12E-01	8.91E-02	6.50E-02	5.94E-02
C11	2.07E+00	4.81E-01	3.98E-01	3.58E-01	3.07E-01	2.70E-01	2.37E-01	1.89E-01	1.89E-01
C12	2.08E+00	5.40E-01	4.88E-01	4.79E-01	4.45E-01	4.24E-01	4.02E-01	3.46E-01	3.71E-01

C13	1.65E+00	4.63E-01	4.44E-01	4.62E-01	4.55E-01	4.58E-01	4.59E-01	4.16E-01	4.71E-01
C14	8.61E-01	2.59E-01	2.61E-01	2.85E-01	2.94E-01	3.11E-01	3.26E-01	3.10E-01	3.67E-01
C15	5.61E-01	1.80E-01	1.89E-01	2.15E-01	2.31E-01	2.54E-01	2.78E-01	2.75E-01	3.38E-01
C16	3.00E-01	1.01E-01	1.10E-01	1.29E-01	1.44E-01	1.63E-01	1.84E-01	1.89E-01	2.39E-01
C17	1.42E-01	5.04E-02	5.66E-02	6.85E-02	7.85E-02	9.19E-02	1.07E-01	1.13E-01	1.47E-01
C18	8.96E-02	3.31E-02	3.80E-02	4.70E-02	5.51E-02	6.60E-02	7.83E-02	8.46E-02	1.12E-01
C19	5.28E-02	2.02E-02	2.38E-02	3.01E-02	3.60E-02	4.40E-02	5.33E-02	5.88E-02	7.97E-02
C20	2.65E-02	1.06E-02	1.28E-02	1.65E-02	2.03E-02	2.53E-02	3.14E-02	3.56E-02	4.92E-02
C21	1.53E-02	6.35E-03	7.85E-03	1.04E-02	1.31E-02	1.67E-02	2.11E-02	2.45E-02	3.45E-02
C22	7.65E-03	3.31E-03	4.19E-03	5.69E-03	7.29E-03	9.53E-03	1.23E-02	1.46E-02	2.10E-02
C23	4.31E-03	1.94E-03	2.52E-03	3.49E-03	4.58E-03	6.10E-03	8.06E-03	9.76E-03	1.43E-02
C24	2.42E-03	1.13E-03	1.50E-03	2.12E-03	2.85E-03	3.87E-03	5.22E-03	6.46E-03	9.62E-03
C25	1.38E-03	6.68E-04	9.08E-04	1.32E-03	1.80E-03	2.50E-03	3.44E-03	4.35E-03	6.60E-03
C26	7.64E-04	3.85E-04	5.35E-04	7.92E-04	1.11E-03	1.57E-03	2.20E-03	2.84E-03	4.38E-03
C27	4.59E-04	2.39E-04	3.40E-04	5.14E-04	7.32E-04	1.06E-03	1.51E-03	1.99E-03	3.12E-03
C28	2.75E-04	1.49E-04	2.16E-04	3.34E-04	4.86E-04	7.16E-04	1.04E-03	1.40E-03	2.23E-03
C29	1.93E-04	1.07E-04	1.59E-04	2.49E-04	3.69E-04	5.53E-04	8.18E-04	1.12E-03	1.81E-03
C30	7.50E-05	4.50E-05	6.98E-05	1.14E-04	1.76E-04	2.75E-04	4.23E-04	6.00E-04	1.00E-03
C31	4.34E-05	2.68E-05	4.23E-05	7.04E-05	1.10E-04	1.75E-04	2.73E-04	3.93E-04	6.66E-04
C32	2.52E-05	1.61E-05	2.60E-05	4.41E-05	7.05E-05	1.14E-04	1.81E-04	2.66E-04	4.58E-04
C33	1.42E-05	9.36E-06	1.54E-05	2.67E-05	4.34E-05	7.13E-05	1.15E-04	1.73E-04	3.02E-04
C34	8.93E-06	6.09E-06	1.02E-05	1.80E-05	2.98E-05	4.98E-05	8.18E-05	1.25E-04	2.21E-04
C35	5.52E-06	3.87E-06	6.61E-06	1.18E-05	1.99E-05	3.39E-05	5.65E-05	8.75E-05	1.58E-04
C36+	5.12E-05	3.76E-05	6.63E-05	1.23E-04	2.14E-04	3.75E-04	6.45E-04	1.02E-03	1.91E-03

Table B.6: Results from simulated steam distillation of crude at different T_{sat+15} & P_{sat} conditions (210 °C to 270 °C) (Run-1).

	Distillation Cuts @ Temp °C						
Mass Flow gm/hr	**210**	**220**	**230**	**240**	**250**	**260**	**270**
WATER	2.86E+01	2.84E+01	2.82E+01	2.79E+01	2.75E+01	2.96E+01	2.42E+01
PROPA-01	0.00E+00	0.00E+00	0.00E+00	0.00E+00	0.00E+00	0.00E+00	0.00E+00
N-PEN-01	0.00E+00	0.00E+00	0.00E+00	0.00E+00	0.00E+00	0.00E+00	0.00E+00
NITROGEN	1.49E+00	1.49E+00	1.48E+00	1.48E+00	1.47E+00	1.48E+00	1.43E+00
METHY-02	0.00E+00	0.00E+00	0.00E+00	0.00E+00	0.00E+00	0.00E+00	0.00E+00
CYCLOHEX	0.00E+00	0.00E+00	0.00E+00	0.00E+00	0.00E+00	0.00E+00	0.00E+00
HEXANES	0.00E+00	0.00E+00	0.00E+00	0.00E+00	0.00E+00	0.00E+00	0.00E+00
METHY-01	1.49E-05	8.58E-06	5.08E-06	3.08E-06	1.92E-06	1.43E-06	6.90E-07
TOLUE-01	0.00E+00	0.00E+00	0.00E+00	0.00E+00	0.00E+00	0.00E+00	0.00E+00
HEPTANES	4.53E-06	2.37E-06	1.29E-06	7.22E-07	4.17E-07	0.00E+00	0.00E+00
OCATANES	3.68E-04	2.28E-04	1.44E-04	9.29E-05	6.09E-05	4.78E-05	2.39E-05
ETHYL-02	5.58E-04	3.89E-04	2.75E-04	1.97E-04	1.42E-04	1.25E-04	6.68E-05
M-XYL-01	2.26E-04	1.60E-04	1.14E-04	8.26E-05	6.02E-05	5.36E-05	2.88E-05
O-XYL-01	2.91E-04	2.11E-04	1.55E-04	1.14E-04	8.51E-05	7.78E-05	4.25E-05
NONANES	5.23E-03	3.75E-03	2.72E-03	1.99E-03	1.46E-03	1.30E-03	7.08E-04
1,2,4-C9	4.13E-03	3.38E-03	2.77E-03	2.27E-03	1.86E-03	1.90E-03	1.11E-03
C10	4.65E-02	3.74E-02	3.01E-02	2.43E-02	1.96E-02	1.95E-02	1.13E-02
C11	1.62E-01	1.41E-01	1.23E-01	1.07E-01	9.27E-02	1.00E-01	6.12E-02
C12	3.40E-01	3.18E-01	2.97E-01	2.75E-01	2.54E-01	2.97E-01	1.90E-01

C13	4.54E-01	4.48E-01	4.40E-01	4.29E-01	4.16E-01	5.18E-01	3.43E-01
C14	3.71E-01	3.83E-01	3.94E-01	4.03E-01	4.08E-01	5.40E-01	3.70E-01
C15	3.56E-01	3.83E-01	4.11E-01	4.37E-01	4.62E-01	6.47E-01	4.57E-01
C16	2.60E-01	2.89E-01	3.20E-01	3.53E-01	3.86E-01	5.66E-01	4.10E-01
C17	1.65E-01	1.89E-01	2.15E-01	2.44E-01	2.76E-01	4.23E-01	3.13E-01
C18	1.29E-01	1.51E-01	1.76E-01	2.04E-01	2.36E-01	3.74E-01	2.81E-01
C19	9.32E-02	1.11E-01	1.33E-01	1.57E-01	1.85E-01	3.03E-01	2.31E-01
C20	5.88E-02	7.18E-02	8.75E-02	1.06E-01	1.28E-01	2.17E-01	1.68E-01
C21	4.21E-02	5.26E-02	6.54E-02	8.11E-02	1.00E-01	1.75E-01	1.37E-01
C22	2.61E-02	3.33E-02	4.23E-02	5.35E-02	6.74E-02	1.21E-01	9.64E-02
C23	1.81E-02	2.36E-02	3.05E-02	3.94E-02	5.07E-02	9.39E-02	7.56E-02
C24	1.25E-02	1.65E-02	2.18E-02	2.87E-02	3.76E-02	7.16E-02	5.83E-02
C25	8.72E-03	1.18E-02	1.58E-02	2.12E-02	2.84E-02	5.56E-02	4.58E-02
C26	5.89E-03	8.10E-03	1.11E-02	1.52E-02	2.06E-02	4.16E-02	3.46E-02
C27	4.27E-03	5.97E-03	8.33E-03	1.16E-02	1.61E-02	3.32E-02	2.79E-02
C28	3.11E-03	4.43E-03	6.30E-03	8.92E-03	1.26E-02	2.67E-02	2.27E-02
C29	2.56E-03	3.70E-03	5.33E-03	7.66E-03	1.10E-02	2.38E-02	2.04E-02
C30	1.47E-03	2.20E-03	3.28E-03	4.87E-03	7.20E-03	1.64E-02	1.43E-02
C31	9.90E-04	1.50E-03	2.27E-03	3.42E-03	5.13E-03	1.19E-02	1.05E-02
C32	6.93E-04	1.07E-03	1.65E-03	2.52E-03	3.85E-03	9.19E-03	8.13E-03
C33	4.65E-04	7.30E-04	1.14E-03	1.78E-03	2.76E-03	6.74E-03	6.02E-03
C34	3.46E-04	5.51E-04	8.73E-04	1.38E-03	2.17E-03	5.43E-03	4.89E-03
C35	2.50E-04	4.03E-04	6.49E-04	1.04E-03	1.66E-03	4.24E-03	3.85E-03
C36+	3.11E-03	5.17E-03	8.57E-03	1.41E-02	2.33E-02	6.37E-02	5.73E-02

Table B.7: Results from simulated steam distillation of crude at different T_{sat+15} & P_{sat} conditions (115°C to 200°C) (Run-2).

	Distillation Cuts @ Temp °C								
Mass Flow gm/hr	**115**	**130**	**140**	**150**	**160**	**170**	**180**	**190**	**200**
WATER	2.97E+01	2.79E+01	2.95E+01	2.89E+01	2.92E+01	2.92E+01	2.90E+01	2.89E+01	2.88E+01
PROPA-01	0.00E+00	0.00E+00	0.00E+00	0.00E+00	0.00E+00	0.00E+00	0.00E+00	0.00E+00	0.00E+00
N-PEN-01	0.00E+00	0.00E+00	0.00E+00	0.00E+00	0.00E+00	0.00E+00	0.00E+00	0.00E+00	0.00E+00
NITROGEN	1.50E+00	1.50E+00	1.50E+00	1.50E+00	1.50E+00	1.50E+00	1.50E+00	1.49E+00	1.49E+00
METHY-02	0.00E+00	0.00E+00	0.00E+00	0.00E+00	0.00E+00	0.00E+00	0.00E+00	0.00E+00	0.00E+00
CYCLOHEX	0.00E+00	0.00E+00	0.00E+00	0.00E+00	0.00E+00	0.00E+00	0.00E+00	0.00E+00	0.00E+00
HEXANES	5.78E-02	1.73E-03	3.75E-04	8.02E-05	2.20E-05	6.57E-06	2.11E-06	7.28E-07	0.00E+00
METHY-01	5.47E-02	3.13E-03	1.25E-03	4.57E-04	2.07E-04	9.90E-05	4.94E-05	2.56E-05	1.38E-05
TOLUE-01	0.00E+00	0.00E+00	0.00E+00	0.00E+00	0.00E+00	0.00E+00	0.00E+00	0.00E+00	0.00E+00
HEPTANES	5.60E-02	2.65E-03	8.83E-04	2.77E-04	1.09E-04	4.54E-05	2.00E-05	9.22E-06	4.45E-06
OCATANES	4.22E-01	2.99E-02	1.43E-02	6.12E-03	3.19E-03	1.73E-03	9.68E-04	5.57E-04	3.29E-04
ETHYL-02	1.47E-01	1.32E-02	7.87E-03	4.08E-03	2.53E-03	1.62E-03	1.06E-03	7.05E-04	4.76E-04
M-XYL-01	4.83E-02	4.51E-03	2.79E-03	1.49E-03	9.48E-04	6.22E-04	4.15E-04	2.81E-04	1.93E-04
O-XYL-01	4.72E-02	4.59E-03	2.96E-03	1.63E-03	1.08E-03	7.30E-04	5.01E-04	3.49E-04	2.47E-04
NONANES	8.47E-01	8.39E-02	5.42E-02	3.01E-02	1.98E-02	1.34E-02	9.18E-03	6.37E-03	4.47E-03
1,2,4-C9	1.50E-01	1.91E-02	1.56E-02	1.05E-02	8.32E-03	6.69E-03	5.39E-03	4.37E-03	3.55E-03
C10	1.93E+00	2.43E-01	1.94E-01	1.29E-01	1.00E-01	7.93E-02	6.28E-02	5.00E-02	3.99E-02
C11	2.78E+00	4.08E-01	3.72E-01	2.78E-01	2.42E-01	2.12E-01	1.86E-01	1.63E-01	1.42E-01
C12	3.02E+00	4.97E-01	5.00E-01	4.07E-01	3.85E-01	3.66E-01	3.46E-01	3.27E-01	3.08E-01

C13	2.53E+00	4.51E-01	4.84E-01	4.18E-01	4.19E-01	4.21E-01	4.21E-01	4.20E-01	4.18E-01
C14	1.37E+00	2.63E-01	2.97E-01	2.70E-01	2.83E-01	2.99E-01	3.13E-01	3.28E-01	3.41E-01
C15	9.14E-01	1.86E-01	2.20E-01	2.09E-01	2.28E-01	2.51E-01	2.74E-01	2.98E-01	3.24E-01
C16	4.94E-01	1.06E-01	1.30E-01	1.27E-01	1.44E-01	1.63E-01	1.84E-01	2.07E-01	2.32E-01
C17	2.35E-01	5.32E-02	6.71E-02	6.79E-02	7.91E-02	9.25E-02	1.07E-01	1.24E-01	1.44E-01
C18	1.49E-01	3.50E-02	4.51E-02	4.68E-02	5.57E-02	6.66E-02	7.90E-02	9.35E-02	1.10E-01
C19	8.78E-02	2.14E-02	2.82E-02	3.00E-02	3.65E-02	4.45E-02	5.39E-02	6.51E-02	7.83E-02
C20	4.40E-02	1.12E-02	1.52E-02	1.65E-02	2.06E-02	2.57E-02	3.18E-02	3.93E-02	4.84E-02
C21	2.54E-02	6.73E-03	9.33E-03	1.04E-02	1.33E-02	1.69E-02	2.14E-02	2.70E-02	3.40E-02
C22	1.27E-02	3.51E-03	4.98E-03	5.68E-03	7.40E-03	9.66E-03	1.25E-02	1.61E-02	2.07E-02
C23	7.18E-03	2.06E-03	2.98E-03	3.49E-03	4.65E-03	6.19E-03	8.17E-03	1.07E-02	1.41E-02
C24	4.02E-03	1.20E-03	1.78E-03	2.12E-03	2.89E-03	3.93E-03	5.30E-03	7.10E-03	9.49E-03
C25	2.29E-03	7.08E-04	1.08E-03	1.31E-03	1.83E-03	2.54E-03	3.49E-03	4.78E-03	6.51E-03
C26	1.27E-03	4.08E-04	6.33E-04	7.91E-04	1.12E-03	1.59E-03	2.23E-03	3.11E-03	4.32E-03
C27	7.63E-04	2.54E-04	4.02E-04	5.13E-04	7.44E-04	1.07E-03	1.53E-03	2.18E-03	3.07E-03
C28	4.57E-04	1.58E-04	2.56E-04	3.33E-04	4.93E-04	7.26E-04	1.06E-03	1.53E-03	2.20E-03
C29	3.20E-04	1.14E-04	1.88E-04	2.49E-04	3.75E-04	5.61E-04	8.29E-04	1.22E-03	1.78E-03
C30	1.25E-04	4.77E-05	8.23E-05	1.14E-04	1.79E-04	2.79E-04	4.29E-04	6.53E-04	9.90E-04
C31	7.20E-05	2.84E-05	4.98E-05	7.03E-05	1.12E-04	1.77E-04	2.76E-04	4.27E-04	6.56E-04
C32	4.18E-05	1.71E-05	3.05E-05	4.40E-05	7.15E-05	1.15E-04	1.83E-04	2.89E-04	4.52E-04
C33	2.35E-05	9.91E-06	1.81E-05	2.66E-05	4.41E-05	7.23E-05	1.17E-04	1.87E-04	2.98E-04
C34	1.48E-05	6.45E-06	1.20E-05	1.80E-05	3.02E-05	5.05E-05	8.29E-05	1.35E-04	2.18E-04
C35	9.14E-06	4.10E-06	7.76E-06	1.18E-05	2.02E-05	3.43E-05	5.73E-05	9.46E-05	1.55E-04
C36+	8.49E-05	3.97E-05	7.80E-05	1.23E-04	2.17E-04	3.79E-04	6.53E-04	1.11E-03	1.88E-03

Table B.8: Results from simulated steam distillation of crude at different T_{sat+15} & P_{sat} conditions (210°C to 280°C) (Run-2).

	Distillation Cuts @ Temp °C							
Mass Flow gm/hr	**210**	**220**	**230**	**240**	**250**	**260**	**270**	**280**
WATER	2.86E+01	2.84E+01	2.82E+01	2.79E+01	2.75E+01	2.88E+01	2.50E+01	2.58E+01
PROPA-01	0.00E+00	0.00E+00	0.00E+00	0.00E+00	0.00E+00	0.00E+00	0.00E+00	0.00E+00
N-PEN-01	0.00E+00	0.00E+00	0.00E+00	0.00E+00	0.00E+00	0.00E+00	0.00E+00	0.00E+00
NITROGEN	1.49E+00	1.49E+00	1.48E+00	1.48E+00	1.47E+00	1.47E+00	1.44E+00	1.44E+00
METHY-02	0.00E+00	0.00E+00	0.00E+00	0.00E+00	0.00E+00	0.00E+00	0.00E+00	0.00E+00
CYCLOHEX	0.00E+00	0.00E+00	0.00E+00	0.00E+00	0.00E+00	0.00E+00	0.00E+00	0.00E+00
HEXANES	0.00E+00	0.00E+00	0.00E+00	0.00E+00	0.00E+00	0.00E+00	0.00E+00	0.00E+00
METHY-01	7.65E-06	4.38E-06	2.58E-06	1.56E-06	9.67E-07	7.46E-07	3.90E-07	0.00E+00
TOLUE-01	0.00E+00	0.00E+00	0.00E+00	0.00E+00	0.00E+00	0.00E+00	0.00E+00	0.00E+00
HEPTANES	2.23E-06	1.16E-06	6.28E-07	3.50E-07	0.00E+00	0.00E+00	0.00E+00	0.00E+00
OCATANES	1.99E-04	1.23E-04	7.72E-05	4.95E-05	3.23E-05	2.60E-05	1.41E-05	1.01E-05
ETHYL-02	3.27E-04	2.27E-04	1.60E-04	1.14E-04	8.19E-05	7.26E-05	4.21E-05	3.28E-05
M-XYL-01	1.34E-04	9.47E-05	6.75E-05	4.86E-05	3.53E-05	3.15E-05	1.84E-05	1.44E-05
O-XYL-01	1.77E-04	1.28E-04	9.31E-05	6.86E-05	5.10E-05	4.65E-05	2.76E-05	2.20E-05
NONANES	3.17E-03	2.27E-03	1.64E-03	1.19E-03	8.75E-04	7.81E-04	4.59E-04	3.61E-04
1,2,4-C9	2.89E-03	2.35E-03	1.92E-03	1.57E-03	1.29E-03	1.29E-03	8.17E-04	7.04E-04
C10	3.20E-02	2.57E-02	2.06E-02	1.66E-02	1.33E-02	1.30E-02	8.18E-03	6.93E-03
C11	1.24E-01	1.08E-01	9.44E-02	8.19E-02	7.08E-02	7.45E-02	4.92E-02	4.43E-02
C12	2.89E-01	2.70E-01	2.52E-01	2.33E-01	2.14E-01	2.42E-01	1.67E-01	1.59E-01

C13	4.14E-01	4.07E-01	3.99E-01	3.89E-01	3.76E-01	4.51E-01	3.23E-01	3.21E-01
C14	3.54E-01	3.65E-01	3.75E-01	3.83E-01	3.87E-01	4.92E-01	3.64E-01	3.78E-01
C15	3.50E-01	3.76E-01	4.02E-01	4.27E-01	4.51E-01	6.06E-01	4.61E-01	5.00E-01
C16	2.59E-01	2.87E-01	3.18E-01	3.50E-01	3.82E-01	5.38E-01	4.19E-01	4.70E-01
C17	1.65E-01	1.89E-01	2.15E-01	2.44E-01	2.75E-01	4.06E-01	3.22E-01	3.74E-01
C18	1.30E-01	1.52E-01	1.77E-01	2.05E-01	2.36E-01	3.60E-01	2.90E-01	3.45E-01
C19	9.39E-02	1.12E-01	1.33E-01	1.58E-01	1.86E-01	2.93E-01	2.39E-01	2.91E-01
C20	5.94E-02	7.25E-02	8.82E-02	1.07E-01	1.29E-01	2.10E-01	1.74E-01	2.17E-01
C21	4.26E-02	5.31E-02	6.60E-02	8.17E-02	1.01E-01	1.69E-01	1.42E-01	1.81E-01
C22	2.64E-02	3.36E-02	4.27E-02	5.40E-02	6.80E-02	1.18E-01	1.00E-01	1.31E-01
C23	1.84E-02	2.38E-02	3.08E-02	3.98E-02	5.11E-02	9.14E-02	7.83E-02	1.05E-01
C24	1.26E-02	1.67E-02	2.20E-02	2.89E-02	3.79E-02	6.99E-02	6.05E-02	8.25E-02
C25	8.81E-03	1.19E-02	1.60E-02	2.14E-02	2.86E-02	5.43E-02	4.75E-02	6.61E-02
C26	5.96E-03	8.18E-03	1.12E-02	1.53E-02	2.08E-02	4.07E-02	3.59E-02	5.09E-02
C27	4.32E-03	6.04E-03	8.42E-03	1.17E-02	1.62E-02	3.25E-02	2.89E-02	4.18E-02
C28	3.15E-03	4.48E-03	6.36E-03	9.00E-03	1.27E-02	2.62E-02	2.35E-02	3.47E-02
C29	2.59E-03	3.74E-03	5.38E-03	7.73E-03	1.11E-02	2.34E-02	2.12E-02	3.16E-02
C30	1.49E-03	2.22E-03	3.31E-03	4.91E-03	7.26E-03	1.61E-02	1.48E-02	2.28E-02
C31	1.00E-03	1.52E-03	2.29E-03	3.45E-03	5.17E-03	1.18E-02	1.09E-02	1.70E-02
C32	7.01E-04	1.08E-03	1.66E-03	2.54E-03	3.88E-03	9.06E-03	8.43E-03	1.35E-02
C33	4.70E-04	7.38E-04	1.15E-03	1.79E-03	2.78E-03	6.65E-03	6.24E-03	1.01E-02
C34	3.49E-04	5.56E-04	8.82E-04	1.39E-03	2.19E-03	5.37E-03	5.07E-03	8.36E-03
C35	2.52E-04	4.08E-04	6.55E-04	1.05E-03	1.68E-03	4.20E-03	3.99E-03	6.68E-03
C36+	3.14E-03	5.22E-03	8.63E-03	1.42E-02	2.34E-02	6.29E-02	5.94E-02	1.03E-01

Table B. 9: Results from simulated steam-propane distillation of crude at different T_{sat+15} & P_{sat} conditions (118°C to 202°C) (Run-1).

	Distillation Cuts @ Temp °C								
Mass Flow gm/hr	**118**	**132**	**139**	**149**	**161**	**170**	**180**	**191**	**202**
WATER	2.95E+01	2.79E+01	2.96E+01	2.89E+01	2.93E+01	2.91E+01	2.90E+01	2.82E+01	2.97E+01
PROPA-01	1.49E+00	1.46E+00	1.49E+00	1.48E+00	1.48E+00	1.48E+00	1.47E+00	1.45E+00	1.49E+00
N-PEN-01	0.00E+00	0.00E+00	0.00E+00	0.00E+00	0.00E+00	0.00E+00	0.00E+00	0.00E+00	0.00E+00
NITROGEN	0.00E+00	0.00E+00	0.00E+00	0.00E+00	0.00E+00	0.00E+00	0.00E+00	0.00E+00	0.00E+00
METHY-02	0.00E+00	0.00E+00	0.00E+00	0.00E+00	0.00E+00	0.00E+00	0.00E+00	0.00E+00	0.00E+00
CYCLOHEX	0.00E+00	0.00E+00	0.00E+00	0.00E+00	0.00E+00	0.00E+00	0.00E+00	0.00E+00	0.00E+00
HEXANES	5.66E-02	2.62E-03	6.09E-04	1.34E-04	3.85E-05	1.14E-05	3.75E-06	1.26E-06	5.35E-07
METHY-01	5.22E-02	4.52E-03	1.90E-03	7.12E-04	3.39E-04	1.60E-04	8.09E-05	4.02E-05	2.50E-05
TOLUE-01	0.00E+00	0.00E+00	0.00E+00	0.00E+00	0.00E+00	0.00E+00	0.00E+00	0.00E+00	0.00E+00
HEPTANES	5.40E-02	3.90E-03	1.38E-03	4.43E-04	1.82E-04	7.54E-05	3.37E-05	1.50E-05	8.35E-06
OCATANES	3.96E-01	4.20E-02	2.10E-02	9.19E-03	5.04E-03	2.69E-03	1.52E-03	8.36E-04	5.71E-04
ETHYL-02	1.34E-01	1.78E-02	1.10E-02	5.79E-03	3.80E-03	2.38E-03	1.57E-03	9.86E-04	7.75E-04
M-XYL-01	4.37E-02	6.02E-03	3.86E-03	2.08E-03	1.41E-03	9.02E-04	6.07E-04	3.88E-04	3.10E-04
O-XYL-01	4.24E-02	6.07E-03	4.04E-03	2.26E-03	1.58E-03	1.04E-03	7.24E-04	4.75E-04	3.91E-04
NONANES	7.59E-01	1.11E-01	7.39E-02	4.15E-02	2.90E-02	1.91E-02	1.32E-02	8.67E-03	7.06E-03
1,2,4-C9	1.25E-01	2.32E-02	1.92E-02	1.30E-02	1.10E-02	8.59E-03	6.97E-03	5.28E-03	5.01E-03
C10	1.63E+00	2.98E-01	2.42E-01	1.62E-01	1.34E-01	1.03E-01	8.22E-02	6.14E-02	5.71E-02
C11	2.21E+00	4.66E-01	4.28E-01	3.21E-01	2.98E-01	2.53E-01	2.23E-01	1.83E-01	1.86E-01
C12	2.27E+00	5.34E-01	5.34E-01	4.36E-01	4.42E-01	4.05E-01	3.85E-01	3.40E-01	3.74E-01

C13	1.83E+00	4.65E-01	4.91E-01	4.25E-01	4.58E-01	4.43E-01	4.45E-01	4.16E-01	4.83E-01
C14	9.71E-01	2.64E-01	2.91E-01	2.64E-01	3.00E-01	3.04E-01	3.20E-01	3.14E-01	3.82E-01
C15	6.42E-01	1.85E-01	2.11E-01	2.00E-01	2.38E-01	2.50E-01	2.74E-01	2.81E-01	3.56E-01
C16	3.46E-01	1.05E-01	1.23E-01	1.20E-01	1.49E-01	1.61E-01	1.82E-01	1.93E-01	2.53E-01
C17	1.66E-01	5.26E-02	6.30E-02	6.37E-02	8.15E-02	9.08E-02	1.06E-01	1.16E-01	1.57E-01
C18	1.05E-01	3.47E-02	4.22E-02	4.37E-02	5.74E-02	6.53E-02	7.77E-02	8.74E-02	1.20E-01
C19	6.25E-02	2.13E-02	2.64E-02	2.79E-02	3.76E-02	4.35E-02	5.29E-02	6.10E-02	8.57E-02
C20	3.16E-02	1.12E-02	1.41E-02	1.53E-02	2.12E-02	2.51E-02	3.12E-02	3.69E-02	5.31E-02
C21	1.84E-02	6.75E-03	8.66E-03	9.63E-03	1.37E-02	1.65E-02	2.10E-02	2.55E-02	3.74E-02
C22	9.27E-03	3.54E-03	4.61E-03	5.25E-03	7.67E-03	9.45E-03	1.23E-02	1.52E-02	2.28E-02
C23	5.26E-03	2.08E-03	2.76E-03	3.22E-03	4.82E-03	6.06E-03	8.03E-03	1.02E-02	1.56E-02
C24	2.97E-03	1.22E-03	1.64E-03	1.96E-03	3.00E-03	3.85E-03	5.20E-03	6.77E-03	1.05E-02
C25	1.70E-03	7.24E-04	9.90E-04	1.21E-03	1.91E-03	2.49E-03	3.43E-03	4.57E-03	7.25E-03
C26	9.53E-04	4.19E-04	5.82E-04	7.27E-04	1.17E-03	1.56E-03	2.19E-03	2.99E-03	4.83E-03
C27	5.76E-04	2.62E-04	3.69E-04	4.71E-04	7.78E-04	1.05E-03	1.51E-03	2.10E-03	3.45E-03
C28	3.48E-04	1.64E-04	2.34E-04	3.05E-04	5.17E-04	7.12E-04	1.04E-03	1.48E-03	2.48E-03
C29	2.45E-04	1.18E-04	1.72E-04	2.28E-04	3.93E-04	5.50E-04	8.17E-04	1.18E-03	2.01E-03
C30	9.67E-05	5.02E-05	7.50E-05	1.04E-04	1.89E-04	2.74E-04	4.22E-04	6.37E-04	1.12E-03
C31	5.63E-05	3.00E-05	4.53E-05	6.40E-05	1.18E-04	1.74E-04	2.72E-04	4.18E-04	7.48E-04
C32	3.28E-05	1.81E-05	2.77E-05	4.00E-05	7.57E-05	1.13E-04	1.81E-04	2.83E-04	5.16E-04
C33	1.86E-05	1.05E-05	1.64E-05	2.42E-05	4.67E-05	7.10E-05	1.15E-04	1.84E-04	3.42E-04
C34	1.18E-05	6.89E-06	1.09E-05	1.63E-05	3.21E-05	4.96E-05	8.18E-05	1.33E-04	2.51E-04
C35	7.32E-06	4.40E-06	7.01E-06	1.07E-05	2.15E-05	3.37E-05	5.66E-05	9.37E-05	1.79E-04
C36+	6.89E-05	4.30E-05	7.03E-05	1.11E-04	2.32E-04	3.73E-04	6.45E-04	1.10E-03	2.18E-03

Table B. 10: Results from simulated steam-propane distillation of crude at different T_{sat+15} & P_{sat} conditions (210°C to 279°C) (Run-1).

	Distillation Cuts @ Temp °C							
Mass Flow gm/hr	**210**	**219**	**230**	**241**	**250**	**260**	**271**	**279**
WATER	2.83E+01	2.82E+01	2.82E+01	2.80E+01	2.72E+01	2.96E+01	2.40E+01	2.58E+01
PROPA-01	1.45E+00	1.45E+00	1.45E+00	1.44E+00	1.41E+00	1.48E+00	1.29E+00	0.00E+00
N-PEN-01	0.00E+00	0.00E+00	0.00E+00	0.00E+00	0.00E+00	0.00E+00	0.00E+00	0.00E+00
NITROGEN	0.00E+00	0.00E+00	0.00E+00	0.00E+00	0.00E+00	0.00E+00	0.00E+00	1.44E+00
METHY-02	0.00E+00	0.00E+00	0.00E+00	0.00E+00	0.00E+00	0.00E+00	0.00E+00	0.00E+00
CYCLOHEX	0.00E+00	0.00E+00	0.00E+00	0.00E+00	0.00E+00	0.00E+00	0.00E+00	0.00E+00
HEXANES	0.00E+00	0.00E+00	0.00E+00	0.00E+00	0.00E+00	0.00E+00	0.00E+00	0.00E+00
METHY-01	1.30E-05	7.49E-06	4.58E-06	2.82E-06	1.71E-06	1.30E-06	6.31E-07	0.00E+00
TOLUE-01	0.00E+00	0.00E+00	0.00E+00	0.00E+00	0.00E+00	0.00E+00	0.00E+00	0.00E+00
HEPTANES	3.95E-06	2.07E-06	1.16E-06	6.60E-07	3.73E-07	0.00E+00	0.00E+00	0.00E+00
OCATANES	3.22E-04	1.99E-04	1.30E-04	8.51E-05	5.43E-05	4.35E-05	2.18E-05	1.01E-05
ETHYL-02	4.94E-04	3.42E-04	2.50E-04	1.82E-04	1.27E-04	1.14E-04	6.12E-05	3.28E-05
M-XYL-01	2.01E-04	1.41E-04	1.04E-04	7.64E-05	5.40E-05	4.91E-05	2.64E-05	1.44E-05
O-XYL-01	2.59E-04	1.86E-04	1.41E-04	1.06E-04	7.66E-05	7.14E-05	3.90E-05	2.20E-05
NONANES	4.65E-03	3.31E-03	2.48E-03	1.84E-03	1.31E-03	1.20E-03	6.50E-04	3.61E-04
1,2,4-C9	3.76E-03	3.03E-03	2.57E-03	2.15E-03	1.70E-03	1.77E-03	1.04E-03	7.04E-04
C10	4.22E-02	3.35E-02	2.79E-02	2.29E-02	1.79E-02	1.81E-02	1.05E-02	6.93E-03
C11	1.50E-01	1.29E-01	1.16E-01	1.03E-01	8.62E-02	9.48E-02	5.81E-02	4.43E-02
C12	3.21E-01	2.95E-01	2.85E-01	2.70E-01	2.40E-01	2.85E-01	1.83E-01	1.59E-01

C13	4.35E-01	4.21E-01	4.28E-01	4.27E-01	3.98E-01	5.05E-01	3.36E-01	3.21E-01
C14	3.59E-01	3.63E-01	3.88E-01	4.06E-01	3.95E-01	5.32E-01	3.67E-01	3.78E-01
C15	3.48E-01	3.65E-01	4.07E-01	4.44E-01	4.51E-01	6.42E-01	4.57E-01	5.00E-01
C16	2.55E-01	2.76E-01	3.19E-01	3.60E-01	3.78E-01	5.64E-01	4.13E-01	4.70E-01
C17	1.62E-01	1.80E-01	2.15E-01	2.51E-01	2.71E-01	4.23E-01	3.17E-01	3.74E-01
C18	1.27E-01	1.44E-01	1.76E-01	2.10E-01	2.33E-01	3.75E-01	2.85E-01	3.45E-01
C19	9.18E-02	1.07E-01	1.33E-01	1.62E-01	1.83E-01	3.05E-01	2.36E-01	2.91E-01
C20	5.80E-02	6.88E-02	8.78E-02	1.10E-01	1.27E-01	2.18E-01	1.72E-01	2.17E-01
C21	4.16E-02	5.04E-02	6.57E-02	8.43E-02	9.93E-02	1.76E-01	1.41E-01	1.81E-01
C22	2.59E-02	3.19E-02	4.26E-02	5.58E-02	6.71E-02	1.23E-01	9.95E-02	1.31E-01
C23	1.80E-02	2.26E-02	3.08E-02	4.12E-02	5.05E-02	9.51E-02	7.82E-02	1.05E-01
C24	1.24E-02	1.58E-02	2.20E-02	3.00E-02	3.75E-02	7.27E-02	6.06E-02	8.25E-02
C25	8.65E-03	1.13E-02	1.60E-02	2.23E-02	2.84E-02	5.65E-02	4.77E-02	6.61E-02
C26	5.85E-03	7.75E-03	1.12E-02	1.60E-02	2.07E-02	4.23E-02	3.62E-02	5.09E-02
C27	4.24E-03	5.72E-03	8.44E-03	1.22E-02	1.61E-02	3.38E-02	2.92E-02	4.18E-02
C28	3.10E-03	4.24E-03	6.38E-03	9.43E-03	1.26E-02	2.73E-02	2.39E-02	3.47E-02
C29	2.54E-03	3.54E-03	5.41E-03	8.12E-03	1.10E-02	2.43E-02	2.15E-02	3.16E-02
C30	1.47E-03	2.10E-03	3.33E-03	5.18E-03	7.26E-03	1.68E-02	1.51E-02	2.28E-02
C31	9.87E-04	1.44E-03	2.31E-03	3.64E-03	5.18E-03	1.23E-02	1.11E-02	1.70E-02
C32	6.92E-04	1.02E-03	1.68E-03	2.69E-03	3.89E-03	9.45E-03	8.66E-03	1.35E-02
C33	4.64E-04	6.97E-04	1.16E-03	1.90E-03	2.79E-03	6.94E-03	6.43E-03	1.01E-02
C34	3.45E-04	5.26E-04	8.91E-04	1.48E-03	2.20E-03	5.60E-03	5.24E-03	8.36E-03
C35	2.49E-04	3.85E-04	6.63E-04	1.12E-03	1.69E-03	4.38E-03	4.13E-03	6.68E-03
C36+	3.11E-03	4.91E-03	8.74E-03	1.52E-02	2.36E-02	6.58E-02	6.19E-02	1.03E-01

Table B 11:: Results from simulated steam-propane distillation of crude at different T_{sat+15} & P_{sat} conditions (115°C to 200°C) (Run-2).

	Distillation Cuts @ Temp °C								
Mass Flow gm/hr	**115**	**130**	**140**	**150**	**160**	**170**	**180**	**190**	**200**
WATER	2.97E+01	2.76E+01	2.98E+01	2.89E+01	2.92E+01	2.91E+01	2.90E+01	2.81E+01	2.96E+01
PROPA-01	1.49E+00	1.46E+00	1.50E+00	1.48E+00	1.48E+00	1.48E+00	1.47E+00	1.45E+00	1.49E+00
N-PEN-01	0.00E+00	0.00E+00	0.00E+00	0.00E+00	0.00E+00	0.00E+00	0.00E+00	0.00E+00	0.00E+00
NITROGEN	0.00E+00	0.00E+00	0.00E+00	0.00E+00	0.00E+00	0.00E+00	0.00E+00	0.00E+00	0.00E+00
METHY-02	0.00E+00	0.00E+00	0.00E+00	0.00E+00	0.00E+00	0.00E+00	0.00E+00	0.00E+00	0.00E+00
CYCLOHEX	0.00E+00	0.00E+00	0.00E+00	0.00E+00	0.00E+00	0.00E+00	0.00E+00	0.00E+00	0.00E+00
HEXANES	5.80E-02	1.53E-03	3.71E-04	7.93E-05	2.19E-05	6.60E-06	2.14E-06	7.09E-07	0.00E+00
METHY-01	5.52E-02	2.71E-03	1.21E-03	4.43E-04	2.02E-04	9.71E-05	4.87E-05	2.37E-05	1.47E-05
TOLUE-01	0.00E+00	0.00E+00	0.00E+00	0.00E+00	0.00E+00	0.00E+00	0.00E+00	0.00E+00	0.00E+00
HEPTANES	5.64E-02	2.31E-03	8.64E-04	2.70E-04	1.07E-04	4.49E-05	1.99E-05	8.68E-06	4.81E-06
OCATANES	4.27E-01	2.57E-02	1.38E-02	5.89E-03	3.08E-03	1.68E-03	9.45E-04	5.08E-04	3.44E-04
ETHYL-02	1.50E-01	1.13E-02	7.55E-03	3.89E-03	2.43E-03	1.56E-03	1.02E-03	6.27E-04	4.88E-04
M-XYL-01	4.92E-02	3.85E-03	2.67E-03	1.42E-03	9.07E-04	5.97E-04	3.99E-04	2.49E-04	1.97E-04
O-XYL-01	4.82E-02	3.91E-03	2.83E-03	1.55E-03	1.03E-03	6.99E-04	4.81E-04	3.08E-04	2.51E-04
NONANES	8.65E-01	7.16E-02	5.19E-02	2.86E-02	1.89E-02	1.28E-02	8.82E-03	5.64E-03	4.54E-03
1,2,4-C9	1.56E-01	1.63E-02	1.49E-02	9.97E-03	7.92E-03	6.38E-03	5.15E-03	3.79E-03	3.54E-03
C10	2.00E+00	2.07E-01	1.85E-01	1.22E-01	9.54E-02	7.56E-02	6.00E-02	4.37E-02	3.99E-02
C11	2.93E+00	3.50E-01	3.58E-01	2.65E-01	2.31E-01	2.03E-01	1.78E-01	1.42E-01	1.42E-01
C12	3.24E+00	4.32E-01	4.87E-01	3.93E-01	3.71E-01	3.53E-01	3.35E-01	2.87E-01	3.08E-01

C13	2.74E+00	3.96E-01	4.75E-01	4.07E-01	4.08E-01	4.10E-01	4.10E-01	3.71E-01	4.20E-01
C14	1.50E+00	2.33E-01	2.94E-01	2.65E-01	2.78E-01	2.93E-01	3.07E-01	2.91E-01	3.45E-01
C15	1.01E+00	1.66E-01	2.19E-01	2.06E-01	2.25E-01	2.47E-01	2.70E-01	2.67E-01	3.29E-01
C16	5.46E-01	9.48E-02	1.29E-01	1.26E-01	1.42E-01	1.61E-01	1.82E-01	1.86E-01	2.36E-01
C17	2.60E-01	4.76E-02	6.70E-02	6.72E-02	7.83E-02	9.16E-02	1.06E-01	1.12E-01	1.46E-01
C18	1.65E-01	3.13E-02	4.51E-02	4.63E-02	5.52E-02	6.60E-02	7.83E-02	8.45E-02	1.13E-01
C19	9.73E-02	1.92E-02	2.82E-02	2.97E-02	3.61E-02	4.41E-02	5.35E-02	5.89E-02	8.00E-02
C20	4.88E-02	1.01E-02	1.52E-02	1.63E-02	2.04E-02	2.55E-02	3.16E-02	3.57E-02	4.95E-02
C21	2.82E-02	6.05E-03	9.33E-03	1.03E-02	1.32E-02	1.68E-02	2.13E-02	2.46E-02	3.48E-02
C22	1.41E-02	3.15E-03	4.98E-03	5.63E-03	7.35E-03	9.60E-03	1.24E-02	1.47E-02	2.12E-02
C23	7.96E-03	1.85E-03	2.99E-03	3.46E-03	4.61E-03	6.15E-03	8.13E-03	9.83E-03	1.44E-02
C24	4.45E-03	1.08E-03	1.78E-03	2.11E-03	2.87E-03	3.91E-03	5.27E-03	6.51E-03	9.72E-03
C25	2.54E-03	6.38E-04	1.08E-03	1.31E-03	1.82E-03	2.53E-03	3.48E-03	4.39E-03	6.67E-03
C26	1.41E-03	3.68E-04	6.34E-04	7.86E-04	1.12E-03	1.58E-03	2.22E-03	2.86E-03	4.43E-03
C27	8.46E-04	2.29E-04	4.03E-04	5.10E-04	7.39E-04	1.07E-03	1.53E-03	2.01E-03	3.16E-03
C28	5.07E-04	1.42E-04	2.56E-04	3.31E-04	4.90E-04	7.23E-04	1.05E-03	1.41E-03	2.26E-03
C29	3.55E-04	1.03E-04	1.88E-04	2.48E-04	3.73E-04	5.59E-04	8.27E-04	1.13E-03	1.83E-03
C30	1.38E-04	4.31E-05	8.25E-05	1.14E-04	1.78E-04	2.78E-04	4.28E-04	6.07E-04	1.02E-03
C31	7.98E-05	2.57E-05	4.99E-05	6.99E-05	1.11E-04	1.76E-04	2.76E-04	3.98E-04	6.76E-04
C32	4.63E-05	1.54E-05	3.06E-05	4.38E-05	7.12E-05	1.15E-04	1.83E-04	2.69E-04	4.65E-04
C33	2.60E-05	8.96E-06	1.81E-05	2.65E-05	4.39E-05	7.21E-05	1.17E-04	1.75E-04	3.07E-04
C34	1.64E-05	5.83E-06	1.20E-05	1.79E-05	3.01E-05	5.03E-05	8.28E-05	1.26E-04	2.25E-04
C35	1.01E-05	3.71E-06	7.78E-06	1.18E-05	2.02E-05	3.42E-05	5.72E-05	8.87E-05	1.60E-04
C36+	9.40E-05	3.59E-05	7.81E-05	1.22E-04	2.16E-04	3.78E-04	6.52E-04	1.04E-03	1.93E-03

Table B. 12: Results from simulated steam-propane distillation of crude at different T_{sat+15} & P_{sat} conditions (210^{o}C to 270^{o}C) (Run-2).

	Distillation Cuts @ Temp ^{o}C						
Mass Flow gm/hr	**210**	**220**	**230**	**240**	**250**	**260**	**270**
WATER	2.86E+01	2.83E+01	2.85E+01	2.74E+01	2.74E+01	2.96E+01	2.37E+01
PROPA-01	1.46E+00	1.45E+00	1.45E+00	1.42E+00	1.42E+00	1.48E+00	1.28E+00
N-PEN-01	0.00E+00	0.00E+00	0.00E+00	0.00E+00	0.00E+00	0.00E+00	0.00E+00
NITROGEN	0.00E+00	0.00E+00	0.00E+00	0.00E+00	0.00E+00	0.00E+00	0.00E+00
METHY-02	0.00E+00	0.00E+00	0.00E+00	0.00E+00	0.00E+00	0.00E+00	0.00E+00
CYCLOHEX	0.00E+00	0.00E+00	0.00E+00	0.00E+00	0.00E+00	0.00E+00	0.00E+00
HEXANES	0.00E+00	0.00E+00	0.00E+00	0.00E+00	0.00E+00	0.00E+00	0.00E+00
METHY-01	7.98E-06	4.59E-06	2.81E-06	1.61E-06	1.02E-06	7.67E-07	3.63E-07
TOLUE-01	0.00E+00	0.00E+00	0.00E+00	0.00E+00	0.00E+00	0.00E+00	0.00E+00
HEPTANES	2.37E-06	1.24E-06	6.93E-07	3.69E-07	0.00E+00	0.00E+00	0.00E+00
OCATANES	2.03E-04	1.26E-04	8.23E-05	5.02E-05	3.33E-05	2.64E-05	1.29E-05
ETHYL-02	3.27E-04	2.28E-04	1.67E-04	1.12E-04	8.23E-05	7.31E-05	3.82E-05
M-XYL-01	1.34E-04	9.47E-05	7.04E-05	4.78E-05	3.53E-05	3.17E-05	1.66E-05
O-XYL-01	1.75E-04	1.27E-04	9.68E-05	6.72E-05	5.07E-05	4.68E-05	2.49E-05
NONANES	3.15E-03	2.26E-03	1.70E-03	1.17E-03	8.71E-04	7.83E-04	4.15E-04
1,2,4-C9	2.81E-03	2.30E-03	1.97E-03	1.51E-03	1.25E-03	1.29E-03	7.34E-04
C10	3.12E-02	2.51E-02	2.11E-02	1.59E-02	1.30E-02	1.30E-02	7.36E-03
C11	1.21E-01	1.05E-01	9.64E-02	7.83E-02	6.86E-02	7.47E-02	4.45E-02
12	2.82E-01	2.63E-01	2.59E-01	2.23E-01	2.08E-01	2.45E-01	1.53E-01

C13	4.05E-01	3.99E-01	4.14E-01	3.75E-01	3.68E-01	4.61E-01	2.98E-01
C14	3.48E-01	3.59E-01	3.92E-01	3.71E-01	3.81E-01	5.07E-01	3.39E-01
C15	3.45E-01	3.71E-01	4.23E-01	4.16E-01	4.45E-01	6.28E-01	4.33E-01
C16	2.56E-01	2.85E-01	3.37E-01	3.42E-01	3.78E-01	5.59E-01	3.95E-01
C17	1.64E-01	1.87E-01	2.29E-01	2.39E-01	2.73E-01	4.22E-01	3.05E-01
C18	1.29E-01	1.51E-01	1.89E-01	2.01E-01	2.35E-01	3.75E-01	2.75E-01
C19	9.34E-02	1.12E-01	1.43E-01	1.55E-01	1.86E-01	3.05E-01	2.28E-01
C20	5.90E-02	7.22E-02	9.49E-02	1.05E-01	1.29E-01	2.19E-01	1.66E-01
C21	4.24E-02	5.29E-02	7.12E-02	8.06E-02	1.01E-01	1.77E-01	1.36E-01
C22	2.63E-02	3.36E-02	4.62E-02	5.33E-02	6.81E-02	1.23E-01	9.61E-02
C23	1.83E-02	2.38E-02	3.35E-02	3.93E-02	5.13E-02	9.56E-02	7.55E-02
C24	1.26E-02	1.67E-02	2.40E-02	2.87E-02	3.81E-02	7.31E-02	5.85E-02
C25	8.81E-03	1.19E-02	1.75E-02	2.13E-02	2.88E-02	5.68E-02	4.60E-02
C26	5.95E-03	8.20E-03	1.23E-02	1.52E-02	2.10E-02	4.25E-02	3.49E-02
C27	4.32E-03	6.05E-03	9.27E-03	1.16E-02	1.63E-02	3.40E-02	2.82E-02
C28	3.15E-03	4.50E-03	7.03E-03	8.96E-03	1.28E-02	2.74E-02	2.30E-02
C29	2.59E-03	3.75E-03	5.96E-03	7.70E-03	1.12E-02	2.45E-02	2.07E-02
C30	1.49E-03	2.24E-03	3.69E-03	4.90E-03	7.37E-03	1.69E-02	1.45E-02
C31	1.00E-03	1.53E-03	2.56E-03	3.45E-03	5.26E-03	1.23E-02	1.07E-02
C32	7.04E-04	1.09E-03	1.86E-03	2.55E-03	3.95E-03	9.49E-03	8.30E-03
C33	4.73E-04	7.44E-04	1.29E-03	1.80E-03	2.83E-03	6.97E-03	6.16E-03
C34	3.51E-04	5.61E-04	9.93E-04	1.40E-03	2.24E-03	5.63E-03	5.01E-03
C35	2.54E-04	4.11E-04	7.40E-04	1.05E-03	1.71E-03	4.40E-03	3.95E-03
C36+	3.16E-03	5.26E-03	9.83E-03	1.43E-02	2.39E-02	6.60E-02	5.88E-02

Table B. 13: Results from simulated steam distillation of crude at field (260psig) conditions (Run-1).

	Distillation Cuts @ Temp ^oC								
Mass Flow gm/hr	**230**	**240**	**244**	**250**	**260**	**270**	**280**	**290**	**300**
WATER	2.53E+01	3.03E+01	3.01E+01	3.05E+01	3.04E+01	3.04E+01	3.04E+01	3.04E+01	3.02E+01
PROPA-01	0.00E+00	0.00E+00	0.00E+00	0.00E+00	0.00E+00	0.00E+00	0.00E+00	0.00E+00	0.00E+00
N-PEN-01	0.00E+00	0.00E+00	0.00E+00	0.00E+00	0.00E+00	0.00E+00	0.00E+00	0.00E+00	0.00E+00
NITROGEN	1.48E+00	1.50E+00	1.50E+00	1.50E+00	1.50E+00	1.50E+00	1.50E+00	1.50E+00	1.50E+00
METHY-02	0.00E+00	0.00E+00	0.00E+00	0.00E+00	0.00E+00	0.00E+00	0.00E+00	0.00E+00	0.00E+00
CYCLOHEX	0.00E+00	0.00E+00	0.00E+00	0.00E+00	0.00E+00	0.00E+00	0.00E+00	0.00E+00	0.00E+00
HEXANES	2.01E-02	5.79E-03	1.28E-03	2.85E-04	5.55E-05	9.66E-06	1.47E-06	0.00E+00	0.00E+00
METHY-01	1.62E-02	7.40E-03	2.57E-03	9.16E-04	2.87E-04	8.07E-05	1.99E-05	4.31E-06	7.86E-07
TOLUE-01	0.00E+00	0.00E+00	0.00E+00	0.00E+00	0.00E+00	0.00E+00	0.00E+00	0.00E+00	0.00E+00
HEPTANES	1.75E-02	6.96E-03	2.11E-03	6.51E-04	1.76E-04	4.28E-05	9.07E-06	1.69E-06	0.00E+00
OCATANES	1.21E-01	6.13E-02	2.35E-02	9.30E-03	3.23E-03	1.01E-03	2.75E-04	6.62E-05	1.33E-05
ETHYL-02	3.87E-02	2.38E-02	1.11E-02	5.36E-03	2.30E-03	8.95E-04	3.05E-04	9.19E-05	2.31E-05
M-XYL-01	1.27E-02	7.93E-03	3.75E-03	1.85E-03	8.09E-04	3.20E-04	1.11E-04	3.40E-05	8.65E-06
O-XYL-01	1.21E-02	7.92E-03	3.93E-03	2.04E-03	9.41E-04	3.94E-04	1.45E-04	4.73E-05	1.28E-05
NONANES	2.24E-01	1.43E-01	6.89E-02	3.46E-02	1.54E-02	6.21E-03	2.19E-03	6.86E-04	1.78E-04
1,2,4-C9	3.72E-02	2.99E-02	1.81E-02	1.17E-02	6.74E-03	3.58E-03	1.68E-03	7.04E-04	2.44E-04
C10	4.94E-01	3.82E-01	2.22E-01	1.37E-01	7.53E-02	3.80E-02	1.69E-02	6.70E-03	2.20E-03
C11	7.34E-01	6.58E-01	4.43E-01	3.21E-01	2.09E-01	1.27E-01	6.83E-02	3.32E-02	1.33E-02
C12	8.94E-01	9.08E-01	6.92E-01	5.75E-01	4.36E-01	3.12E-01	2.01E-01	1.18E-01	5.73E-02

C13	8.91E-01	9.93E-01	8.29E-01	7.67E-01	6.54E-01	5.34E-01	3.96E-01	2.73E-01	1.55E-01
C14	6.16E-01	7.42E-01	6.69E-01	6.78E-01	6.40E-01	5.87E-01	4.95E-01	3.96E-01	2.62E-01
C15	5.48E-01	7.02E-01	6.73E-01	7.34E-01	7.53E-01	7.62E-01	7.19E-01	6.54E-01	4.95E-01
C16	3.92E-01	5.25E-01	5.25E-01	6.04E-01	6.58E-01	7.17E-01	7.35E-01	7.40E-01	6.20E-01
C17	2.49E-01	3.46E-01	3.58E-01	4.29E-01	4.91E-01	5.67E-01	6.22E-01	6.81E-01	6.22E-01
C18	1.98E-01	2.81E-01	2.97E-01	3.66E-01	4.32E-01	5.18E-01	5.95E-01	6.88E-01	6.66E-01
C19	1.46E-01	2.12E-01	2.27E-01	2.87E-01	3.47E-01	4.30E-01	5.12E-01	6.21E-01	6.30E-01
C20	9.51E-02	1.40E-01	1.53E-01	1.97E-01	2.44E-01	3.11E-01	3.84E-01	4.87E-01	5.16E-01
C21	7.02E-02	1.05E-01	1.16E-01	1.52E-01	1.92E-01	2.52E-01	3.20E-01	4.21E-01	4.63E-01
C22	4.50E-02	6.82E-02	7.63E-02	1.01E-01	1.30E-01	1.74E-01	2.27E-01	3.08E-01	3.50E-01
C23	3.22E-02	4.95E-02	5.59E-02	7.52E-02	9.81E-02	1.34E-01	1.77E-01	2.48E-01	2.88E-01
C24	2.28E-02	3.55E-02	4.04E-02	5.50E-02	7.26E-02	1.00E-01	1.36E-01	1.94E-01	2.30E-01
C25	1.65E-02	2.59E-02	2.97E-02	4.09E-02	5.47E-02	7.67E-02	1.05E-01	1.54E-01	1.86E-01
C26	1.15E-02	1.82E-02	2.11E-02	2.93E-02	3.96E-02	5.62E-02	7.83E-02	1.17E-01	1.43E-01
C27	8.60E-03	1.38E-02	1.60E-02	2.25E-02	3.06E-02	4.40E-02	6.20E-02	9.39E-02	1.16E-01
C28	6.47E-03	1.04E-02	1.22E-02	1.73E-02	2.38E-02	3.46E-02	4.94E-02	7.59E-02	9.52E-02
C29	5.46E-03	8.88E-03	1.04E-02	1.49E-02	2.06E-02	3.03E-02	4.36E-02	6.78E-02	8.59E-02
C30	3.35E-03	5.55E-03	6.60E-03	9.59E-03	1.35E-02	2.02E-02	2.98E-02	4.76E-02	6.12E-02
C31	2.31E-03	3.85E-03	4.60E-03	6.73E-03	9.53E-03	1.44E-02	2.13E-02	3.45E-02	4.46E-02
C32	1.67E-03	2.81E-03	3.37E-03	4.97E-03	7.09E-03	1.08E-02	1.62E-02	2.65E-02	3.45E-02
C33	1.15E-03	1.95E-03	2.36E-03	3.50E-03	5.03E-03	7.75E-03	1.17E-02	1.93E-02	2.54E-02
C34	8.80E-04	1.50E-03	1.82E-03	2.72E-03	3.94E-03	6.11E-03	9.29E-03	1.55E-02	2.05E-02
C35	6.53E-04	1.12E-03	1.36E-03	2.05E-03	2.99E-03	4.67E-03	7.16E-03	1.21E-02	1.60E-02
C36+	8.96E-03	1.56E-02	1.92E-02	2.95E-02	4.38E-02	7.02E-02	1.10E-01	1.92E-01	2.58E-01

Table B.14: Results from simulated steam distillation of crude at field (260psig) conditions (Run-2).

	Distillation Cuts @ Temp ^oC								
Mass Flow gm/hr	**228**	**240**	**249**	**260.5**	**270**	**276**	**280**	**290**	**300**
WATER	2.42E+01	3.10E+01	3.03E+01	3.07E+01	3.05E+01	3.03E+01	3.02E+01	3.03E+01	3.03E+01
PROPA-01	0.00E+00	0.00E+00	0.00E+00	0.00E+00	0.00E+00	0.00E+00	0.00E+00	0.00E+00	0.00E+00
N-PEN-01	0.00E+00	0.00E+00	0.00E+00	0.00E+00	0.00E+00	0.00E+00	0.00E+00	0.00E+00	0.00E+00
NITROGEN	1.47E+00	1.51E+00	1.50E+00	1.50E+00	1.50E+00	1.50E+00	1.50E+00	1.50E+00	1.50E+00
METHY-02	0.00E+00	0.00E+00	0.00E+00	0.00E+00	0.00E+00	0.00E+00	0.00E+00	0.00E+00	0.00E+00
CYCLOHEX	0.00E+00	0.00E+00	0.00E+00	0.00E+00	0.00E+00	0.00E+00	0.00E+00	0.00E+00	0.00E+00
HEXANES	2.03E-02	7.44E-03	1.77E-03	4.06E-04	7.84E-05	1.33E-05	2.04E-06	0.00E+00	0.00E+00
METHY-01	1.57E-02	9.11E-03	3.40E-03	1.24E-03	3.83E-04	1.03E-04	2.53E-05	5.87E-06	1.19E-06
TOLUE-01	0.00E+00	0.00E+00	0.00E+00	0.00E+00	0.00E+00	0.00E+00	0.00E+00	0.00E+00	0.00E+00
HEPTANES	1.73E-02	8.70E-03	2.83E-03	8.98E-04	2.40E-04	5.60E-05	1.19E-05	2.38E-06	4.17E-07
OCATANES	1.16E-01	7.46E-02	3.08E-02	1.25E-02	4.25E-03	1.26E-03	3.42E-04	8.76E-05	1.96E-05
ETHYL-02	3.61E-02	2.82E-02	1.41E-02	7.02E-03	2.95E-03	1.08E-03	3.61E-04	1.15E-04	3.22E-05
M-XYL-01	1.18E-02	9.39E-03	4.78E-03	2.42E-03	1.03E-03	3.85E-04	1.30E-04	4.22E-05	1.20E-05
O-XYL-01	1.12E-02	9.31E-03	4.97E-03	2.65E-03	1.20E-03	4.70E-04	1.69E-04	5.81E-05	1.75E-05
NONANES	2.08E-01	1.68E-01	8.75E-02	4.51E-02	1.96E-02	7.46E-03	2.58E-03	8.52E-04	2.46E-04
1,2,4-C9	3.33E-02	3.40E-02	2.23E-02	1.48E-02	8.34E-03	4.11E-03	1.85E-03	8.11E-04	3.12E-04
C10	4.46E-01	4.37E-01	2.75E-01	1.74E-01	9.37E-02	4.41E-02	1.89E-02	7.85E-03	2.86E-03
C11	6.47E-01	7.33E-01	5.35E-01	3.99E-01	2.56E-01	1.43E-01	7.35E-02	3.70E-02	1.64E-02
C12	7.71E-01	9.88E-01	8.20E-01	7.08E-01	5.29E-01	3.47E-01	2.10E-01	1.26E-01	6.77E-02

C13	7.55E-01	1.06E+00	9.71E-01	9.37E-01	7.90E-01	5.89E-01	4.05E-01	2.83E-01	1.77E-01
C14	5.13E-01	7.81E-01	7.76E-01	8.27E-01	7.76E-01	6.46E-01	4.99E-01	3.99E-01	2.89E-01
C15	4.50E-01	7.30E-01	7.77E-01	8.97E-01	9.21E-01	8.43E-01	7.18E-01	6.45E-01	5.32E-01
C16	3.18E-01	5.41E-01	6.05E-01	7.42E-01	8.14E-01	7.98E-01	7.30E-01	7.17E-01	6.55E-01
C17	2.01E-01	3.55E-01	4.13E-01	5.31E-01	6.14E-01	6.36E-01	6.16E-01	6.52E-01	6.47E-01
C18	1.58E-01	2.87E-01	3.43E-01	4.56E-01	5.46E-01	5.86E-01	5.89E-01	6.54E-01	6.86E-01
C19	1.16E-01	2.16E-01	2.64E-01	3.60E-01	4.43E-01	4.89E-01	5.07E-01	5.86E-01	6.44E-01
C20	7.51E-02	1.42E-01	1.78E-01	2.49E-01	3.15E-01	3.57E-01	3.80E-01	4.56E-01	5.25E-01
C21	5.51E-02	1.07E-01	1.36E-01	1.94E-01	2.52E-01	2.91E-01	3.17E-01	3.93E-01	4.69E-01
C22	3.51E-02	6.92E-02	8.94E-02	1.31E-01	1.72E-01	2.03E-01	2.25E-01	2.86E-01	3.52E-01
C23	2.50E-02	5.01E-02	6.58E-02	9.78E-02	1.31E-01	1.57E-01	1.76E-01	2.29E-01	2.89E-01
C24	1.77E-02	3.59E-02	4.78E-02	7.21E-02	9.83E-02	1.19E-01	1.35E-01	1.79E-01	2.31E-01
C25	1.27E-02	2.62E-02	3.53E-02	5.41E-02	7.47E-02	9.14E-02	1.05E-01	1.41E-01	1.86E-01
C26	8.82E-03	1.85E-02	2.52E-02	3.91E-02	5.46E-02	6.75E-02	7.79E-02	1.07E-01	1.43E-01
C27	6.56E-03	1.39E-02	1.92E-02	3.02E-02	4.27E-02	5.31E-02	6.17E-02	8.57E-02	1.16E-01
C28	4.92E-03	1.06E-02	1.48E-02	2.35E-02	3.35E-02	4.20E-02	4.92E-02	6.91E-02	9.50E-02
C29	4.13E-03	8.98E-03	1.27E-02	2.03E-02	2.93E-02	3.70E-02	4.34E-02	6.16E-02	8.56E-02
C30	2.51E-03	5.61E-03	8.09E-03	1.33E-02	1.96E-02	2.50E-02	2.96E-02	4.30E-02	6.10E-02
C31	1.73E-03	3.90E-03	5.67E-03	9.41E-03	1.39E-02	1.79E-02	2.13E-02	3.11E-02	4.45E-02
C32	1.24E-03	2.84E-03	4.17E-03	7.01E-03	1.05E-02	1.35E-02	1.61E-02	2.38E-02	3.44E-02
C33	8.54E-04	1.98E-03	2.93E-03	4.98E-03	7.49E-03	9.72E-03	1.17E-02	1.73E-02	2.53E-02
C34	6.49E-04	1.52E-03	2.27E-03	3.89E-03	5.90E-03	7.70E-03	9.27E-03	1.39E-02	2.04E-02
C35	4.80E-04	1.13E-03	1.71E-03	2.96E-03	4.52E-03	5.92E-03	7.14E-03	1.08E-02	1.60E-02
C36+	6.45E-03	1.59E-02	2.45E-02	4.38E-02	6.84E-02	9.06E-02	1.10E-01	1.70E-01	2.57E-01

Table B.15: Results from simulated steam-propane distillation of crude at field (260psig) conditions (Run-1).

	Distillation Cuts @ Temp °C								
Mass Flow gm/hr	**230**	**235**	**245**	**250**	**260**	**270**	**280**	**290**	**300**
WATER	2.50E+01	3.02E+01	3.03E+01	3.05E+01	3.05E+01	3.05E+01	3.04E+01	3.04E+01	3.02E+01
PROPA-01	1.37E+00	1.51E+00	1.51E+00	1.51E+00	1.51E+00	1.51E+00	1.51E+00	1.51E+00	1.50E+00
N-PEN-01	0.00E+00	0.00E+00	0.00E+00	0.00E+00	0.00E+00	0.00E+00	0.00E+00	0.00E+00	0.00E+00
NITROGEN	0.00E+00	0.00E+00	0.00E+00	0.00E+00	0.00E+00	0.00E+00	0.00E+00	0.00E+00	0.00E+00
METHY-02	0.00E+00	0.00E+00	0.00E+00	0.00E+00	0.00E+00	0.00E+00	0.00E+00	0.00E+00	0.00E+00
CYCLOHEX	0.00E+00	0.00E+00	0.00E+00	0.00E+00	0.00E+00	0.00E+00	0.00E+00	0.00E+00	0.00E+00
HEXANES	1.97E-02	5.99E-03	1.45E-03	3.26E-04	6.55E-05	1.16E-05	1.79E-06	0.00E+00	0.00E+00
METHY-01	1.57E-02	7.49E-03	2.86E-03	1.02E-03	3.31E-04	9.45E-05	2.36E-05	5.21E-06	9.64E-07
TOLUE-01	0.00E+00	0.00E+00	0.00E+00	0.00E+00	0.00E+00	0.00E+00	0.00E+00	0.00E+00	0.00E+00
HEPTANES	1.70E-02	7.11E-03	2.36E-03	7.34E-04	2.05E-04	5.06E-05	1.09E-05	2.06E-06	0.00E+00
OCATANES	1.17E-01	6.16E-02	2.61E-02	1.03E-02	3.69E-03	1.17E-03	3.24E-04	7.91E-05	1.61E-05
ETHYL-02	3.69E-02	2.35E-02	1.21E-02	5.87E-03	2.60E-03	1.02E-03	3.53E-04	1.08E-04	2.75E-05
M-XYL-01	1.21E-02	7.83E-03	4.11E-03	2.03E-03	9.12E-04	3.65E-04	1.28E-04	3.98E-05	1.03E-05
O-XYL-01	1.15E-02	7.78E-03	4.29E-03	2.22E-03	1.06E-03	4.48E-04	1.67E-04	5.51E-05	1.52E-05
NONANES	2.13E-01	1.41E-01	7.53E-02	3.77E-02	1.73E-02	7.05E-03	2.52E-03	8.00E-04	2.11E-04
1,2,4-C9	3.49E-02	2.87E-02	1.94E-02	1.24E-02	7.40E-03	3.97E-03	1.88E-03	7.97E-04	2.80E-04
C10	4.66E-01	3.69E-01	2.39E-01	1.46E-01	8.28E-02	4.22E-02	1.90E-02	7.61E-03	2.53E-03
C11	6.86E-01	6.23E-01	4.70E-01	3.36E-01	2.25E-01	1.38E-01	7.49E-02	3.67E-02	1.49E-02
C12	8.29E-01	8.44E-01	7.24E-01	5.93E-01	4.62E-01	3.33E-01	2.15E-01	1.28E-01	6.26E-02

C13	8.20E-01	9.08E-01	8.58E-01	7.78E-01	6.82E-01	5.59E-01	4.17E-01	2.89E-01	1.66E-01
C14	5.63E-01	6.68E-01	6.86E-01	6.79E-01	6.59E-01	6.06E-01	5.14E-01	4.13E-01	2.75E-01
C15	4.98E-01	6.23E-01	6.85E-01	7.28E-01	7.68E-01	7.79E-01	7.37E-01	6.74E-01	5.12E-01
C16	3.54E-01	4.60E-01	5.32E-01	5.94E-01	6.66E-01	7.26E-01	7.47E-01	7.54E-01	6.34E-01
C17	2.24E-01	3.01E-01	3.61E-01	4.20E-01	4.94E-01	5.71E-01	6.28E-01	6.89E-01	6.31E-01
C18	1.78E-01	2.43E-01	2.99E-01	3.57E-01	4.33E-01	5.20E-01	5.98E-01	6.94E-01	6.72E-01
C19	1.31E-01	1.82E-01	2.29E-01	2.78E-01	3.47E-01	4.30E-01	5.13E-01	6.24E-01	6.34E-01
C20	8.48E-02	1.19E-01	1.54E-01	1.91E-01	2.44E-01	3.11E-01	3.84E-01	4.88E-01	5.18E-01
C21	6.24E-02	8.89E-02	1.17E-01	1.47E-01	1.92E-01	2.51E-01	3.19E-01	4.21E-01	4.64E-01
C22	3.99E-02	5.74E-02	7.66E-02	9.79E-02	1.30E-01	1.74E-01	2.26E-01	3.08E-01	3.49E-01
C23	2.85E-02	4.14E-02	5.61E-02	7.26E-02	9.79E-02	1.33E-01	1.77E-01	2.47E-01	2.88E-01
C24	2.01E-02	2.95E-02	4.06E-02	5.30E-02	7.25E-02	1.00E-01	1.35E-01	1.94E-01	2.30E-01
C25	1.45E-02	2.15E-02	2.99E-02	3.94E-02	5.46E-02	7.65E-02	1.05E-01	1.54E-01	1.85E-01
C26	1.01E-02	1.50E-02	2.12E-02	2.82E-02	3.95E-02	5.61E-02	7.81E-02	1.16E-01	1.43E-01
C27	7.53E-03	1.13E-02	1.61E-02	2.16E-02	3.06E-02	4.39E-02	6.19E-02	9.37E-02	1.16E-01
C28	5.65E-03	8.53E-03	1.23E-02	1.67E-02	2.38E-02	3.46E-02	4.93E-02	7.58E-02	9.51E-02
C29	4.76E-03	7.22E-03	1.05E-02	1.43E-02	2.06E-02	3.02E-02	4.35E-02	6.78E-02	8.58E-02
C30	2.91E-03	4.47E-03	6.66E-03	9.21E-03	1.35E-02	2.02E-02	2.97E-02	4.75E-02	6.11E-02
C31	2.00E-03	3.09E-03	4.65E-03	6.46E-03	9.55E-03	1.44E-02	2.14E-02	3.45E-02	4.46E-02
C32	1.44E-03	2.24E-03	3.41E-03	4.77E-03	7.11E-03	1.08E-02	1.62E-02	2.65E-02	3.45E-02
C33	9.93E-04	1.55E-03	2.39E-03	3.36E-03	5.05E-03	7.76E-03	1.17E-02	1.93E-02	2.54E-02
C34	7.56E-04	1.19E-03	1.84E-03	2.61E-03	3.95E-03	6.12E-03	9.31E-03	1.55E-02	2.05E-02
C35	5.59E-04	8.84E-04	1.38E-03	1.97E-03	3.00E-03	4.69E-03	7.18E-03	1.21E-02	1.61E-02
C36+	7.59E-03	1.21E-02	1.94E-02	2.82E-02	4.41E-02	7.05E-02	1.11E-01	1.92E-01	2.58E-01

Table B.16: Results from simulated steam-propane distillation of crude at field (260psig) conditions (Run-2).

	Distillation Cuts @ Temp ^oC								
Mass Flow gm/hr	**229**	**240**	**249**	**257**	**265**	**270**	**279**	**290**	**299**
WATER	2.41E+01	3.10E+01	3.03E+01	3.06E+01	3.05E+01	3.03E+01	3.04E+01	3.04E+01	3.03E+01
PROPA-01	1.34E+00	1.54E+00	1.50E+00	1.51E+00	1.51E+00	1.51E+00	1.51E+00	1.51E+00	1.51E+00
N-PEN-01	0.00E+00	0.00E+00	0.00E+00	0.00E+00	0.00E+00	0.00E+00	0.00E+00	0.00E+00	0.00E+00
NITROGEN	0.00E+00	0.00E+00	0.00E+00	0.00E+00	0.00E+00	0.00E+00	0.00E+00	0.00E+00	0.00E+00
METHY-02	0.00E+00	0.00E+00	0.00E+00	0.00E+00	0.00E+00	0.00E+00	0.00E+00	0.00E+00	0.00E+00
CYCLOHEX	0.00E+00	0.00E+00	0.00E+00	0.00E+00	0.00E+00	0.00E+00	0.00E+00	0.00E+00	0.00E+00
HEXANES	2.02E-02	7.48E-03	1.80E-03	4.14E-04	8.41E-05	1.51E-05	2.53E-06	3.74E-07	0.00E+00
METHY-01	1.57E-02	9.11E-03	3.43E-03	1.25E-03	4.02E-04	1.15E-04	3.09E-05	7.36E-06	1.52E-06
TOLUE-01	0.00E+00	0.00E+00	0.00E+00	0.00E+00	0.00E+00	0.00E+00	0.00E+00	0.00E+00	0.00E+00
HEPTANES	1.72E-02	8.71E-03	2.87E-03	9.07E-04	2.54E-04	6.30E-05	1.46E-05	3.00E-06	5.36E-07
OCATANES	1.16E-01	7.45E-02	3.10E-02	1.24E-02	4.43E-03	1.40E-03	4.14E-04	1.09E-04	2.48E-05
ETHYL-02	3.60E-02	2.81E-02	1.42E-02	6.94E-03	3.03E-03	1.18E-03	4.32E-04	1.42E-04	4.01E-05
M-XYL-01	1.18E-02	9.35E-03	4.80E-03	2.39E-03	1.06E-03	4.18E-04	1.56E-04	5.19E-05	1.49E-05
O-XYL-01	1.11E-02	9.26E-03	4.98E-03	2.61E-03	1.22E-03	5.08E-04	2.01E-04	7.10E-05	2.17E-05
NONANES	2.08E-01	1.68E-01	8.77E-02	4.44E-02	2.01E-02	8.06E-03	3.07E-03	1.04E-03	3.05E-04
1,2,4-C9	3.32E-02	3.38E-02	2.22E-02	1.44E-02	8.36E-03	4.32E-03	2.15E-03	9.68E-04	3.76E-04
C10	4.46E-01	4.34E-01	2.74E-01	1.69E-01	9.41E-02	4.65E-02	2.20E-02	9.38E-03	3.46E-03
C11	6.47E-01	7.27E-01	5.33E-01	3.84E-01	2.52E-01	1.47E-01	8.37E-02	4.32E-02	1.94E-02
C12	7.73E-01	9.80E-01	8.16E-01	6.74E-01	5.12E-01	3.48E-01	2.33E-01	1.44E-01	7.74E-02

C13	7.58E-01	1.05E+00	9.65E-01	8.84E-01	7.52E-01	5.75E-01	4.40E-01	3.14E-01	1.97E-01
C14	5.17E-01	7.75E-01	7.71E-01	7.72E-01	7.26E-01	6.15E-01	5.31E-01	4.34E-01	3.14E-01
C15	4.55E-01	7.25E-01	7.72E-01	8.31E-01	8.49E-01	7.83E-01	7.48E-01	6.87E-01	5.64E-01
C16	3.23E-01	5.38E-01	6.02E-01	6.83E-01	7.40E-01	7.27E-01	7.49E-01	7.52E-01	6.80E-01
C17	2.04E-01	3.53E-01	4.11E-01	4.86E-01	5.52E-01	5.69E-01	6.24E-01	6.74E-01	6.61E-01
C18	1.61E-01	2.86E-01	3.42E-01	4.15E-01	4.87E-01	5.18E-01	5.91E-01	6.71E-01	6.93E-01
C19	1.19E-01	2.15E-01	2.63E-01	3.26E-01	3.92E-01	4.28E-01	5.04E-01	5.97E-01	6.45E-01
C20	7.68E-02	1.42E-01	1.77E-01	2.25E-01	2.77E-01	3.09E-01	3.76E-01	4.62E-01	5.21E-01
C21	5.66E-02	1.06E-01	1.35E-01	1.75E-01	2.20E-01	2.50E-01	3.12E-01	3.96E-01	4.62E-01
C22	3.61E-02	6.91E-02	8.94E-02	1.17E-01	1.50E-01	1.73E-01	2.20E-01	2.87E-01	3.46E-01
C23	2.58E-02	5.01E-02	6.58E-02	8.74E-02	1.13E-01	1.32E-01	1.72E-01	2.29E-01	2.83E-01
C24	1.82E-02	3.59E-02	4.78E-02	6.43E-02	8.43E-02	9.95E-02	1.31E-01	1.79E-01	2.25E-01
C25	1.31E-02	2.62E-02	3.54E-02	4.81E-02	6.38E-02	7.60E-02	1.02E-01	1.41E-01	1.81E-01
C26	9.15E-03	1.85E-02	2.53E-02	3.47E-02	4.64E-02	5.58E-02	7.56E-02	1.06E-01	1.38E-01
C27	6.82E-03	1.40E-02	1.93E-02	2.67E-02	3.61E-02	4.36E-02	5.98E-02	8.54E-02	1.13E-01
C28	5.12E-03	1.06E-02	1.48E-02	2.07E-02	2.82E-02	3.44E-02	4.76E-02	6.88E-02	9.19E-02
C29	4.31E-03	9.02E-03	1.27E-02	1.79E-02	2.46E-02	3.01E-02	4.20E-02	6.14E-02	8.27E-02
C30	2.63E-03	5.65E-03	8.14E-03	1.16E-02	1.63E-02	2.01E-02	2.86E-02	4.28E-02	5.88E-02
C31	1.81E-03	3.92E-03	5.70E-03	8.21E-03	1.15E-02	1.43E-02	2.05E-02	3.10E-02	4.29E-02
C32	1.31E-03	2.86E-03	4.20E-03	6.09E-03	8.64E-03	1.08E-02	1.56E-02	2.37E-02	3.31E-02
C33	9.00E-04	1.99E-03	2.96E-03	4.32E-03	6.16E-03	7.72E-03	1.12E-02	1.73E-02	2.44E-02
C34	6.85E-04	1.53E-03	2.29E-03	3.37E-03	4.84E-03	6.09E-03	8.93E-03	1.39E-02	1.96E-02
C35	5.07E-04	1.14E-03	1.73E-03	2.56E-03	3.69E-03	4.66E-03	6.88E-03	1.08E-02	1.54E-02
C36+	6.85E-03	1.60E-02	2.48E-02	3.74E-02	5.51E-02	7.02E-02	1.06E-01	1.70E-01	2.47E-01

APPENDIX C

GC-FID Analysis of Distillation Yields

In this section data from GC-FID analysis of distillation yields are presented. Compositional analysis was performed on elemental basis.

GC was operated in split mode with $10^{o}C$/min temperature from $35^{o}C$ to $300^{o}C$ with split ration of 1:50 and purge rate of 2 ml/min.

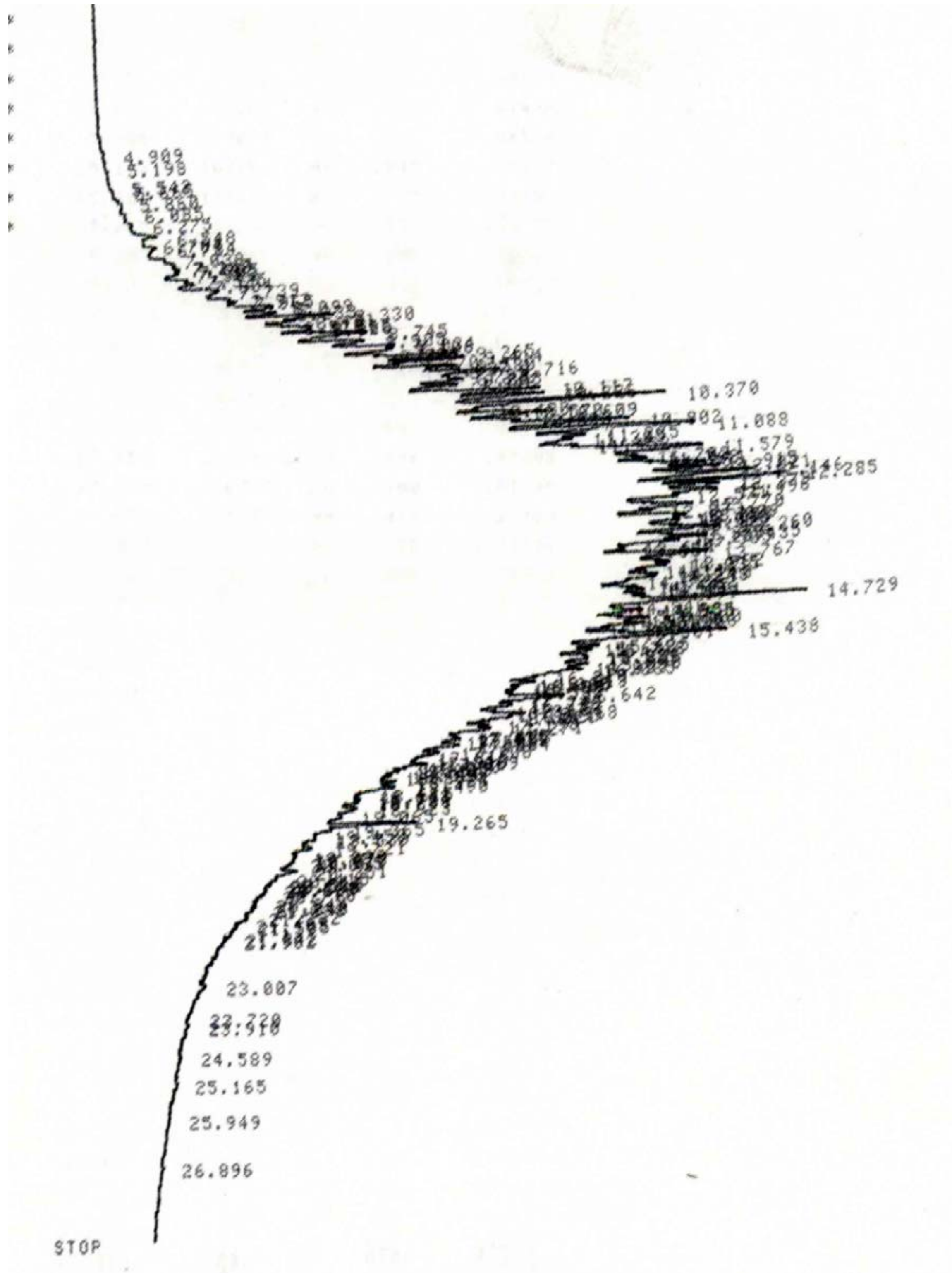

Figure C.1: Steam- distillation yields at 140°C for Psat.

Table C.1: Composition of steam distillation yield at 140°C.

Type : Steam Distillation Yield at Psat

Temperature - 140°C

Component	weight %
C5	0.0000
C6	0.0000
C7	0.0010
C8	0.0081
C9	0.0374
C10	0.1047
C11	0.1683
C12	0.2057
C13	0.1879
C14	0.1104
C15	0.0795
C16	0.0451
C17	0.0234
C18	0.0161
C19	0.0096
C20	0.0039
C21	0.0030
C22	0.0006
C23	0.0000
C24	0.0000
C25	0.0000
C26	0.0002
C27	0.0000
C28	0.0000
C29	0.0000
C30+	0.0000

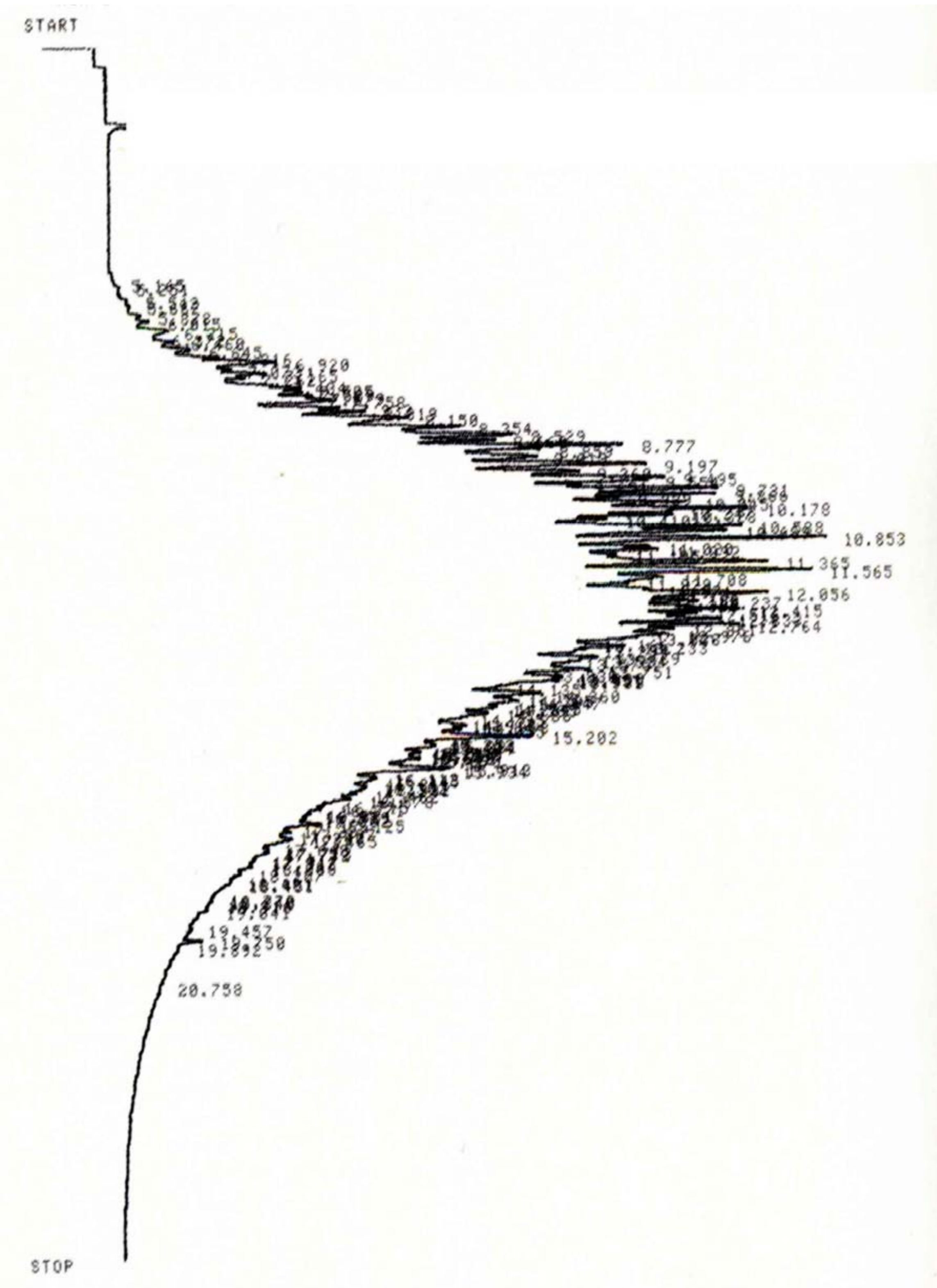

Figure C.2: Steam- distillation yields at 180^oC for Psat.

Table C.2: Composition of steam distillation yield at 180^{o}C.

Type : Steam Distillation Yield at Psat

Temperature - 180^{o}C

Component	weight %
C5	0.0000
C6	0.0000
C7	0.0000
C8	0.0002
C9	0.0069
C10	0.0420
C11	0.1030
C12	0.1747
C13	0.1987
C14	0.1420
C15	0.1196
C16	0.0788
C17	0.0461
C18	0.0337
C19	0.0230
C20	0.0128
C21	0.0079
C22	0.0053
C23	0.0035
C24	0.0010
C25	0.0013
C26	0.0006
C27	0.0000
C28	0.0000
C29	0.0001
C30+	0.0000

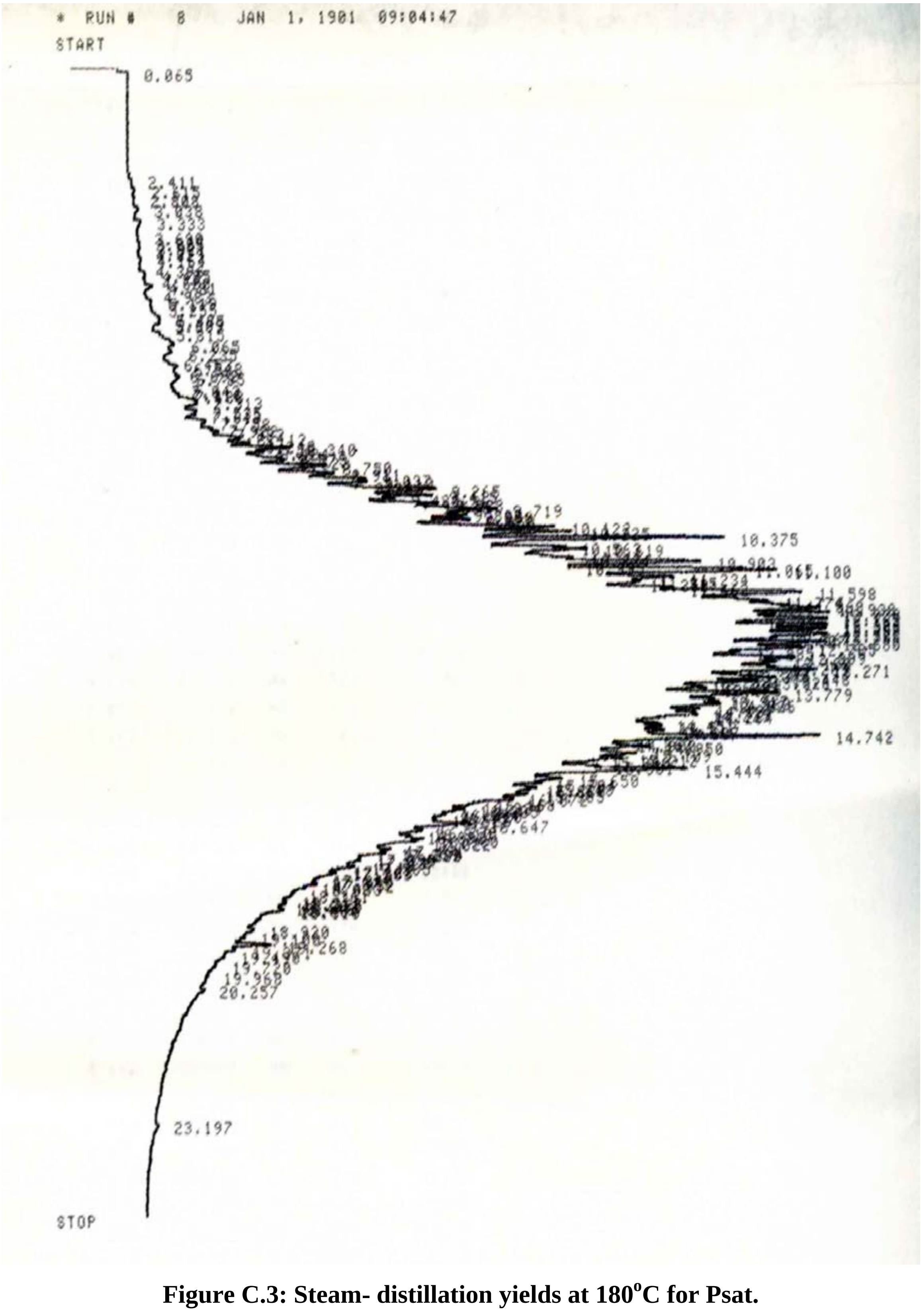

Figure C.3: Steam- distillation yields at 180^oC for Psat.

Table C.3: Composition of steam distillation yield at 220^{o}C.

Type : Steam Distillation Yield at Psat

Temperature - 220^{o}C

Component	weight %
C5	0.0000
C6	0.0000
C7	0.0000
C8	0.0000
C9	0.0012
C10	0.0143
C11	0.0530
C12	0.1196
C13	0.1689
C14	0.1445
C15	0.1436
C16	0.1079
C17	0.0700
C18	0.0556
C19	0.0408
C20	0.0269
C21	0.0185
C22	0.0110
C23	0.0079
C24	0.0052
C25	0.0037
C26	0.0025
C27	0.0020
C28	0.0008
C29	0.0006
C30+	0.0013

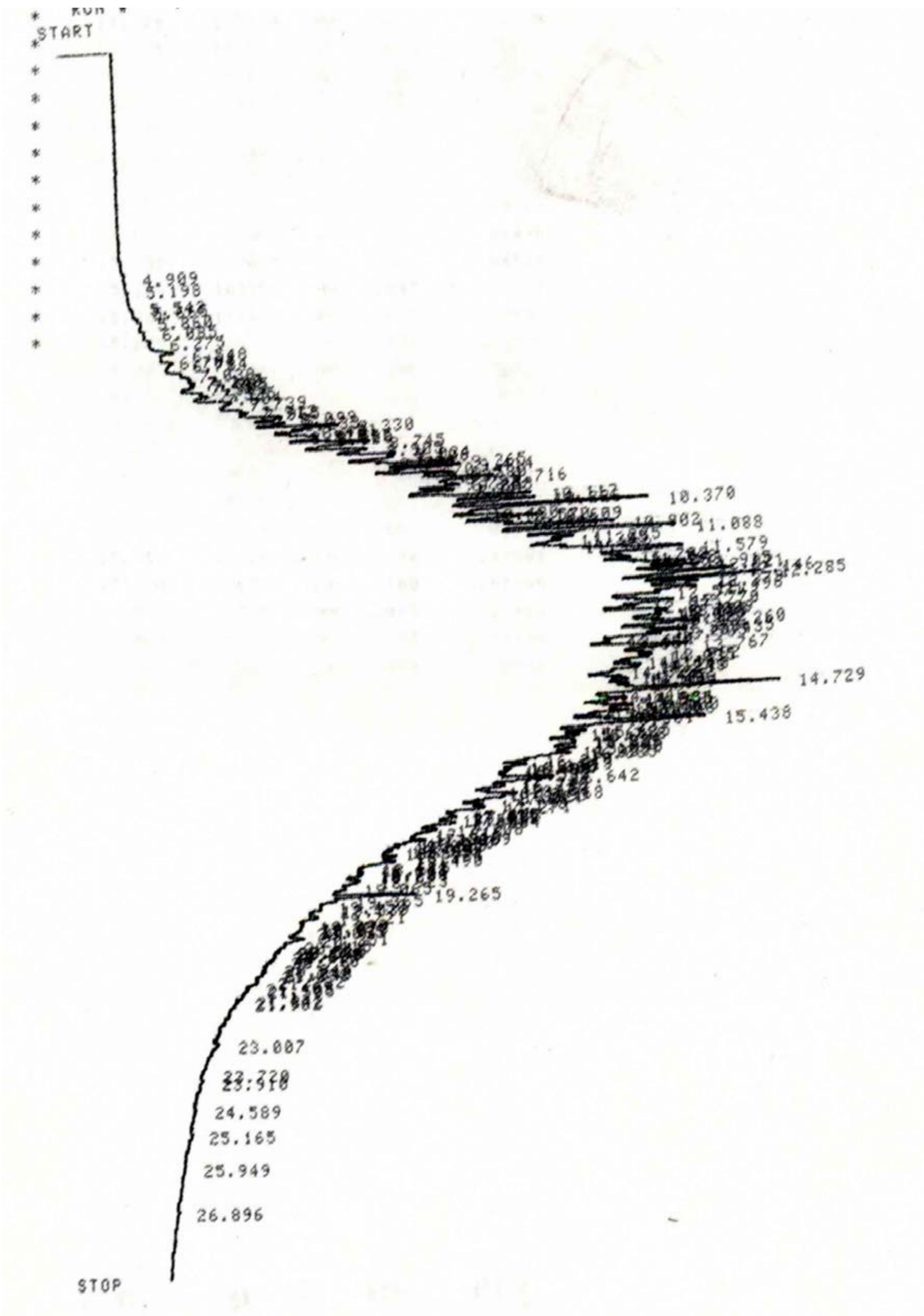

Figure C.4: Steam- distillation yields at 260^oC for Psat.

Table C.4: Composition of steam distillation yield at 260^{o}C.

Type: Steam Distillation Yield at Psat

Temperature - 260^{o}C

Component	weight %
C5	0.0000
C6	0.0000
C7	0.0000
C8	0.0000
C9	0.0000
C10	0.0044
C11	0.0208
C12	0.0625
C13	0.1102
C14	0.1143
C15	0.1376
C16	0.1193
C17	0.0886
C18	0.0786
C19	0.0645
C20	0.0455
C21	0.0371
C22	0.0247
C23	0.0188
C24	0.0149
C25	0.0114
C26	0.0075
C27	0.0066
C28	0.0050
C29	0.0045
C30+	0.0233

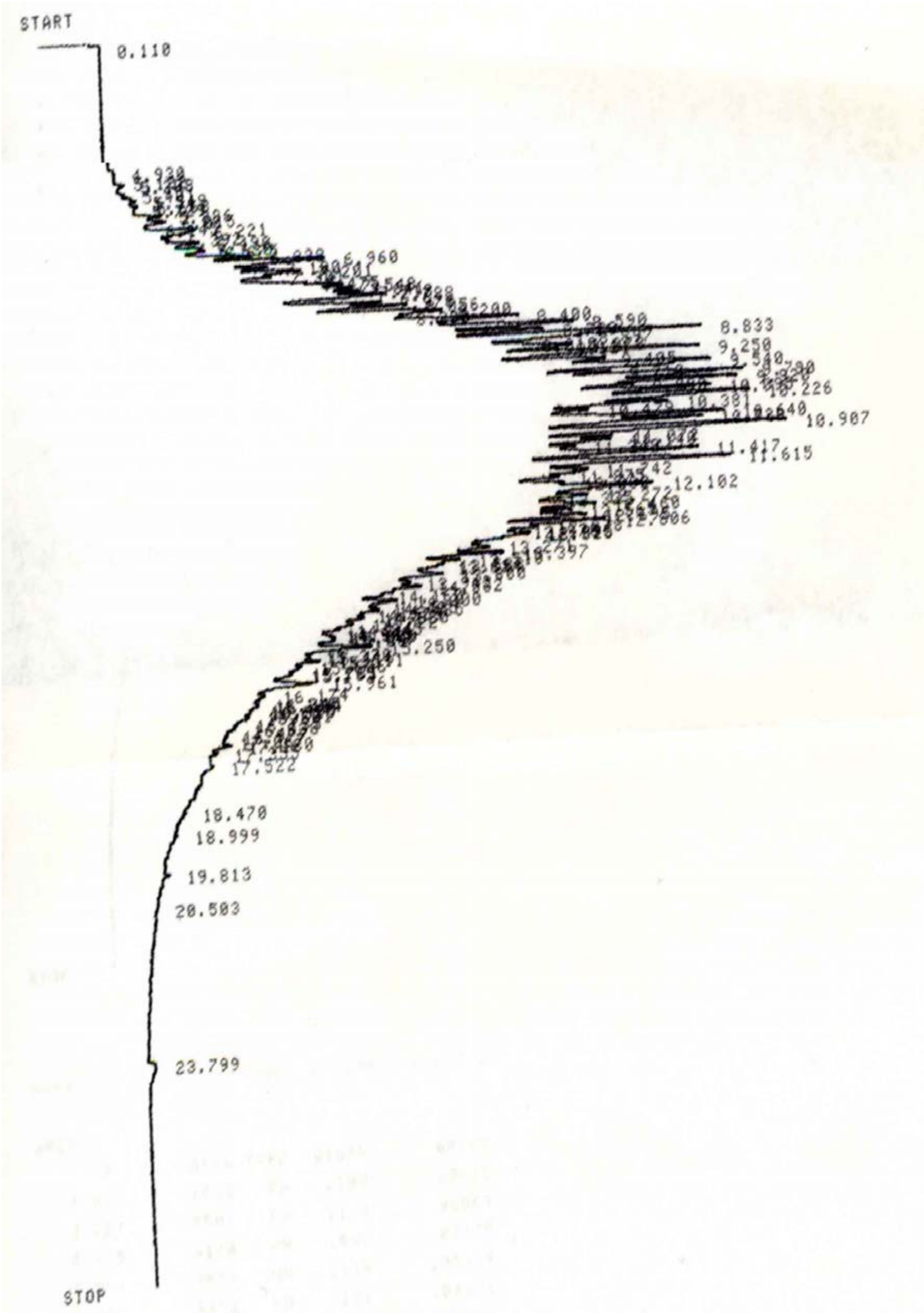

Figure C.5: Steam-propane distillation yields at 139°C for Psat.

Table C.5: Composition of steam-propane distillation yield at 139^{o}C.

Type : Steam-Propane Distillation Yield at Psat

Temperature - 140^{o}C

Component	weight %
C5	0.0000
C6	0.0000
C7	0.0001
C8	0.0030
C9	0.0238
C10	0.0807
C11	0.1494
C12	0.2036
C13	0.1972
C14	0.1222
C15	0.0933
C16	0.0560
C17	0.0290
C18	0.0195
C19	0.0130
C20	0.0057
C21	0.0036
C22	0.0022
C23	0.0015
C24	0.0001
C25	0.0000
C26	0.0000
C27	0.0000
C28	0.0000
C29	0.0000
C30+	0.0000

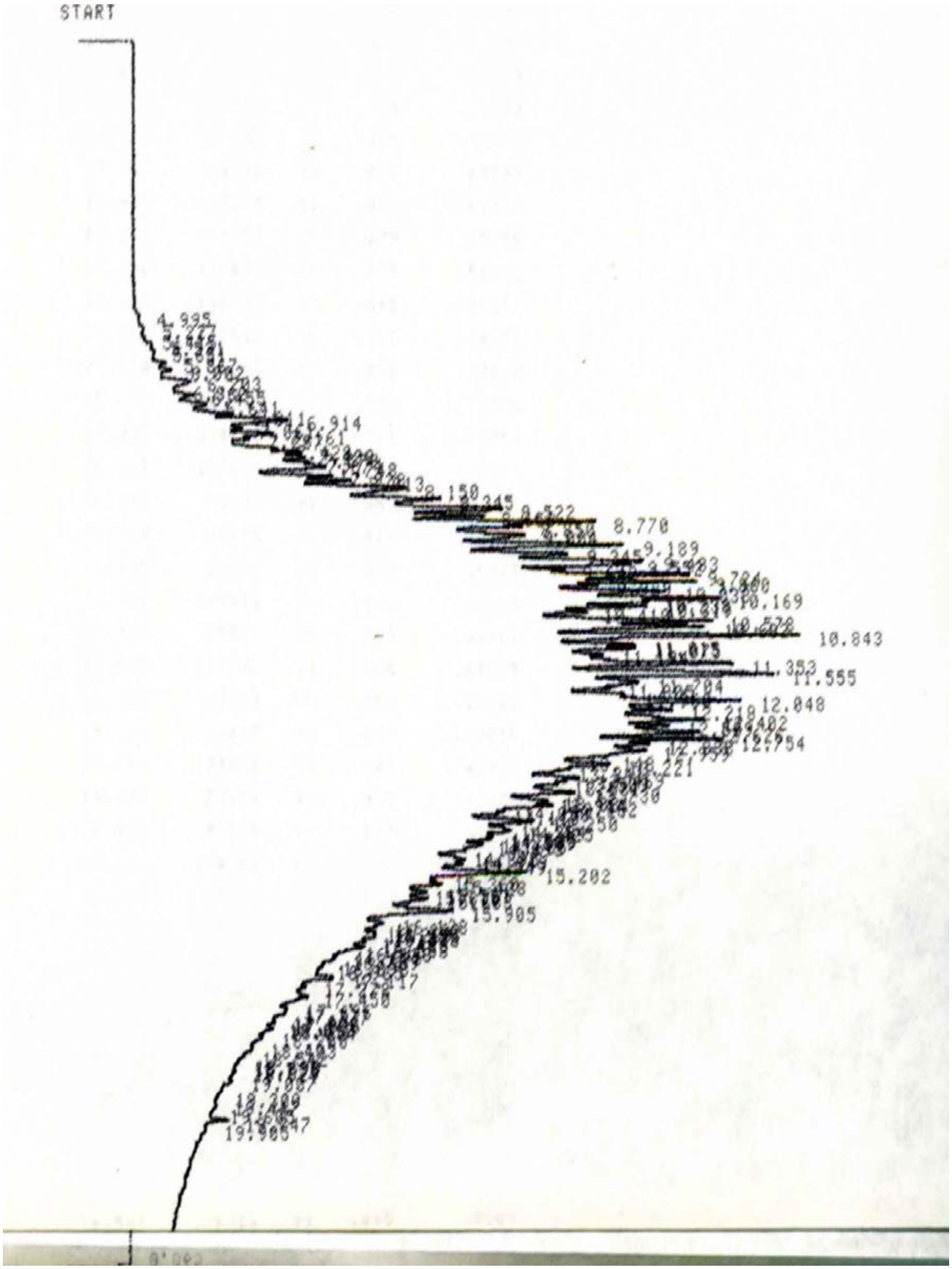

Figure C.6 Steam-propane distillation yields at 179°C for Psat.

Table C.6: Composition of steam-propane distillation yield at 179°C.

Type : Steam-Propane Distillation Yield at Psat

Temperature - 179°C

Component	weight %
C5	0.0000
C6	0.0000
C7	0.0000
C8	0.0000
C9	0.0041
C10	0.0302
C11	0.0844
C12	0.1582
C13	0.1938
C14	0.1463
C15	0.1299
C16	0.0896
C17	0.0529
C18	0.0403
C19	0.0272
C20	0.0164
C21	0.0118
C22	0.0065
C23	0.0042
C24	0.0025
C25	0.0014
C26	0.0007
C27	0.0004
C28	0.0000
C29	0.0000
C30+	0.0000

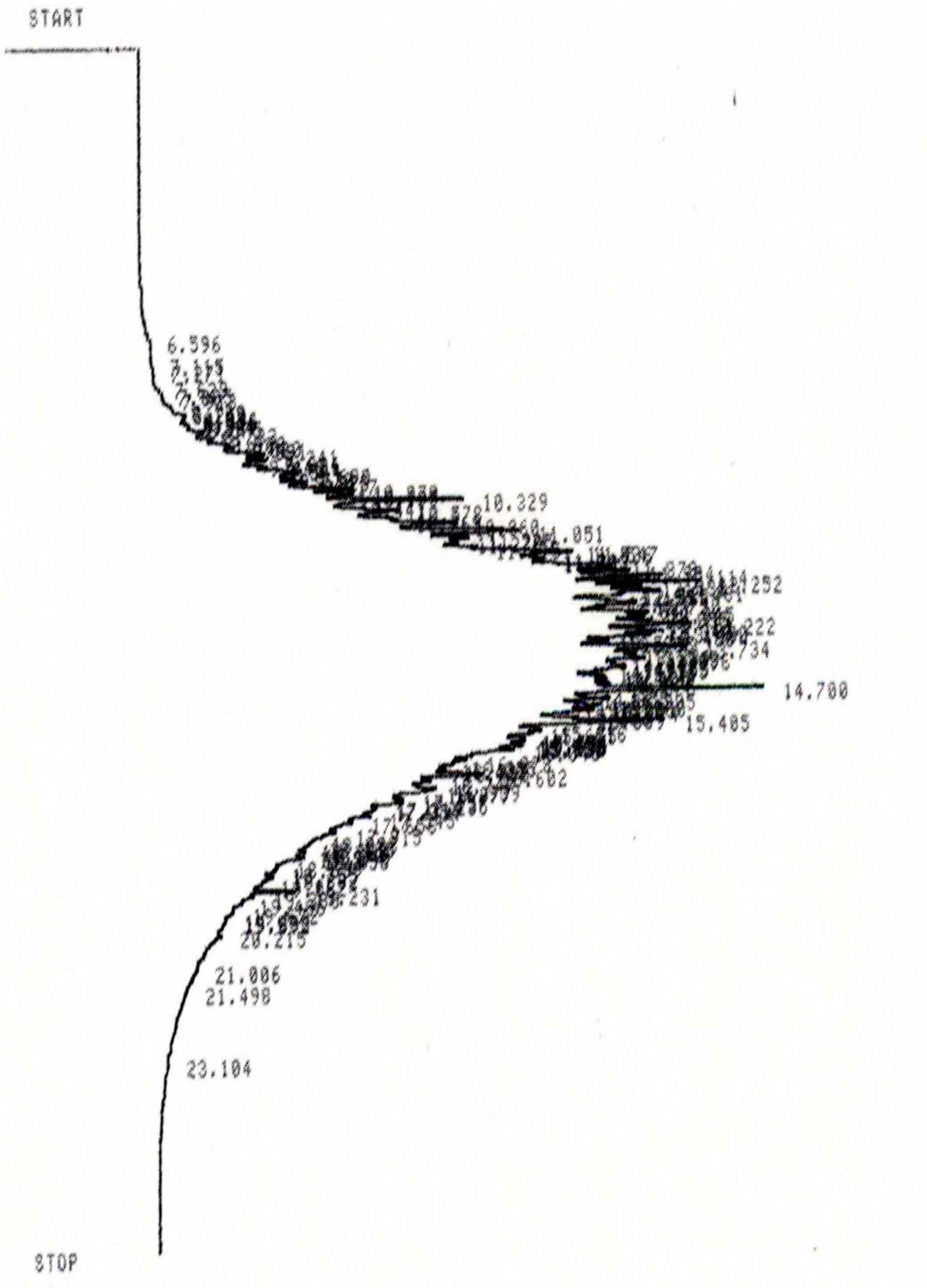

Figure C.7: Steam-propane distillation yields at 220^{o}C for Psat.

Table C.7: Composition of steam-propane distillation yield at 220°C.

Type: Steam-Propane Distillation Yield at Psat

Temperature - 220°C

Component	weight %
C5	0.0000
C6	0.0000
C7	0.0000
C8	0.0000
C9	0.0007
C10	0.0138
C11	0.0503
C12	0.1178
C13	0.1678
C14	0.1447
C15	0.1446
C16	0.1093
C17	0.0721
C18	0.0567
C19	0.0417
C20	0.0260
C21	0.0187
C22	0.0115
C23	0.0080
C24	0.0056
C25	0.0034
C26	0.0026
C27	0.0018
C28	0.0006
C29	0.0002
C30+	0.0024

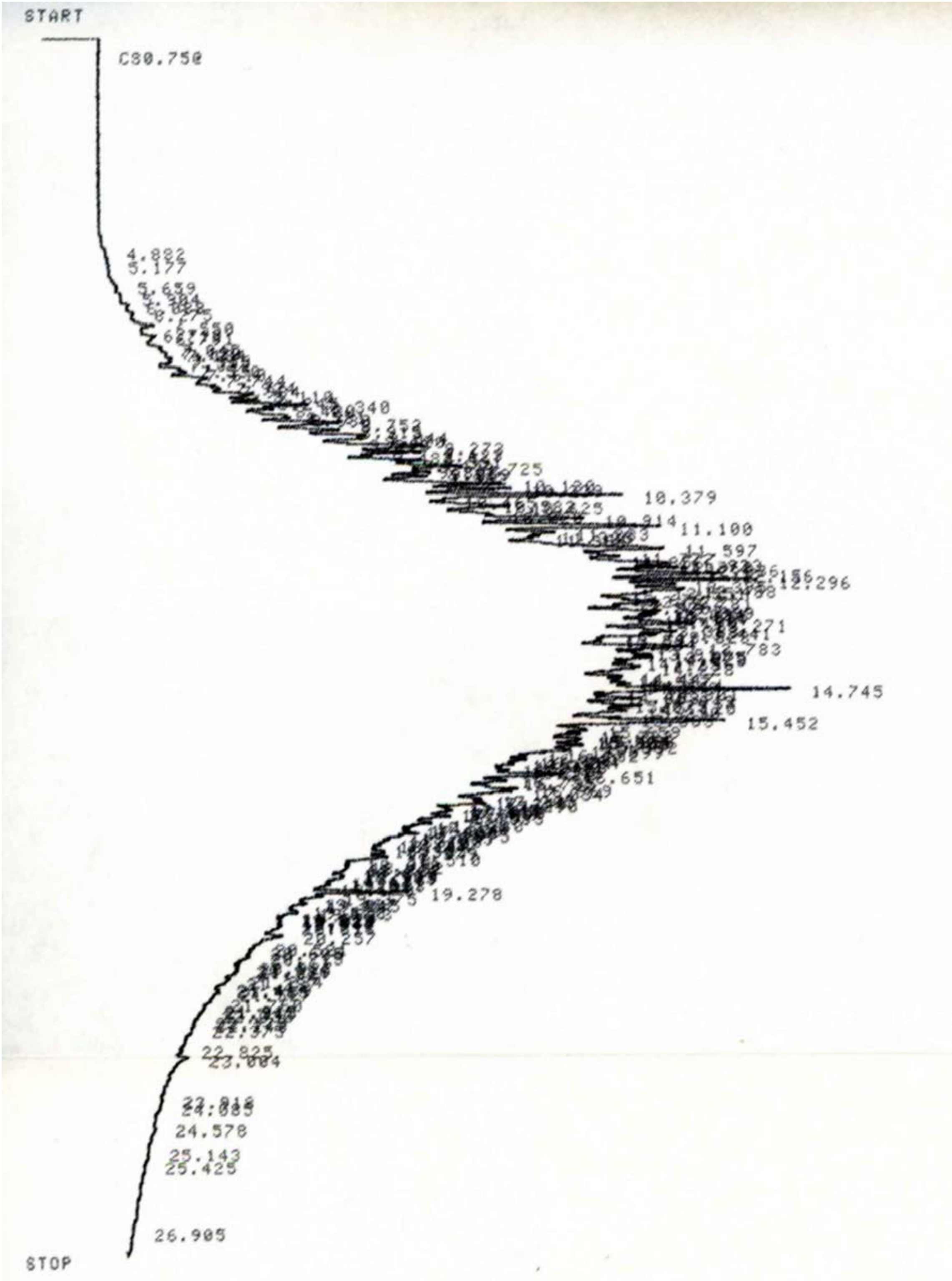

Figure C.8: Steam-propane distillation yields at 260°C for Psat.

Table C.8: Composition of steam-propane distillation yield at 260°C.

Type : Steam-Propane Distillation Yield at Psat

Temperature - 260°C

Component	weight %
C5	0.0000
C6	0.0000
C7	0.0000
C8	0.0000
C9	0.0000
C10	0.0032
C11	0.0165
C12	0.0533
C13	0.0980
C14	0.1069
C15	0.1325
C16	0.1202
C17	0.0915
C18	0.0828
C19	0.0672
C20	0.0493
C21	0.0406
C22	0.0275
C23	0.0216
C24	0.0163
C25	0.0133
C26	0.0103
C27	0.0083
C28	0.0063
C29	0.0052
C30+	0.0293

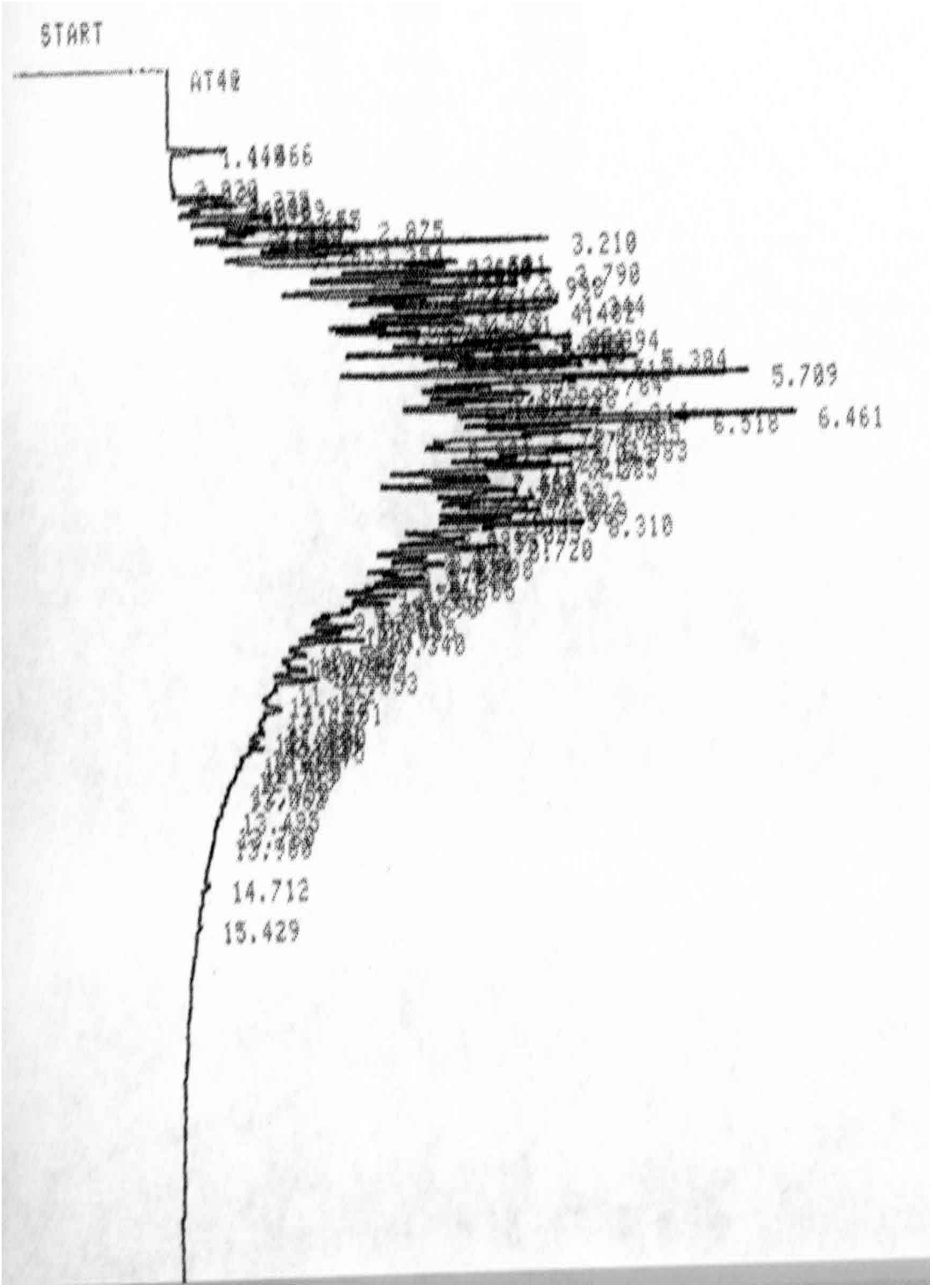

Figure C.9: Steam distillation yields at 230°C for 260psig.

Table C.9: Composition of distillation yield at 230^{o}C.

Type : Steam Distillation Yield at Field condition

Temperature - 230 ^{o}C

Component	weight %
C5	0.0000
C6	0.0028
C7	0.0043
C8	0.0194
C9	0.0472
C10	0.0884
C11	0.1209
C12	0.1482
C13	0.1479
C14	0.1014
C15	0.0913
C16	0.0640
C17	0.0404
C18	0.0321
C19	0.0244
C20	0.0148
C21	0.0107
C22	0.0068
C23	0.0040
C24	0.0033
C25	0.0017
C26	0.0017
C27	0.0010
C28	0.0000
C29	0.0005
C30+	0.0230

Figure C.10: Steam distillation yields at 250°C for 260psig.

Table C.10: Composition of distillation yield at 250°C.

Type : Steam Distillation Yield at Field condition

Temperature - 250°C

Component	weight %
C5	0.0000
C6	0.0000
C7	0.0003
C8	0.0011
C9	0.0064
C10	0.0234
C11	0.0523
C12	0.0951
C13	0.1268
C14	0.1124
C15	0.1218
C16	0.1004
C17	0.0710
C18	0.0599
C19	0.0464
C20	0.0320
C21	0.0247
C22	0.0157
C23	0.0112
C24	0.0091
C25	0.0055
C26	0.0036
C27	0.0030
C28	0.0023
C29	0.0016
C30+	0.0741

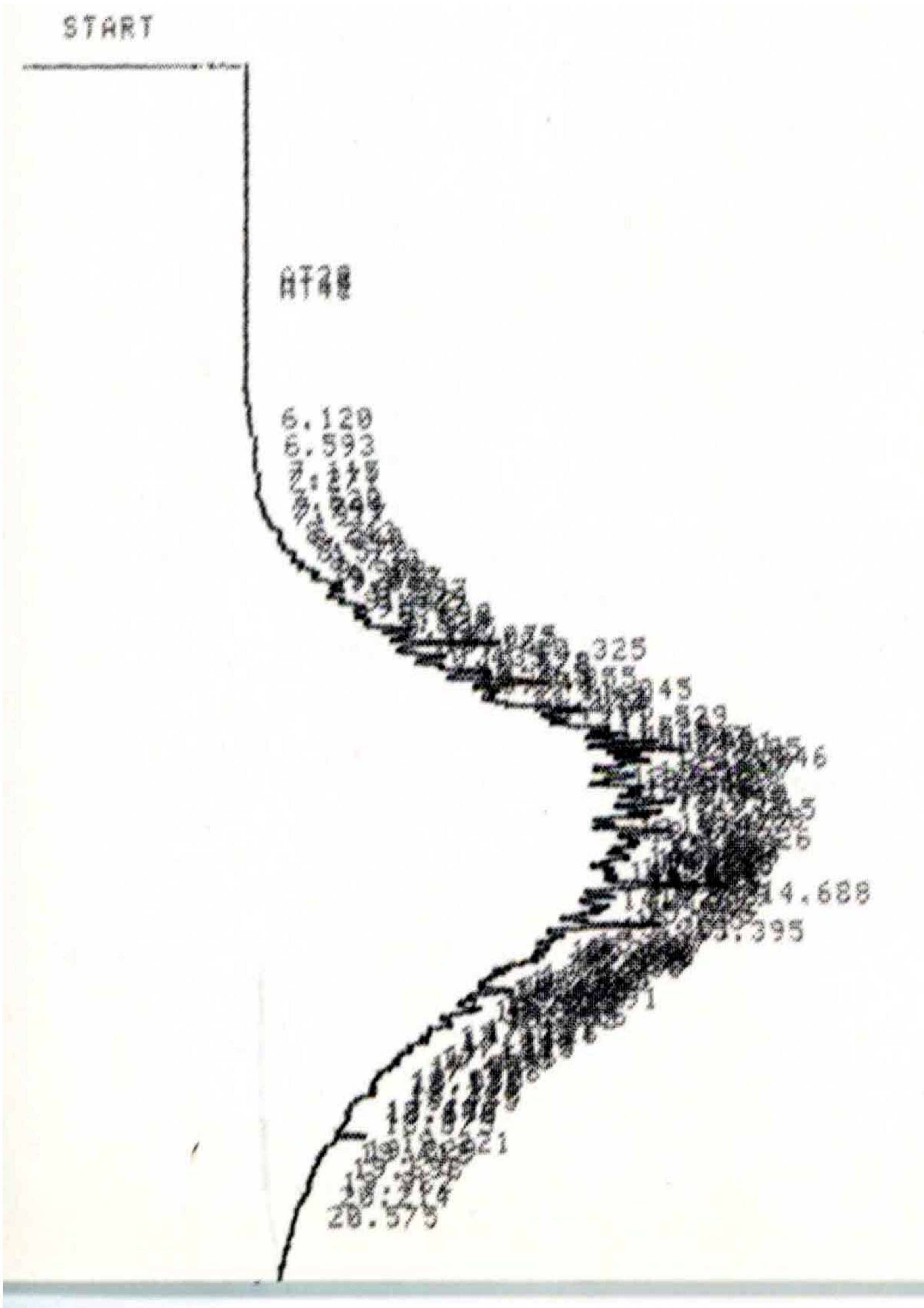

Figure C.11: Steam distillation yields at 270°C for 260psig.

Table C.11: Composition of distillation yield at 270^{o}C.

Type : Steam Distillation Yield at Field condition

Temperature - 270^{o}C

Component	weight %
C5	0.0000
C6	0.0000
C7	0.0000
C8	0.0000
C9	0.0000
C10	0.0022
C11	0.0111
C12	0.0327
C13	0.0650
C14	0.0823
C15	0.1199
C16	0.1216
C17	0.1024
C18	0.0978
C19	0.0846
C20	0.0626
C21	0.0531
C22	0.0378
C23	0.0283
C24	0.0214
C25	0.0165
C26	0.0118
C27	0.0101
C28	0.0073
C29	0.0068
C30+	0.0246

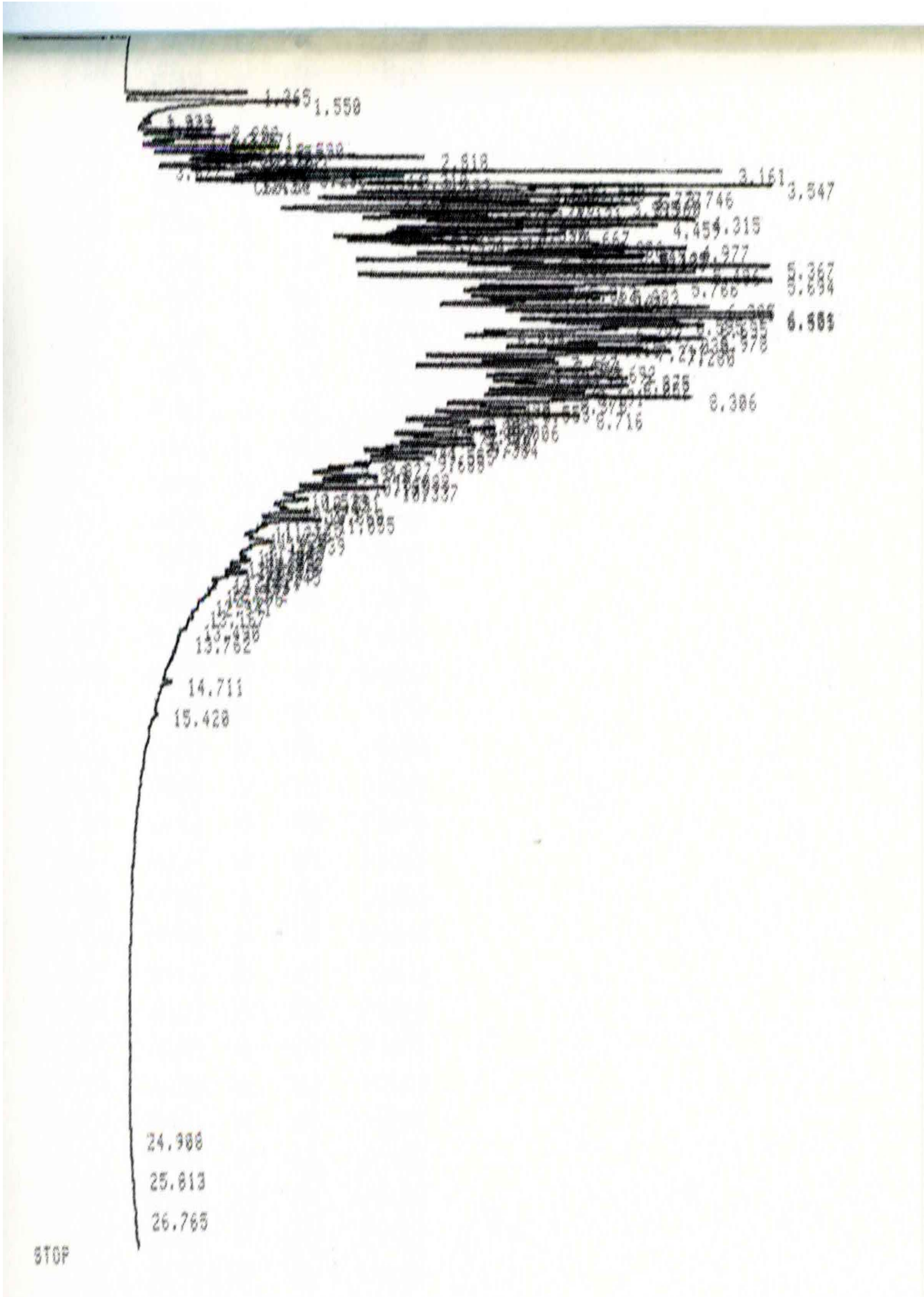

Figure C.12: Steam distillation yields at 229°C for 260psig.

Table C.12: Composition of steam-propane distillation yield at 229°C.

Type: Steam-Propane Distillation Yield at Field condition

Temperature - 229°C

Component	weight %
C5	0.0000
C6	0.0026
C7	0.0062
C8	0.0216
C9	0.0523
C10	0.0937
C11	0.1279
C12	0.1524
C13	0.1500
C14	0.1016
C15	0.0899
C16	0.0639
C17	0.0391
C18	0.0309
C19	0.0235
C20	0.0148
C21	0.0109
C22	0.0068
C23	0.0051
C24	0.0028
C25	0.0018
C26	0.0003
C27	0.0001
C28	0.0000
C29	0.0000
C30+	0.0017

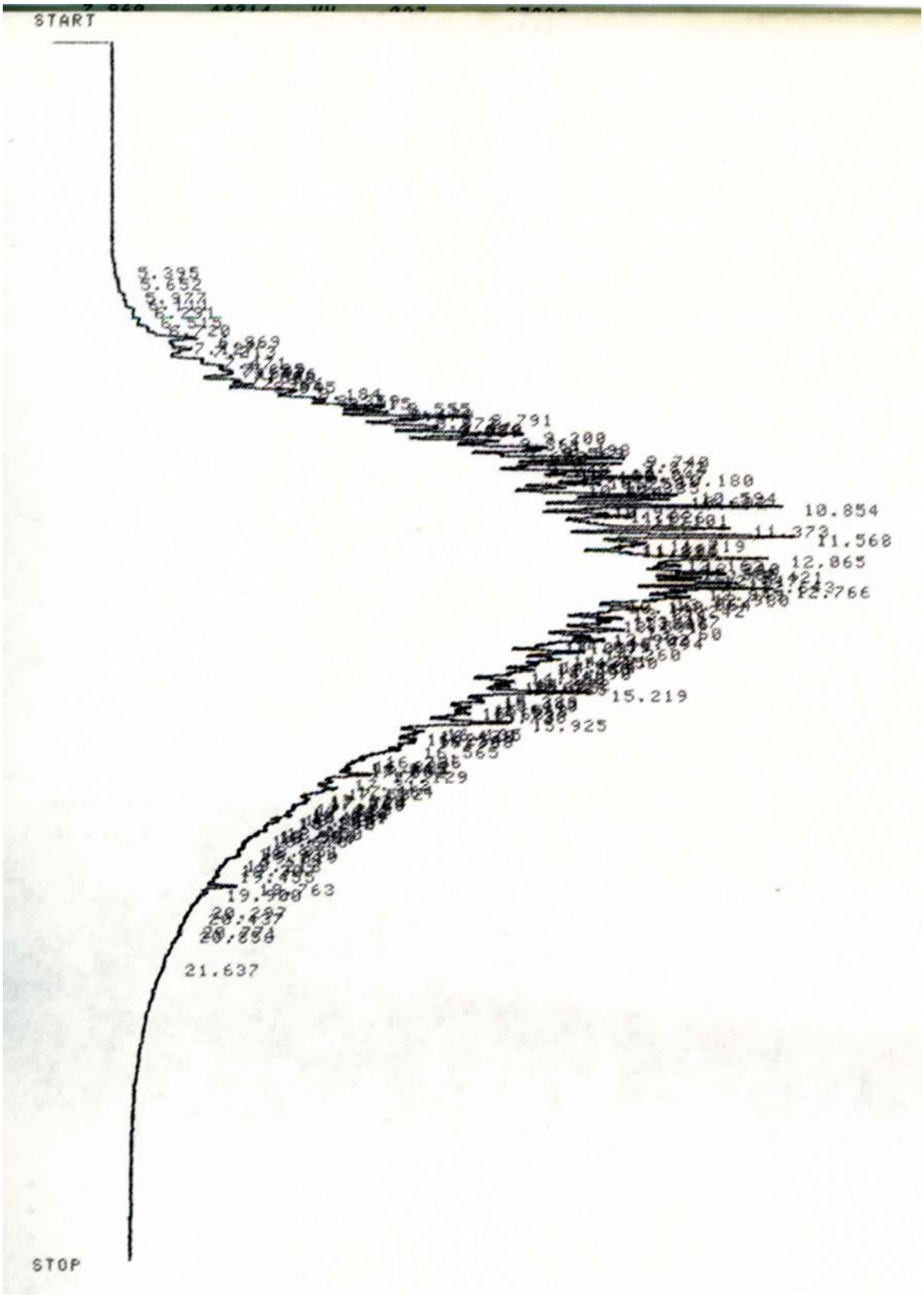

Figure C.13: Steam-propane distillation yields at 249°C for 260psig.

Table C.13: Composition of steam-propane distillation yield at 249^{o}C.

Type : Steam-Propane Distillation Yield at Field condition

Temperature - 249^{o}C

Component	weight %
C5	0.0000
C6	0.0000
C7	0.0003
C8	0.0034
C9	0.0168
C10	0.0448
C11	0.0818
C12	0.1248
C13	0.1479
C14	0.1179
C15	0.1189
C16	0.0924
C17	0.0628
C18	0.0524
C19	0.0402
C20	0.0263
C21	0.0208
C22	0.0126
C23	0.0092
C24	0.0061
C25	0.0040
C26	0.0031
C27	0.0026
C28	0.0021
C29	0.0019
C30+	0.0068

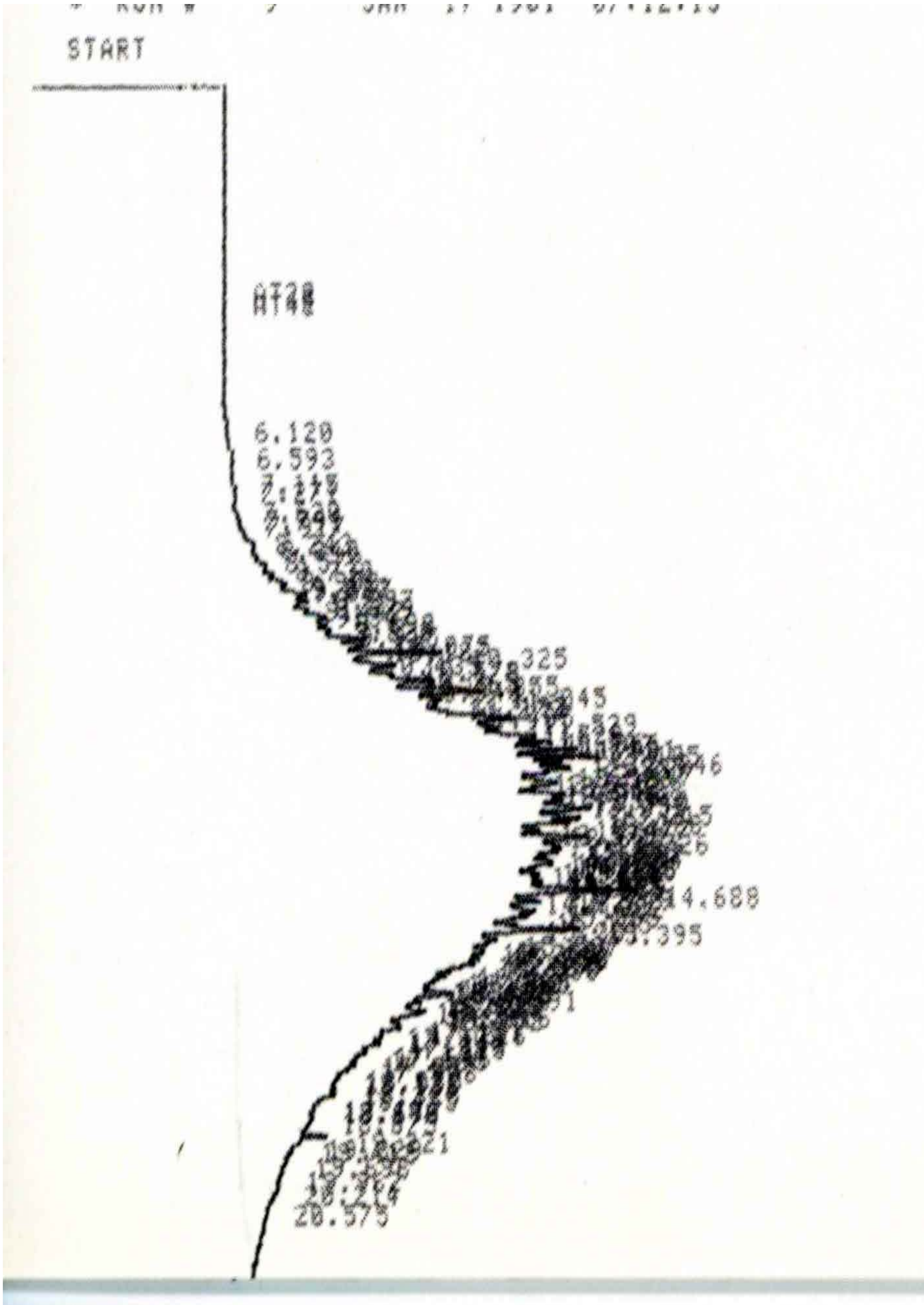

Figure C.14: Steam-propane distillation yields at 279^{o}C for 260psig.

Table C.14: Composition of steam-propane distillation yield at 279^oC.

Type : Steam-Propane Distillation Yield at Field condition

Temperature - 279^oC

Component	weight %
C5	0.0000
C6	0.0000
C7	0.0000
C8	0.0000
C9	0.0006
C10	0.0074
C11	0.0234
C12	0.0572
C13	0.0958
C14	0.1027
C15	0.1300
C16	0.1205
C17	0.0944
C18	0.0854
C19	0.0708
C20	0.0510
C21	0.0401
C22	0.0278
C23	0.0220
C24	0.0156
C25	0.0118
C26	0.0088
C27	0.0065
C28	0.0047
C29	0.0043
C30+	0.0193

VITA

Name:	Namit Jaiswal
Permanent Address:	Plot 86, Bandhu Nagar,
	Jhingabai Takli Road,
	Nagpur, M.S. 440002
	India
Email:	NamitJaiswal@GMAIL.com
Education:	University of Mumbai, Institute of Chemical Technology (UICT)
	Bachelor of Chemical Engineering
	June 2002
	University of Alaska Fairbanks (UAF)
	Master of Science in Petroleum Engineering
	August 2004
	Texas A & M University, College Station, TX
	Ph.D. in Petroleum Engineering
	May 2006